

In Situ database Analyses Report

prepared by the Pi-MEP Consortium

December 15, 2020

Contents

1 Overview	8
1.1 <i>In situ</i> datasets	8
1.1.1 Argo	9
1.1.2 TSG	9
1.1.3 Surface drifters	10
1.1.4 Sea mammals	11
1.1.5 Moorings	11
1.2 Auxiliary geophysical datasets	11
1.2.1 CMORPH	12
1.2.2 ASCAT	13
1.2.3 ISAS	13
1.2.4 World Ocean Atlas Climatology	13
2 Argo	14
2.1 Introduction	14
2.2 Number of SSS data as a function of time and distance to coast	14
2.3 Histograms of SSS	15
2.4 Distribution of <i>in situ</i> SSS depth measurements	15
2.5 Spatial distribution of SSS	15
2.6 Spatial Maps of the Temporal mean and Std of <i>in situ</i> and ISAS SSS and of the difference (Δ SSS)	16
2.7 Time series of the monthly median and Std of <i>in situ</i> and ISAS SSS and of the difference (Δ SSS)	17
2.8 Zonal mean and Std of <i>in situ</i> and ISAS SSS and of the difference Δ SSS	18
2.9 Scatterplots of ISAS vs <i>in situ</i> SSS by latitudinal bands	19
2.10 Time series of the monthly median and Std of the difference Δ SSS sorted by latitudinal bands	20
2.11 Δ SSS sorted as geophysical conditions	21
2.12 Δ SSS maps and statistics for different geophysical conditions	22
2.13 Summary	24
3 TSG	25
3.1 TSG (LEGOS-DM)	26
3.1.1 Introduction	26
3.1.2 Number of SSS data as a function of time and distance to coast	26
3.1.3 Histograms of SSS	26
3.1.4 Distribution of <i>in situ</i> SSS depth measurements	27
3.1.5 Spatial distribution of SSS	27
3.1.6 Spatial Maps of the Temporal mean and Std of <i>in situ</i> and ISAS SSS and of the difference (Δ SSS)	27
3.1.7 Time series of the monthly median and Std of <i>in situ</i> and ISAS SSS and of the difference (Δ SSS)	28
3.1.8 Zonal mean and Std of <i>in situ</i> and ISAS SSS and of the difference Δ SSS	29
3.1.9 Scatterplots of ISAS vs <i>in situ</i> SSS by latitudinal bands	30
3.1.10 Time series of the monthly median and Std of the difference Δ SSS sorted by latitudinal bands	31
3.1.11 Δ SSS sorted as geophysical conditions	32

3.1.12	ΔSSS maps and statistics for different geophysical conditions	33
3.1.13	Summary	35
3.2	TSG (GOSUD-Research-vessel)	36
3.2.1	Introduction	36
3.2.2	Number of SSS data as a function of time and distance to coast	36
3.2.3	Histograms of SSS	37
3.2.4	Distribution of <i>in situ</i> SSS depth measurements	37
3.2.5	Spatial distribution of SSS	38
3.2.6	Spatial Maps of the Temporal mean and Std of <i>in situ</i> and ISAS SSS and of the difference (Δ SSS)	38
3.2.7	Time series of the monthly median and Std of <i>in situ</i> and ISAS SSS and of the difference (Δ SSS)	39
3.2.8	Zonal mean and Std of <i>in situ</i> and ISAS SSS and of the difference Δ SSS	40
3.2.9	Scatterplots of ISAS vs <i>in situ</i> SSS by latitudinal bands	41
3.2.10	Time series of the monthly median and Std of the difference Δ SSS sorted by latitudinal bands	42
3.2.11	Δ SSS sorted as geophysical conditions	43
3.2.12	Δ SSS maps and statistics for different geophysical conditions	44
3.2.13	Summary	46
3.3	TSG (GOSUD-Sailing-ship)	47
3.3.1	Introduction	47
3.3.2	Number of SSS data as a function of time and distance to coast	47
3.3.3	Histograms of SSS	48
3.3.4	Distribution of <i>in situ</i> SSS depth measurements	48
3.3.5	Spatial distribution of SSS	49
3.3.6	Spatial Maps of the Temporal mean and Std of <i>in situ</i> and ISAS SSS and of the difference (Δ SSS)	49
3.3.7	Time series of the monthly median and Std of <i>in situ</i> and ISAS SSS and of the difference (Δ SSS)	50
3.3.8	Zonal mean and Std of <i>in situ</i> and ISAS SSS and of the difference Δ SSS	51
3.3.9	Scatterplots of ISAS vs <i>in situ</i> SSS by latitudinal bands	52
3.3.10	Time series of the monthly median and Std of the difference Δ SSS sorted by latitudinal bands	53
3.3.11	Δ SSS sorted as geophysical conditions	54
3.3.12	Δ SSS maps and statistics for different geophysical conditions	55
3.3.13	Summary	57
3.4	TSG (SAMOS)	58
3.4.1	Introduction	58
3.4.2	Number of SSS data as a function of time and distance to coast	58
3.4.3	Histograms of SSS	59
3.4.4	Distribution of <i>in situ</i> SSS depth measurements	59
3.4.5	Spatial distribution of SSS	60
3.4.6	Spatial Maps of the Temporal mean and Std of <i>in situ</i> and ISAS SSS and of the difference (Δ SSS)	60
3.4.7	Time series of the monthly median and Std of <i>in situ</i> and ISAS SSS and of the difference (Δ SSS)	61
3.4.8	Zonal mean and Std of <i>in situ</i> and ISAS SSS and of the difference Δ SSS	62
3.4.9	Scatterplots of ISAS vs <i>in situ</i> SSS by latitudinal bands	63

3.4.10	Time series of the monthly median and Std of the difference ΔSSS sorted by latitudinal bands	64
3.4.11	ΔSSS sorted as geophysical conditions	65
3.4.12	ΔSSS maps and statistics for different geophysical conditions	66
3.4.13	Summary	68
3.5	TSG (LEGOS-Survostral)	69
3.5.1	Introduction	69
3.5.2	Number of SSS data as a function of time and distance to coast	69
3.5.3	Histograms of SSS	70
3.5.4	Distribution of <i>in situ</i> SSS depth measurements	70
3.5.5	Spatial distribution of SSS	71
3.5.6	Spatial Maps of the Temporal mean and Std of <i>in situ</i> and ISAS SSS and of the difference (ΔSSS)	72
3.5.7	Time series of the monthly median and Std of <i>in situ</i> and ISAS SSS and of the difference (ΔSSS)	74
3.5.8	Zonal mean and Std of <i>in situ</i> and ISAS SSS and of the difference ΔSSS	74
3.5.9	Scatterplots of ISAS vs <i>in situ</i> SSS by latitudinal bands	75
3.5.10	Time series of the monthly median and Std of the difference ΔSSS sorted by latitudinal bands	77
3.5.11	ΔSSS sorted as geophysical conditions	77
3.5.12	ΔSSS maps and statistics for different geophysical conditions	78
3.5.13	Summary	81
3.6	TSG (LEGOS-Survostral-Adelie)	82
3.6.1	Introduction	82
3.6.2	Number of SSS data as a function of time and distance to coast	82
3.6.3	Histograms of SSS	83
3.6.4	Distribution of <i>in situ</i> SSS depth measurements	83
3.6.5	Spatial distribution of SSS	84
3.6.6	Spatial Maps of the Temporal mean and Std of <i>in situ</i> and ISAS SSS and of the difference (ΔSSS)	85
3.6.7	Time series of the monthly median and Std of <i>in situ</i> and ISAS SSS and of the difference (ΔSSS)	87
3.6.8	Zonal mean and Std of <i>in situ</i> and ISAS SSS and of the difference ΔSSS	87
3.6.9	Scatterplots of ISAS vs <i>in situ</i> SSS by latitudinal bands	88
3.6.10	Time series of the monthly median and Std of the difference ΔSSS sorted by latitudinal bands	90
3.6.11	ΔSSS sorted as geophysical conditions	90
3.6.12	ΔSSS maps and statistics for different geophysical conditions	91
3.6.13	Summary	94
3.7	TSG (Polarstern)	95
3.7.1	Introduction	95
3.7.2	Number of SSS data as a function of time and distance to coast	95
3.7.3	Histograms of SSS	96
3.7.4	Distribution of <i>in situ</i> SSS depth measurements	96
3.7.5	Spatial distribution of SSS	97
3.7.6	Spatial Maps of the Temporal mean and Std of <i>in situ</i> and ISAS SSS and of the difference (ΔSSS)	97
3.7.7	Time series of the monthly median and Std of <i>in situ</i> and ISAS SSS and of the difference (ΔSSS)	98

3.7.8	Zonal mean and Std of <i>in situ</i> and ISAS SSS and of the difference ΔSSS	99
3.7.9	Scatterplots of ISAS vs <i>in situ</i> SSS by latitudinal bands	100
3.7.10	Time series of the monthly median and Std of the difference ΔSSS sorted by latitudinal bands	101
3.7.11	ΔSSS sorted as geophysical conditions	102
3.7.12	ΔSSS maps and statistics for different geophysical conditions	103
3.7.13	Summary	105
3.8	TSG (NCEI-0170743)	106
3.8.1	Introduction	106
3.8.2	Number of SSS data as a function of time and distance to coast	107
3.8.3	Histograms of SSS	107
3.8.4	Distribution of <i>in situ</i> SSS depth measurements	108
3.8.5	Spatial distribution of SSS	108
3.8.6	Spatial Maps of the Temporal mean and Std of <i>in situ</i> and ISAS SSS and of the difference (ΔSSS)	109
3.8.7	Time series of the monthly median and Std of <i>in situ</i> and ISAS SSS and of the difference (ΔSSS)	110
3.8.8	Zonal mean and Std of <i>in situ</i> and ISAS SSS and of the difference ΔSSS	111
3.8.9	Scatterplots of ISAS vs <i>in situ</i> SSS by latitudinal bands	112
3.8.10	Time series of the monthly median and Std of the difference ΔSSS sorted by latitudinal bands	113
3.8.11	ΔSSS sorted as geophysical conditions	114
3.8.12	ΔSSS maps and statistics for different geophysical conditions	115
3.8.13	Summary	117
4	Surface drifters	118
4.1	Introduction	118
4.2	Number of SSS data as a function of time and distance to coast	118
4.3	Histograms of SSS	119
4.4	Distribution of <i>in situ</i> SSS depth measurements	119
4.5	Spatial distribution of SSS	120
4.6	Spatial Maps of the Temporal mean and Std of <i>in situ</i> and ISAS SSS and of the difference (ΔSSS)	120
4.7	Time series of the monthly median and Std of <i>in situ</i> and ISAS SSS and of the difference (ΔSSS)	121
4.8	Zonal mean and Std of <i>in situ</i> and ISAS SSS and of the difference ΔSSS	122
4.9	Scatterplots of ISAS vs <i>in situ</i> SSS by latitudinal bands	123
4.10	Time series of the monthly median and Std of the difference ΔSSS sorted by latitudinal bands	124
4.11	ΔSSS sorted as geophysical conditions	125
4.12	ΔSSS maps and statistics for different geophysical conditions	126
4.13	Summary	128
5	Sea mammals	129
5.1	Introduction	129
5.2	Number of SSS data as a function of time and distance to coast	130
5.3	Histograms of SSS	130
5.4	Distribution of <i>in situ</i> SSS depth measurements	130
5.5	Spatial distribution of SSS	131

5.6	Spatial Maps of the Temporal mean and Std of <i>in situ</i> and ISAS SSS and of the difference (Δ SSS)	131
5.7	Time series of the monthly median and Std of <i>in situ</i> and ISAS SSS and of the difference (Δ SSS)	132
5.8	Zonal mean and Std of <i>in situ</i> and ISAS SSS and of the difference Δ SSS	133
5.9	Scatterplots of ISAS vs <i>in situ</i> SSS by latitudinal bands	134
5.10	Time series of the monthly median and Std of the difference Δ SSS sorted by latitudinal bands	135
5.11	Δ SSS sorted as geophysical conditions	136
5.12	Δ SSS maps and statistics for different geophysical conditions	137
5.13	Summary	139
6	Moorings	140
6.1	Introduction	140
6.2	Number of SSS data as a function of time and distance to coast	141
6.3	Histogram of SSS	141
6.4	Temporal mean of shallowest salinity	141
6.5	Temporal Std of shallowest salinity	142
6.6	Number of shallowest salinity	142
6.7	Time series of shallowest salinity	143
7	Summary	144
7.1	Number of SSS data as a function of time	144
7.2	Histogram of SSS	145
7.3	Temporal mean of SSS	146
7.4	Temporal Std of SSS	147
7.5	Spatial density of SSS	148
7.6	Characteristics for each Pi-MEP region	149

Acronym

Aquarius	NASA/CONAE Salinity mission
ASCAT	Advanced Scatterometer
ATBD	Algorithm Theoretical Baseline Document
BLT	Barrier Layer Thickness
CMORPH	CPC MORPHing technique (precipitation analyses)
CPC	Climate Prediction Center
CTD	Instrument used to measure the conductivity, temperature, and pressure of seawater
DM	Delayed Mode
EO	Earth Observation
ESA	European Space Agency
FTP	File Transfer Protocol
GOSUD	Global Ocean Surface Underway Data
GTMBA	The Global Tropical Moored Buoy Array
Ifremer	Institut français de recherche pour l'exploitation de la mer
IPEV	Institut polaire français Paul-Émile Victor
IQR	Interquartile range
ISAS	<i>In Situ</i> Analysis System
Kurt	Kurtosis (fourth central moment divided by fourth power of the standard deviation)
L2	Level 2
LEGOS	Laboratoire d'Etudes en Géophysique et Océanographie Spatiales
LOCEAN	Laboratoire d'Océanographie et du Climat : Expérimentations et Approches Numériques
LOPS	Laboratoire d'Océanographie Physique et Spatiale
MDB	Match-up Data Base
MEOP	Marine Mammals Exploring the Oceans Pole to Pole
MLD	Mixed Layer Depth
NCEI	National Centers for Environmental Information
NRT	Near Real Time
NTAS	Northwest Tropical Atlantic Station
OI	Optimal interpolation
Pi-MEP	Pilot-Mission Exploitation Platform
PIRATA	Prediction and Researched Moored Array in the Atlantic
QC	Quality control
R_{sat}	Spatial resolution of the satellite SSS product
RAMA	Research Moored Array for African-Asian-Australian Monsoon Analysis and Prediction
r^2	Square of the Pearson correlation coefficient
RMS	Root mean square
RR	Rain rate
SAMOS	Shipboard Automated Meteorological and Oceanographic System
Skew	Skewness (third central moment divided by the cube of the standard deviation)
SMAP	Soil Moisture Active Passive (NASA mission)
SMOS	Soil Moisture and Ocean Salinity (ESA mission)
SPURS	Salinity Processes in the Upper Ocean Regional Study
SSS	Sea Surface Salinity
SSS_{insitu}	<i>In situ</i> SSS data considered for the match-up

SSS _{SAT}	Satellite SSS product considered for the match-up
ΔSSS	Difference between satellite and <i>in situ</i> SSS at colocalized point ($\Delta\text{SSS} = \text{SSS}_{\text{SAT}} - \text{SSS}_{\text{insitu}}$)
SST	Sea Surface Temperature
Std	Standard deviation
Std*	Robust Standard deviation = $\text{median}(\text{abs}(\text{x}-\text{median}(\text{x}))) / 0.67$ (less affected by outliers than Std)
Stratus	Surface buoy located in the eastern tropical Pacific
Survostral	SURVeillance de l'Océan AuSTRAL (Monitoring the Southern Ocean)
TAO	Tropical Atmosphere Ocean
TSG	ThermoSalinoGraph
WHOI	Woods Hole Oceanographic Institution
WHOTS	WHOI Hawaii Ocean Time-series Station
WOA	World Ocean Atlas

1 Overview

This report presents some characteristics of the 5 major *in situ* datasets ([Argo](#), [TSG](#), [Moorings](#), [surface drifters](#) and [Sea mammals](#)) used by the Pi-MEP to validate SMOS, SMAP and Aquarius satellite SSS products. For each *in situ* datasets, a series of plots show:

- Number of SSS data as a function of time and distance to coast
- Histogram of shallowest salinity and pressure (if relevant)
- Temporal mean of shallowest salinity pressure measurements (if relevant)
- Spatial density of shallowest salinity
- Spatial Maps of the Time-mean and temporal Std of *in situ* and satellite SSS and of the Δ SSS
- Time series of the monthly median and Std of *in situ* and satellite SSS and of the Δ SSS
- Zonal mean and Std of *in situ* and satellite SSS and of the Δ SSS
- Scatterplots of ISAS vs *in situ* SSS by latitudinal bands
- Time series of the monthly median and Std of the Δ SSS sorted by latitudinal bands
- Δ SSS sorted as function of geophysical parameters
- Δ SSS maps and statistics for different geophysical conditions

1.1 *In situ* datasets

The following table resumes some characteristics (number of points, first and last date, minimum, maximum and mean value of the SSS distribution) of the different *in situ* datasets used by the Pi-MEP.

<i>In situ</i> datasets	#	Time_{min}	Time_{max}	S_{min}	S_{max}	S_{Mean}
Argo	1413783	01/01/2010	31/10/2020	2.14	40.45	34.76
TSG (LEGOS-DM)	5888360	01/01/2010	30/08/2019	0.03	42.74	34.60
TSG (GOSUD-Research-vessel)	5413749	05/01/2010	06/12/2019	0.01	42.00	35.68
TSG (GOSUD-Sailing-ship)	1472098	08/01/2010	29/08/2017	0.01	42.00	33.68
TSG (SAMOS)	23008724	07/01/2010	26/09/2020	5.03	39.80	33.32
Sea mammals	199580	01/01/2010	14/01/2018	4.06	36.67	33.95
Surface drifters	2161177	01/01/2010	31/12/2018	1.03	38.58	35.62
TSG (LEGOS-Survostral)	654661	01/01/2010	02/03/2020	22.67	35.73	34.17
TSG (LEGOS-Surv-Adel)	38903	09/01/2010	25/01/2012	28.14	34.37	34.04
Moorings	6320250	01/01/2010	05/11/2020	27.02	37.81	34.94
TSG (NCEI-0170743)	590389	08/12/2010	02/02/2017	32.41	35.78	34.26
TSG (Polarstern)	447592	01/01/2010	28/06/2019	20.30	37.75	34.27
Salinity Snake	3428541	20/08/2016	13/11/2017	24.04	34.34	33.12
Saildrone	9218	16/10/2017	17/11/2017	30.75	33.85	33.29
Waveglider	642340	24/08/2016	10/11/2017	27.48	34.47	33.51
Seaglider	73542	24/08/2016	07/11/2017	28.99	34.86	33.27
Total	51762907	01/01/2010	05/11/2020	0.01	42.74	34.16

1.1.1 Argo

Argo is a global array of 3,000 free-drifting profiling floats that measures the temperature and salinity of the upper 2000 m of the ocean. This allows continuous monitoring of the temperature and salinity of the upper ocean, with all data being relayed and made publicly available within hours after collection. The array provides around 100,000 temperature/salinity profiles per year distributed over the global oceans at an average of 3-degree spacing. Only Argo salinity and temperature float data with quality index set to 1 or 2 and data mode set to real time (RT), real time adjusted (RTA) and delayed mode (DM) are considered in the Pi-MEP. Argo floats which may have problems with one or more sensors appearing in the grey list maintained at the Coriolis/GDACs are discarded. Furthermore, Pi-MEP provides an additional list of ~1000 "suspicious" argo salinity profiles that are also removed before analysis. The upper ocean salinity and temperature values recorded between 0m and 10m depth are considered as Argo sea surface salinities (SSS) and sea surface temperatures (SST). These data were collected and made freely available by the international Argo project and the national programs that contribute to it ([Argo \(2000\)](#)).

1.1.2 TSG

The TSG dataset is subdivided into 8 subdatasets following TSG data providers subdivisions:

- **LEGOS-DM:**
The TSG-LEGOS-DM dataset correspond to sea surface salinity delayed mode data derived from voluntary observing ships collected, validated, archived, and made freely available by the [French Sea Surface Salinity Observation Service \(Alory et al. \(2015\)\)](#). Adjusted values when available and only collected TSG data that exhibit quality flags=1 and 2 were used.
- **GOSUD-Research-vessel:**
The TSG-GOSUD-Research-vessel dataset correspond to French research vessels that have been collecting thermo-salinometer (TSG) data since the early 2000 in contribution to the [GOSUD](#) program. The set of homogeneous instruments is permanently monitored and regularly calibrated. Water samples are taken on a daily basis by the crew and later analysed in the laboratory. The careful calibration and instrument maintenance, complemented with a rigorous adjustment on water samples lead to reach an accuracy of a few 10^{-2} PSS in salinity. This delayed mode dataset ([Kolodziejczyk et al. \(2015a\)](#)) is updated annually and freely available [here](#). Adjusted values when available and only collected TSG data that exhibit quality flags 1 or 2 were used.
- **GOSUD-Sailing-ship:** The TSG-GOSUD-Sailing-ship dataset correspond to Observations of Sea surface salinity obtained from voluntary sailing ships using medium or small size sensors. They complement the networks installed on research vessels or commercial ships. This delayed mode dataset ([Reynaud et al. \(2015\)](#)) is updated annually as a contribution to GOSUD (<http://www.gosud.org>) and freely available [here](#). Adjusted values when available and only collected TSG data that exhibit quality flags=1 and 2 were used.
- **SAMOS:** The TSG-SAMOS dataset correspond to "Research" quality data from the US Shipboard Automated Meteorological and Oceanographic System (SAMOS) initiative ([Smith et al. \(2009\)](#)). Data are available at <http://samos.coaps.fsu.edu/html/>. Adjusted values when available and only collected TSG data that exhibit quality flags=1 and 2 were used. After visual inspection, data from the NANCY FOSTER (ID="WTER", IMO="008993227") with date 2011/03/21 and all data from the ATLANTIS (ID="KAQP", IMO="009105798") for year 2010 has been remove from this dataset.

- **LEGOS-Survostral:** The TSG-LEGOS-Survostral dataset correspond to delayed mode regional data from TSG installed on the Astrolabe vessel (IPEV) during the round trips between Hobart (Tasmania) and the French Antarctic base at Dumont d'Urville ([Morrow and Kestenare \(2014\)](#)). It is provided by the [Survostral project](#) and available via [ftp](#). Adjusted values when available and only collected TSG data that exhibit quality flags=1 and 2 were used.
- **LEGOS-Survostral-Adélie:** The TSG-LEGOS-Surv-Adel dataset correspond to delayed mode regional dataset along the Adelie coast provided by the [Survostral project](#) and available via [ftp](#). Adjusted values when available and only collected TSG data that exhibit quality flags=1 and 2 were used.
- **Polarstern:** The TSG-POLARSTERN dataset has been gathered through the <https://www.pangaea.de/> data warehouse utility using the following criteria: basis:"Polarstern" , device:"Underway cruise track measurements (CT)" , time coverage form 2010/01/01 to present. The result of the query is a collection of 77 different datasets with the following identification numbers: [736345](#), [742729](#), [753224](#), [753225](#), [753226](#), [753227](#), [758080](#), [760120](#), [760121](#), [761277](#), [770034](#), [770035](#), [770828](#), [776596](#), [776597](#), [780004](#), [802809](#), [802810](#), [802811](#), [802812](#), [803312](#), [803431](#), [808835](#), [808836](#), [808838](#), [809727](#), [810678](#), [816055](#), [819831](#), [823259](#), [831976](#), [832269](#), [839406](#), [839407](#), [839408](#), [845130](#), [848615](#), [858879](#), [858880](#), [858881](#), [858882](#), [858883](#), [858884](#), [858885](#), [863228](#), [863229](#), [863230](#), [863231](#), [863232](#), [863234](#), [873145](#), [873147](#), [873151](#), [873153](#), [873155](#), [873156](#), [873158](#), [887767](#), [889444](#), [889513](#), [889515](#), [889516](#), [889517](#), [889535](#), [889542](#), [889548](#), [895578](#), [895579](#), [895581](#), [898225](#), [898233](#), [898266](#), [905555](#), [905562](#), [905608](#), [905610](#), [905734](#).
- **NCEI-0170743:** The TSG-NCEI-0170743 dataset ([Aulicino et al. \(2018\)](#)) contains sea surface temperature and salinity data collected from 2010 to 2017 in the South Atlantic Ocean and Southern Ocean from S.A. Agulhas and Agulhas-II research vessels, in the framework of South African National Antarctic Programme ([SANAP](#)), South African Department of Environmental Affairs ([DEA](#)) and Italian National Antarctic Research Programme ([PNRA](#)) scientific activities. Measurements have been obtained through termosalinograph (TSG) during several cruises to both Antarctica and sub-Antarctic islands. On-board TSG devices have been regularly calibrated and continuously monitored in-between cruises; no appreciable sensor drift emerged. Independent water samples taken along the cruises have been used to validate the data; salinity measurement error was a few hundredths of a unit on the practical salinity scale. A careful quality control allowed to discard bad data for each single campaign.

1.1.3 Surface drifters

The skin depth of the L-band radiometer signal over the ocean is about 1 cm whereas classical surface salinity measured by ships or Argo floats are performed at a few meters depth. In order to improve the knowledge of the SSS variability in the first 50 cm depth, to better document the SSS variability in a satellite pixel and to provide ground-truth as close as possible to the sea surface for validating satellite SSS, the L-band remotely sensed community proposed to deploy numerous surface drifters over various parts of the ocean. Surface drifter data are provided by the LOCEAN (see <https://www.locean-ipsl.upmc.fr/smos/drifters/>). Only validated data are considered with uncertainty order of 0.01 and 0.1.

1.1.4 Sea mammals

Instrumentation of southern elephant seals with satellite-linked CTD tags proposes unique temporal and spatial coverage. This includes extensive data from the Antarctic continental slope and shelf regions during the winter months, which is outside the conventional areas of Argo autonomous floats and ship-based studies. The use of elephant seals has been particularly effective to sample the Southern Ocean and the North Pacific. Other seal species have been successfully used in the North Atlantic, such as hooded seals. The marine mammal dataset ([MEOP-CTD database](#)) is quality controlled and calibrated using delayed-mode techniques involving comparisons with other existing profiles as well as cross-comparisons similar to established protocols within the Argo community, with a resulting accuracy of ± 0.03 °C in temperature and ± 0.05 in salinity or better ([Treasure et al. \(2017\)](#)). The marine mammal data were collected and made freely available by the International MEOP Consortium and the national programs that contribute to it (<http://www.meop.net>). This dataset is updated once a year and can be downloaded [here](#) ([Roquet et al. \(2018\)](#)). A preprocessing stage is applied to the database before being used by the Pi-MEP which consist to keep only profile with salinity, temperature and pressure quality flags set to 1 or 2 and if at least one measurement is in the top 10 m depth. Marine mammal SSS correspond to the top (shallowest) profile salinity data provided that profile depth is 10 m or less.

1.1.5 Moorings

The Pi-MEP collects data from the Global Tropical Moored Buoy Array ([GTMBA](#)), a multi-national effort to provide data in real-time for climate research and forecasting. Major components include the TAO/TRITON array in the Pacific, PIRATA in the Atlantic, and RAMA in the Indian Ocean. Data collected within TAO/TRITON, PIRATA and RAMA comes primarily from ATLAS and TRITON moorings. These two mooring systems are functionally equivalent in terms of sensors, sample rates, and data quality. The data are directly downloaded from <ftp://pmel.noaa.gov> every day and stored in the Pi-MEP. Only salinity data measured at 1 or 1.5 meter depth with standard (pre-deployment calibration applied) and highest quality (pre/post calibration agree) are considered. A careful filtering of suspicious bad mooring salinity data when compared with all satellite data has also been performed (cf. [presentation](#)). The Pi-MEP project acknowledges the GTMBA Project Office of NOAA/PMEL for providing the data. Data from the Ocean Station [PAPA](#) are also added to the Pi-MEP *in situ* database.

From the [Upper Ocean Processes Group](#) at Woods Hole Oceanographic Institution ([WHOI](#)), delayed mode surface mooring salinity records under the stratus cloud deck in the eastern tropical Pacific ([Stratus](#)), in the trade wind region of the northwest tropical Atlantic ([NTAS](#)), 100 km north of Oahu at the WHOI Hawaii Ocean Time-series Site ([WHOTS](#)), in the salinity maximum region of the subtropical North Atlantic ([SPURS-1](#)) and in the Pacific intertropical convergence zone ([SPURS-2](#)) are also included in the Pi-MEP.

1.2 Auxiliary geophysical datasets

Additional EO datasets are used to characterize the geophysical conditions at the *in situ* measurement locations and time, and 10 days prior the measurements to get an estimate of the geophysical condition and history. As discussed in [Boutin et al. \(2016\)](#), the presence of vertical gradients in, and horizontal variability of, sea surface salinity indeed complicates comparison of satellite and *in situ* measurements. The additional EO data are used here to get a first estimates of conditions for which L-band satellite SSS measured in the first centimeters of the upper ocean

within a 50-150 km diameter footprint might differ from pointwise *in situ* measurements performed in general between 10 and 5 m depth below the surface. The spatio-temporal variability of SSS within a satellite footprint (50-150 km) is a major issue for satellite SSS validation in the vicinity of river plumes, frontal zones, and significant precipitation. Rainfall can in some cases produce vertical salinity gradients exceeding 1 pss m⁻¹; consequently, it is recommended that satellite and *in situ* SSS measurements less than 3–6 h after rain events should be considered with care when used in satellite calibration/validation analyses. To identify such situation, the Pi-MEP platform is first using CMORPH products to characterize the local value and history of rain rate and ASCAT gridded data are used to characterize the local surface wind speed and history. For validation purpose, the ISAS monthly SSS *in situ* analysed fields at 5 m depth are collocated and compared with the *in situ* SSS value. The use of ISAS is motivated by the fact that it is used in the SMOS L2 official validation protocol in which systematic comparisons of SMOS L2 retrieved SSS with ISAS are done. In complement to ISAS, annual std climatological field from the World Ocean Atlas (WOA13) at the *in situ* location are also used to have an a priori information of the local SSS variability.

1.2.1 CMORPH

Precipitation are estimated using the CMORPH 3-hourly products at 1/4° resolution (Joyce et al. (2004)). CMORPH (CPC MORPHing technique) produces global precipitation analyses at very high spatial and temporal resolution. This technique uses precipitation estimates that have been derived from low orbiter satellite microwave observations exclusively, and whose features are transported via spatial propagation information that is obtained entirely from geostationary satellite IR data. At present NOAA incorporate precipitation estimates derived from the passive microwaves aboard the DMSP 13, 14 and 15 (SSM/I), the NOAA-15, 16, 17 and 18 (AMSU-B), and AMSR-E and TMI aboard NASA's Aqua, TRMM and GPM spacecraft, respectively. These estimates are generated by algorithms of Ferraro (1997) for SSM/I, Ferraro et al. (2000) for AMSU-B and Kummerow et al. (2001) for TMI. Note that this technique is not a precipitation estimation algorithm but a means by which estimates from existing microwave rainfall algorithms can be combined. Therefore, this method is extremely flexible such that any precipitation estimates from any microwave satellite source can be incorporated.

With regard to spatial resolution, although the precipitation estimates are available on a grid with a spacing of 8 km (at the equator), the resolution of the individual satellite-derived estimates is coarser than that - more on the order of 12 x 15 km or so. The finer "resolution" is obtained via interpolation.

In effect, IR data are used as a means to transport the microwave-derived precipitation features during periods when microwave data are not available at a location. Propagation vector matrices are produced by computing spatial lag correlations on successive images of geostationary satellite IR which are then used to propagate the microwave derived precipitation estimates. This process governs the movement of the precipitation features only. At a given location, the shape and intensity of the precipitation features in the intervening half hour periods between microwave scans are determined by performing a time-weighting interpolation between microwave-derived features that have been propagated forward in time from the previous microwave observation and those that have been propagated backward in time from the following microwave scan. NOAA refer to this latter step as "morphing" of the features.

For the present Pi-MEP products, we only considered the 3-hourly products at 1/4 degree resolution. The entire CMORPH record (December 2002-present) for 3-hourly, 1/4 degree lat/lon resolution can be found at: ftp://ftp.cpc.ncep.noaa.gov/precip/CMORPH_V1.0/CRT/. CMORPH estimates cover a global belt (-180°W to 180°E) extending from 60°S to 60°N

latitude and are available for the complete period of the Pi-MEP core datasets (Jan 2010-now).

1.2.2 ASCAT

Advanced SCATterometer (ASCAT) daily data produced and made available at Ifremer/CERSAT on a $0.25^\circ \times 0.25^\circ$ resolution grid ([Bentamy and Fillon \(2012\)](#)) since March 2007 are used to characterize the mean daily wind at the match-up pair location as well as the wind history during the 10-days period preceding the in situ measurement date. These wind fields are calculated based on a geostatistical method with external drift. Remotely sensed data from ASCAT are considered as observations while those from numerical model analysis (ECMWF) are associated with the external drift. The spatial and temporal structure functions for wind speed, zonal and meridional wind components are estimated from ASCAT retrievals. Furthermore, the new procedure includes a temporal interpolation of the retrievals based on the complex empirical orthogonal function (CEOF) approach, in order to enhance the sampling length of the scatterometer observations. The resulting daily wind fields involves the main known surface wind patterns as well as some variation modes associated with temporal and spatial moving features. The accuracy of the gridded winds was investigated through comparisons with moored buoy data in [Bentamy et al. \(2012\)](#) and resulted in rms differences for wind speed and direction are about 1.50 m.s^{-1} and 20° .

1.2.3 ISAS

The In Situ Analysis System (ISAS), as described in [Gaillard et al. \(2016\)](#) is a data based reanalysis of temperature and salinity fields over the global ocean. It was initially designed to synthesize the temperature and salinity profiles collected by the Argo program. It has been later extended to accommodate all type of vertical profile as well as time series. ISAS gridded fields are entirely based on *in situ* measurements. The methodology and configuration have been conceived to preserve as much as possible the data information content and resolution. ISAS is developed and run in a research laboratory ([LOPS](#)) in close collaboration with Coriolis, one of Argo Global Data Assembly Center and unique data provider for the Mercator operational oceanography system. At the moment the period covered starts in 2002 and only the upper 2000 m are considered. The gridded fields were produced over the global ocean 70°N – 70°S on a $1/2^\circ$ grid by the ISAS project with datasets downloaded from the Coriolis data center (for more details on ISAS see [Gaillard et al. \(2009\)](#)). In the Pi-MEP, the product in used is the [INSITU_GLO_TS_OA_NRT_OBSERVATIONS_013_002.a](#) v6.2 NRT derived at the Coriolis data center and provided by the Copernicus Marine Environment Monitoring Service ([CMEMS](#)). The major contribution to the data set is from Argo array of profiling floats, reaching an approximate resolution of one profile every 10-days and every 3-degrees over the satellite SSS period (<http://www.umr-lops.fr/SNO-Argo/Products/ISAS-T-S-fields/>); in this version SSS from ship of opportunity thermosalinographs are not used, so that we can consider SMOS SSS validation using these measurements independent of ISAS. The ISAS optimal interpolation involves a structure function modeled as the sum of two Gaussian functions, each associated with specific time and space scales, resulting in a smoothing over typically 3 degrees. The smallest scale which can be retrieved with ISAS analysis is not smaller than 300–500 km ([Kolodziejczyk et al. \(2015b\)](#)). For validation purpose, the ISAS monthly SSS fields at 5 m depth are collocated and compared with the satellite SSS products and included in the Pi-MEP Match-up files. In addition, the "percentage of variance" fields (PCTVAR) contained in the ISAS analyses provide information on the local variability of *in situ* SSS measurements within $1/2^\circ \times 1/2^\circ$ boxes.

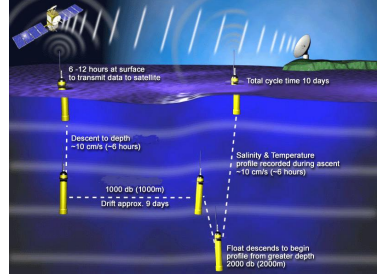
1.2.4 World Ocean Atlas Climatology

The World Ocean Atlas 2013 version 2 ([WOA13 V2](#)) is a set of objectively analyzed (1° grid) climatological fields of *in situ* temperature, salinity and other variables provided at standard depth levels for annual, seasonal, and monthly compositing periods for the World Ocean. It also includes associated statistical fields of observed oceanographic profile data interpolated to standard depth levels on 5° , 1° , and 0.25° grids. We use these fields in complement to ISAS to characterize the climatological fields (annual mean and std) at the match-up pairs location and date.

2 Argo

2.1 Introduction

Argo is a global array of 3,000 free-drifting profiling floats that measures the temperature and salinity of the upper 2000 m of the ocean. This allows continuous monitoring of the temperature and salinity of the upper ocean, with all data being relayed and made publicly available within hours after collection. The array provides around 100,000 temperature/salinity profiles per year distributed over the global oceans at an average of 3-degree spacing. Only Argo salinity and temperature float data with quality index set to 1 or 2 and data mode set to real time (RT), real time adjusted (RTA) and delayed mode (DM) are considered in the Pi-MEP. Argo floats which may have problems with one or more sensors appearing in the [grey list](#) maintained at the Coriolis/GDACs are discarded. Furthermore, Pi-MEP provides an additional [list](#) of ~ 1000 "suspicious" argo salinity profiles that are also removed before analysis. The upper ocean salinity and temperature values recorded between 0m and 10m depth are considered as Argo sea surface salinities (SSS) and sea surface temperatures (SST). These data were collected and made freely available by the international Argo project and the national programs that contribute to it ([Argo \(2000\)](#)).



2.2 Number of SSS data as a function of time and distance to coast

Figure 1 shows the time (a) and distance to coast (b) distributions of the Argo *in situ* dataset.

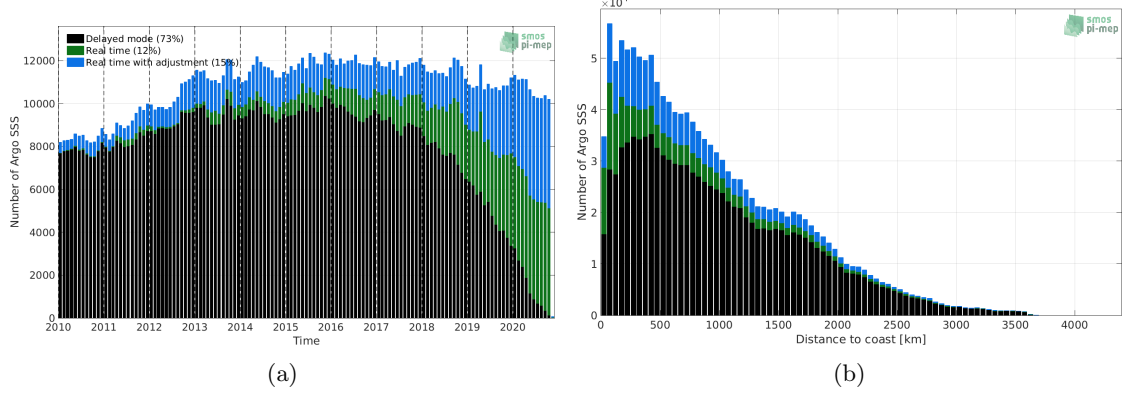


Figure 1: Number of SSS from Argo as a function of time (a) and distance to coast (b).

2.3 Histograms of SSS

Figure 2 shows the SSS distribution of the Argo (a) and colocalized ISAS (b) dataset.

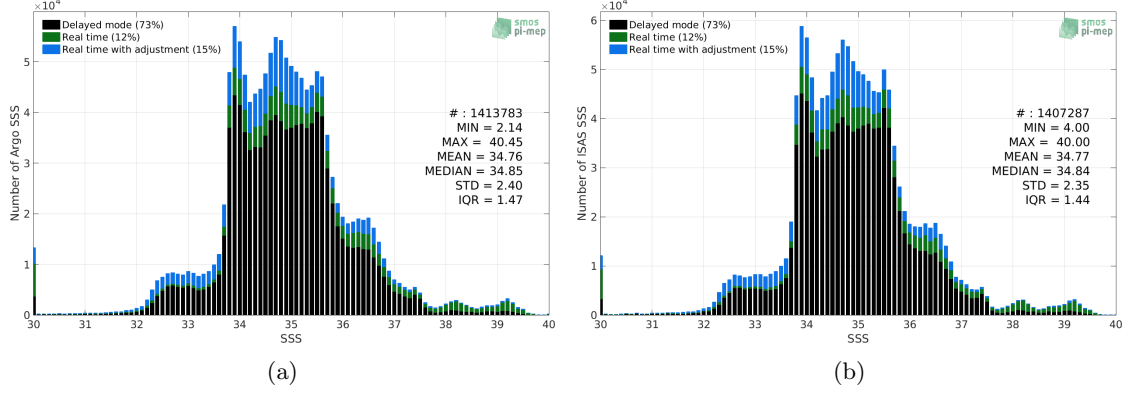


Figure 2: Histograms of SSS from Argo (a) and ISAS (b) per bins of 0.1.

2.4 Distribution of *in situ* SSS depth measurements

In Figure 3, we show the depth distribution of the *in situ* salinity dataset (a) and the spatial distribution of the depth temporal mean in $1^\circ \times 1^\circ$ boxes and considering the full *in situ* dataset period (b).

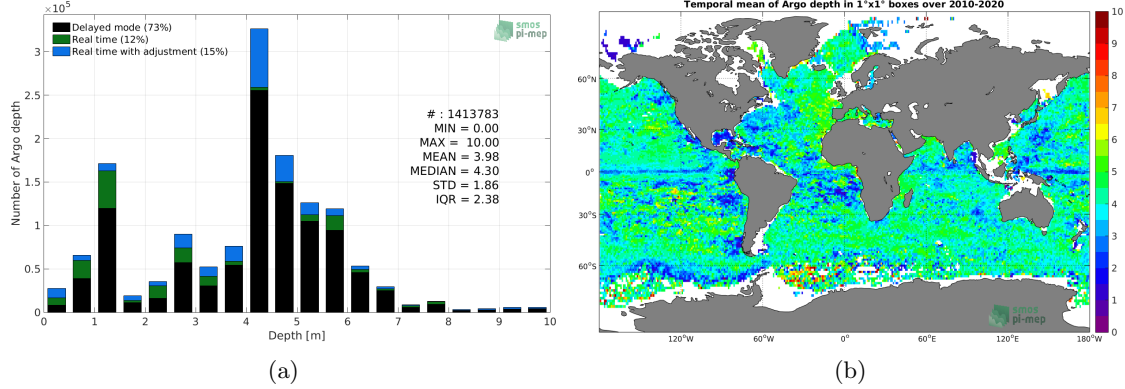


Figure 3: Depth distribution of the upper level SSS measurements from Argo (a) and spatial distribution of the *in situ* SSS depth measurements showing the mean value in $1^\circ \times 1^\circ$ boxes and considering the full *in situ* dataset period (b).

2.5 Spatial distribution of SSS

In Figure 4, the number of Argo SSS measurements in $1^\circ \times 1^\circ$ boxes is shown.

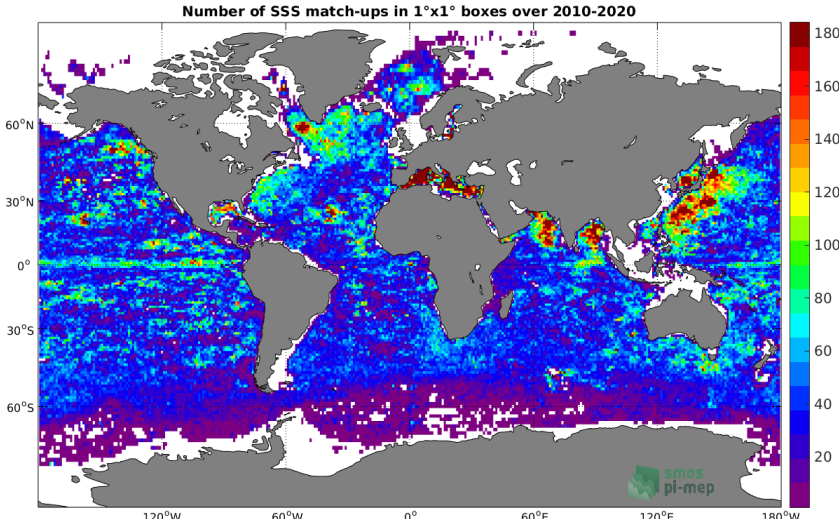


Figure 4: Number of SSS from Argo in $1^\circ \times 1^\circ$ boxes.

2.6 Spatial Maps of the Temporal mean and Std of *in situ* and ISAS SSS and of the difference (Δ SSS)

In Figure 5, we show maps of temporal mean (left) and standard deviation (right) of ISAS (top), Argo *in situ* dataset (middle) and the difference Δ SSS(ISAS - Argo) (bottom). The temporal mean and std are calculated using all match-up pairs falling in spatial boxes of size $1^\circ \times 1^\circ$ over the full Argo dataset period.

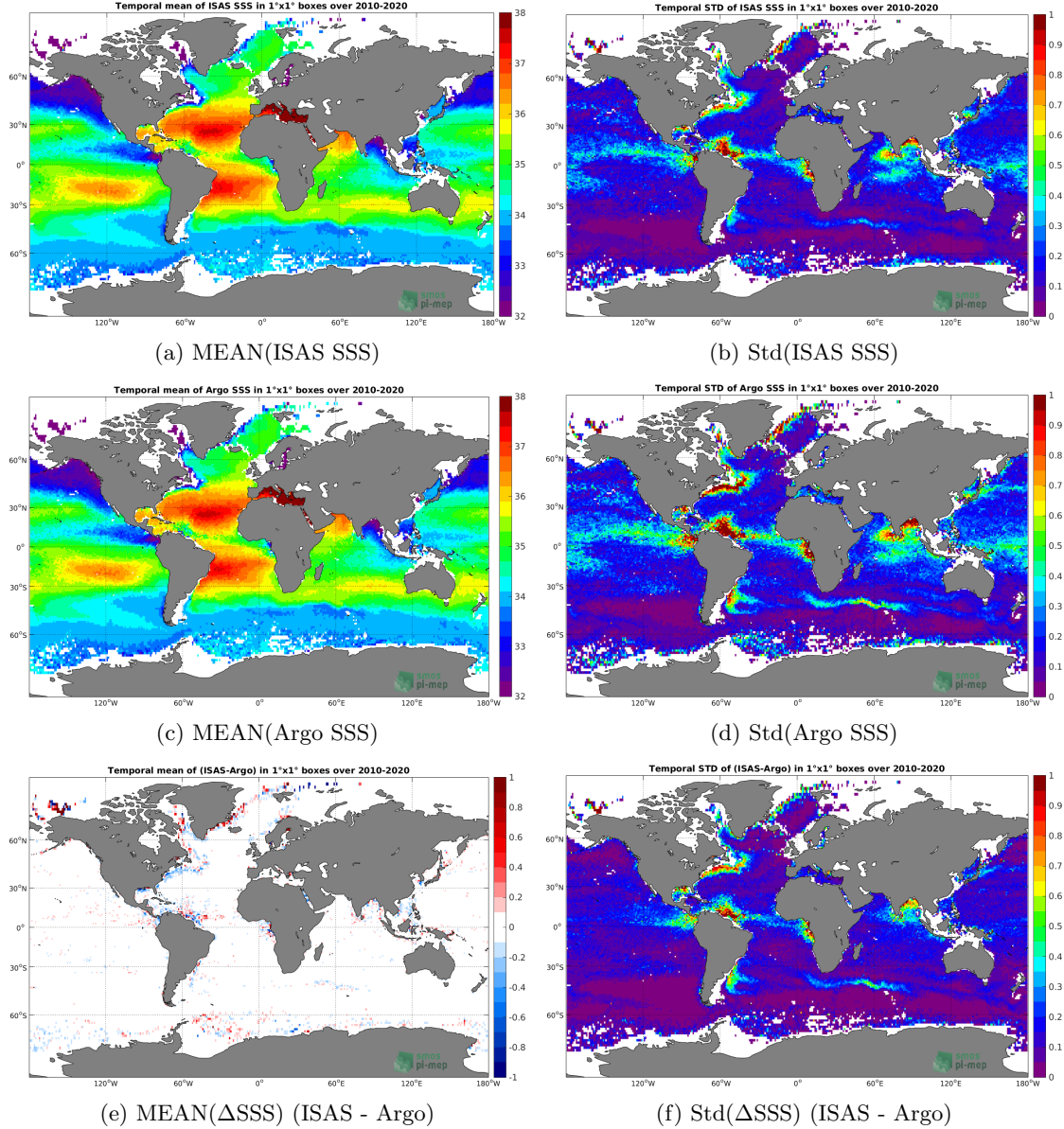


Figure 5: Temporal mean (left) and Std (right) of SSS from ISAS (top), Argo (middle), and of Δ SSS (ISAS - Argo). Only match-up pairs are used to generate these maps.

2.7 Time series of the monthly median and Std of *in situ* and ISAS SSS and of the difference (Δ SSS)

In the top panel of Figure 6, we show the time series of the monthly median SSS estimated for both ISAS SSS product (in black) and the Argo *in situ* dataset (in blue) at the collected Pi-MEP match-up pairs.

In the middle panel of Figure 6, we show the time series of the monthly median of Δ SSS (ISAS - Argo) for the collected Pi-MEP match-up pairs.

In the bottom panel of Figure 6, we show the time series of the monthly standard deviation of the Δ SSS (ISAS - Argo) for the collected Pi-MEP match-up pairs.



Figure 6: Time series of the monthly median SSS (top), median of Δ SSS (ISAS - Argo) and Std of Δ SSS (ISAS - Argo) considering all match-ups collected by the Pi-MEP.

2.8 Zonal mean and Std of *in situ* and ISAS SSS and of the difference Δ SSS

In Figure 7 left panel, we show the zonal mean SSS considering all Pi-MEP match-up pairs for both ISAS SSS product (in black) and the Argo *in situ* dataset (in blue). The full *in situ* dataset period is used to derive the mean.

In the right panel of Figure 7, we show the zonal mean of Δ SSS (ISAS - Argo) for all the collected Pi-MEP match-up pairs estimated over the full *in situ* dataset period.

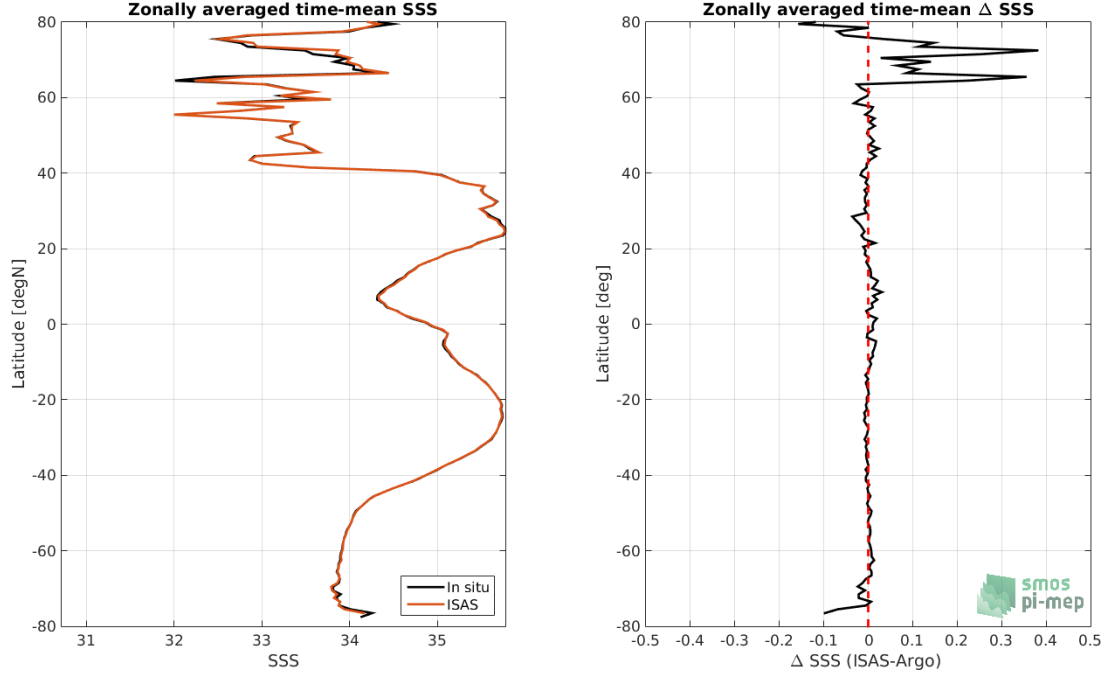


Figure 7: Left panel: Zonal mean SSS from ISAS product (black) and from Argo (blue). Right panel: Zonal mean of Δ SSS (ISAS - Argo) for all the collected Pi-MEP match-up pairs estimated over the full *in situ* dataset period.

2.9 Scatterplots of ISAS vs *in situ* SSS by latitudinal bands

In Figure 8, contour maps of the concentration of ISAS SSS (y-axis) versus Argo SSS (x-axis) at match-up pairs for different latitude bands: (a) 80°S-80°N, (b) 20°S-20°N, (c) 40°S-20°S and 20°N-40°N and (d) 60°S-40°S and 40°N-60°N. For each plot, the red line shows $x=y$. The black thin and dashed lines indicate a linear fit through the data cloud and the $\pm 95\%$ confidence levels, respectively. The number match-up pairs n , the slope and R^2 coefficient of the linear fit, the root mean square (RMS) and the mean bias between ISAS and *in situ* data are indicated for each latitude band in each plots.

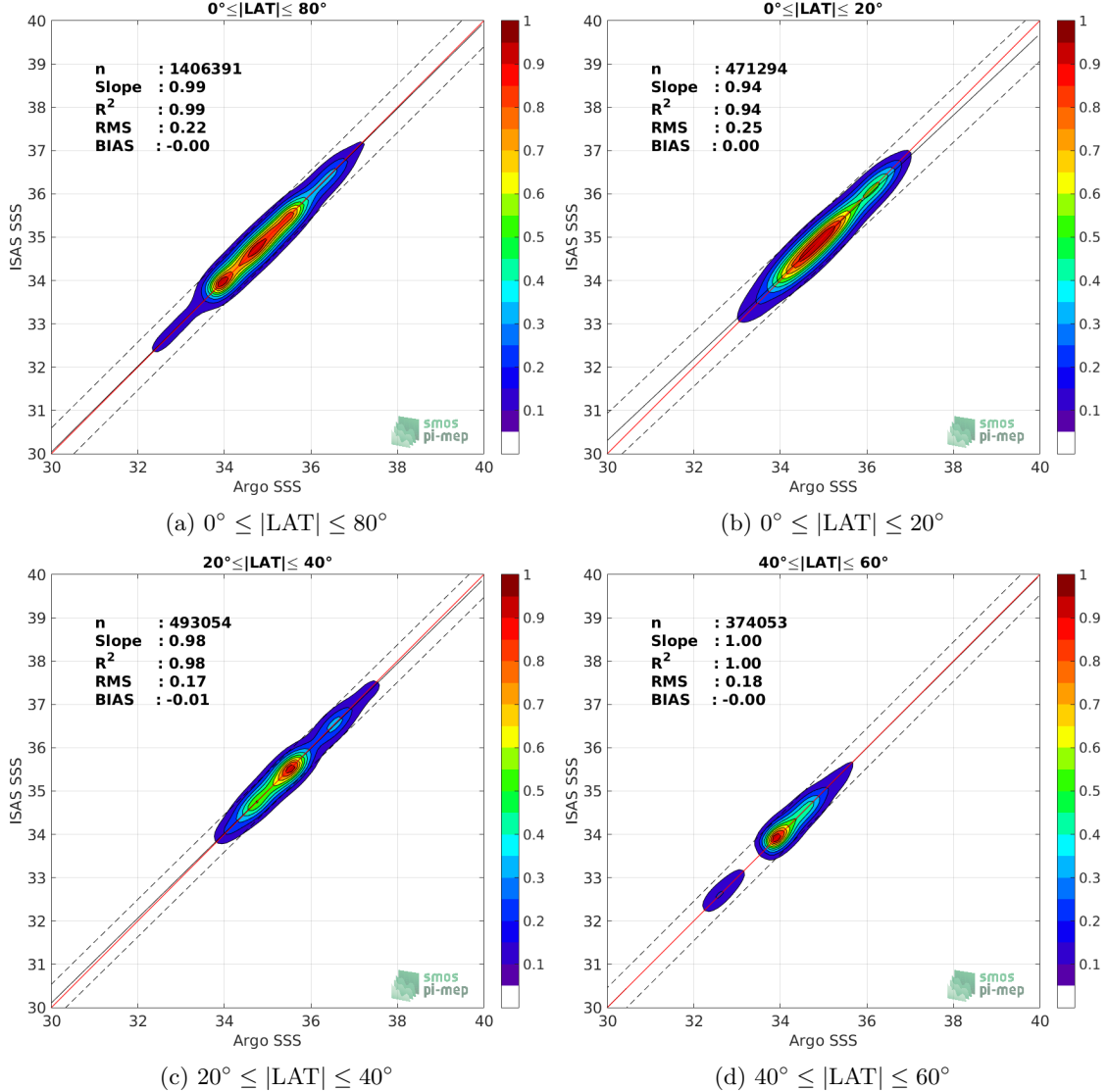


Figure 8: Contour maps of the concentration of ISAS SSS (y-axis) versus Argo SSS (x-axis) at match-up pairs for different latitude bands. For each plot, the red line shows $x=y$. The black thin and dashed lines indicate a linear fit through the data cloud and the $\pm 95\%$ confidence levels, respectively. The number match-up pairs n , the slope and R^2 coefficient of the linear fit, the root mean square (RMS) and the mean bias between ISAS and *in situ* data are indicated for each latitude band in each plots.

2.10 Time series of the monthly median and Std of the difference ΔSSS sorted by latitudinal bands

In Figure 9, time series of the monthly median (red curves) of ΔSSS (ISAS - Argo) and ± 1 Std (black vertical thick bars) as function of time for all the collected Pi-MEP match-up pairs estimated for the full *in situ* dataset period are shown for different latitude bands: (a) $80^\circ\text{S}-80^\circ\text{N}$, (b) $20^\circ\text{S}-20^\circ\text{N}$, (c) $40^\circ\text{S}-20^\circ\text{S}$ and $20^\circ\text{N}-40^\circ\text{N}$ and (d) $60^\circ\text{S}-40^\circ\text{S}$ and $40^\circ\text{N}-60^\circ\text{N}$.

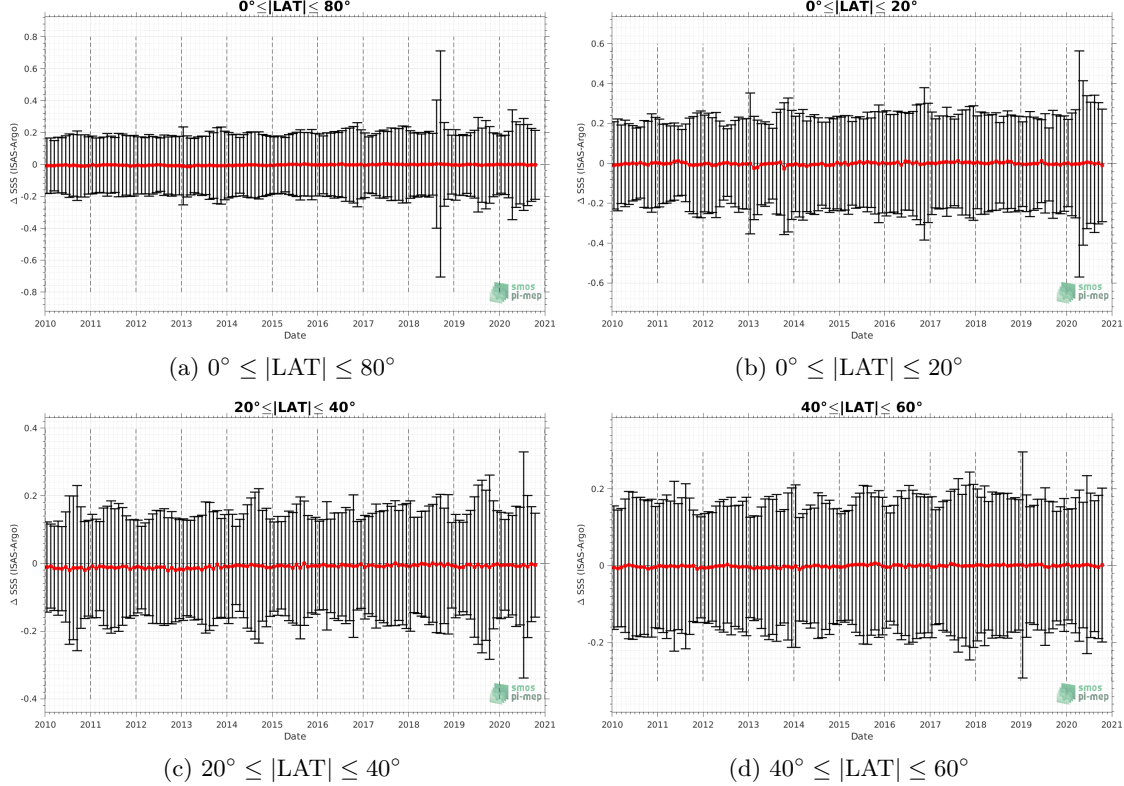


Figure 9: Monthly median (red curves) of ΔSSS (ISAS - Argo) and ± 1 Std (black vertical thick bars) as function of time for all the collected Pi-MEP match-up pairs for the full *in situ* dataset period are shown for different latitude bands: (a) $80^\circ\text{S}-80^\circ\text{N}$, (b) $20^\circ\text{S}-20^\circ\text{N}$, (c) $40^\circ\text{S}-20^\circ\text{S}$ and $20^\circ\text{N}-40^\circ\text{N}$ and (d) $60^\circ\text{S}-40^\circ\text{S}$ and $40^\circ\text{N}-60^\circ\text{N}$.

2.11 ΔSSS sorted as geophysical conditions

In Figure 10, we classify the match-up differences ΔSSS (ISAS - *in situ*) as function of the geophysical conditions at match-up points. The mean and std of ΔSSS (ISAS - Argo) is thus evaluated as function of the

- *in situ* SSS values per bins of width 0.2,
- *in situ* SST values per bins of width 1°C ,
- ASCAT daily wind values per bins of width 1 m/s,
- CMORPH 3-hourly rain rates per bins of width 1 mm/h, and,
- distance to coasts per bins of width 50 km,
- *in situ* measurement depth (if relevant).

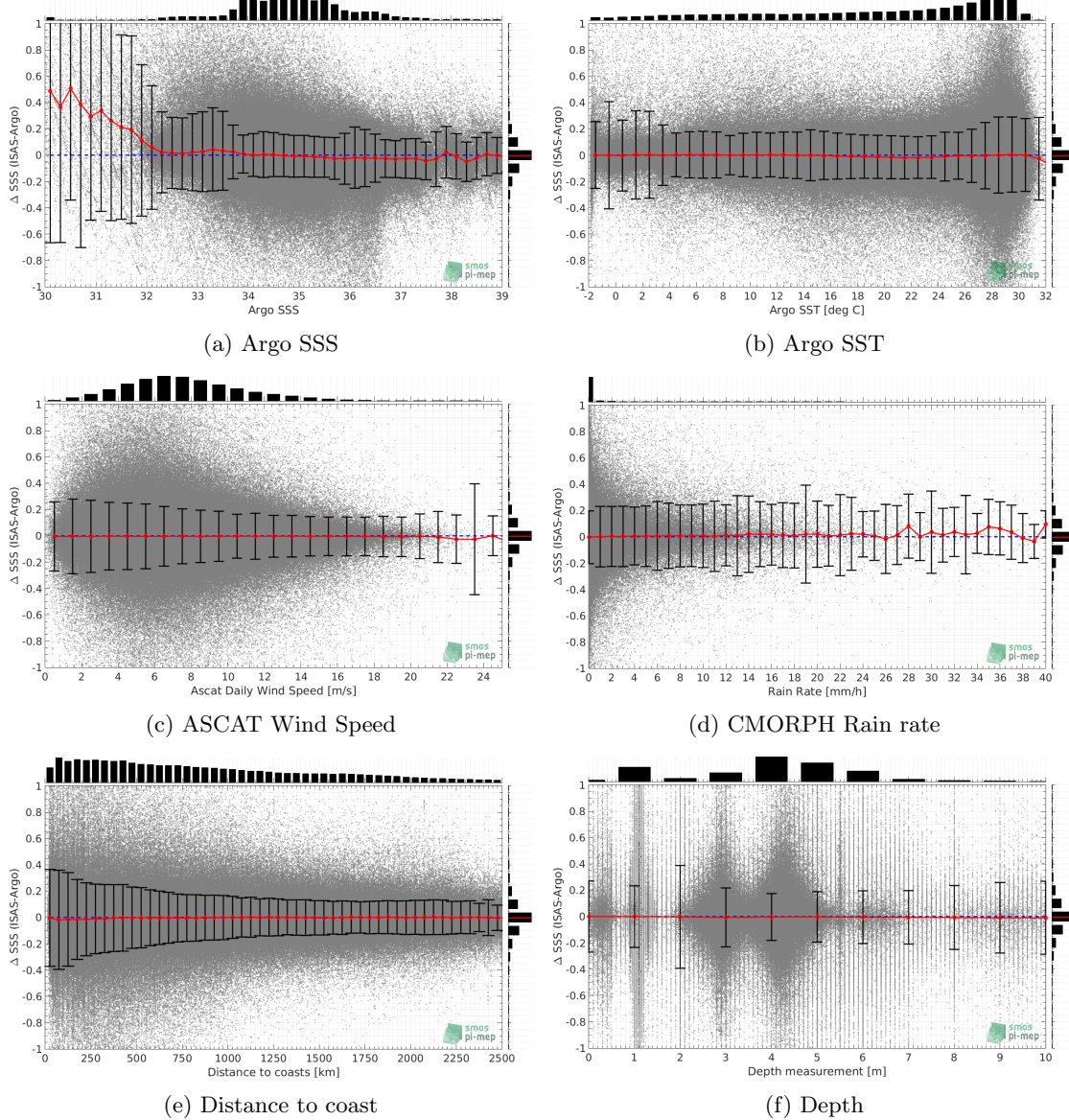


Figure 10: Δ SSS (ISAS - Argo) sorted as geophysical conditions: Argo SSS a), Argo SST b), ASCAT Wind speed c), CMORPH rain rate d), distance to coast (e) and depth measurements (f).

2.12 Δ SSS maps and statistics for different geophysical conditions

In Figures 11 and 12, we focus on sub-datasets of the match-up differences Δ SSS (*ISAS - in situ*) for the following specific geophysical conditions:

- **C1:** if the local value at *in situ* location of estimated rain rate is zero, mean daily wind is in the range [3, 12] m/s, the SST is $> 5^{\circ}\text{C}$ and distance to coast is > 800 km.
- **C2:** if the local value at *in situ* location of estimated rain rate is zero, mean daily wind is

in the range [3, 12] m/s.

- **C3:**if the local value at *in situ* location of estimated rain rate is high (ie. $> 1 \text{ mm/h}$) and mean daily wind is low (ie. $< 4 \text{ m/s}$).
- **C4:**if the mixed layer is shallow with depth $< 20\text{m}$.
- **C5:**if the *in situ* data is located where the climatological SSS standard deviation is low (ie. above < 0.2).
- **C6:**if the *in situ* data is located where the climatological SSS standard deviation is high (ie. above > 0.2).

For each of these conditions, the temporal mean (gridded over spatial boxes of size $1^\circ \times 1^\circ$) and the histogram of the difference ΔSSS (ISAS - *in situ*) are presented.

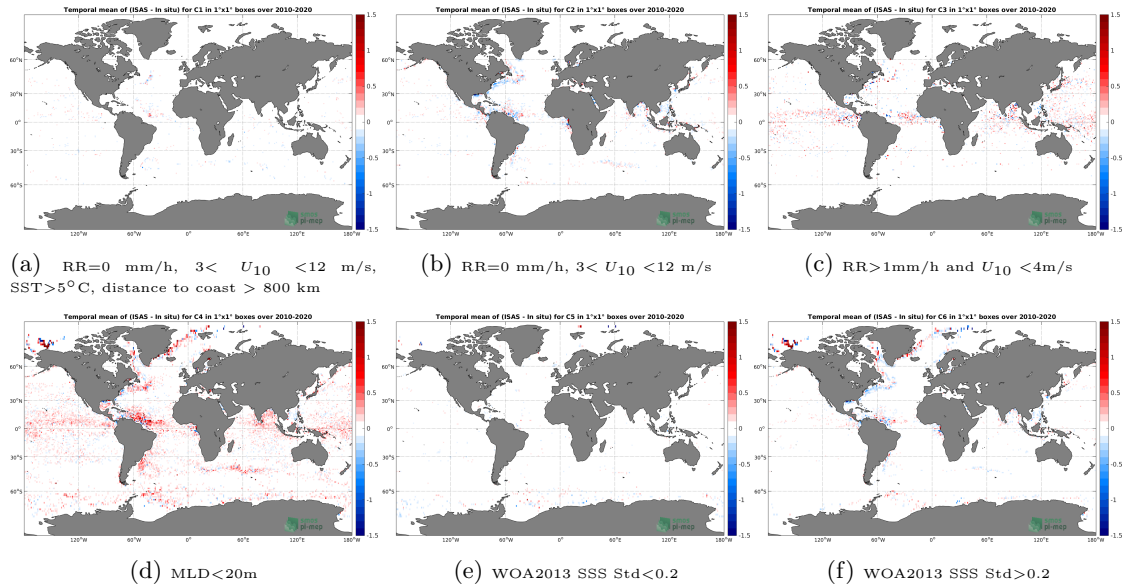


Figure 11: Temporal mean gridded over spatial boxes of size $1^\circ \times 1^\circ$ of ΔSSS (ISAS - Argo) for 6 different subdatasets corresponding to: RR = 0 mm/h, $3 < U_{10} < 12 \text{ m/s}$, SST $> 5^\circ\text{C}$, distance to coast $> 800 \text{ km}$ (a), RR = 0 mm/h, $3 < U_{10} < 12 \text{ m/s}$ (b), RR $> 1\text{mm/h}$ and $U_{10} < 4\text{m/s}$ (c), MLD $< 20\text{m}$ (d), WOA2013 SSS Std < 0.2 (e), WOA2013 SSS Std > 0.2 (f).

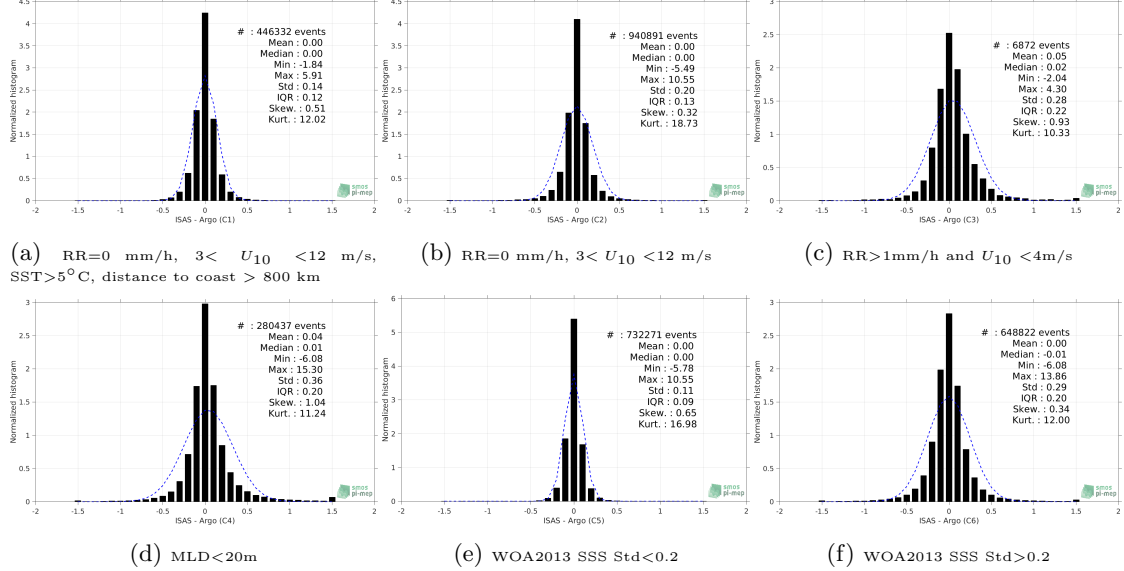


Figure 12: Normalized histogram of ΔSSS (ISAS - Argo) for 6 different subdatasets corresponding to: RR=0 mm/h, $3 < U_{10} < 12$ m/s, SST > 5°C, distance to coast > 800 km (a), RR=0 mm/h, $3 < U_{10} < 12$ m/s (b), RR > 1mm/h and $U_{10} < 4$ m/s (c), WOA2013 SSS Std < 0.2 (d), WOA2013 SSS Std > 0.2 (e).

2.13 Summary

Table 1 shows the mean, median, standard deviation (Std), root mean square (RMS), interquartile range (IQR), correlation coefficient (r^2) and robust standard deviation (Std*) of the match-up differences ΔSSS (ISAS - Argo) for the following conditions:

- all: All the match-up pairs satellite/in situ SSS are used to derive the statistics
- C1: only pairs where RR=0 mm/h, $3 < U_{10} < 12$ m/s, SST > 5°C, distance to coast > 800 km
- C2: only pairs where RR=0 mm/h, $3 < U_{10} < 12$ m/s
- C3: only pairs where RR > 1mm/h and $U_{10} < 4$ m/s
- C4: only pairs where MLD < 20m
- C5: only pairs where WOA2013 SSS Std < 0.2
- C6: only pairs where WOA2013 SSS Std > 0.2
- C7a: only pairs where distance to coast is < 150 km.
- C7b: only pairs where distance to coast is in the range [150, 800] km.
- C7c: only pairs where distance to coast is > 800 km.
- C8a: only pairs where in situ SST is < 5°C.
- C8b: only pairs where in situ SST is in the range [5, 15]°C.

- C8c: only pairs where in situ SST is $> 15^{\circ}\text{C}$.
- C9a: only pairs where in situ SSS is < 33 .
- C9b: only pairs where in situ SSS is in the range [33, 37].
- C9c: only pairs where in situ SSS is > 37 .

Table 1: Statistics of ΔSSS (ISAS - Argo)

Condition	#	Median	Mean	Std	RMS	IQR	r^2	Std*
all	1407287	0.00	0.00	0.22	0.22	0.13	0.99	0.10
C1	446332	0.00	0.00	0.14	0.14	0.12	0.98	0.09
C2	940891	0.00	0.00	0.20	0.20	0.13	0.99	0.10
C3	6872	0.02	0.05	0.28	0.28	0.22	0.98	0.16
C4	280437	0.01	0.04	0.36	0.36	0.20	0.99	0.15
C5	732271	0.00	0.00	0.11	0.11	0.09	0.99	0.07
C6	648822	-0.01	0.00	0.29	0.29	0.20	0.99	0.15
C7a	139430	-0.01	0.00	0.37	0.37	0.17	1.00	0.13
C7b	590494	-0.01	-0.01	0.24	0.24	0.13	0.97	0.10
C7c	676193	0.00	0.00	0.14	0.14	0.12	0.98	0.09
C8a	128929	0.00	0.01	0.28	0.28	0.06	0.99	0.05
C8b	298160	0.00	0.01	0.17	0.17	0.09	1.00	0.07
C8c	979624	-0.01	0.00	0.22	0.22	0.15	0.99	0.12
C9a	82872	0.02	0.12	0.54	0.55	0.17	0.99	0.11
C9b	1253244	0.00	-0.01	0.18	0.18	0.13	0.96	0.09
C9c	71171	-0.03	-0.03	0.15	0.15	0.14	0.96	0.10

Table 1 numerical values can be downloaded as a csv file [here](#).

3 TSG

The TSG dataset is subdivided into 8 subdatasets following TSG data providers subdivisions.

- [LEGOS-DM](#)
- [GOSUD-Research-vessel](#)
- [GOSUD-Sailing-ship](#)
- [SAMOS](#)
- [LEGOS-Survostral](#)
- [LEGOS-Survostral-Adélie](#)
- [Polarstern](#)
- [NCEI-0170743](#)

3.1 TSG (LEGOS-DM)

3.1.1 Introduction

The TSG-LEGOS-DM dataset correspond to sea surface salinity delayed mode data derived from voluntary observing ships collected, validated, archived, and made freely available by the French Sea Surface Salinity Observation Service (Alory et al. (2015)). Adjusted values when available and only collected TSG data that exhibit quality flags=1 and 2 were used.

3.1.2 Number of SSS data as a function of time and distance to coast

Figure 13 shows the time (a) and distance to coast (b) distributions of the TSG (LEGOS-DM) *in situ* dataset.

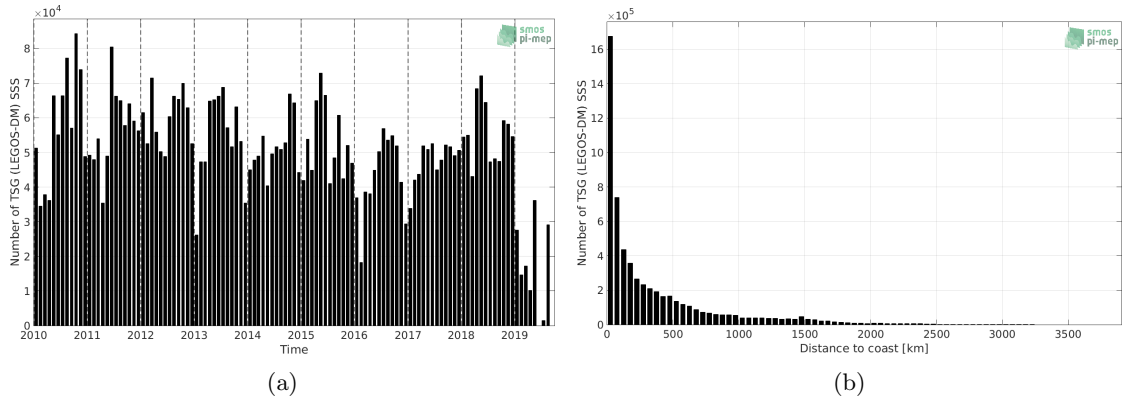


Figure 13: Number of SSS from TSG (LEGOS-DM) as a function of time (a) and distance to coast (b).

3.1.3 Histograms of SSS

Figure 14 shows the SSS distribution of the TSG (LEGOS-DM) (a) and colocalized ISAS (b) dataset.

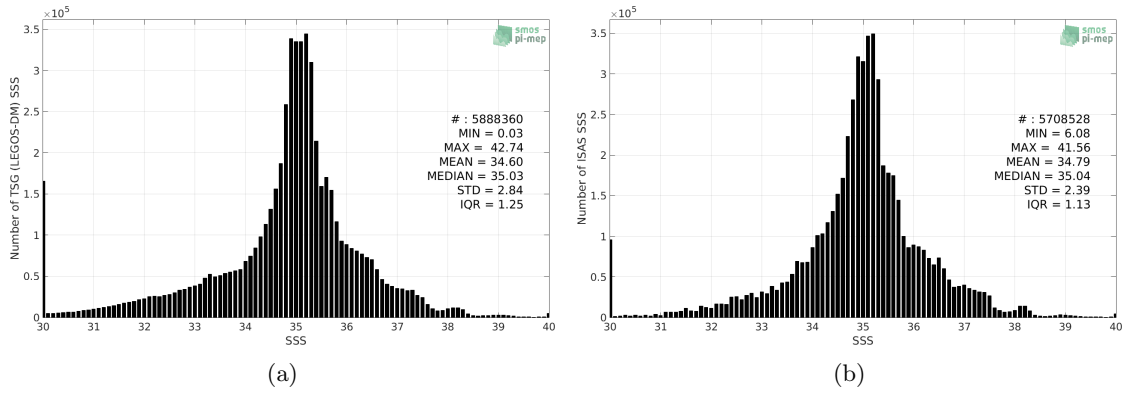


Figure 14: Histograms of SSS from TSG (LEGOS-DM) (a) and ISAS (b) per bins of 0.1.

3.1.4 Distribution of *in situ* SSS depth measurements

In Figure 15, we show the depth distribution of the *in situ* salinity dataset (a) and the spatial distribution of the depth temporal mean in $1^\circ \times 1^\circ$ boxes and considering the full *in situ* dataset period (b).

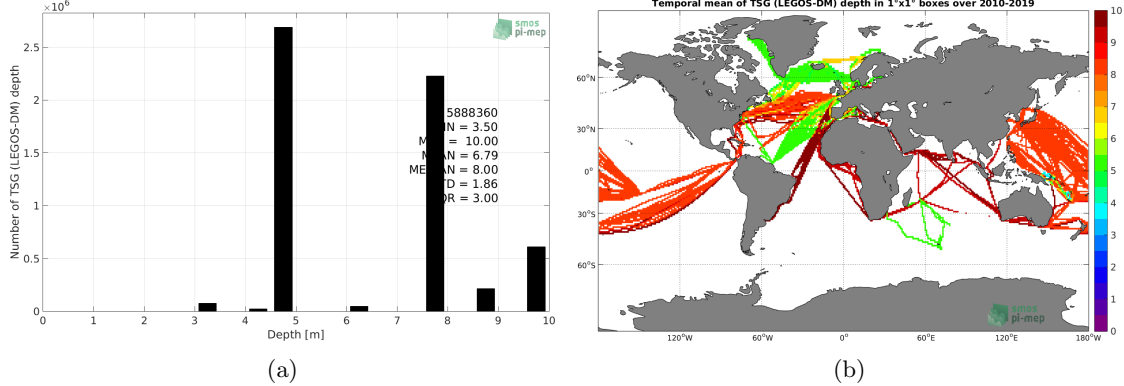


Figure 15: Depth distribution of the upper level SSS measurements from TSG (LEGOS-DM) (a) and spatial distribution of the *in situ* SSS depth measurements showing the mean value in $1^\circ \times 1^\circ$ boxes and considering the full *in situ* dataset period (b).

3.1.5 Spatial distribution of SSS

In Figure 16, the number of TSG (LEGOS-DM) SSS measurements in $1^\circ \times 1^\circ$ boxes is shown.

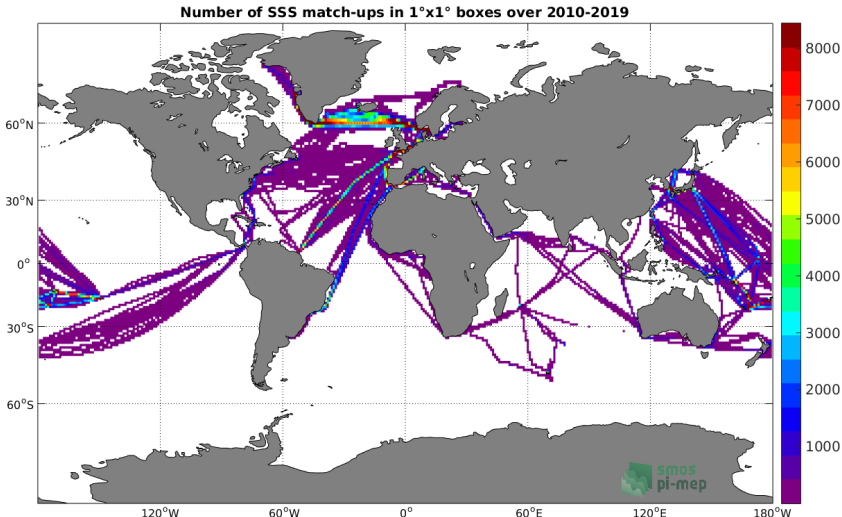


Figure 16: Number of SSS from TSG (LEGOS-DM) in $1^\circ \times 1^\circ$ boxes.

3.1.6 Spatial Maps of the Temporal mean and Std of *in situ* and ISAS SSS and of the difference (Δ SSS)

In Figure 17, we show maps of temporal mean (left) and standard deviation (right) of ISAS (top), TSG (LEGOS-DM) *in situ* dataset (middle) and the difference Δ SSS(ISAS -TSG (LEGOS-DM))

(bottom). The temporal mean and std are calculated using all match-up pairs falling in spatial boxes of size $1^\circ \times 1^\circ$ over the full TSG (LEGOS-DM) dataset period.

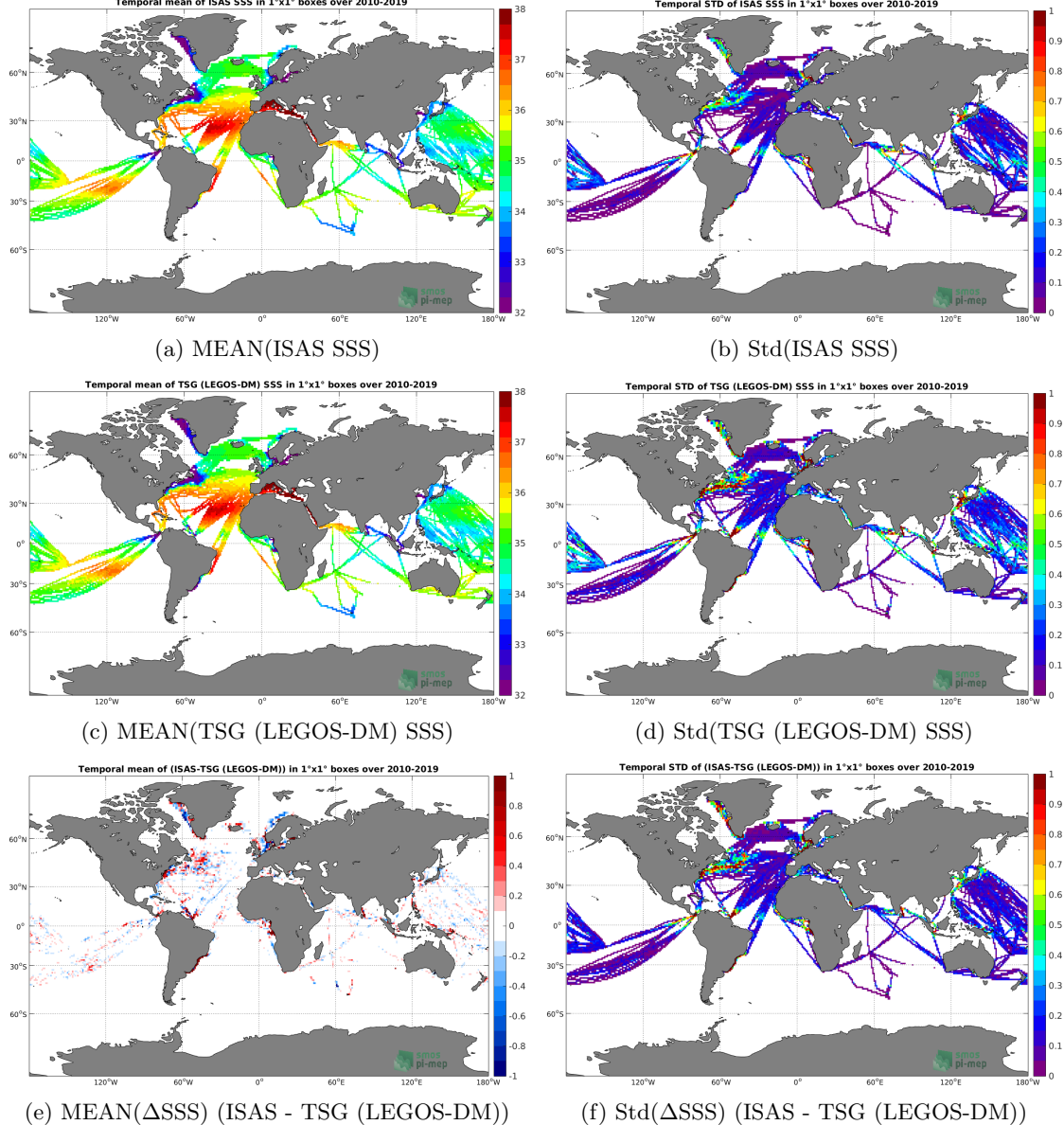


Figure 17: Temporal mean (left) and Std (right) of SSS from ISAS (top), TSG (LEGOS-DM) (middle), and of Δ SSS (ISAS - TSG (LEGOS-DM)). Only match-up pairs are used to generate these maps.

3.1.7 Time series of the monthly median and Std of *in situ* and ISAS SSS and of the difference (Δ SSS)

In the top panel of Figure 18, we show the time series of the monthly median SSS estimated for both ISAS SSS product (in black) and the TSG (LEGOS-DM) *in situ* dataset (in blue) at the

collected Pi-MEP match-up pairs.

In the middle panel of Figure 18, we show the time series of the monthly median of ΔSSS (ISAS - TSG (LEGOS-DM)) for the collected Pi-MEP match-up pairs.

In the bottom panel of Figure 18, we show the time series of the monthly standard deviation of the ΔSSS (ISAS - TSG (LEGOS-DM)) for the collected Pi-MEP match-up pairs.

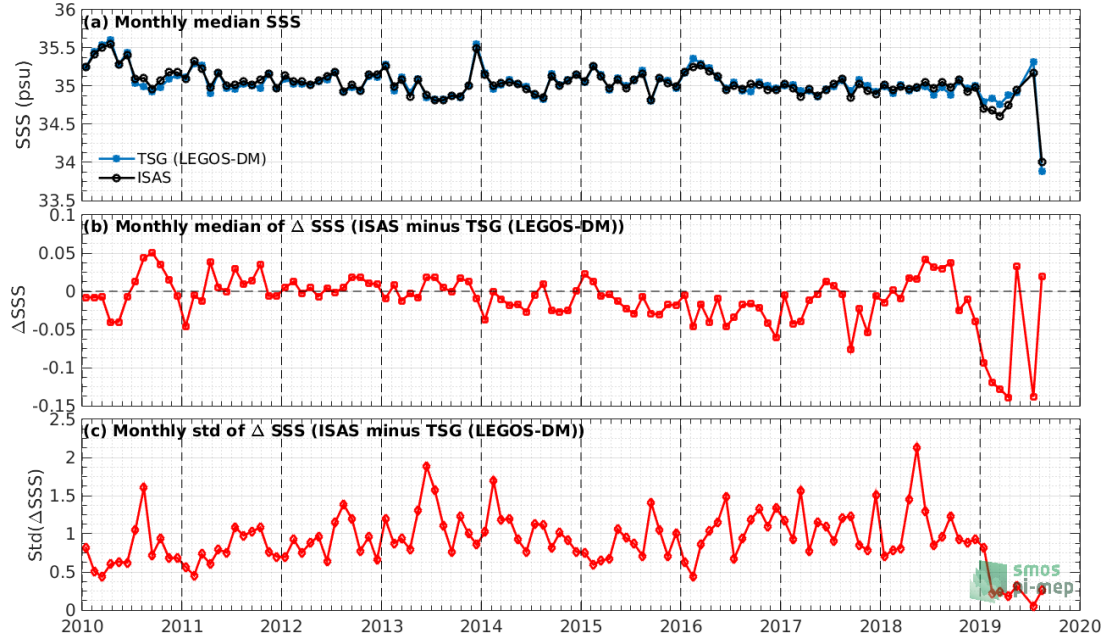


Figure 18: Time series of the monthly median SSS (top), median of ΔSSS (ISAS - TSG (LEGOS-DM)) and Std of ΔSSS (ISAS - TSG (LEGOS-DM)) considering all match-ups collected by the Pi-MEP.

3.1.8 Zonal mean and Std of *in situ* and ISAS SSS and of the difference ΔSSS

In Figure 19 left panel, we show the zonal mean SSS considering all Pi-MEP match-up pairs for both ISAS SSS product (in black) and the TSG (LEGOS-DM) *in situ* dataset (in blue). The full *in situ* dataset period is used to derive the mean.

In the right panel of Figure 19, we show the zonal mean of ΔSSS (ISAS - TSG (LEGOS-DM)) for all the collected Pi-MEP match-up pairs estimated over the full *in situ* dataset period.

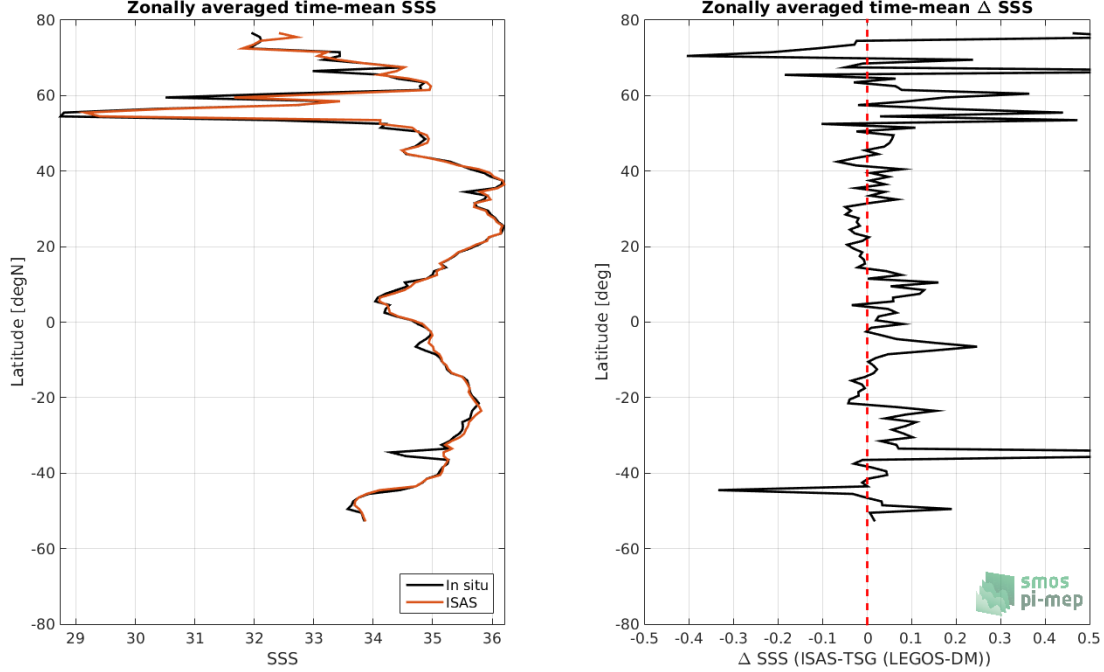


Figure 19: Left panel: Zonal mean SSS from ISAS product (black) and from TSG (LEGOS-DM) (blue). Right panel: Zonal mean of Δ SSS (ISAS - TSG (LEGOS-DM)) for all the collected Pi-MEP match-up pairs estimated over the full *in situ* dataset period.

3.1.9 Scatterplots of ISAS vs *in situ* SSS by latitudinal bands

In Figure 20, contour maps of the concentration of ISAS SSS (y-axis) versus TSG (LEGOS-DM) SSS (x-axis) at match-up pairs for different latitude bands: (a) 80°S-80°N, (b) 20°S-20°N, (c) 40°S-20°S and 20°N-40°N and (d) 60°S-40°S and 40°N-60°N. For each plot, the red line shows $x=y$. The black thin and dashed lines indicate a linear fit through the data cloud and the $\pm 95\%$ confidence levels, respectively. The number match-up pairs n , the slope and R^2 coefficient of the linear fit, the root mean square (RMS) and the mean bias between ISAS and *in situ* data are indicated for each latitude band in each plots.

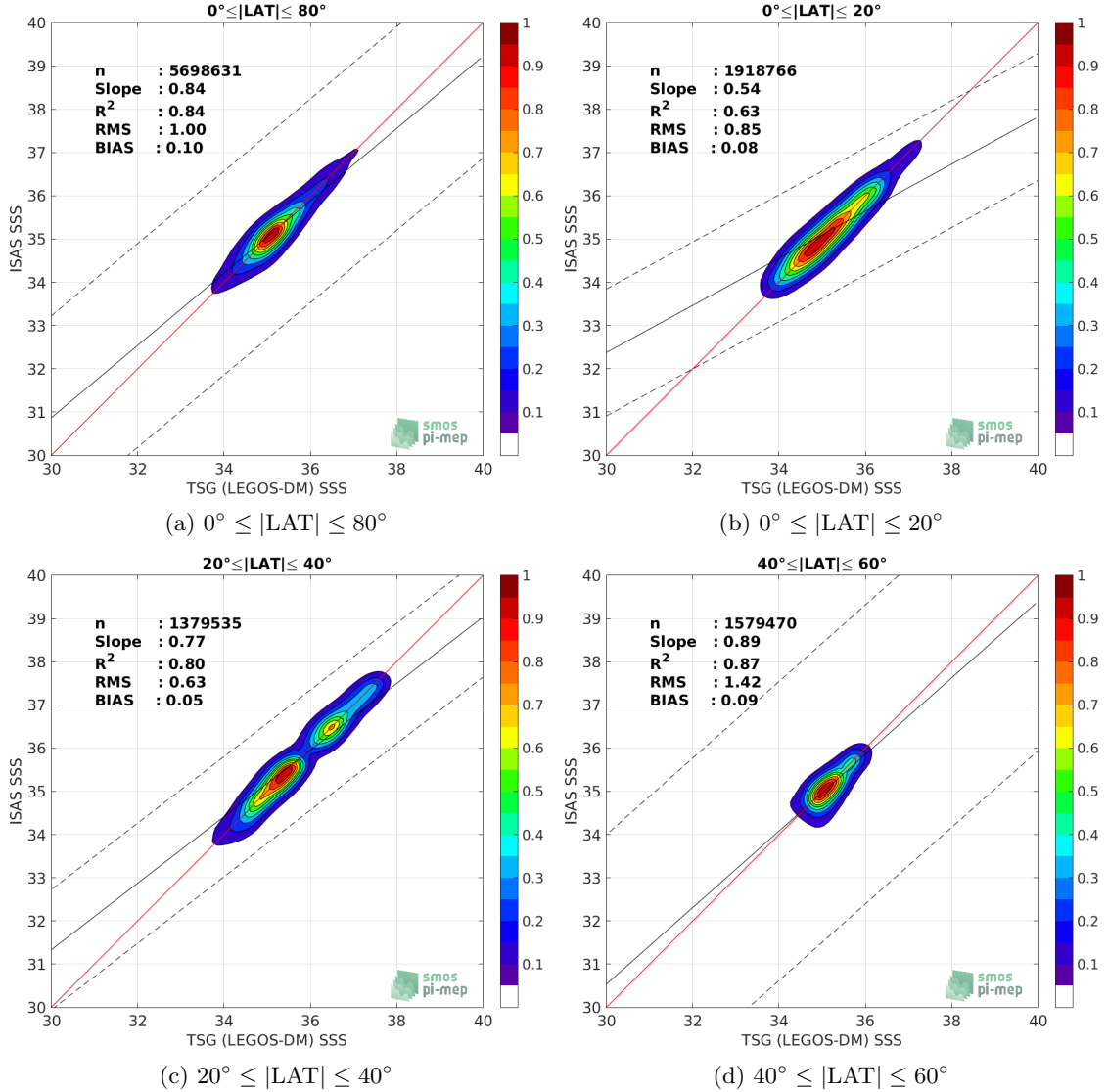


Figure 20: Contour maps of the concentration of ISAS SSS (y-axis) versus TSG (LEGOS-DM) SSS (x-axis) at match-up pairs for different latitude bands. For each plot, the red line shows $y=x$. The black thin and dashed lines indicate a linear fit through the data cloud and the $\pm 95\%$ confidence levels, respectively. The number match-up pairs n , the slope and R^2 coefficient of the linear fit, the root mean square (RMS) and the mean bias between ISAS and *in situ* data are indicated for each latitude band in each plots.

3.1.10 Time series of the monthly median and Std of the difference ΔSSS sorted by latitudinal bands

In Figure 21, time series of the monthly median (red curves) of ΔSSS (ISAS - TSG (LEGOS-DM)) and ± 1 Std (black vertical thick bars) as function of time for all the collected Pi-MEP match-up pairs estimated for the full *in situ* dataset period are shown for different latitude bands: (a) $80^\circ\text{S}-80^\circ\text{N}$, (b) $20^\circ\text{S}-20^\circ\text{N}$, (c) $40^\circ\text{S}-20^\circ\text{N}$ and $20^\circ\text{N}-40^\circ\text{N}$ and (d) $60^\circ\text{S}-40^\circ\text{S}$ and $40^\circ\text{N}-60^\circ\text{N}$.

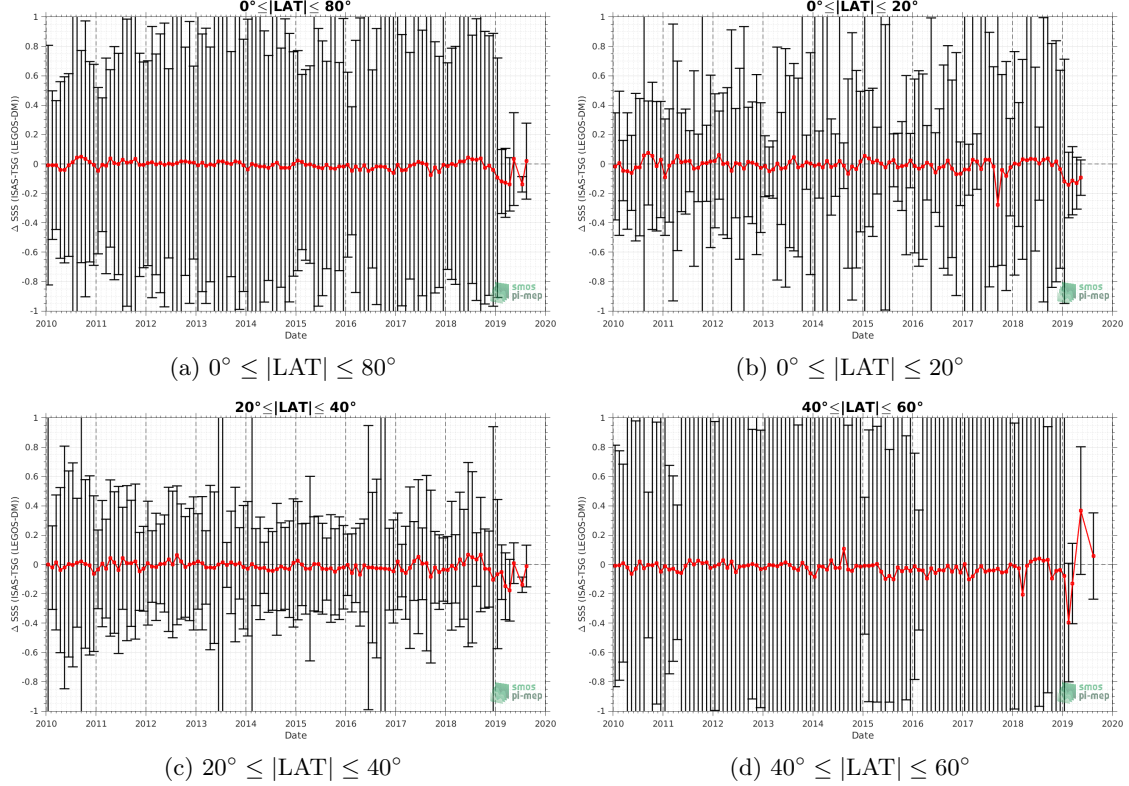


Figure 21: Monthly median (red curves) of ΔSSS (ISAS - TSG (LEGOS-DM)) and ± 1 Std (black vertical thick bars) as function of time for all the collected Pi-MEP match-up pairs for the full *in situ* dataset period are shown for different latitude bands: (a) $80^\circ\text{S}-80^\circ\text{N}$, (b) $20^\circ\text{S}-20^\circ\text{N}$, (c) $40^\circ\text{S}-20^\circ\text{S}$ and $20^\circ\text{N}-40^\circ\text{N}$ and (d) $60^\circ\text{S}-40^\circ\text{S}$ and $40^\circ\text{N}-60^\circ\text{N}$.

3.1.11 ΔSSS sorted as geophysical conditions

In Figure 22, we classify the match-up differences ΔSSS (ISAS - *in situ*) as function of the geophysical conditions at match-up points. The mean and std of ΔSSS (ISAS - TSG (LEGOS-DM)) is thus evaluated as function of the

- *in situ* SSS values per bins of width 0.2,
- *in situ* SST values per bins of width 1°C ,
- ASCAT daily wind values per bins of width 1 m/s,
- CMORPH 3-hourly rain rates per bins of width 1 mm/h, and,
- distance to coasts per bins of width 50 km,
- *in situ* measurement depth (if relevant).

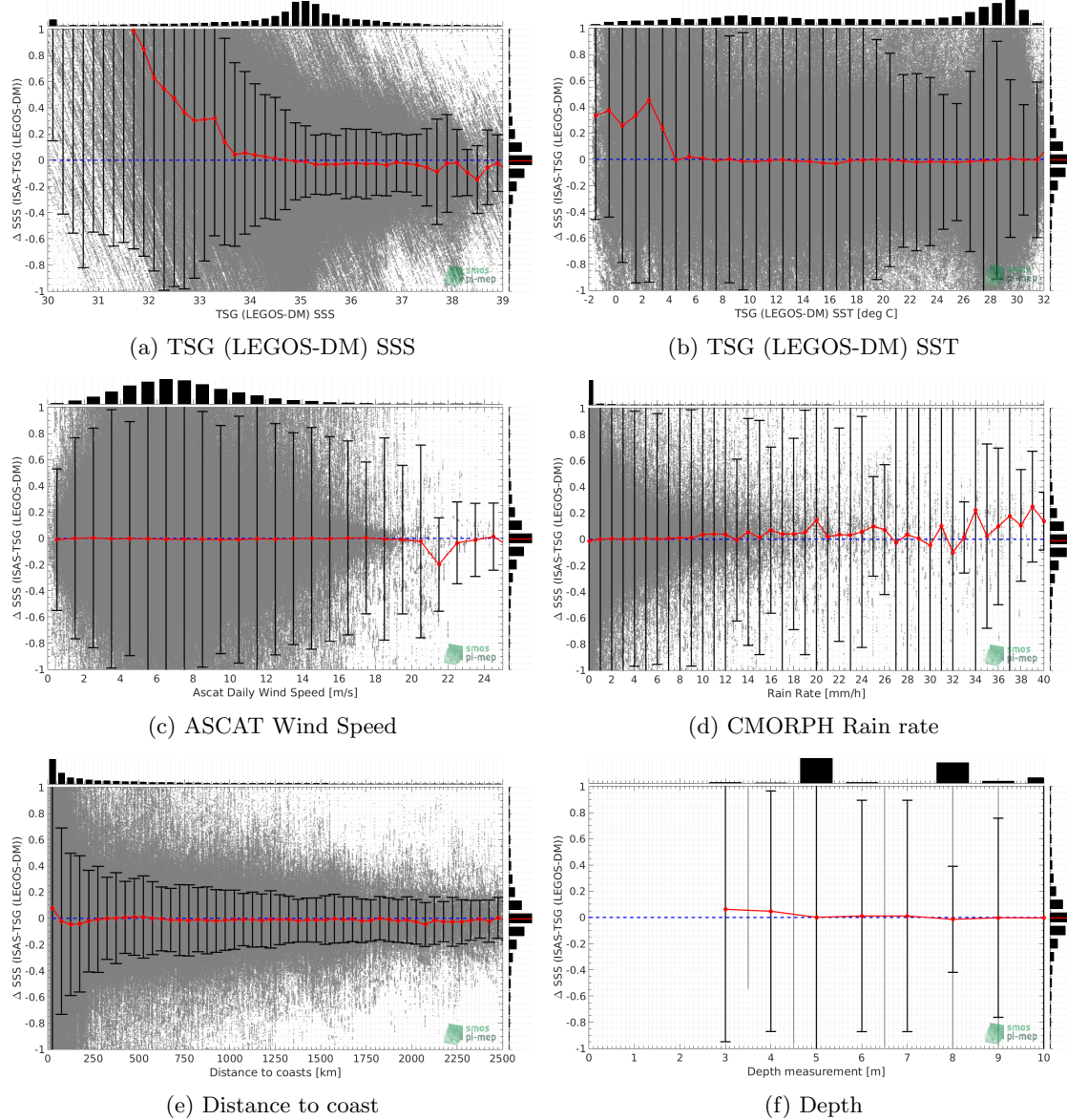


Figure 22: Δ SSS (ISAS - TSG (LEGOS-DM)) sorted as geophysical conditions: TSG (LEGOS-DM) SSS a), TSG (LEGOS-DM) SST b), ASCAT Wind speed c), CMORPH rain rate d), distance to coast (e) and depth measurements (f).

3.1.12 Δ SSS maps and statistics for different geophysical conditions

In Figures 23 and 24, we focus on sub-datasets of the match-up differences Δ SSS (*ISAS - in situ*) for the following specific geophysical conditions:

- **C1:** if the local value at *in situ* location of estimated rain rate is zero, mean daily wind is in the range [3, 12] m/s, the SST is $> 5^{\circ}\text{C}$ and distance to coast is > 800 km.
- **C2:** if the local value at *in situ* location of estimated rain rate is zero, mean daily wind is

in the range [3, 12] m/s.

- **C3:** if the local value at *in situ* location of estimated rain rate is high (ie. $> 1 \text{ mm/h}$) and mean daily wind is low (ie. $< 4 \text{ m/s}$).
- **C5:** if the *in situ* data is located where the climatological SSS standard deviation is low (ie. above < 0.2).
- **C6:** if the *in situ* data is located where the climatological SSS standard deviation is high (ie. above > 0.2).

For each of these conditions, the temporal mean (gridded over spatial boxes of size $1^\circ \times 1^\circ$) and the histogram of the difference ΔSSS (ISAS - *in situ*) are presented.

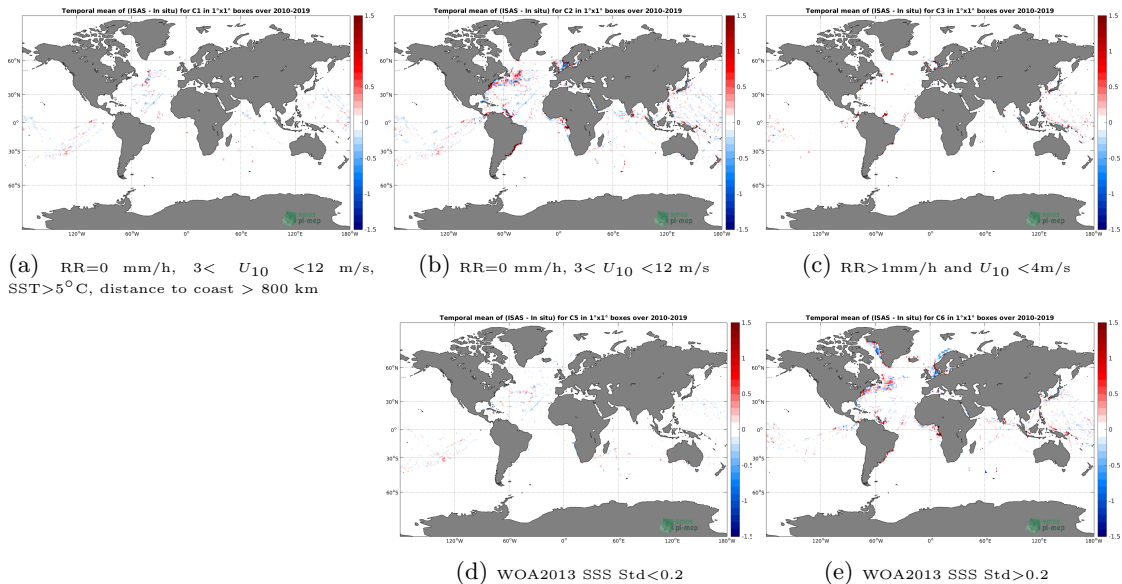


Figure 23: Temporal mean gridded over spatial boxes of size $1^\circ \times 1^\circ$ of ΔSSS (ISAS - TSG (LEGOS-DM)) for 5 different subdatasets corresponding to: $\text{RR}=0 \text{ mm/h}$, $3 < U_{10} < 12 \text{ m/s}$, $\text{SST} > 5^\circ\text{C}$, distance to coast $> 800 \text{ km}$ (a), $\text{RR}=0 \text{ mm/h}$, $3 < U_{10} < 12 \text{ m/s}$ (b), $\text{RR} > 1 \text{ mm/h}$ and $U_{10} < 4 \text{ m/s}$ (c), WOA2013 SSS Std < 0.2 (d), WOA2013 SSS Std > 0.2 (e).

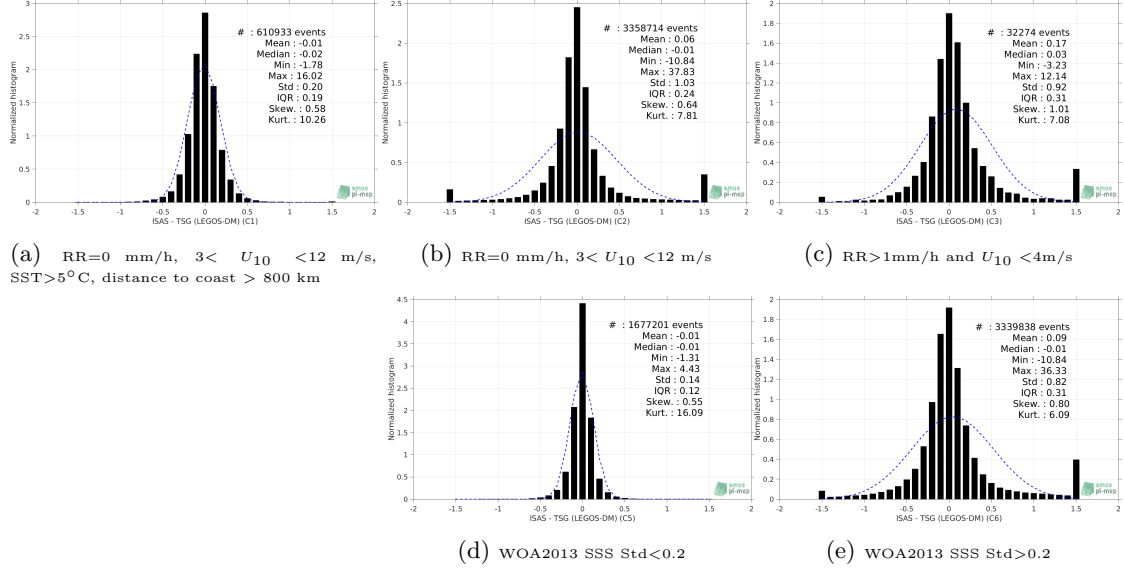


Figure 24: Normalized histogram of ΔSSS (ISAS - TSG (LEGOS-DM)) for 5 different subdatasets corresponding to: RR=0 mm/h, $3 < U_{10} < 12$ m/s, SST > 5°C, distance to coast > 800 km (a), RR=0 mm/h, $3 < U_{10} < 12$ m/s (b), RR > 1 mm/h and $U_{10} < 4$ m/s (c), WOA2013 SSS Std < 0.2 (d), WOA2013 SSS Std > 0.2 (e).

3.1.13 Summary

Table 1 shows the mean, median, standard deviation (Std), root mean square (RMS), interquartile range (IQR), correlation coefficient (r^2) and robust standard deviation (Std*) of the match-up differences ΔSSS (ISAS - TSG (LEGOS-DM)) for the following conditions:

- all: All the match-up pairs satellite/in situ SSS values are used to derive the statistics
- C1: only pairs where RR=0 mm/h, $3 < U_{10} < 12$ m/s, SST > 5°C, distance to coast > 800 km
- C2: only pairs where RR=0 mm/h, $3 < U_{10} < 12$ m/s
- C3: only pairs where RR > 1 mm/h and $U_{10} < 4$ m/s
- C5: only pairs where WOA2013 SSS Std < 0.2
- C6: only pairs where WOA2013 SSS Std > 0.2
- C7a: only pairs with a distance to coast < 150 km.
- C7b: only pairs with a distance to coast in the range [150, 800] km.
- C7c: only pairs with a distance to coast > 800 km.
- C8a: only pairs where SST is < 5°C.
- C8b: only pairs where SST is in the range [5, 15]°C.
- C8c: only pairs where SST is > 15°C.

- C9a: only pairs where SSS is < 33 .
- C9b: only pairs where SSS is in the range [33, 37].
- C9c: only pairs where SSS is > 37 .

Table 1: Statistics of Δ SSS (ISAS - TSG (LEGOS-DM))

Condition	#	Median	Mean	Std	RMS	IQR	r^2	Std*
all	5708528	0.00	0.10	1.03	1.03	0.25	0.85	0.18
C1	610933	-0.02	-0.01	0.20	0.20	0.19	0.96	0.14
C2	3358714	-0.01	0.06	1.03	1.03	0.24	0.85	0.18
C3	32274	0.03	0.17	0.92	0.93	0.31	0.80	0.23
C5	1677201	-0.01	-0.01	0.14	0.14	0.12	0.97	0.09
C6	3339838	-0.01	0.09	0.82	0.83	0.31	0.86	0.23
C7a	2671981	0.01	0.22	1.45	1.47	0.47	0.84	0.33
C7b	2180135	-0.01	0.00	0.37	0.37	0.15	0.84	0.11
C7c	851844	-0.01	-0.01	0.20	0.20	0.19	0.95	0.15
C8a	508558	0.17	0.48	1.27	1.36	1.04	0.73	0.68
C8b	1599329	-0.01	0.05	1.21	1.21	0.19	0.88	0.14
C8c	3600641	-0.01	0.07	0.88	0.88	0.24	0.81	0.18
C9a	577040	0.98	1.27	2.76	3.04	2.14	0.78	1.55
C9b	4839794	-0.01	-0.03	0.39	0.39	0.21	0.79	0.16
C9c	291694	-0.05	-0.07	0.29	0.30	0.22	0.83	0.16

Table 1 numerical values can be downloaded as a csv file [here](#).

3.2 TSG (GOSUD-Research-vessel)

3.2.1 Introduction

The TSG-GOSUD-Research-vessel dataset correspond to French research vessels that have been collecting thermo-salinometer (TSG) data since the early 2000 in contribution to the [GOSUD](#) program. The set of homogeneous instruments is permanently monitored and regularly calibrated. Water samples are taken on a daily basis by the crew and later analysed in the laboratory. The careful calibration and instrument maintenance, complemented with a rigorous adjustment on water samples lead to reach an accuracy of a few 10^{-2} PSS in salinity. This delayed mode dataset ([Kolodziejczyk et al. \(2015a\)](#)) is updated annually and freely available [here](#). Adjusted values when available and only collected TSG data that exhibit quality flags 1 or 2 were used.

3.2.2 Number of SSS data as a function of time and distance to coast

Figure 25 shows the time (a) and distance to coast (b) distributions of the TSG (GOSUD-Research-vessel) *in situ* dataset.

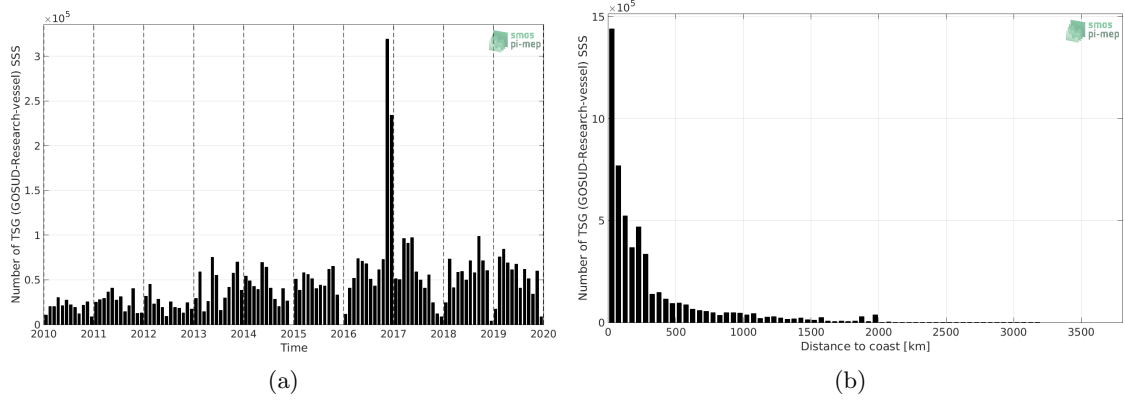


Figure 25: Number of SSS from TSG (GOSUD-Research-vessel) as a function of time (a) and distance to coast (b).

3.2.3 Histograms of SSS

Figure 26 shows the SSS distribution of the TSG (GOSUD-Research-vessel) (a) and colocalized ISAS (b) dataset.

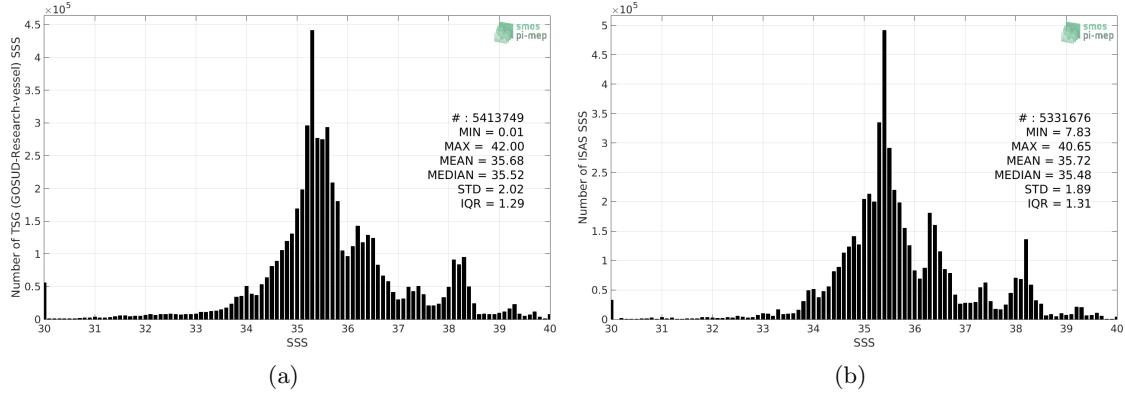


Figure 26: Histograms of SSS from TSG (GOSUD-Research-vessel) (a) and ISAS (b) per bins of 0.1.

3.2.4 Distribution of *in situ* SSS depth measurements

In Figure 27, we show the depth distribution of the *in situ* salinity dataset (a) and the spatial distribution of the depth temporal mean in $1^\circ \times 1^\circ$ boxes and considering the full *in situ* dataset period (b).

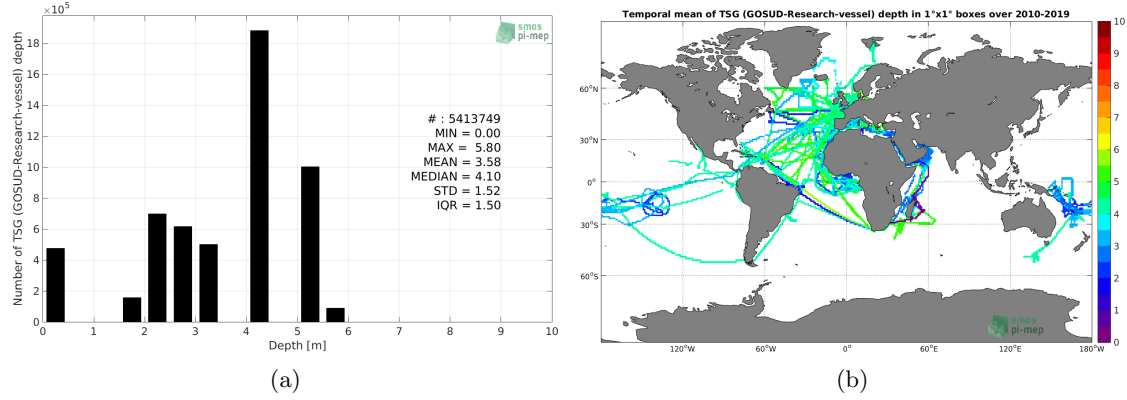


Figure 27: Depth distribution of the upper level SSS measurements from TSG (GOSUD-Research-vessel) (a) and spatial distribution of the *in situ* SSS depth measurements showing the mean value in $1^\circ \times 1^\circ$ boxes and considering the full *in situ* dataset period (b).

3.2.5 Spatial distribution of SSS

In Figure 28, the number of TSG (GOSUD-Research-vessel) SSS measurements in $1^\circ \times 1^\circ$ boxes is shown.

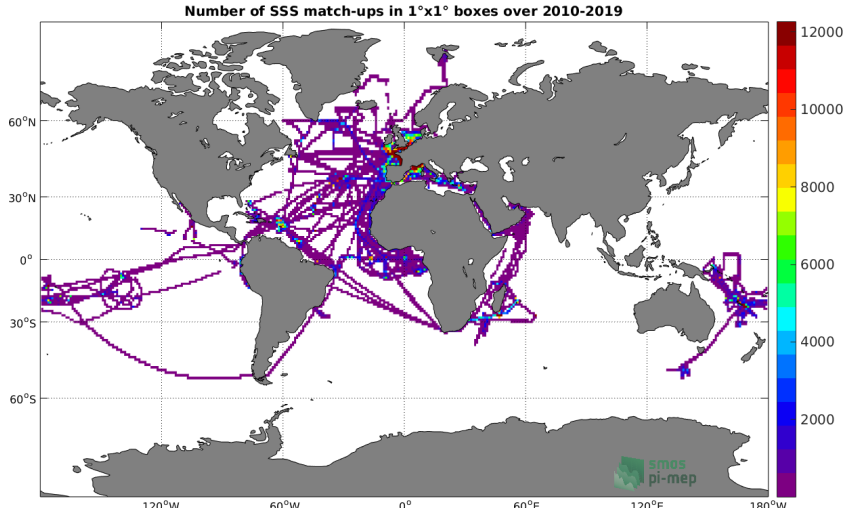


Figure 28: Number of SSS from TSG (GOSUD-Research-vessel) in $1^\circ \times 1^\circ$ boxes.

3.2.6 Spatial Maps of the Temporal mean and Std of *in situ* and ISAS SSS and of the difference (Δ SSS)

In Figure 29, we show maps of temporal mean (left) and standard deviation (right) of ISAS (top), TSG (GOSUD-Research-vessel) *in situ* dataset (middle) and the difference Δ SSS(ISAS - TSG (GOSUD-Research-vessel)) (bottom). The temporal mean and std are calculated using all match-up pairs falling in spatial boxes of size $1^\circ \times 1^\circ$ over the full TSG (GOSUD-Research-vessel) dataset period.

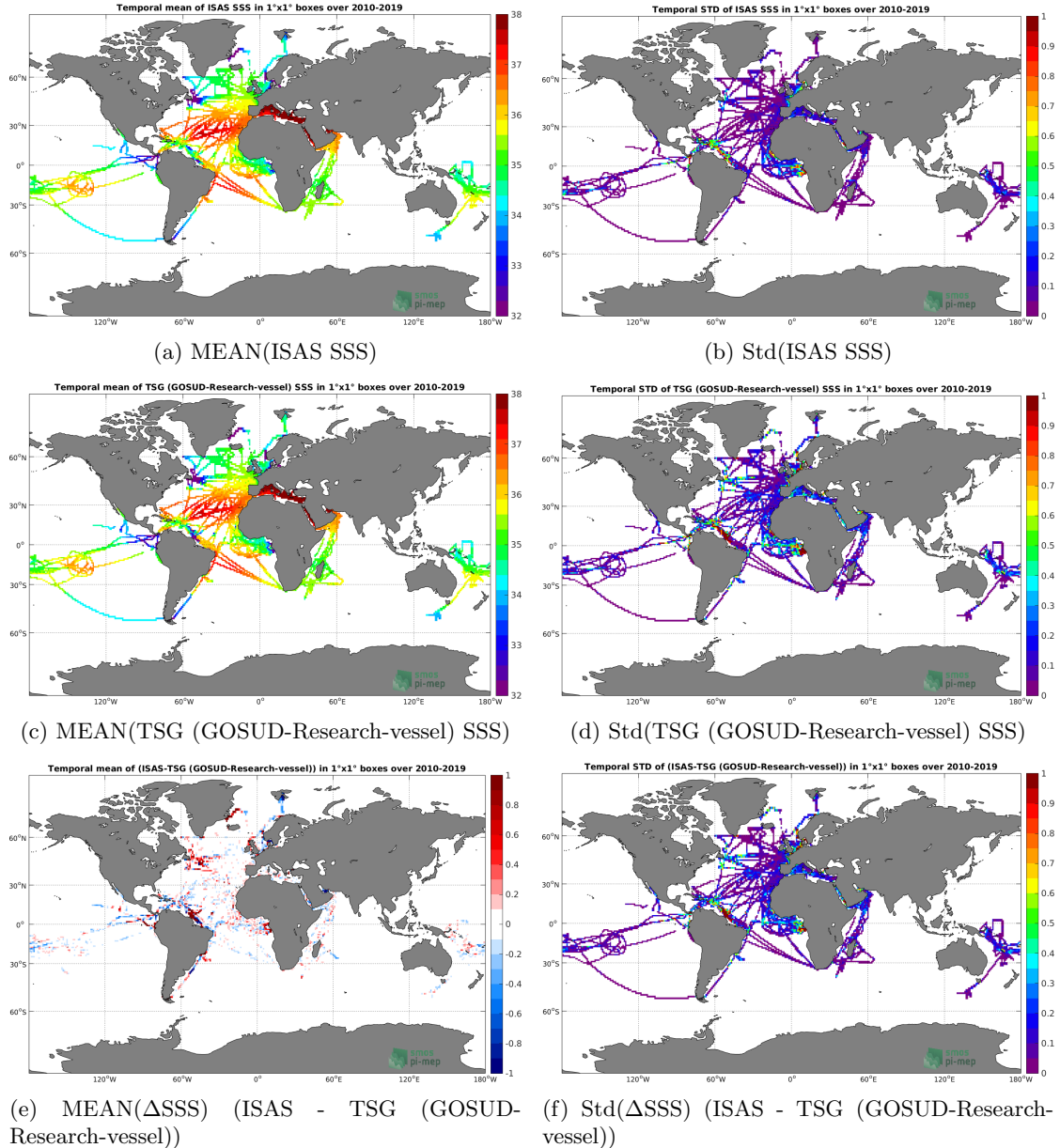


Figure 29: Temporal mean (left) and Std (right) of SSS from ISAS (top), TSG (GOSUD-Research-vessel) (middle), and of Δ SSS (ISAS - TSG (GOSUD-Research-vessel)). Only match-up pairs are used to generate these maps.

3.2.7 Time series of the monthly median and Std of *in situ* and ISAS SSS and of the difference (Δ SSS)

In the top panel of Figure 30, we show the time series of the monthly median SSS estimated for both ISAS SSS product (in black) and the TSG (GOSUD-Research-vessel) *in situ* dataset (in blue) at the collected Pi-MEP match-up pairs.

In the middle panel of Figure 30, we show the time series of the monthly median of Δ SSS

(ISAS - TSG (GOSUD-Research-vessel)) for the collected Pi-MEP match-up pairs.

In the bottom panel of Figure 30, we show the time series of the monthly standard deviation of the ΔSSS (ISAS - TSG (GOSUD-Research-vessel)) for the collected Pi-MEP match-up pairs.

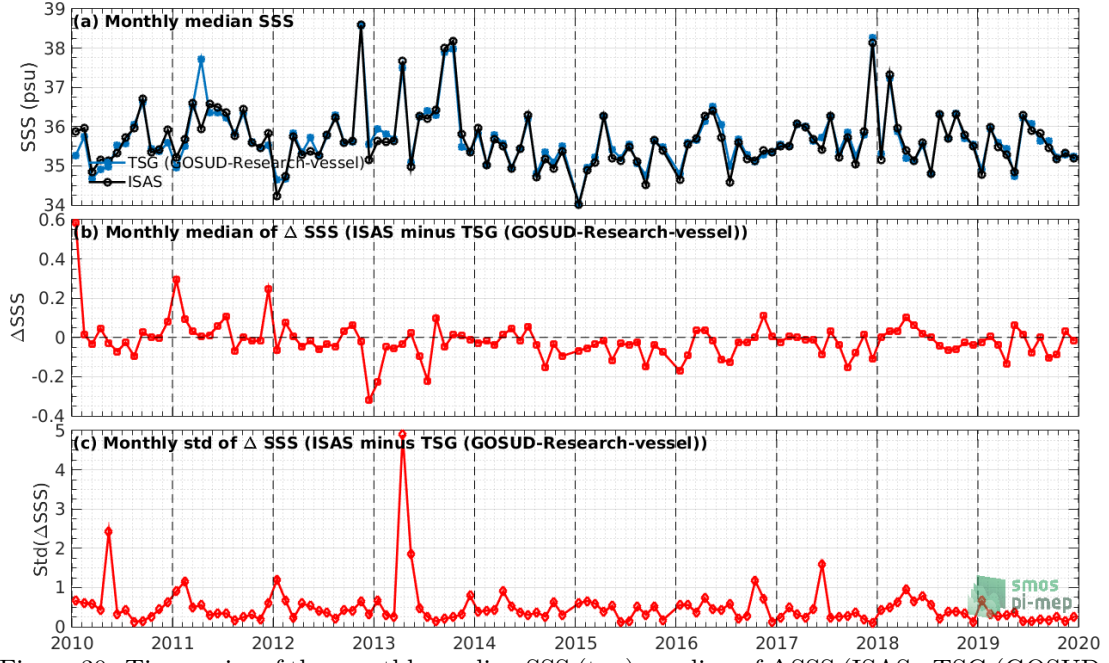


Figure 30: Time series of the monthly median SSS (top), median of ΔSSS (ISAS - TSG (GOSUD-Research-vessel)) and Std of ΔSSS (ISAS - TSG (GOSUD-Research-vessel)) considering all match-ups collected by the Pi-MEP.

3.2.8 Zonal mean and Std of *in situ* and ISAS SSS and of the difference ΔSSS

In Figure 31 left panel, we show the zonal mean SSS considering all Pi-MEP match-up pairs for both ISAS SSS product (in black) and the TSG (GOSUD-Research-vessel) *in situ* dataset (in blue). The full *in situ* dataset period is used to derive the mean.

In the right panel of Figure 31, we show the zonal mean of ΔSSS (ISAS - TSG (GOSUD-Research-vessel)) for all the collected Pi-MEP match-up pairs estimated over the full *in situ* dataset period.

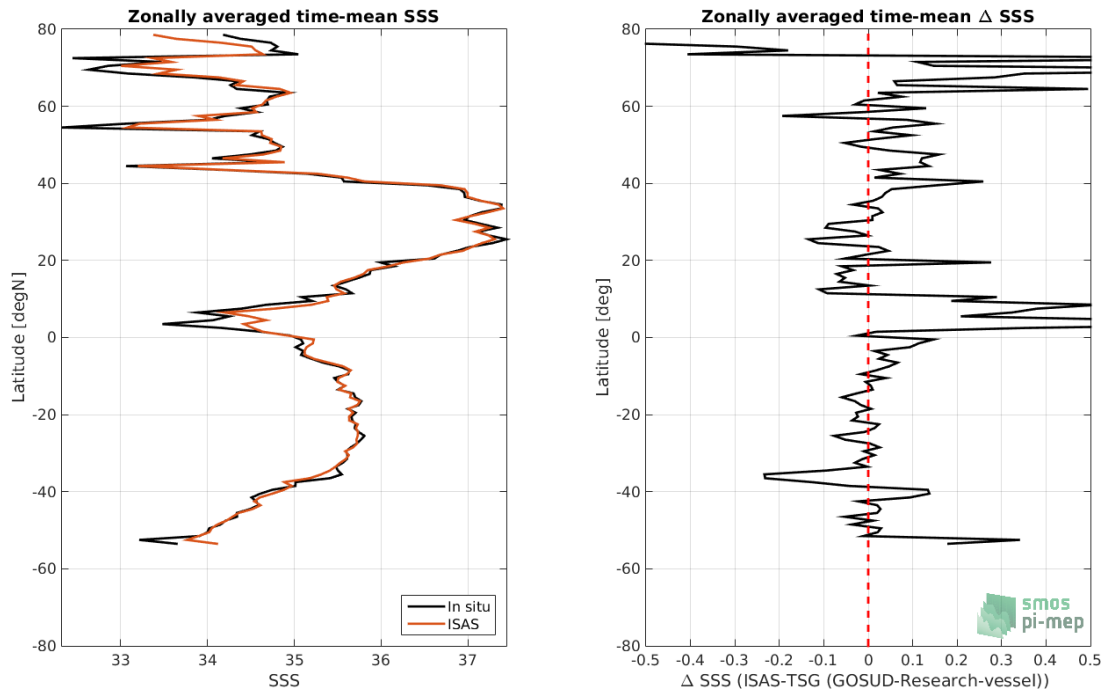


Figure 31: Left panel: Zonal mean SSS from ISAS product (black) and from TSG (GOSUD-Research-vessel) (blue). Right panel: Zonal mean of Δ SSS (ISAS - TSG (GOSUD-Research-vessel)) for all the collected Pi-MEP match-up pairs estimated over the full *in situ* dataset period.

3.2.9 Scatterplots of ISAS vs *in situ* SSS by latitudinal bands

In Figure 32, contour maps of the concentration of ISAS SSS (y-axis) versus TSG (GOSUD-Research-vessel) SSS (x-axis) at match-up pairs for different latitude bands: (a) 80°S-80°N, (b) 20°S-20°N, (c) 40°S-20°S and 20°N-40°N and (d) 60°S-40°S and 40°N-60°N. For each plot, the red line shows $x=y$. The black thin and dashed lines indicate a linear fit through the data cloud and the $\pm 95\%$ confidence levels, respectively. The number match-up pairs n , the slope and R^2 coefficient of the linear fit, the root mean square (RMS) and the mean bias between ISAS and *in situ* data are indicated for each latitude band in each plots.

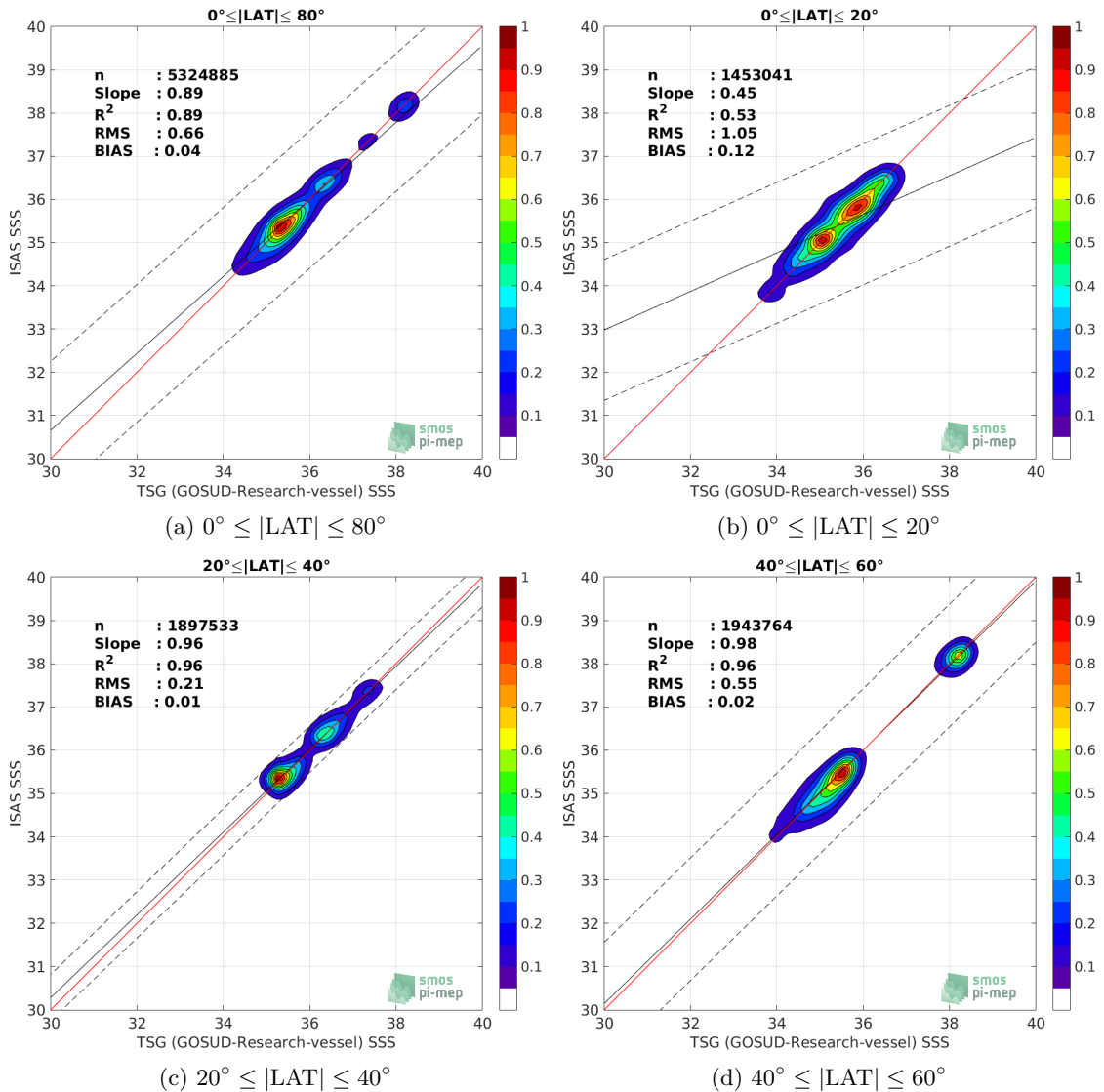


Figure 32: Contour maps of the concentration of ISAS SSS (y-axis) versus TSG (GOSUD-Research-vessel) SSS (x-axis) at match-up pairs for different latitude bands. For each plot, the red line shows $x=y$. The black thin and dashed lines indicate a linear fit through the data cloud and the $\pm 95\%$ confidence levels, respectively. The number match-up pairs n , the slope and R^2 coefficient of the linear fit, the root mean square (RMS) and the mean bias between ISAS and *in situ* data are indicated for each latitude band in each plots.

3.2.10 Time series of the monthly median and Std of the difference ΔSSS sorted by latitudinal bands

In Figure 33, time series of the monthly median (red curves) of ΔSSS (ISAS - TSG (GOSUD-Research-vessel)) and ± 1 Std (black vertical thick bars) as function of time for all the collected Pi-MEP match-up pairs estimated for the full *in situ* dataset period are shown for different latitude bands: (a) $80^\circ\text{S}-80^\circ\text{N}$, (b) $20^\circ\text{S}-20^\circ\text{N}$, (c) $40^\circ\text{S}-20^\circ\text{S}$ and $20^\circ\text{N}-40^\circ\text{N}$ and (d) $60^\circ\text{S}-40^\circ\text{S}$

and 40°N-60°N.

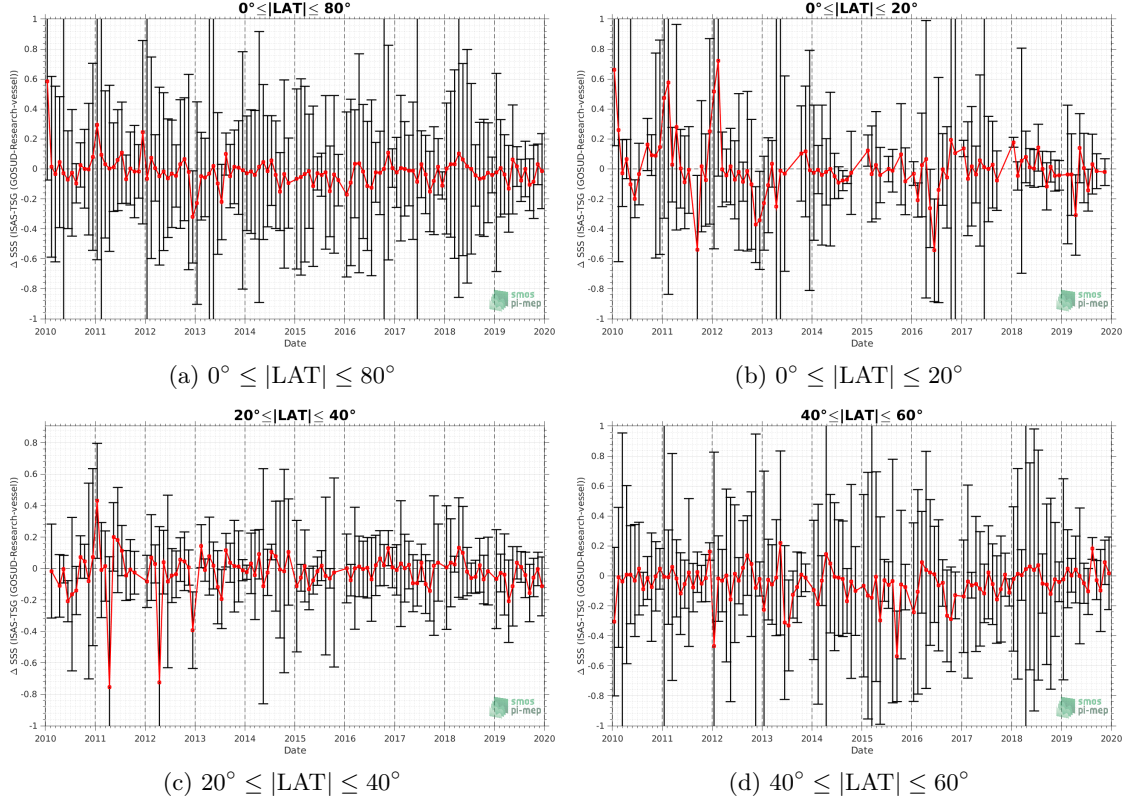


Figure 33: Monthly median (red curves) of ΔSSS (ISAS - TSG (GOSUD-Research-vessel)) and ± 1 Std (black vertical thick bars) as function of time for all the collected Pi-MEP match-up pairs for the full *in situ* dataset period are shown for different latitude bands: (a) $80^\circ\text{S}-80^\circ\text{N}$, (b) $20^\circ\text{S}-20^\circ\text{N}$, (c) $40^\circ\text{S}-20^\circ\text{N}$ and $20^\circ\text{N}-40^\circ\text{N}$ and (d) $60^\circ\text{S}-40^\circ\text{S}$ and $40^\circ\text{N}-60^\circ\text{N}$.

3.2.11 ΔSSS sorted as geophysical conditions

In Figure 34, we classify the match-up differences ΔSSS (ISAS - *in situ*) as function of the geophysical conditions at match-up points. The mean and std of ΔSSS (ISAS - TSG (GOSUD-Research-vessel)) is thus evaluated as function of the

- *in situ* SSS values per bins of width 0.2,
- *in situ* SST values per bins of width 1°C,
- ASCAT daily wind values per bins of width 1 m/s,
- CMORPH 3-hourly rain rates per bins of width 1 mm/h, and,
- distance to coasts per bins of width 50 km,
- *in situ* measurement depth (if relevant).

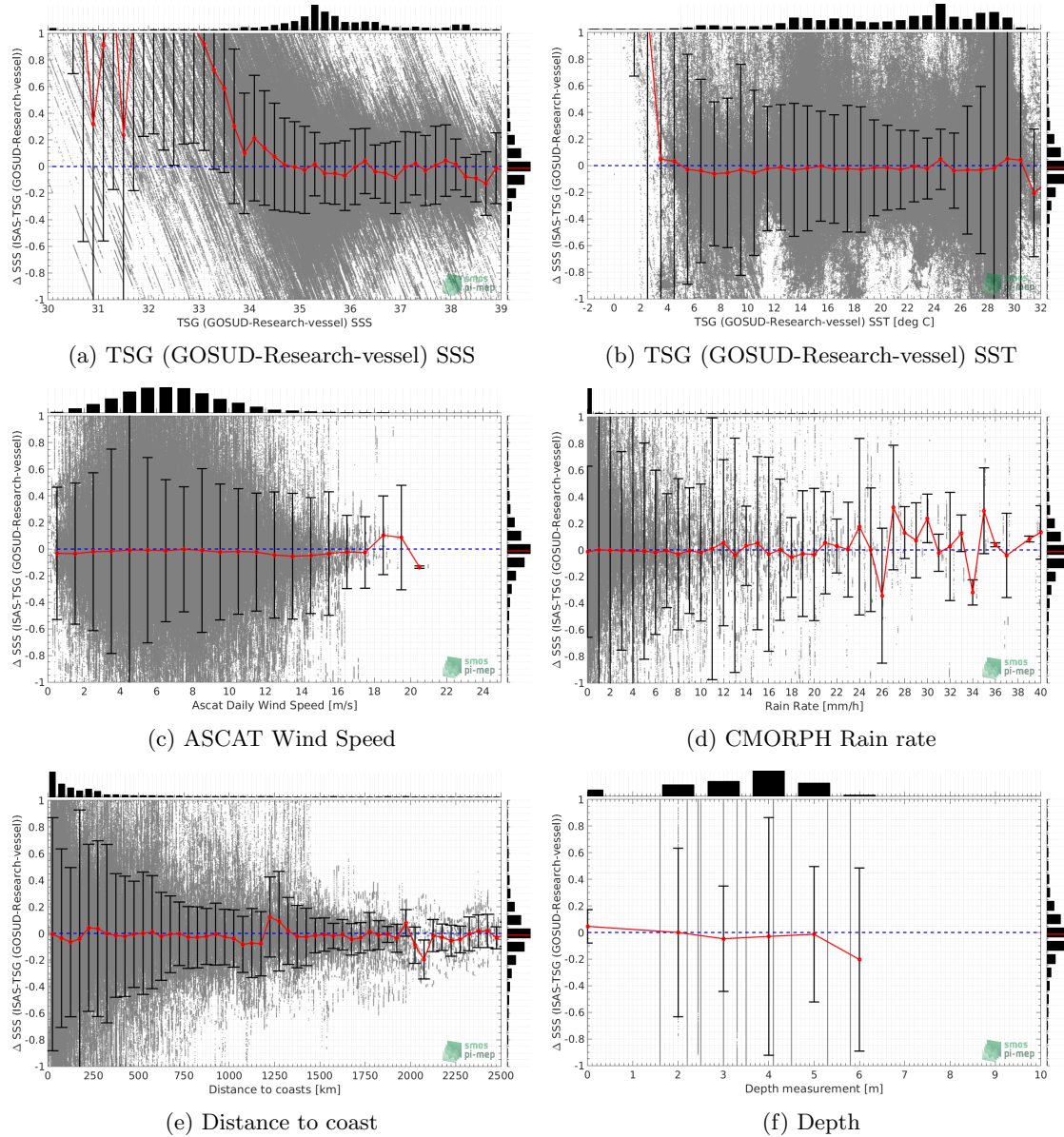


Figure 34: ΔSSS (ISAS - TSG (GOSUD-Research-vessel)) sorted as geophysical conditions: TSG (GOSUD-Research-vessel) SSS a), TSG (GOSUD-Research-vessel) SST b), ASCAT Wind speed c), CMORPH rain rate d), distance to coast (e) and depth measurements (f).

3.2.12 ΔSSS maps and statistics for different geophysical conditions

In Figures 35 and 36, we focus on sub-datasets of the match-up differences ΔSSS (ISAS - *in situ*) for the following specific geophysical conditions:

- **C1:** if the local value at *in situ* location of estimated rain rate is zero, mean daily wind is in the range [3, 12] m/s, the SST is $> 5^\circ\text{C}$ and distance to coast is > 800 km.
- **C2:** if the local value at *in situ* location of estimated rain rate is zero, mean daily wind is

in the range [3, 12] m/s.

- **C3:** if the local value at *in situ* location of estimated rain rate is high (ie. $> 1 \text{ mm/h}$) and mean daily wind is low (ie. $< 4 \text{ m/s}$).
- **C5:** if the *in situ* data is located where the climatological SSS standard deviation is low (ie. above < 0.2).
- **C6:** if the *in situ* data is located where the climatological SSS standard deviation is high (ie. above > 0.2).

For each of these conditions, the temporal mean (gridded over spatial boxes of size $1^\circ \times 1^\circ$) and the histogram of the difference ΔSSS (ISAS - *in situ*) are presented.

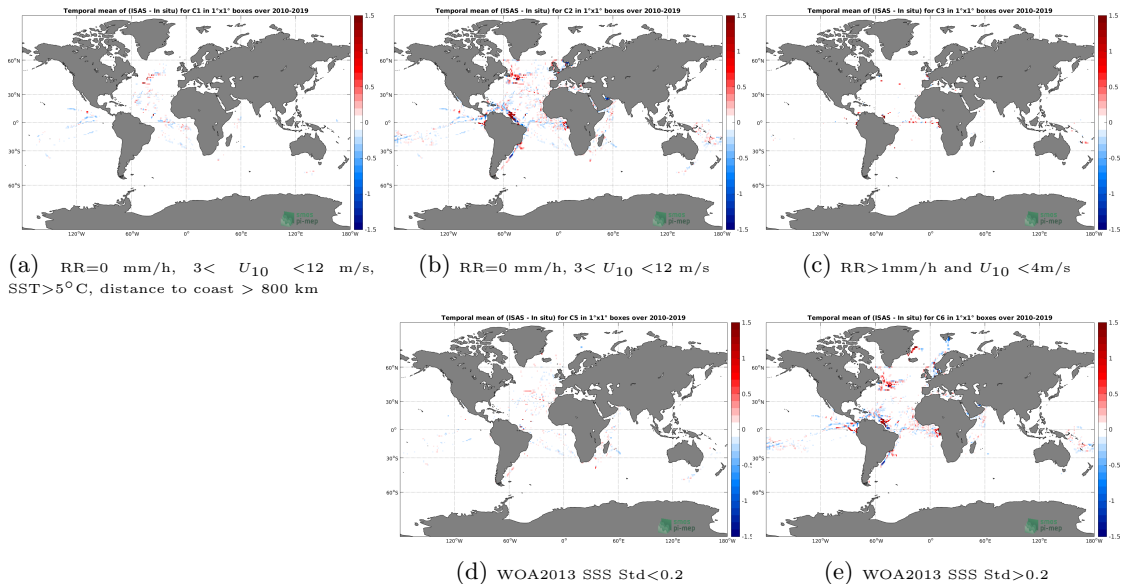


Figure 35: Temporal mean gridded over spatial boxes of size $1^\circ \times 1^\circ$ of ΔSSS (ISAS - TSG (GOSUD-Research-vessel)) for 5 different subdatasets corresponding to: $\text{RR}=0 \text{ mm/h}$, $3 < U_{10} < 12 \text{ m/s}$, $\text{SST} > 5^\circ\text{C}$, distance to coast $> 800 \text{ km}$ (a), $\text{RR}=0 \text{ mm/h}$, $3 < U_{10} < 12 \text{ m/s}$ (b), $\text{RR} > 1 \text{ mm/h}$ and $U_{10} < 4 \text{ m/s}$ (c), WOA2013 SSS Std < 0.2 (d), WOA2013 SSS Std > 0.2 (e).

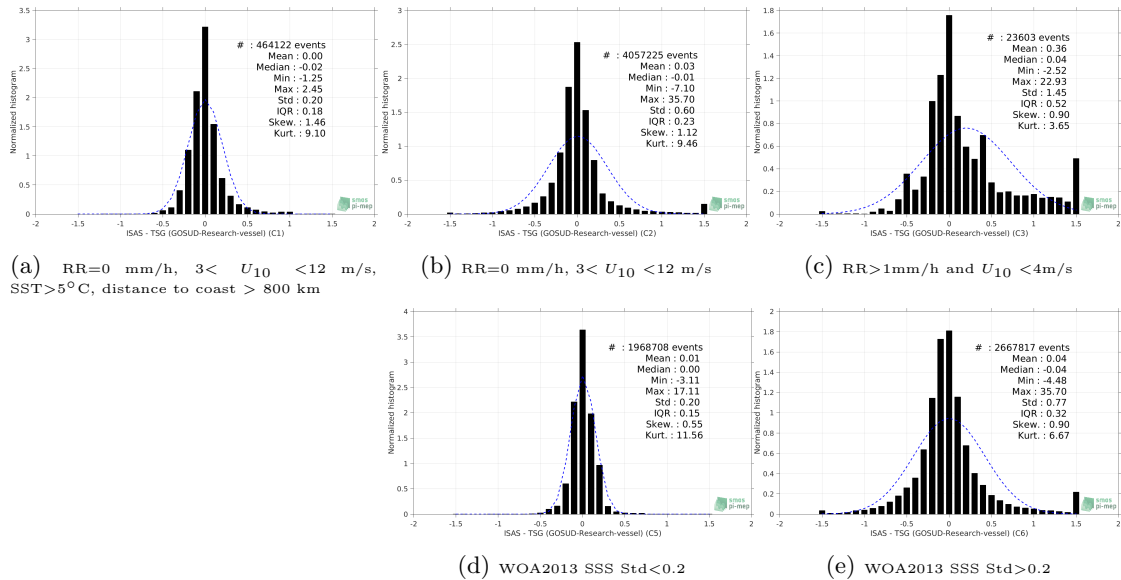


Figure 36: Normalized histogram of ΔSSS (ISAS - TSG (GOSUD-Research-vessel)) for 5 different subdatasets corresponding to: RR=0 mm/h, $3 < U_{10} < 12$ m/s, SST> 5°C , distance to coast > 800 km (a), RR=0 mm/h, $3 < U_{10} < 12$ m/s (b), RR>1mm/h and $U_{10} < 4$ m/s (c), WOA2013 SSS Std<0.2 (d), WOA2013 SSS Std>0.2 (e).

3.2.13 Summary

Table 1 shows the mean, median, standard deviation (Std), root mean square (RMS), interquartile range (IQR), correlation coefficient (r^2) and robust standard deviation (Std*) of the match-up differences ΔSSS (ISAS - TSG (GOSUD-Research-vessel)) for the following conditions:

- all: All the match-up pairs satellite/in situ SSS values are used to derive the statistics
- C1: only pairs where RR=0 mm/h, $3 < U_{10} < 12$ m/s, SST> 5°C , distance to coast > 800 km
- C2: only pairs where RR=0 mm/h, $3 < U_{10} < 12$ m/s
- C3: only pairs where RR>1mm/h and $U_{10} < 4$ m/s
- C5: only pairs where WOA2013 SSS Std<0.2
- C6: only pairs where WOA2013 SSS Std>0.2
- C7a: only pairs with a distance to coast < 150 km.
- C7b: only pairs with a distance to coast in the range [150, 800] km.
- C7c: only pairs with a distance to coast > 800 km.
- C8a: only pairs where SST is < 5°C .
- C8b: only pairs where SST is in the range [$5, 15$]°C.
- C8c: only pairs where SST is > 15°C .

- C9a: only pairs where SSS is < 33 .
- C9b: only pairs where SSS is in the range [33, 37].
- C9c: only pairs where SSS is > 37 .

Table 1: Statistics of Δ SSS (ISAS - TSG (GOSUD-Research-vessel))

Condition	#	Median	Mean	Std	RMS	IQR	r^2	Std*
all	5331676	-0.01	0.04	0.68	0.68	0.23	0.89	0.18
C1	464122	-0.02	0.00	0.20	0.20	0.18	0.96	0.13
C2	4057225	-0.01	0.03	0.60	0.60	0.23	0.91	0.17
C3	23603	0.04	0.36	1.45	1.50	0.52	0.65	0.35
C5	1968708	0.00	0.01	0.20	0.20	0.15	0.96	0.11
C6	2667817	-0.04	0.04	0.77	0.77	0.32	0.89	0.23
C7a	2655019	-0.03	0.04	0.77	0.77	0.28	0.91	0.21
C7b	2077492	0.00	0.05	0.65	0.65	0.20	0.77	0.15
C7c	598402	-0.02	0.00	0.22	0.22	0.18	0.95	0.13
C8a	27428	0.14	0.51	1.47	1.56	1.51	0.92	1.16
C8b	1054872	-0.03	0.01	0.55	0.55	0.23	0.84	0.17
C8c	3972161	-0.01	0.04	0.71	0.71	0.23	0.89	0.17
C9a	177760	1.04	1.56	2.93	3.32	2.42	0.77	1.80
C9b	4312398	-0.01	-0.01	0.33	0.33	0.23	0.81	0.17
C9c	841518	-0.03	-0.04	0.25	0.26	0.19	0.86	0.14

Table 1 numerical values can be downloaded as a csv file [here](#).

3.3 TSG (GOSUD-Sailing-ship)

3.3.1 Introduction

The TSG-GOSUD-Sailing-ship dataset correspond to Observations of Sea surface salinity obtained from voluntary sailing ships using medium or small size sensors. They complement the networks installed on research vessels or commercial ships. This delayed mode dataset ([Reynaud et al. \(2015\)](#)) is updated annually as a contribution to GOSUD (<http://www.gosud.org>) and freely available [here](#). Adjusted values when available and only collected TSG data that exhibit quality flags=1 and 2 were used.

3.3.2 Number of SSS data as a function of time and distance to coast

Figure 37 shows the time (a) and distance to coast (b) distributions of the TSG (GOSUD-Sailing-ship) *in situ* dataset.

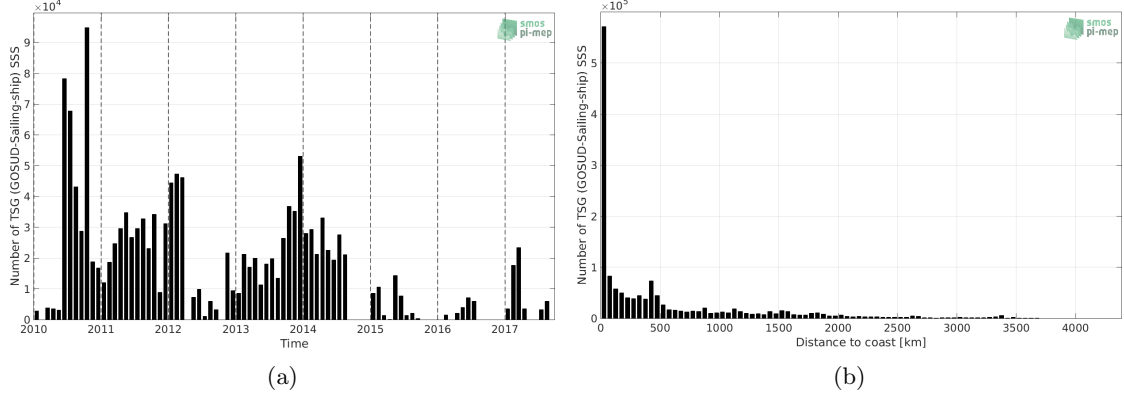


Figure 37: Number of SSS from TSG (GOSUD-Sailing-ship) as a function of time (a) and distance to coast (b).

3.3.3 Histograms of SSS

Figure 38 shows the SSS distribution of the TSG (GOSUD-Sailing-ship) (a) and colocalized ISAS (b) dataset.

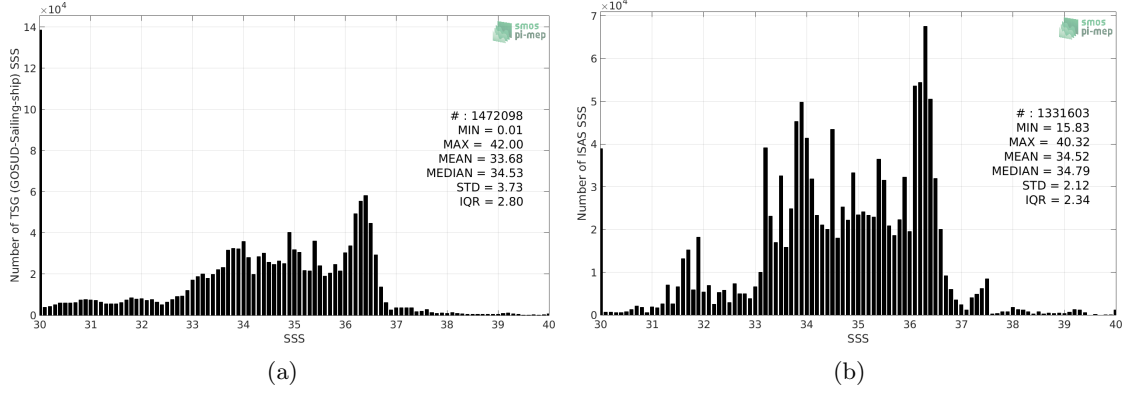


Figure 38: Histograms of SSS from TSG (GOSUD-Sailing-ship) (a) and ISAS (b) per bins of 0.1.

3.3.4 Distribution of *in situ* SSS depth measurements

In Figure 39, we show the depth distribution of the *in situ* salinity dataset (a) and the spatial distribution of the depth temporal mean in $1^\circ \times 1^\circ$ boxes and considering the full *in situ* dataset period (b).

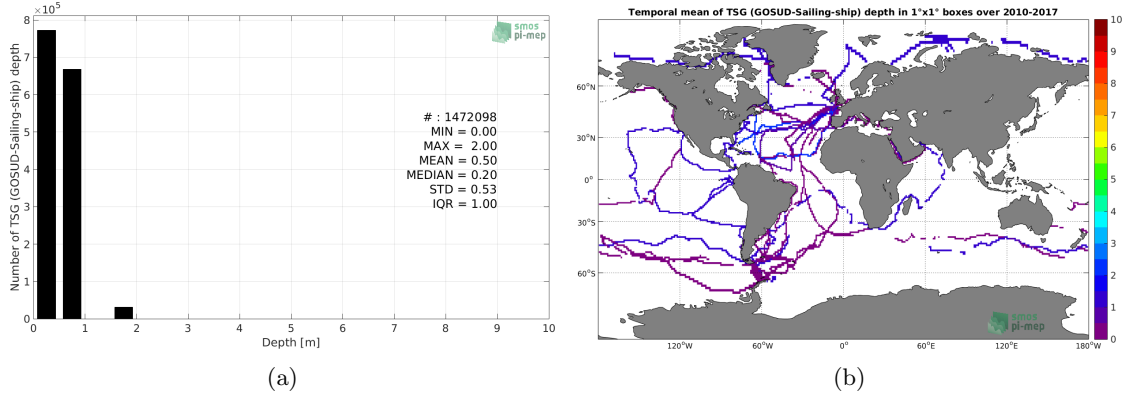


Figure 39: Depth distribution of the upper level SSS measurements from TSG (GOSUD-Sailing-ship) (a) and spatial distribution of the *in situ* SSS depth measurements showing the mean value in $1^\circ \times 1^\circ$ boxes and considering the full *in situ* dataset period (b).

3.3.5 Spatial distribution of SSS

In Figure 40, the number of TSG (GOSUD-Sailing-ship) SSS measurements in $1^\circ \times 1^\circ$ boxes is shown.

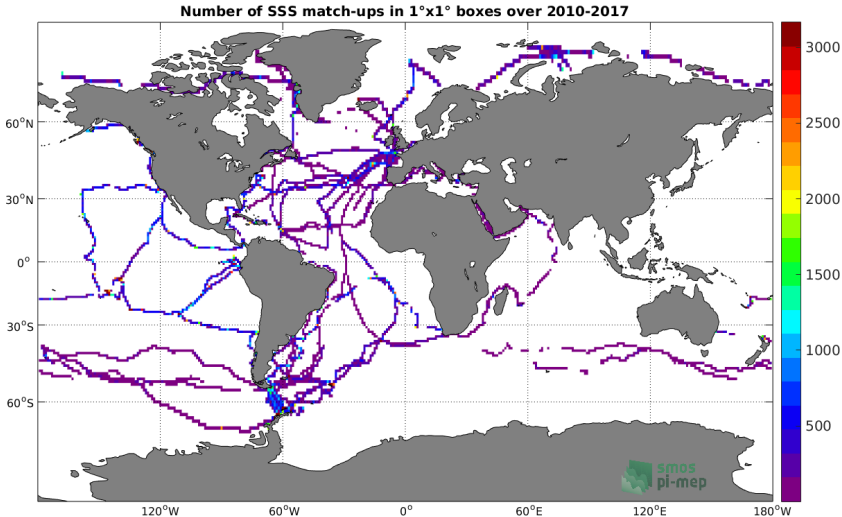


Figure 40: Number of SSS from TSG (GOSUD-Sailing-ship) in $1^\circ \times 1^\circ$ boxes.

3.3.6 Spatial Maps of the Temporal mean and Std of *in situ* and ISAS SSS and of the difference (Δ SSS)

In Figure 41, we show maps of temporal mean (left) and standard deviation (right) of ISAS (top), TSG (GOSUD-Sailing-ship) *in situ* dataset (middle) and the difference Δ SSS(ISAS -TSG (GOSUD-Sailing-ship)) (bottom). The temporal mean and std are calculated using all match-up pairs falling in spatial boxes of size $1^\circ \times 1^\circ$ over the full TSG (GOSUD-Sailing-ship) dataset period.

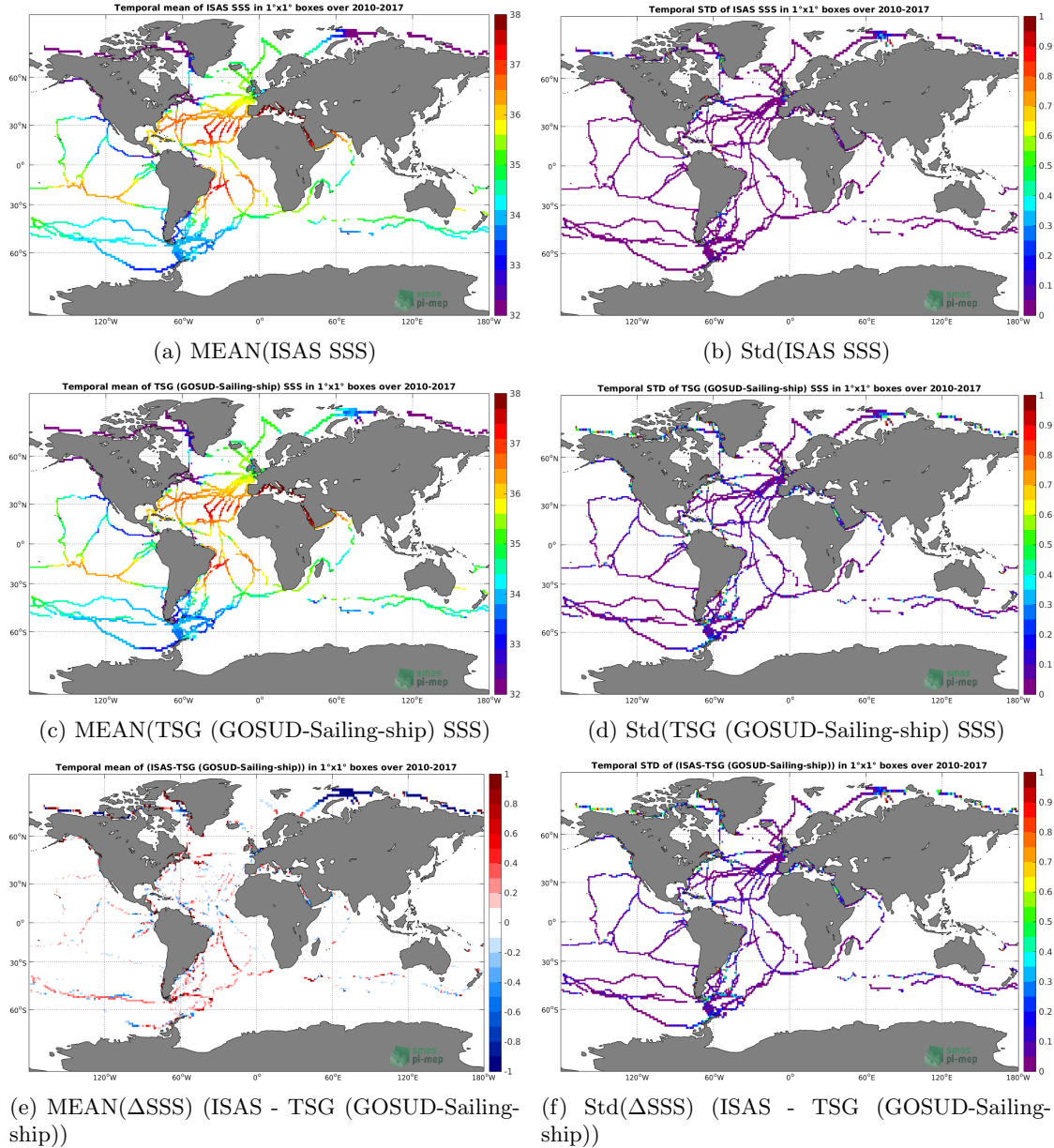


Figure 41: Temporal mean (left) and Std (right) of SSS from ISAS (top), TSG (GOSUD-Sailing-ship) (middle), and of Δ SSS (ISAS - TSG (GOSUD-Sailing-ship)). Only match-up pairs are used to generate these maps.

3.3.7 Time series of the monthly median and Std of *in situ* and ISAS SSS and of the difference (Δ SSS)

In the top panel of Figure 42, we show the time series of the monthly median SSS estimated for both ISAS SSS product (in black) and the TSG (GOSUD-Sailing-ship) *in situ* dataset (in blue) at the collected Pi-MEP match-up pairs.

In the middle panel of Figure 42, we show the time series of the monthly median of Δ SSS

(ISAS - TSG (GOSUD-Sailing-ship)) for the collected Pi-MEP match-up pairs.

In the bottom panel of Figure 42, we show the time series of the monthly standard deviation of the Δ SSS (ISAS - TSG (GOSUD-Sailing-ship)) for the collected Pi-MEP match-up pairs.

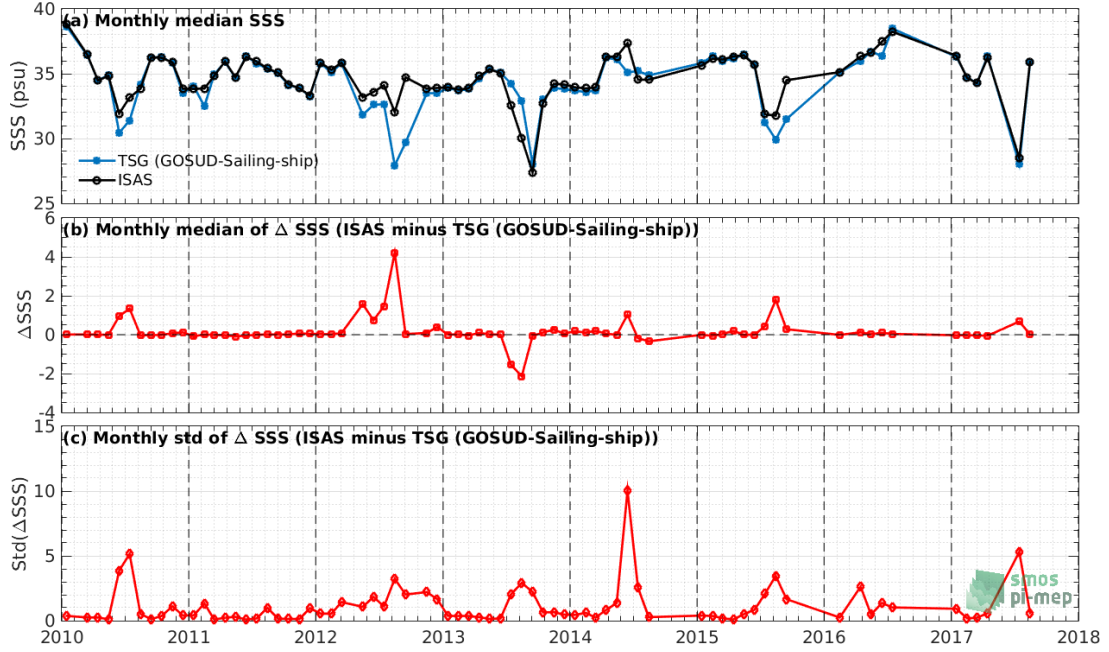


Figure 42: Time series of the monthly median SSS (top), median of Δ SSS (ISAS - TSG (GOSUD-Sailing-ship)) and Std of Δ SSS (ISAS - TSG (GOSUD-Sailing-ship)) considering all match-ups collected by the Pi-MEP.

3.3.8 Zonal mean and Std of *in situ* and ISAS SSS and of the difference Δ SSS

In Figure 43 left panel, we show the zonal mean SSS considering all Pi-MEP match-up pairs for both ISAS SSS product (in black) and the TSG (GOSUD-Sailing-ship) *in situ* dataset (in blue). The full *in situ* dataset period is used to derive the mean.

In the right panel of Figure 43, we show the zonal mean of Δ SSS (ISAS - TSG (GOSUD-Sailing-ship)) for all the collected Pi-MEP match-up pairs estimated over the full *in situ* dataset period.

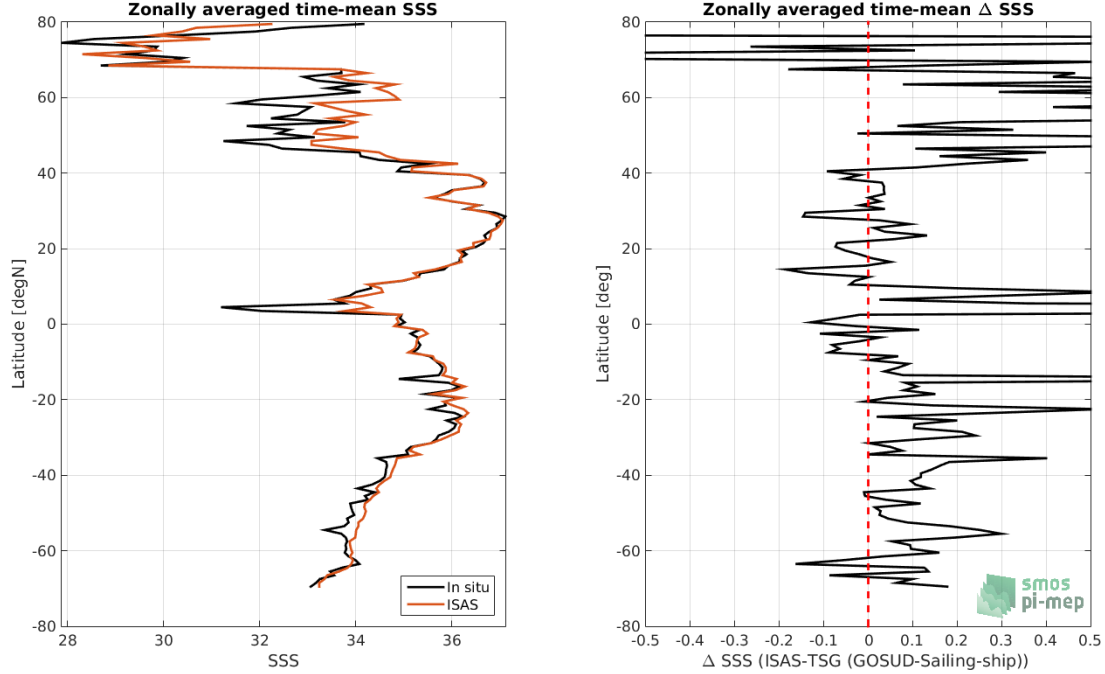


Figure 43: Left panel: Zonal mean SSS from ISAS product (black) and from TSG (GOSUD-Sailing-ship) (blue). Right panel: Zonal mean of Δ SSS (ISAS - TSG (GOSUD-Sailing-ship)) for all the collected Pi-MEP match-up pairs estimated over the full *in situ* dataset period.

3.3.9 Scatterplots of ISAS vs *in situ* SSS by latitudinal bands

In Figure 44, contour maps of the concentration of ISAS SSS (y-axis) versus TSG (GOSUD-Sailing-ship) SSS (x-axis) at match-up pairs for different latitude bands: (a) 80°S-80°N, (b) 20°S-20°N, (c) 40°S-20°S and 20°N-40°N and (d) 60°S-40°S and 40°N-60°N. For each plot, the red line shows $x=y$. The black thin and dashed lines indicate a linear fit through the data cloud and the $\pm 95\%$ confidence levels, respectively. The number match-up pairs n , the slope and R^2 coefficient of the linear fit, the root mean square (RMS) and the mean bias between ISAS and *in situ* data are indicated for each latitude band in each plots.

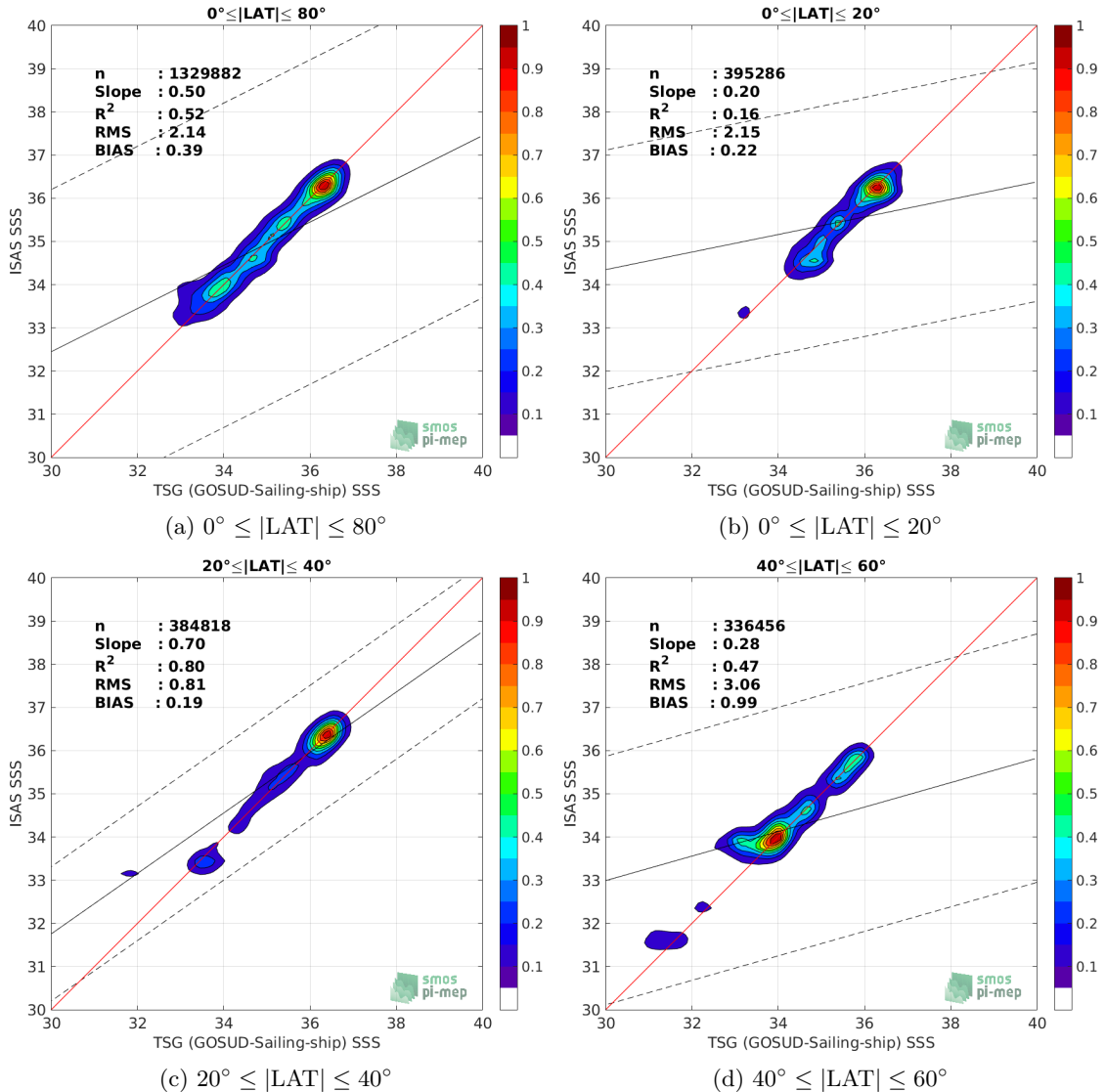


Figure 44: Contour maps of the concentration of ISAS SSS (y-axis) versus TSG (GOSUD-Sailing-ship) SSS (x-axis) at match-up pairs for different latitude bands. For each plot, the red line shows $x=y$. The black thin and dashed lines indicate a linear fit through the data cloud and the $\pm 95\%$ confidence levels, respectively. The number match-up pairs n , the slope and R^2 coefficient of the linear fit, the root mean square (RMS) and the mean bias between ISAS and *in situ* data are indicated for each latitude band in each plots.

3.3.10 Time series of the monthly median and Std of the difference ΔSSS sorted by latitudinal bands

In Figure 45, time series of the monthly median (red curves) of ΔSSS (ISAS - TSG (GOSUD-Sailing-ship)) and ± 1 Std (black vertical thick bars) as function of time for all the collected Pi-MEP match-up pairs estimated for the full *in situ* dataset period are shown for different latitude bands: (a) $80^\circ\text{S}-80^\circ\text{N}$, (b) $20^\circ\text{S}-20^\circ\text{N}$, (c) $40^\circ\text{S}-20^\circ\text{S}$ and $20^\circ\text{N}-40^\circ\text{N}$ and (d) $60^\circ\text{S}-40^\circ\text{S}$

and 40°N-60°N.

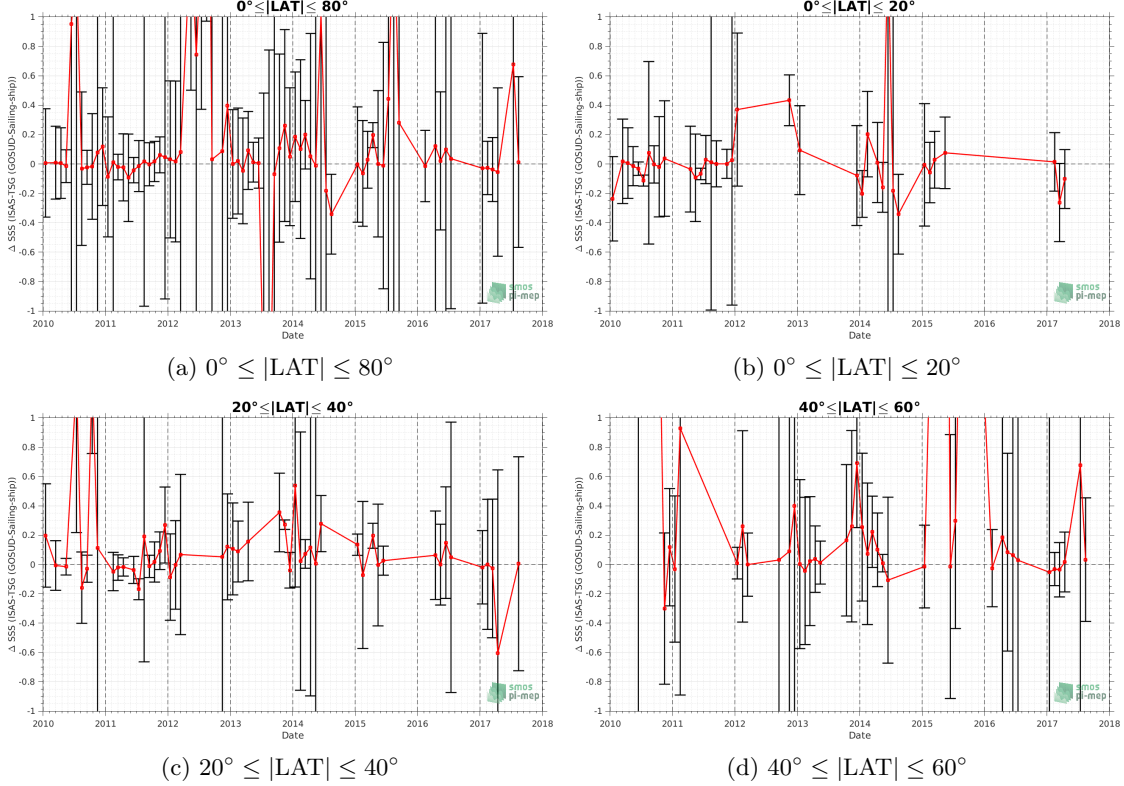


Figure 45: Monthly median (red curves) of ΔSSS (ISAS - TSG (GOSUD-Sailing-ship)) and ± 1 Std (black vertical thick bars) as function of time for all the collected Pi-MEP match-up pairs for the full *in situ* dataset period are shown for different latitude bands: (a) $80^\circ\text{S}-80^\circ\text{N}$, (b) $20^\circ\text{S}-20^\circ\text{N}$, (c) $40^\circ\text{S}-20^\circ\text{S}$ and $20^\circ\text{N}-40^\circ\text{N}$ and (d) $60^\circ\text{S}-40^\circ\text{S}$ and $40^\circ\text{N}-60^\circ\text{N}$.

3.3.11 ΔSSS sorted as geophysical conditions

In Figure 46, we classify the match-up differences ΔSSS (ISAS - *in situ*) as function of the geophysical conditions at match-up points. The mean and std of ΔSSS (ISAS - TSG (GOSUD-Sailing-ship)) is thus evaluated as function of the

- *in situ* SSS values per bins of width 0.2,
- *in situ* SST values per bins of width 1°C ,
- ASCAT daily wind values per bins of width 1 m/s,
- CMORPH 3-hourly rain rates per bins of width 1 mm/h, and,
- distance to coasts per bins of width 50 km,
- *in situ* measurement depth (if relevant).

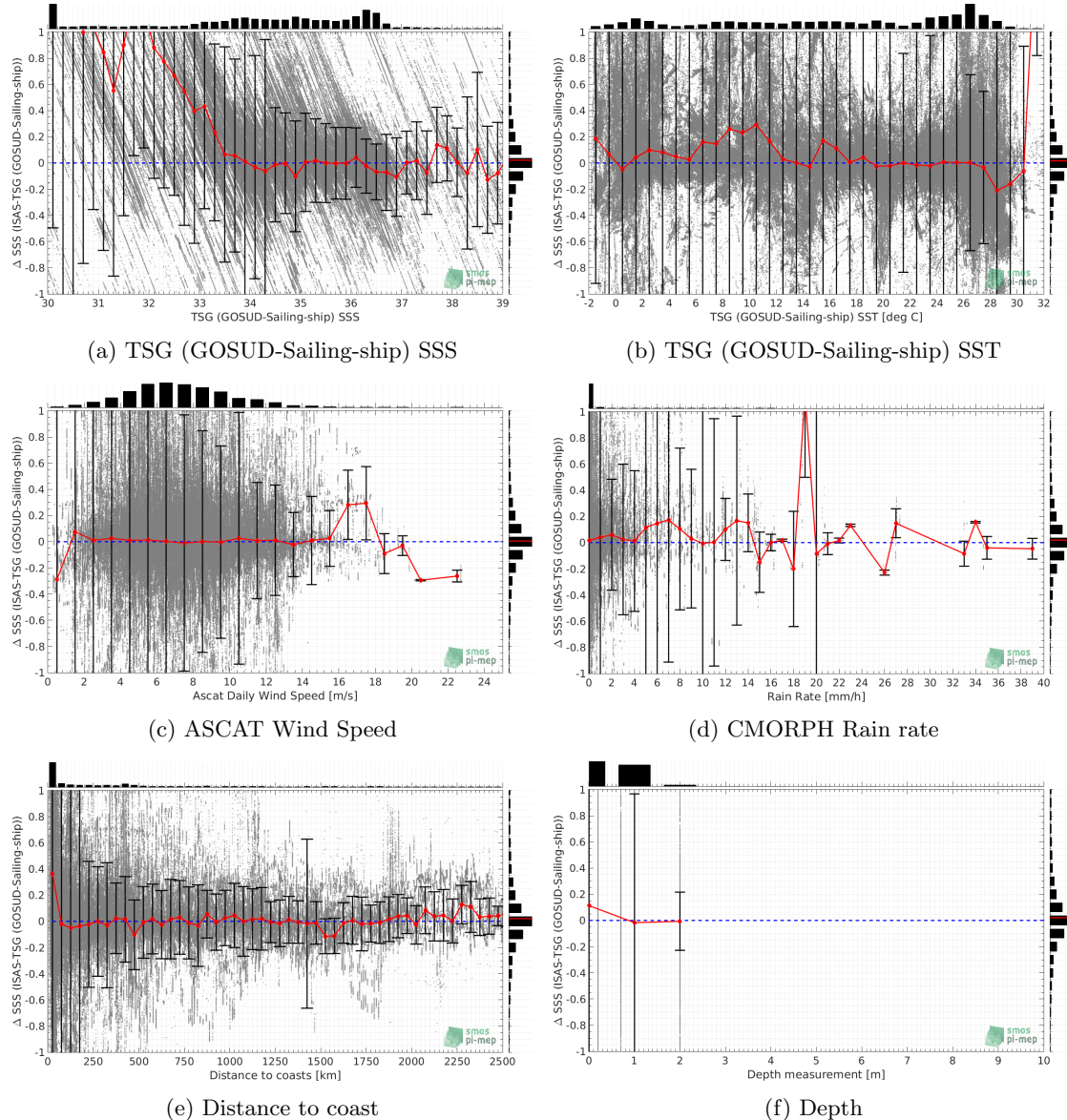


Figure 46: ΔSSS (ISAS - TSG (GOSUD-Sailing-ship)) sorted as geophysical conditions: TSG (GOSUD-Sailing-ship) SSS a), TSG (GOSUD-Sailing-ship) SST b), ASCAT Wind speed c), CMORPH rain rate d), distance to coast (e) and depth measurements (f).

3.3.12 ΔSSS maps and statistics for different geophysical conditions

In Figures 47 and 48, we focus on sub-datasets of the match-up differences ΔSSS (ISAS - *in situ*) for the following specific geophysical conditions:

- **C1:** if the local value at *in situ* location of estimated rain rate is zero, mean daily wind is in the range [3, 12] m/s, the SST is $> 5^\circ\text{C}$ and distance to coast is > 800 km.
- **C2:** if the local value at *in situ* location of estimated rain rate is zero, mean daily wind is

in the range [3, 12] m/s.

- **C3:** if the local value at *in situ* location of estimated rain rate is high (ie. $> 1 \text{ mm/h}$) and mean daily wind is low (ie. $< 4 \text{ m/s}$).
- **C5:** if the *in situ* data is located where the climatological SSS standard deviation is low (ie. above < 0.2).
- **C6:** if the *in situ* data is located where the climatological SSS standard deviation is high (ie. above > 0.2).

For each of these conditions, the temporal mean (gridded over spatial boxes of size $1^\circ \times 1^\circ$) and the histogram of the difference ΔSSS (ISAS - *in situ*) are presented.

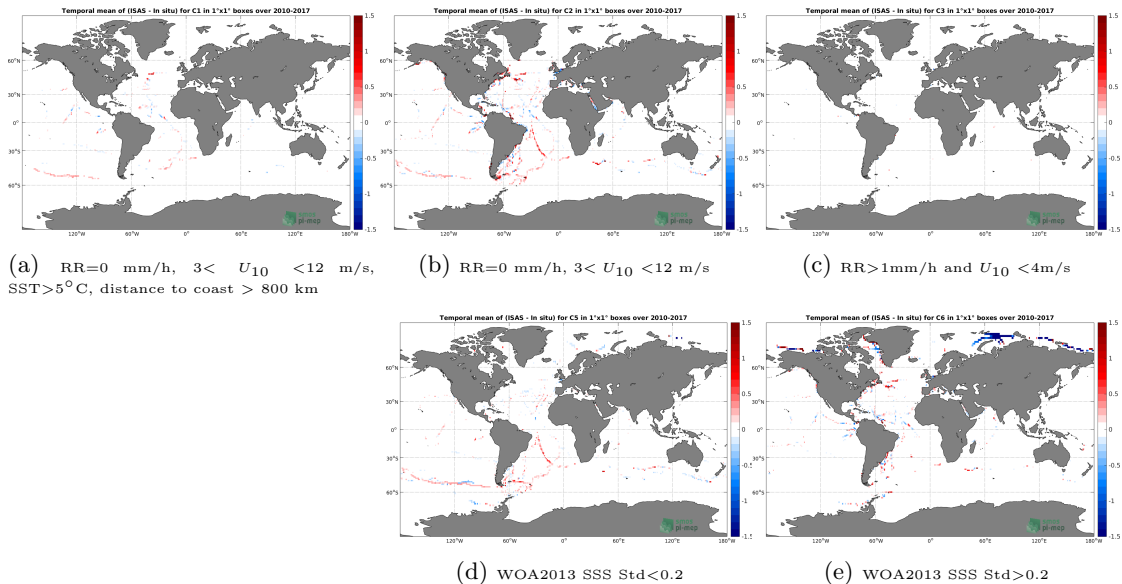


Figure 47: Temporal mean gridded over spatial boxes of size $1^\circ \times 1^\circ$ of ΔSSS (ISAS - TSG (GOSUD-Sailing-ship)) for 5 different subdatasets corresponding to: $\text{RR}=0 \text{ mm/h}$, $3 < U_{10} < 12 \text{ m/s}$, $\text{SST}>5^\circ\text{C}$, distance to coast $> 800 \text{ km}$ (a), $\text{RR}=0 \text{ mm/h}$, $3 < U_{10} < 12 \text{ m/s}$ (b), $\text{RR}>1\text{mm/h}$ and $U_{10} < 4\text{m/s}$ (c), WOA2013 SSS Std<0.2 (d), WOA2013 SSS Std>0.2 (e).

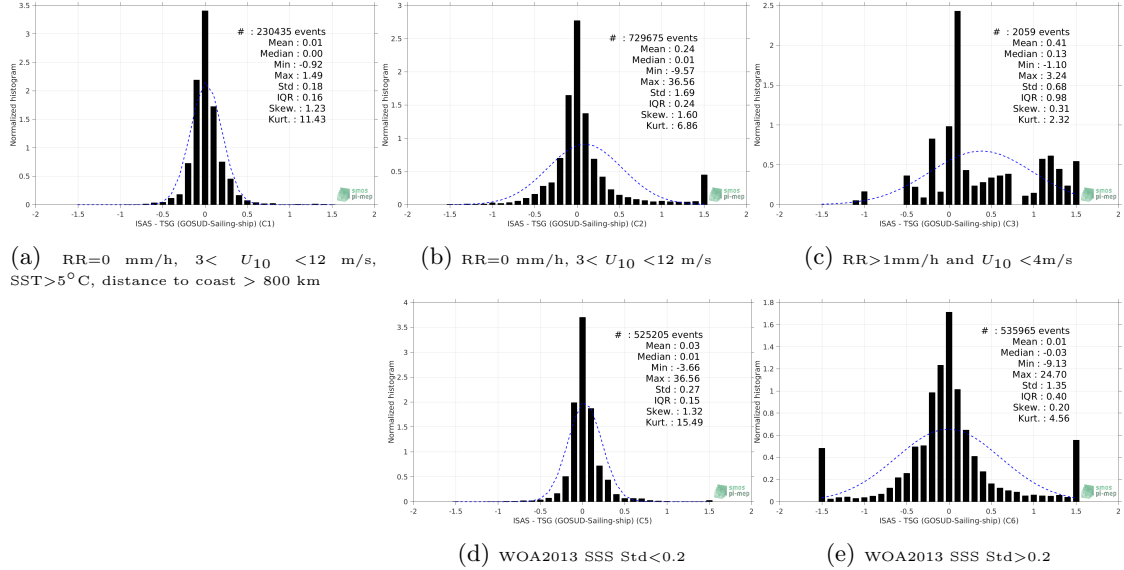


Figure 48: Normalized histogram of ΔSSS (ISAS - TSG (GOSUD-Sailing-ship)) for 5 different subdatasets corresponding to: RR=0 mm/h, $3 < U_{10} < 12$ m/s, SST > 5°C, distance to coast > 800 km (a), RR=0 mm/h, $3 < U_{10} < 12$ m/s (b), RR > 1mm/h and $U_{10} < 4$ m/s (c), WOA2013 SSS Std < 0.2 (d), WOA2013 SSS Std > 0.2 (e).

3.3.13 Summary

Table 1 shows the mean, median, standard deviation (Std), root mean square (RMS), interquartile range (IQR), correlation coefficient (r^2) and robust standard deviation (Std*) of the match-up differences ΔSSS (ISAS - TSG (GOSUD-Sailing-ship)) for the following conditions:

- all: All the match-up pairs satellite/in situ SSS values are used to derive the statistics
- C1: only pairs where RR=0 mm/h, $3 < U_{10} < 12$ m/s, SST > 5°C, distance to coast > 800 km
- C2: only pairs where RR=0 mm/h, $3 < U_{10} < 12$ m/s
- C3: only pairs where RR > 1mm/h and $U_{10} < 4$ m/s
- C5: only pairs where WOA2013 SSS Std < 0.2
- C6: only pairs where WOA2013 SSS Std > 0.2
- C7a: only pairs with a distance to coast < 150 km.
- C7b: only pairs with a distance to coast in the range [150, 800] km.
- C7c: only pairs with a distance to coast > 800 km.
- C8a: only pairs where SST is < 5°C.
- C8b: only pairs where SST is in the range [5, 15]°C.
- C8c: only pairs where SST is > 15°C.

- C9a: only pairs where SSS is < 33 .
- C9b: only pairs where SSS is in the range [33, 37].
- C9c: only pairs where SSS is > 37 .

Table 1: Statistics of Δ SSS (ISAS - TSG (GOSUD-Sailing-ship))

Condition	#	Median	Mean	Std	RMS	IQR	r^2	Std*
all	1331603	0.02	0.40	2.21	2.24	0.36	0.50	0.24
C1	230435	0.00	0.01	0.18	0.18	0.16	0.97	0.12
C2	729675	0.01	0.24	1.69	1.71	0.24	0.46	0.17
C3	2059	0.13	0.41	0.68	0.79	0.98	0.94	0.48
C5	525205	0.01	0.03	0.27	0.28	0.15	0.95	0.11
C6	535965	-0.03	0.01	1.35	1.35	0.40	0.75	0.30
C7a	571269	0.15	0.96	3.24	3.38	1.14	0.36	0.66
C7b	429024	-0.01	-0.04	0.60	0.61	0.22	0.88	0.16
C7c	331189	0.00	0.01	0.23	0.23	0.17	0.96	0.12
C8a	210154	0.06	-0.12	1.68	1.68	0.64	0.67	0.47
C8b	278177	0.08	0.65	2.03	2.14	0.64	0.59	0.30
C8c	793950	0.00	0.37	2.34	2.37	0.24	0.36	0.18
C9a	247568	1.07	2.23	4.54	5.06	2.23	0.10	1.50
C9b	1050983	-0.01	-0.02	0.58	0.58	0.23	0.77	0.17
C9c	33052	-0.01	-0.03	0.36	0.36	0.26	0.84	0.19

Table 1 numerical values can be downloaded as a csv file [here](#).

3.4 TSG (SAMOS)

3.4.1 Introduction

The TSG-SAMOS dataset correspond to "Research" quality data from the US Shipboard Automated Meteorological and Oceanographic System (SAMOS) initiative ([Smith et al. \(2009\)](#)). Data are available at <http://samos.coaps.fsu.edu/html/>. Adjusted values when available and only collected TSG data that exhibit quality flags=1 and 2 were used. After visual inspection, data from the NANCY FOSTER (ID="WTER", IMO="008993227") with date 2011/03/21 and all data from the ATLANTIS (ID="KAQP", IMO="009105798") for year 2010 has been remove from this dataset.

3.4.2 Number of SSS data as a function of time and distance to coast

Figure 49 shows the time (a) and distance to coast (b) distributions of the TSG (SAMOS) *in situ* dataset.

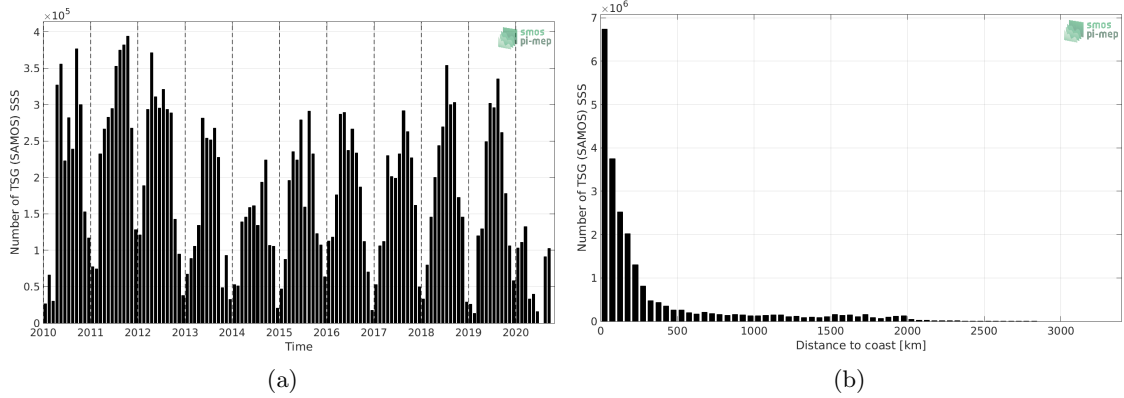


Figure 49: Number of SSS from TSG (SAMOS) as a function of time (a) and distance to coast (b).

3.4.3 Histograms of SSS

Figure 50 shows the SSS distribution of the TSG (SAMOS) (a) and colocalized ISAS (b) dataset.

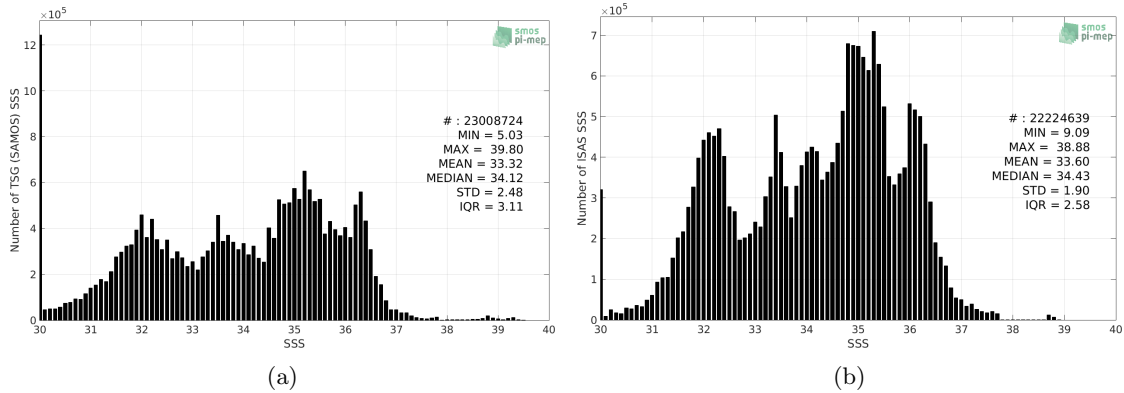


Figure 50: Histograms of SSS from TSG (SAMOS) (a) and ISAS (b) per bins of 0.1.

3.4.4 Distribution of *in situ* SSS depth measurements

In Figure 51, we show the depth distribution of the *in situ* salinity dataset (a) and the spatial distribution of the depth temporal mean in $1^\circ \times 1^\circ$ boxes and considering the full *in situ* dataset period (b).

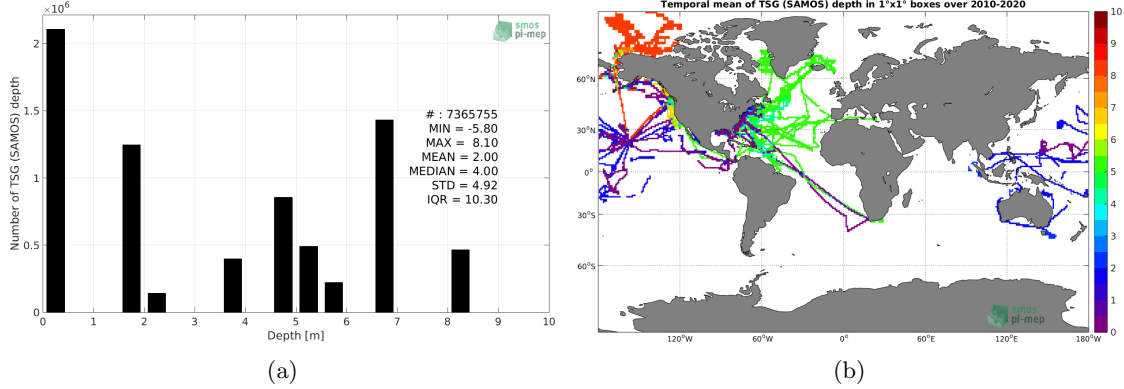


Figure 51: Depth distribution of the upper level SSS measurements from TSG (SAMOS) (a) and spatial distribution of the *in situ* SSS depth measurements showing the mean value in $1^\circ \times 1^\circ$ boxes and considering the full *in situ* dataset period (b).

3.4.5 Spatial distribution of SSS

In Figure 52, the number of TSG (SAMOS) SSS measurements in $1^\circ \times 1^\circ$ boxes is shown.

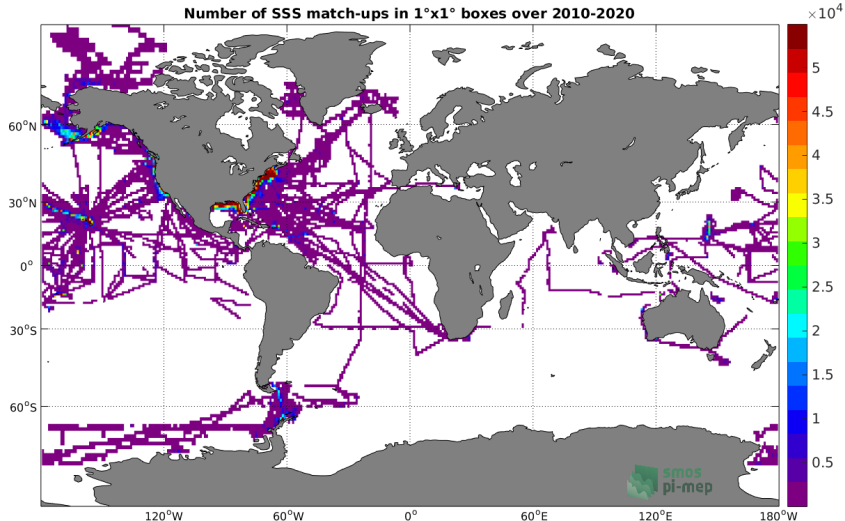


Figure 52: Number of SSS from TSG (SAMOS) in $1^\circ \times 1^\circ$ boxes.

3.4.6 Spatial Maps of the Temporal mean and Std of *in situ* and ISAS SSS and of the difference (Δ SSS)

In Figure 53, we show maps of temporal mean (left) and standard deviation (right) of ISAS (top), TSG (SAMOS) *in situ* dataset (middle) and the difference Δ SSS(ISAS - TSG (SAMOS)) (bottom). The temporal mean and std are calculated using all match-up pairs falling in spatial boxes of size $1^\circ \times 1^\circ$ over the full TSG (SAMOS) dataset period.

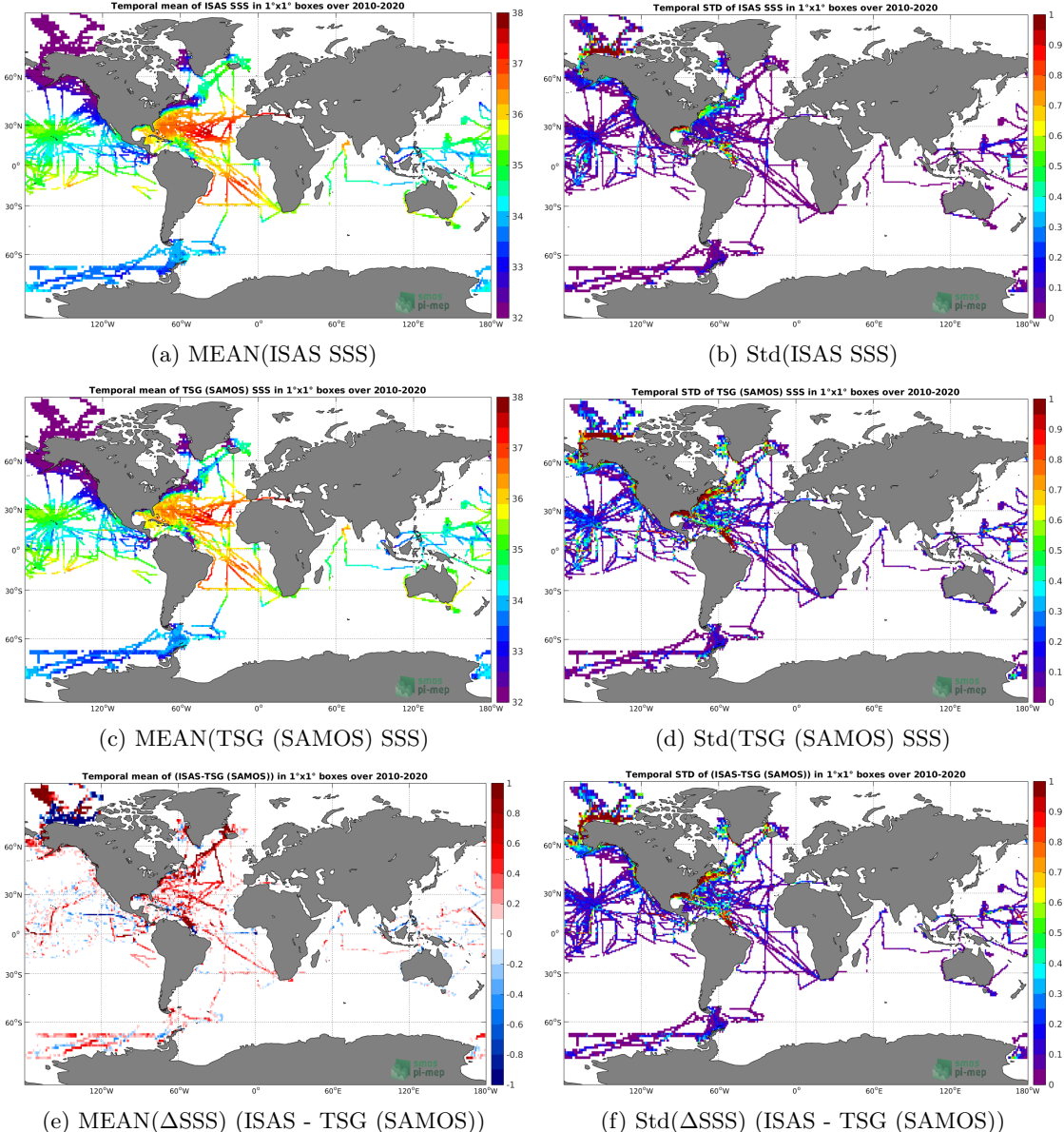


Figure 53: Temporal mean (left) and Std (right) of SSS from ISAS (top), TSG (SAMOS) (middle), and of Δ SSS (ISAS - TSG (SAMOS)). Only match-up pairs are used to generate these maps.

3.4.7 Time series of the monthly median and Std of *in situ* and ISAS SSS and of the difference (Δ SSS)

In the top panel of Figure 54, we show the time series of the monthly median SSS estimated for both ISAS SSS product (in black) and the TSG (SAMOS) *in situ* dataset (in blue) at the collected Pi-MEP match-up pairs.

In the middle panel of Figure 54, we show the time series of the monthly median of Δ SSS (ISAS - TSG (SAMOS)) for the collected Pi-MEP match-up pairs.

In the bottom panel of Figure 54, we show the time series of the monthly standard deviation of the ΔSSS (ISAS - TSG (SAMOS)) for the collected Pi-MEP match-up pairs.

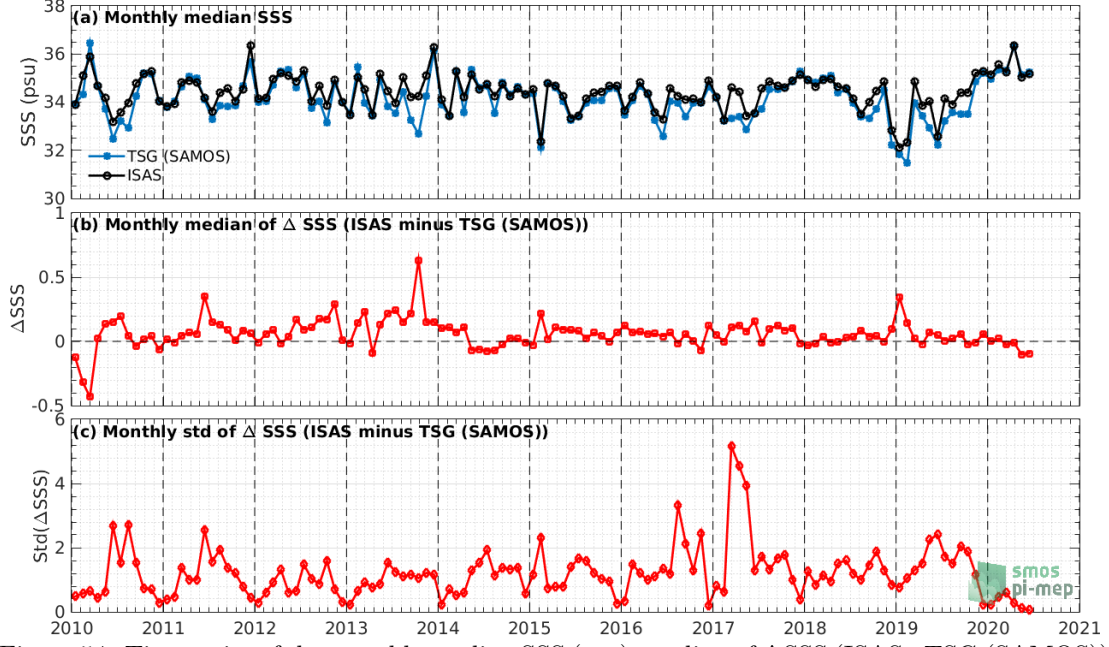


Figure 54: Time series of the monthly median SSS (top), median of ΔSSS (ISAS - TSG (SAMOS)) and Std of ΔSSS (ISAS - TSG (SAMOS)) considering all match-ups collected by the Pi-MEP.

3.4.8 Zonal mean and Std of *in situ* and ISAS SSS and of the difference ΔSSS

In Figure 55 left panel, we show the zonal mean SSS considering all Pi-MEP match-up pairs for both ISAS SSS product (in black) and the TSG (SAMOS) *in situ* dataset (in blue). The full *in situ* dataset period is used to derive the mean.

In the right panel of Figure 55, we show the zonal mean of ΔSSS (ISAS - TSG (SAMOS)) for all the collected Pi-MEP match-up pairs estimated over the full *in situ* dataset period.

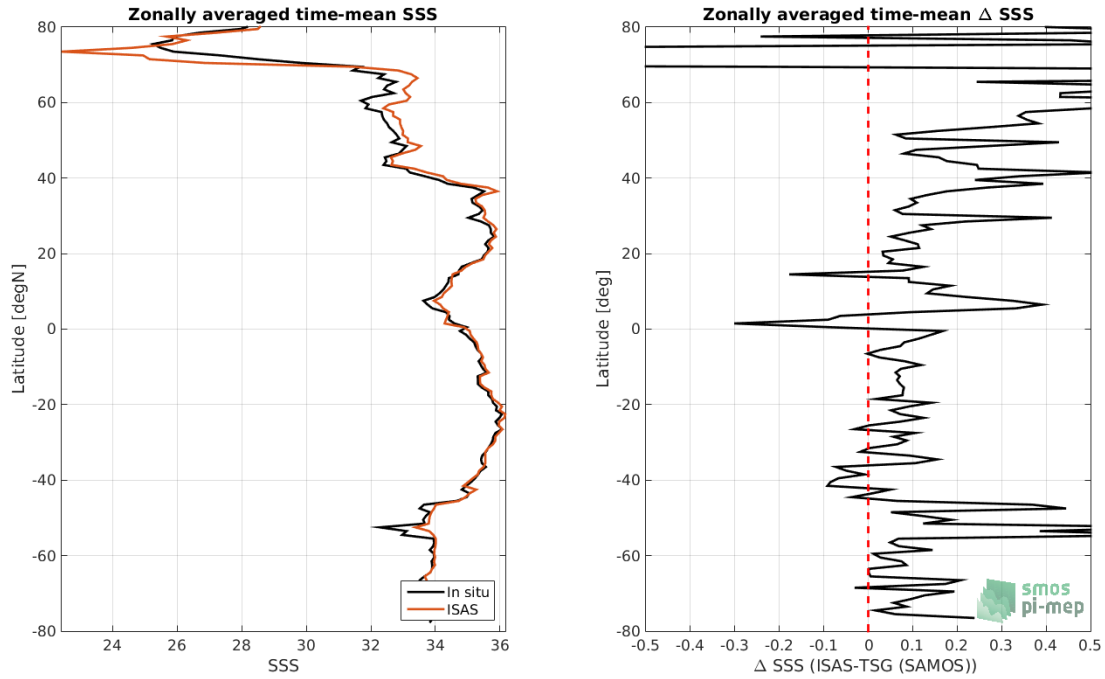


Figure 55: Left panel: Zonal mean SSS from ISAS product (black) and from TSG (SAMOS) (blue). Right panel: Zonal mean of Δ SSS (ISAS - TSG (SAMOS)) for all the collected Pi-MEP match-up pairs estimated over the full *in situ* dataset period.

3.4.9 Scatterplots of ISAS vs *in situ* SSS by latitudinal bands

In Figure 56, contour maps of the concentration of ISAS SSS (y-axis) versus TSG (SAMOS) SSS (x-axis) at match-up pairs for different latitude bands: (a) 80°S-80°N, (b) 20°S-20°N, (c) 40°S-20°S and 20°N-40°N and (d) 60°S-40°S and 40°N-60°N. For each plot, the red line shows $x=y$. The black thin and dashed lines indicate a linear fit through the data cloud and the $\pm 95\%$ confidence levels, respectively. The number match-up pairs n , the slope and R^2 coefficient of the linear fit, the root mean square (RMS) and the mean bias between ISAS and *in situ* data are indicated for each latitude band in each plots.

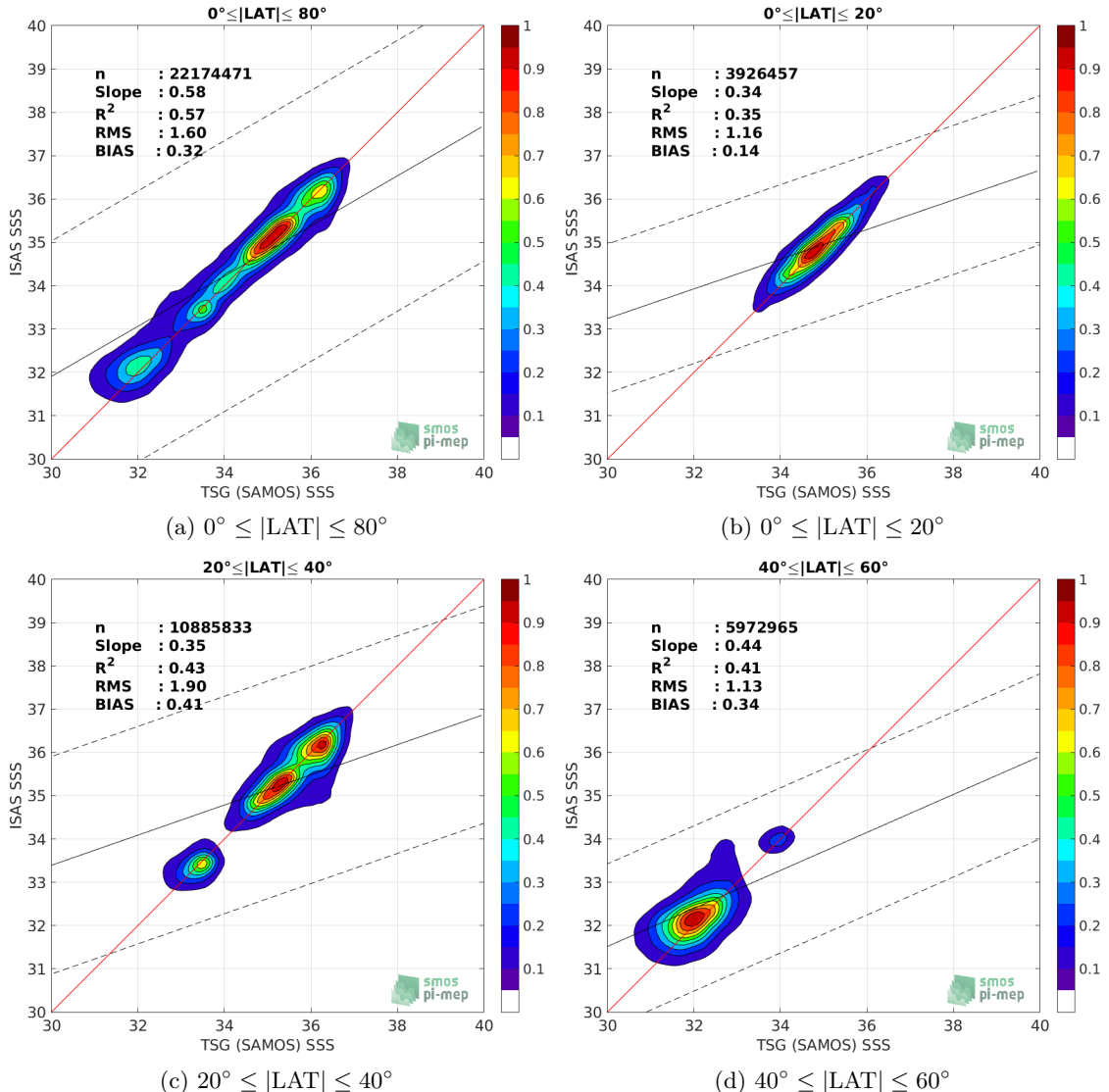


Figure 56: Contour maps of the concentration of ISAS SSS (y-axis) versus TSG (SAMOS) SSS (x-axis) at match-up pairs for different latitude bands. For each plot, the red line shows $x=y$. The black thin and dashed lines indicate a linear fit through the data cloud and the $\pm 95\%$ confidence levels, respectively. The number match-up pairs n , the slope and R^2 coefficient of the linear fit, the root mean square (RMS) and the mean bias between ISAS and *in situ* data are indicated for each latitude band in each plots.

3.4.10 Time series of the monthly median and Std of the difference ΔSSS sorted by latitudinal bands

In Figure 57, time series of the monthly median (red curves) of ΔSSS ($\text{ISAS} - \text{TSG (SAMOS)}$) and ± 1 Std (black vertical thick bars) as function of time for all the collected Pi-MEP match-up pairs estimated for the full *in situ* dataset period are shown for different latitude bands: (a) $80^\circ\text{S}-80^\circ\text{N}$, (b) $20^\circ\text{S}-20^\circ\text{N}$, (c) $40^\circ\text{S}-20^\circ\text{N}$ and $20^\circ\text{N}-40^\circ\text{N}$ and (d) $60^\circ\text{S}-40^\circ\text{S}$ and $40^\circ\text{N}-60^\circ\text{N}$.

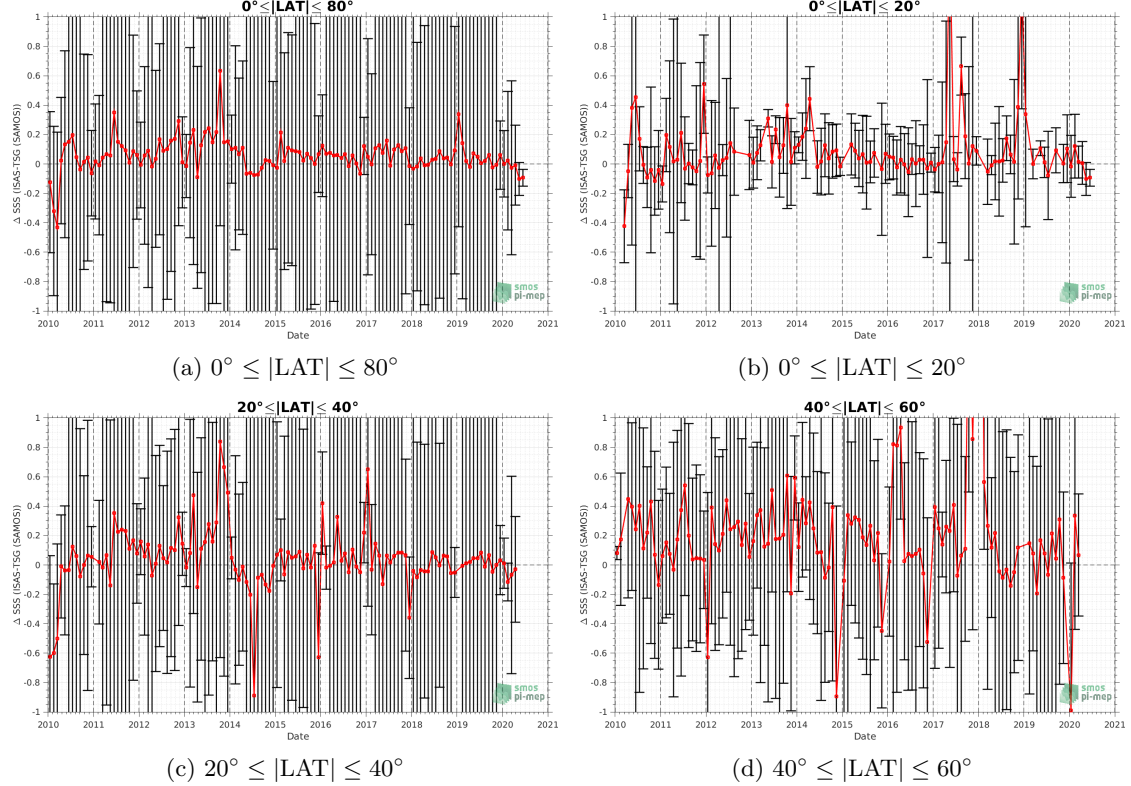


Figure 57: Monthly median (red curves) of ΔSSS (ISAS - TSG (SAMOS)) and $\pm 1 \text{ Std}$ (black vertical thick bars) as function of time for all the collected Pi-MEP match-up pairs for the full *in situ* dataset period are shown for different latitude bands: (a) $80^\circ\text{S}-80^\circ\text{N}$, (b) $20^\circ\text{S}-20^\circ\text{N}$, (c) $40^\circ\text{S}-20^\circ\text{S}$ and $20^\circ\text{N}-40^\circ\text{N}$ and (d) $60^\circ\text{S}-40^\circ\text{S}$ and $40^\circ\text{N}-60^\circ\text{N}$.

3.4.11 ΔSSS sorted as geophysical conditions

In Figure 58, we classify the match-up differences ΔSSS (ISAS - *in situ*) as function of the geophysical conditions at match-up points. The mean and std of ΔSSS (ISAS - TSG (SAMOS)) is thus evaluated as function of the

- *in situ* SSS values per bins of width 0.2,
- *in situ* SST values per bins of width 1°C ,
- ASCAT daily wind values per bins of width 1 m/s,
- CMORPH 3-hourly rain rates per bins of width 1 mm/h, and,
- distance to coasts per bins of width 50 km,
- *in situ* measurement depth (if relevant).

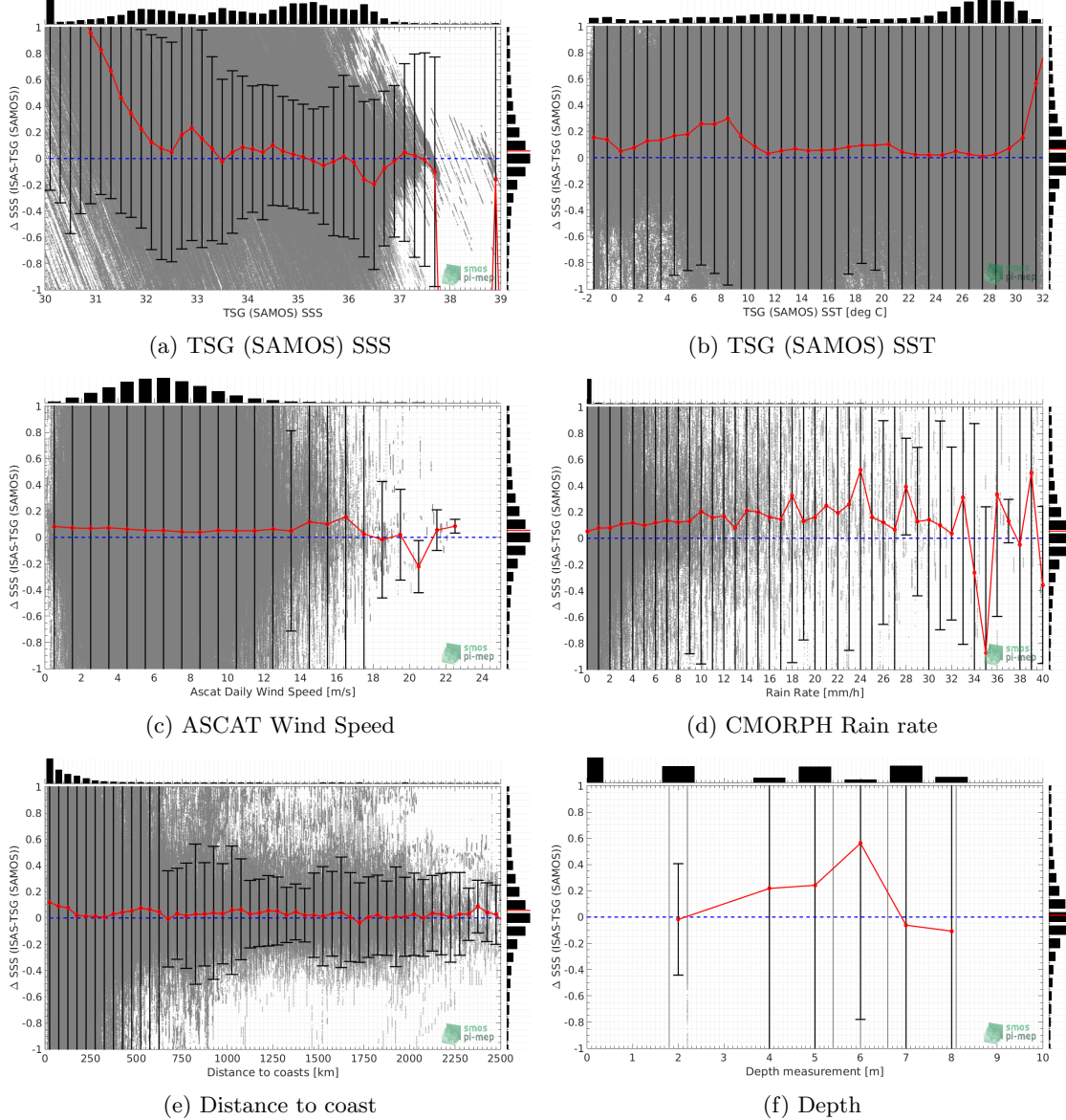


Figure 58: ΔSSS (ISAS - TSG (SAMOS)) sorted as geophysical conditions: TSG (SAMOS) SSS a), TSG (SAMOS) SST b), ASCAT Wind speed c), CMORPH rain rate d), distance to coast e) and depth measurements f).

3.4.12 ΔSSS maps and statistics for different geophysical conditions

In Figures 59 and 60, we focus on sub-datasets of the match-up differences ΔSSS (ISAS - *in situ*) for the following specific geophysical conditions:

- **C1:** if the local value at *in situ* location of estimated rain rate is zero, mean daily wind is in the range [3, 12] m/s, the SST is $> 5^{\circ}\text{C}$ and distance to coast is > 800 km.
- **C2:** if the local value at *in situ* location of estimated rain rate is zero, mean daily wind is

in the range [3, 12] m/s.

- **C3:** if the local value at *in situ* location of estimated rain rate is high (ie. $> 1 \text{ mm/h}$) and mean daily wind is low (ie. $< 4 \text{ m/s}$).
- **C5:** if the *in situ* data is located where the climatological SSS standard deviation is low (ie. above < 0.2).
- **C6:** if the *in situ* data is located where the climatological SSS standard deviation is high (ie. above > 0.2).

For each of these conditions, the temporal mean (gridded over spatial boxes of size $1^\circ \times 1^\circ$) and the histogram of the difference ΔSSS (ISAS - *in situ*) are presented.

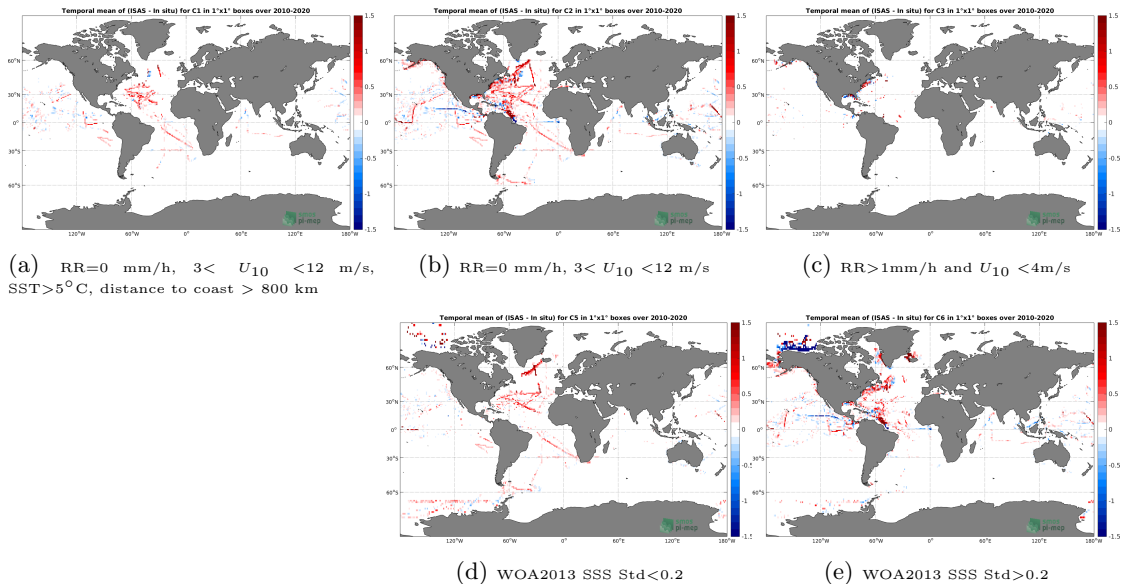


Figure 59: Temporal mean gridded over spatial boxes of size $1^\circ \times 1^\circ$ of ΔSSS (ISAS - TSG (SAMOS)) for 5 different subdatasets corresponding to: $\text{RR}=0 \text{ mm/h}, 3 < U_{10} < 12 \text{ m/s}, \text{SST} > 5^\circ\text{C}, \text{distance to coast} > 800 \text{ km}$ (a), $\text{RR}=0 \text{ mm/h}, 3 < U_{10} < 12 \text{ m/s}$ (b), $\text{RR} > 1 \text{ mm/h and } U_{10} < 4 \text{ m/s}$ (c), WOA2013 SSS Std < 0.2 (d), WOA2013 SSS Std > 0.2 (e).

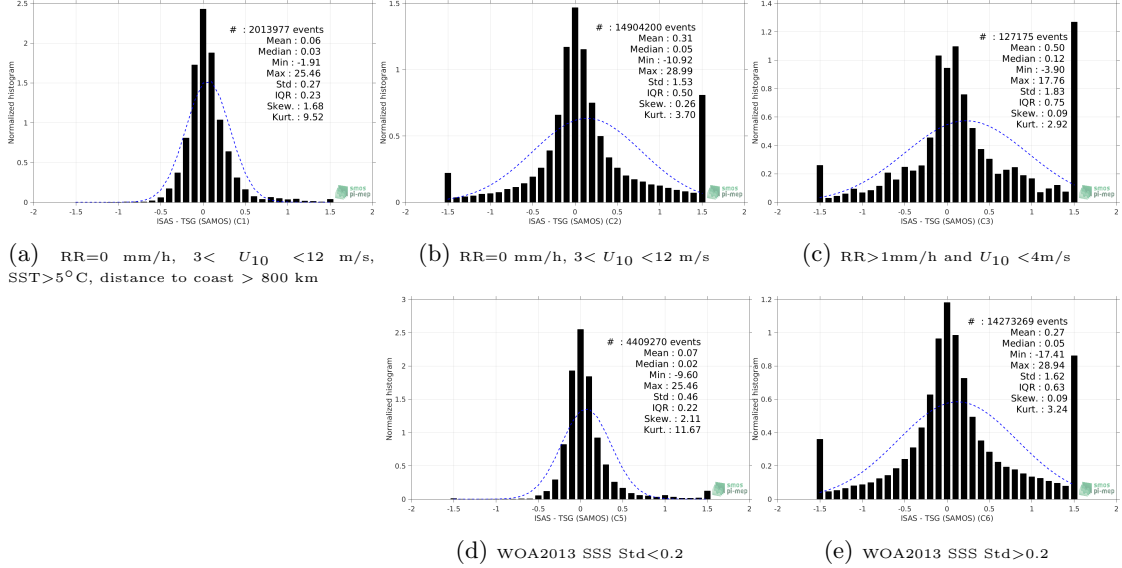


Figure 60: Normalized histogram of ΔSSS (ISAS - TSG (SAMOS)) for 5 different subdatasets corresponding to: RR=0 mm/h, $3 < U_{10} < 12$ m/s, SST > 5°C, distance to coast > 800 km (a), RR=0 mm/h, $3 < U_{10} < 12$ m/s (b), RR > 1mm/h and $U_{10} < 4$ m/s (c), WOA2013 SSS Std < 0.2 (d), WOA2013 SSS Std > 0.2 (e).

3.4.13 Summary

Table 1 shows the mean, median, standard deviation (Std), root mean square (RMS), interquartile range (IQR), correlation coefficient (r^2) and robust standard deviation (Std*) of the match-up differences ΔSSS (ISAS - TSG (SAMOS)) for the following conditions:

- all: All the match-up pairs satellite/in situ SSS values are used to derive the statistics
- C1: only pairs where RR=0 mm/h, $3 < U_{10} < 12$ m/s, SST > 5°C, distance to coast > 800 km
- C2: only pairs where RR=0 mm/h, $3 < U_{10} < 12$ m/s
- C3: only pairs where RR > 1mm/h and $U_{10} < 4$ m/s
- C5: only pairs where WOA2013 SSS Std < 0.2
- C6: only pairs where WOA2013 SSS Std > 0.2
- C7a: only pairs with a distance to coast < 150 km.
- C7b: only pairs with a distance to coast in the range [150, 800] km.
- C7c: only pairs with a distance to coast > 800 km.
- C8a: only pairs where SST is < 5°C.
- C8b: only pairs where SST is in the range [5, 15]°C.
- C8c: only pairs where SST is > 15°C.

- C9a: only pairs where SSS is < 33.
- C9b: only pairs where SSS is in the range [33, 37].
- C9c: only pairs where SSS is > 37.

Table 1: Statistics of ΔSSS (ISAS - TSG (SAMOS))

Condition	#	Median	Mean	Std	RMS	IQR	r^2	Std*
all	22224639	0.06	0.32	1.56	1.60	0.54	0.57	0.37
C1	2013977	0.03	0.06	0.27	0.27	0.23	0.91	0.17
C2	14904200	0.05	0.31	1.53	1.56	0.50	0.56	0.35
C3	127175	0.12	0.50	1.83	1.90	0.75	0.44	0.49
C5	4409270	0.02	0.07	0.46	0.46	0.22	0.87	0.16
C6	14273269	0.05	0.27	1.62	1.64	0.63	0.54	0.45
C7a	12280524	0.10	0.48	1.83	1.89	0.77	0.47	0.51
C7b	6783202	0.03	0.13	1.35	1.36	0.45	0.61	0.33
C7c	3134630	0.03	0.09	0.35	0.36	0.24	0.91	0.18
C8a	1854121	0.12	0.06	1.31	1.31	0.52	0.75	0.37
C8b	5273777	0.12	0.31	1.29	1.33	0.77	0.35	0.54
C8c	13476278	0.04	0.37	1.70	1.74	0.45	0.47	0.31
C9a	7383598	0.42	1.01	2.44	2.64	1.31	0.07	0.84
C9b	14579216	0.00	-0.01	0.56	0.56	0.33	0.71	0.25
C9c	261825	-0.10	-1.07	1.53	1.87	2.79	0.06	0.44

Table 1 numerical values can be downloaded as a csv file [here](#).

3.5 TSG (LEGOS-Survostral)

3.5.1 Introduction

The TSG-LEGOS-Survostral dataset correspond to delayed mode regional data from TSG installed on the Astrolabe vessel (IPEV) during the round trips between Hobart (Tasmania) and the French Antarctic base at Dumont d'Urville ([Morrow and Kestenare \(2014\)](#)). It is provided by the [Survostral project](#) and available via [ftp](#). Adjusted values when available and only collected TSG data that exhibit quality flags=1 and 2 were used.

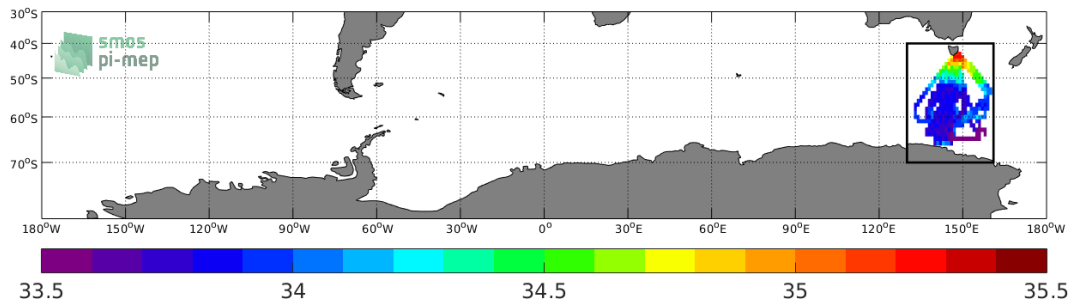


Figure 61: Location of the TSG (LEGOS-Survostral) dataset.

3.5.2 Number of SSS data as a function of time and distance to coast

Figure 62 shows the time (a) and distance to coast (b) distributions of the TSG (LEGOS-Survostral) *in situ* dataset.

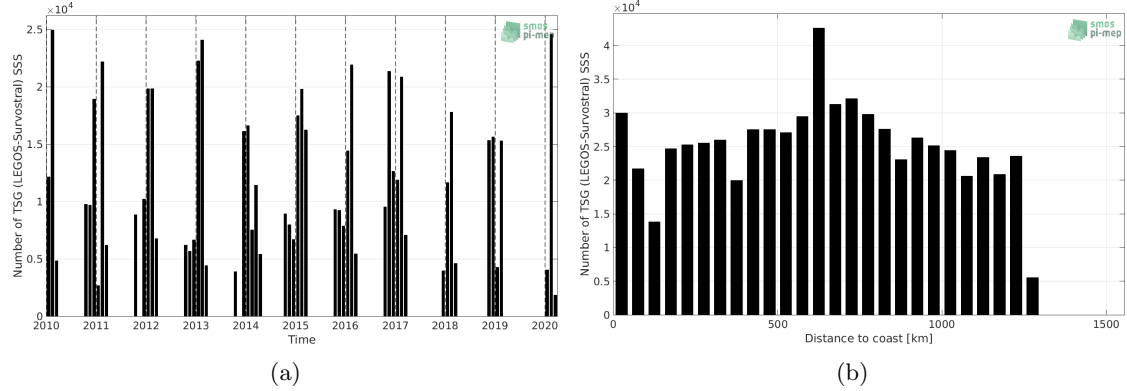


Figure 62: Number of SSS from TSG (LEGOS-Survostral) as a function of time (a) and distance to coast (b).

3.5.3 Histograms of SSS

Figure 63 shows the SSS distribution of the TSG (LEGOS-Survostral) (a) and colocalized ISAS (b) dataset.

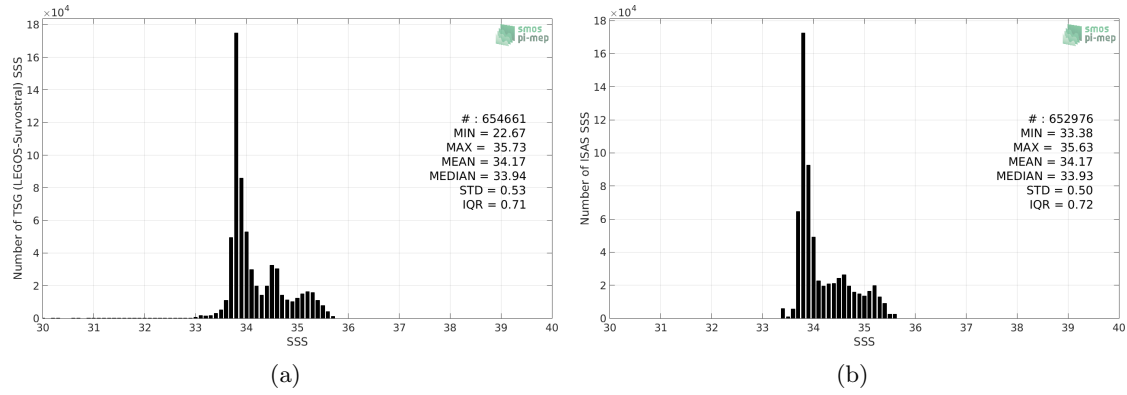


Figure 63: Histograms of SSS from TSG (LEGOS-Survostral) (a) and ISAS (b) per bins of 0.1.

3.5.4 Distribution of *in situ* SSS depth measurements

In Figure 64, we show the depth distribution of the *in situ* salinity dataset (a) and the spatial distribution of the depth temporal mean in $1^\circ \times 1^\circ$ boxes and considering the full *in situ* dataset period (b).

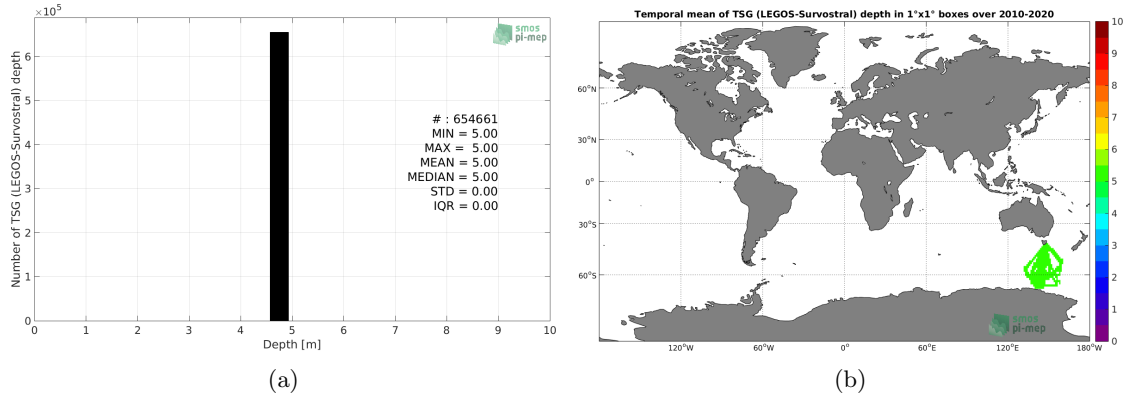


Figure 64: Depth distribution of the upper level SSS measurements from TSG (LEGOS-Survostral) (a) and spatial distribution of the *in situ* SSS depth measurements showing the mean value in $1^\circ \times 1^\circ$ boxes and considering the full *in situ* dataset period (b).

3.5.5 Spatial distribution of SSS

In Figure 65, the number of TSG (LEGOS-Survostral) SSS measurements in $1^\circ \times 1^\circ$ boxes is shown.

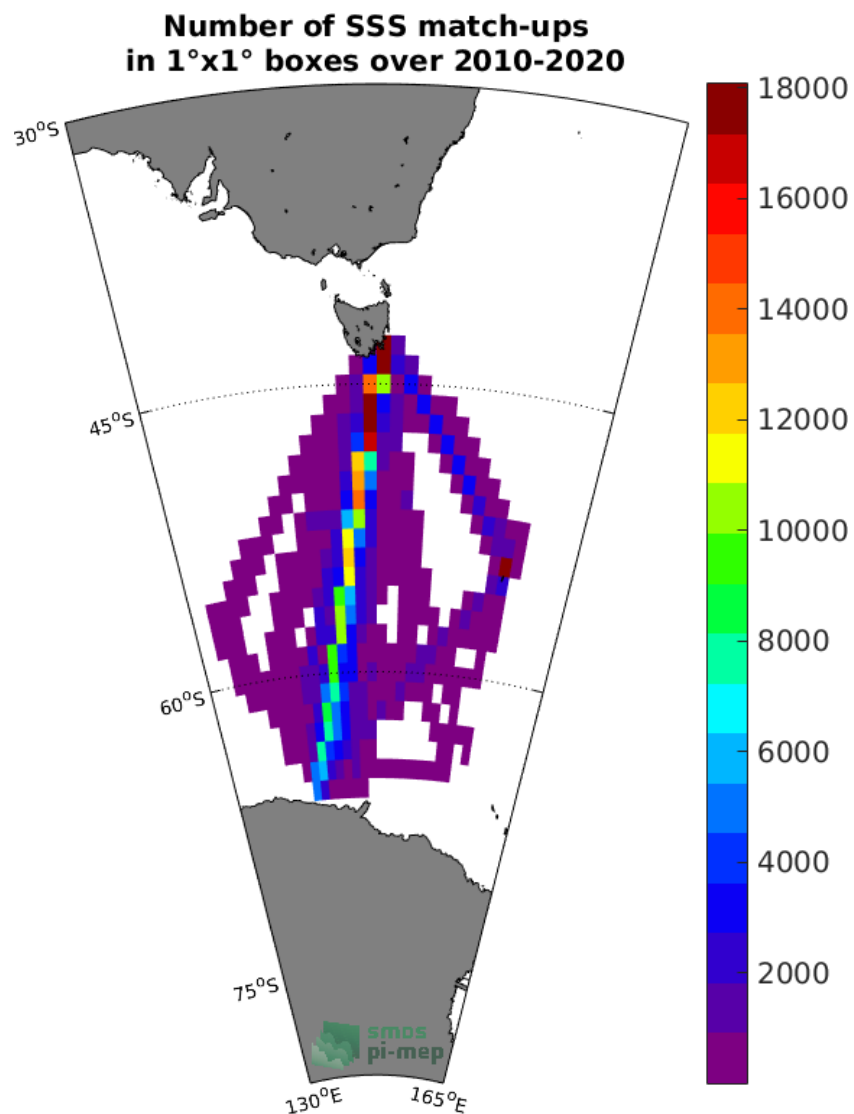


Figure 65: Number of SSS from TSG (LEGOS-Survostral) in $1^\circ \times 1^\circ$ boxes.

3.5.6 Spatial Maps of the Temporal mean and Std of *in situ* and ISAS SSS and of the difference (Δ SSS)

In Figure 66, we show maps of temporal mean (left) and standard deviation (right) of ISAS (top), TSG (LEGOS-Survostral) *in situ* dataset (middle) and the difference Δ SSS(ISAS -TSG (LEGOS-Survostral)) (bottom). The temporal mean and std are calculated using all match-up pairs falling in spatial boxes of size $1^\circ \times 1^\circ$ over the full TSG (LEGOS-Survostral) dataset period.

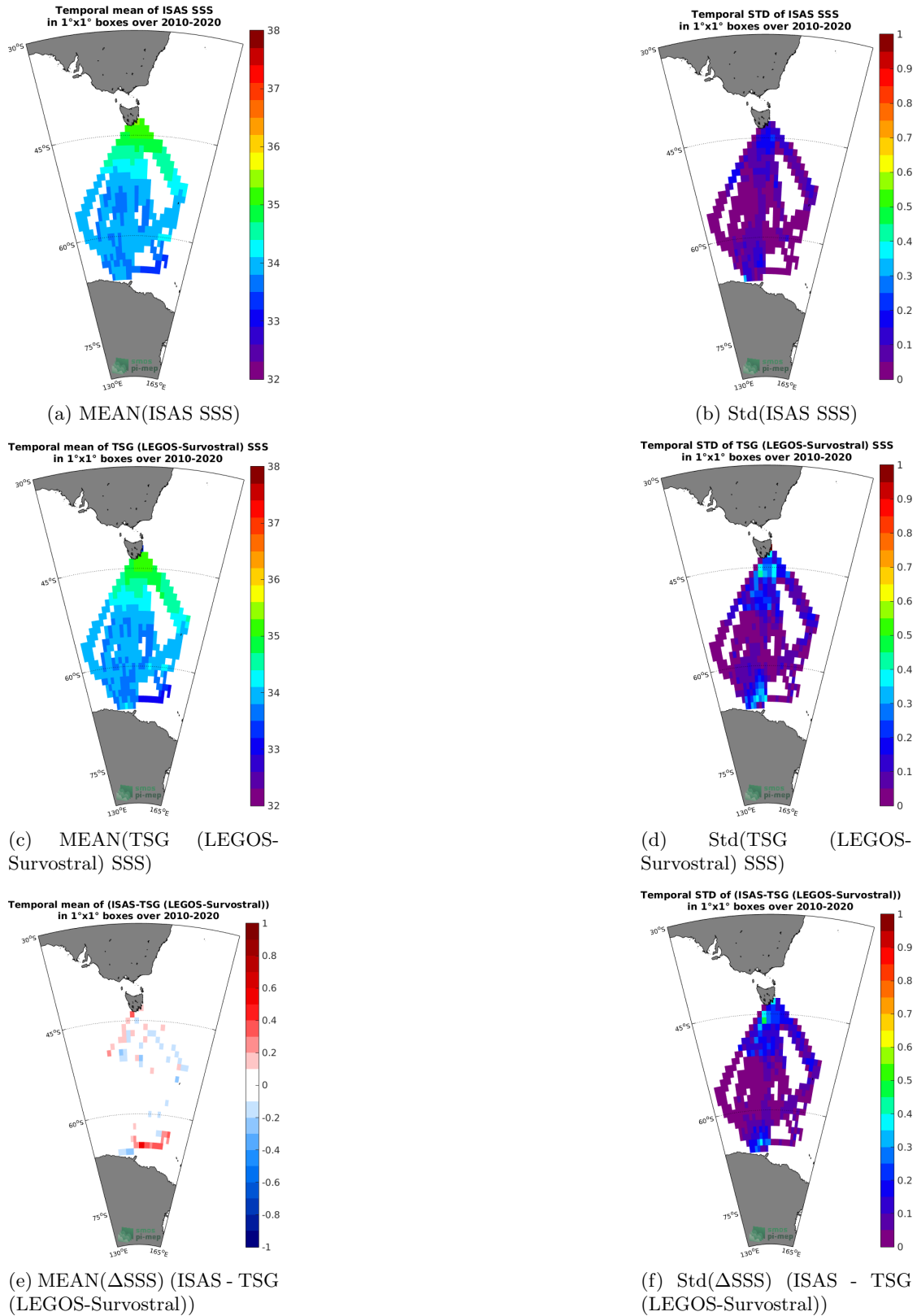


Figure 66: Temporal mean (left) and Std (right) of SSS from ISAS (top), TSG (LEGOS-Survostral) (middle), and of Δ SSS (ISAS - TSG (LEGOS-Survostral)). Only match-up pairs are used to generate these maps.

3.5.7 Time series of the monthly median and Std of *in situ* and ISAS SSS and of the difference (Δ SSS)

In the top panel of Figure 67, we show the time series of the monthly median SSS estimated for both ISAS SSS product (in black) and the TSG (LEGOS-Survostral) *in situ* dataset (in blue) at the collected Pi-MEP match-up pairs.

In the middle panel of Figure 67, we show the time series of the monthly median of Δ SSS (ISAS - TSG (LEGOS-Survostral)) for the collected Pi-MEP match-up pairs.

In the bottom panel of Figure 67, we show the time series of the monthly standard deviation of the Δ SSS (ISAS - TSG (LEGOS-Survostral)) for the collected Pi-MEP match-up pairs.

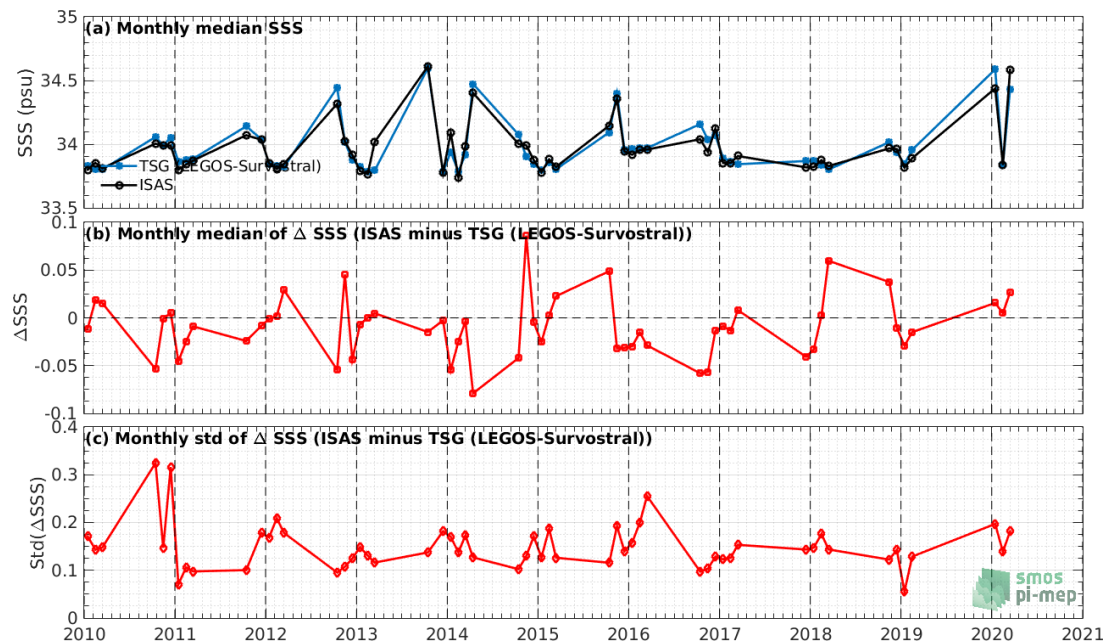


Figure 67: Time series of the monthly median SSS (top), median of Δ SSS (ISAS - TSG (LEGOS-Survostral)) and Std of Δ SSS (ISAS - TSG (LEGOS-Survostral)) considering all match-ups collected by the Pi-MEP.

3.5.8 Zonal mean and Std of *in situ* and ISAS SSS and of the difference Δ SSS

In Figure 68 left panel, we show the zonal mean SSS considering all Pi-MEP match-up pairs for both ISAS SSS product (in black) and the TSG (LEGOS-Survostral) *in situ* dataset (in blue). The full *in situ* dataset period is used to derive the mean.

In the right panel of Figure 68, we show the zonal mean of Δ SSS (ISAS - TSG (LEGOS-Survostral)) for all the collected Pi-MEP match-up pairs estimated over the full *in situ* dataset period.

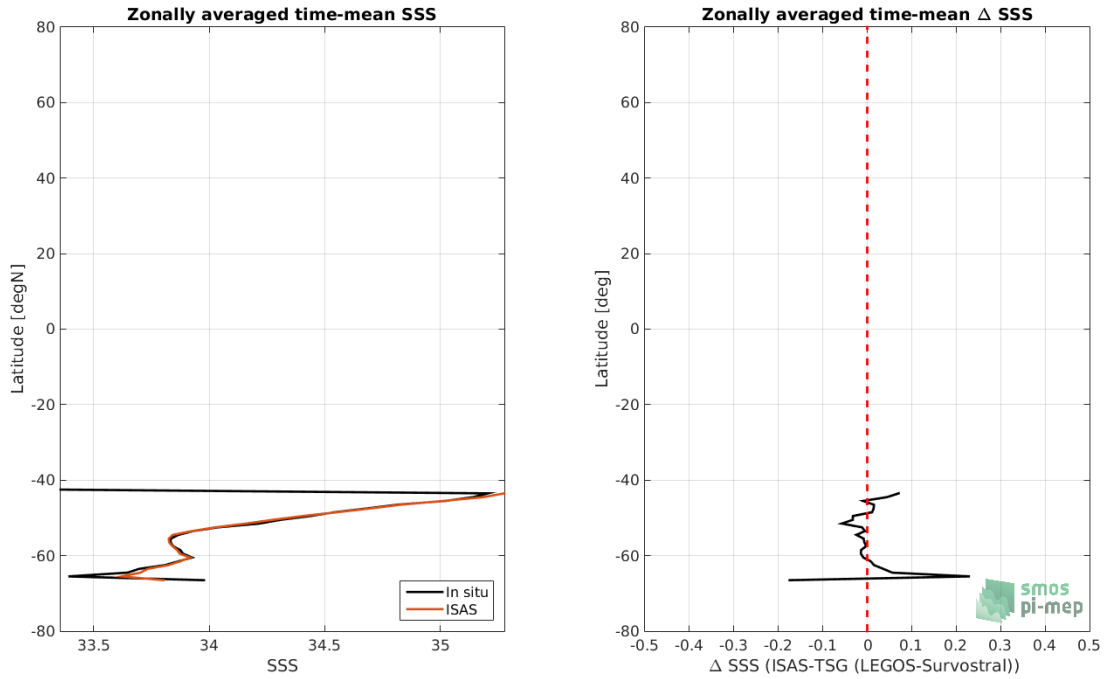


Figure 68: Left panel: Zonal mean SSS from ISAS product (black) and from TSG (LEGOS-Survostral) (blue). Right panel: Zonal mean of Δ SSS (ISAS - TSG (LEGOS-Survostral)) for all the collected Pi-MEP match-up pairs estimated over the full *in situ* dataset period.

3.5.9 Scatterplots of ISAS vs *in situ* SSS by latitudinal bands

In Figure 69, contour maps of the concentration of ISAS SSS (y-axis) versus TSG (LEGOS-Survostral) SSS (x-axis) at match-up pairs for different latitude bands: (a) 80°S-80°N, (b) 20°S-20°N, (c) 40°S-20°S and 20°N-40°N and (d) 60°S-40°S and 40°N-60°N. For each plot, the red line shows $x=y$. The black thin and dashed lines indicate a linear fit through the data cloud and the $\pm 95\%$ confidence levels, respectively. The number match-up pairs n , the slope and R^2 coefficient of the linear fit, the root mean square (RMS) and the mean bias between ISAS and *in situ* data are indicated for each latitude band in each plots.

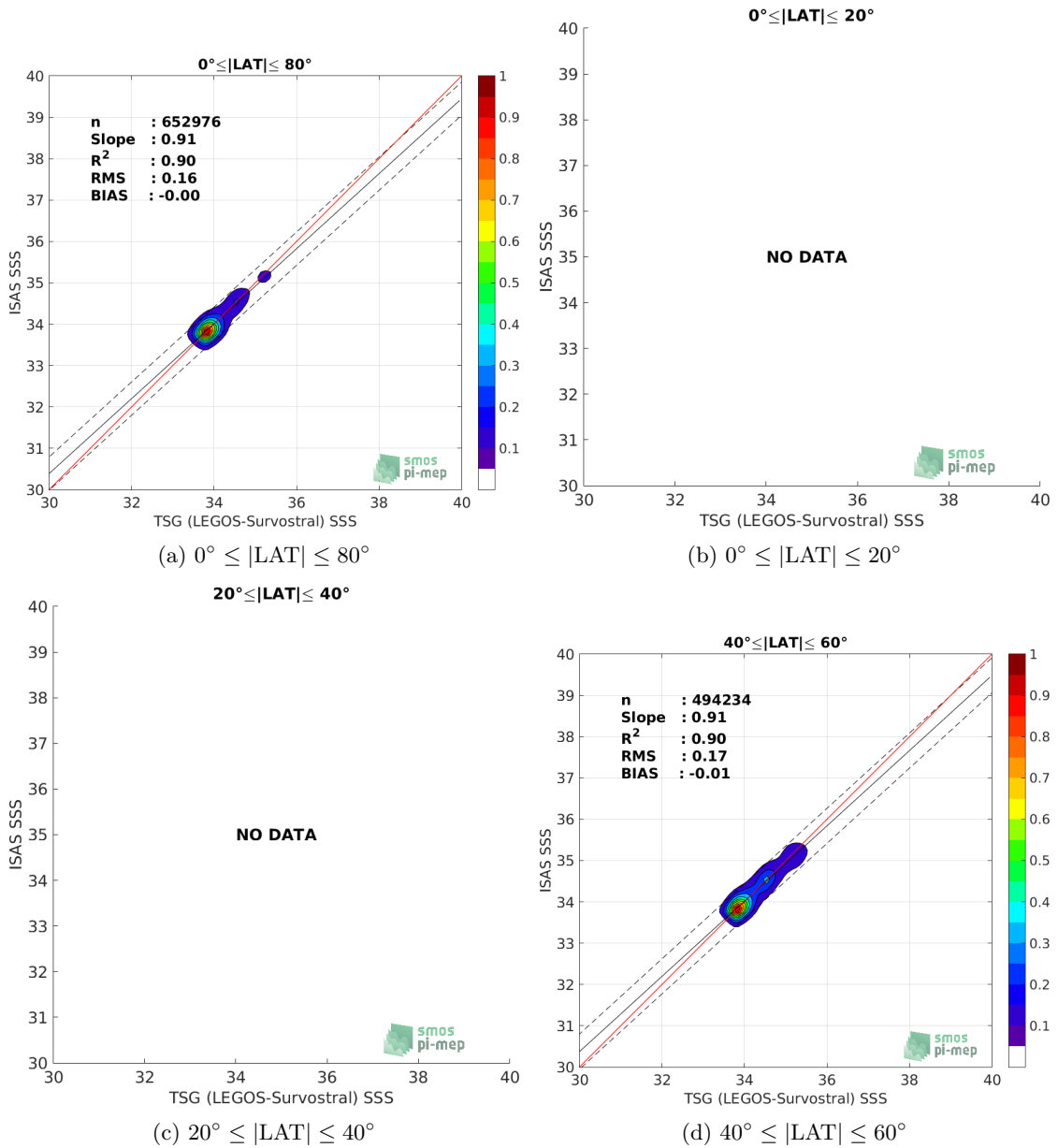


Figure 69: Contour maps of the concentration of ISAS SSS (y-axis) versus TSG (LEGOS-Survostral) SSS (x-axis) at match-up pairs for different latitude bands. For each plot, the red line shows $x=y$. The black thin and dashed lines indicate a linear fit through the data cloud and the $\pm 95\%$ confidence levels, respectively. The number match-up pairs n , the slope and R^2 coefficient of the linear fit, the root mean square (RMS) and the mean bias between ISAS and *in situ* data are indicated for each latitude band in each plots.

3.5.10 Time series of the monthly median and Std of the difference ΔSSS sorted by latitudinal bands

In Figure 70, time series of the monthly median (red curves) of ΔSSS (ISAS - TSG (LEGOS-Survostral)) and ± 1 Std (black vertical thick bars) as function of time for all the collected Pi-MEP match-up pairs estimated for the full *in situ* dataset period are shown for different latitude bands: (a) $80^{\circ}\text{S}-80^{\circ}\text{N}$, (b) $20^{\circ}\text{S}-20^{\circ}\text{N}$, (c) $40^{\circ}\text{S}-20^{\circ}\text{S}$ and $20^{\circ}\text{N}-40^{\circ}\text{N}$ and (d) $60^{\circ}\text{S}-40^{\circ}\text{S}$ and $40^{\circ}\text{N}-60^{\circ}\text{N}$.

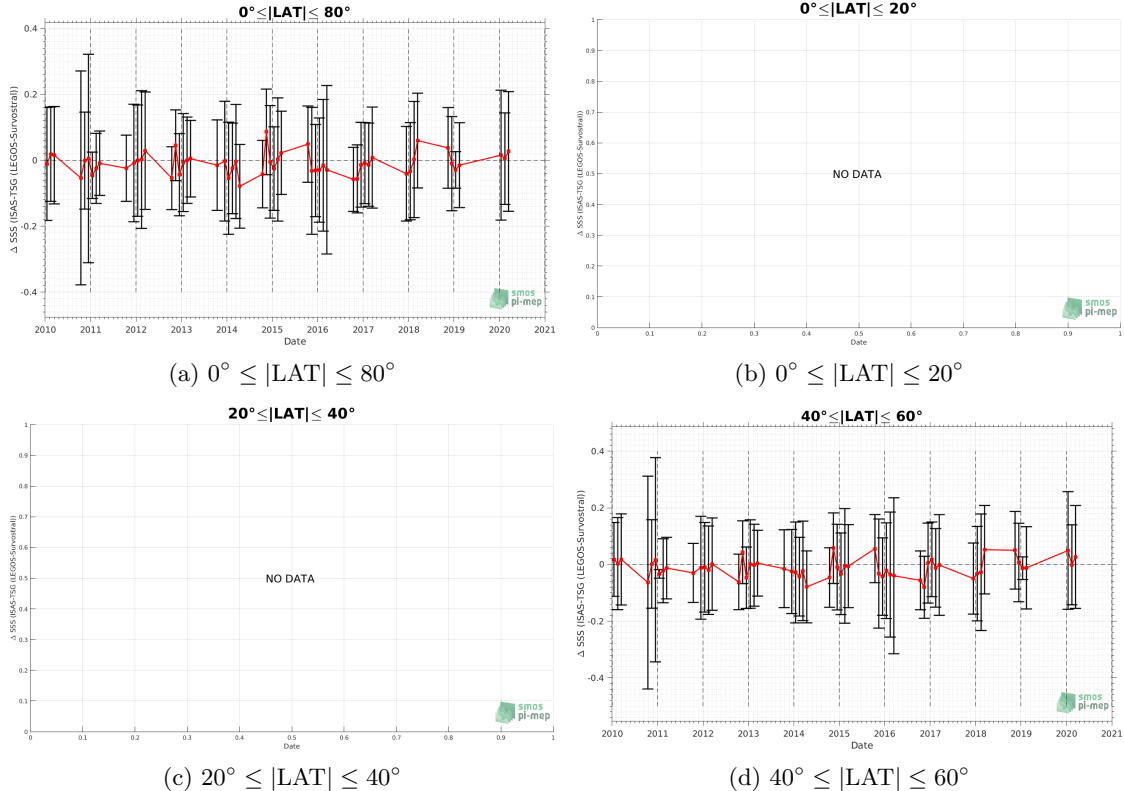


Figure 70: Monthly median (red curves) of ΔSSS (ISAS - TSG (LEGOS-Survostral)) and ± 1 Std (black vertical thick bars) as function of time for all the collected Pi-MEP match-up pairs for the full *in situ* dataset period are shown for different latitude bands: (a) $80^{\circ}\text{S}-80^{\circ}\text{N}$, (b) $20^{\circ}\text{S}-20^{\circ}\text{N}$, (c) $40^{\circ}\text{S}-20^{\circ}\text{S}$ and $20^{\circ}\text{N}-40^{\circ}\text{N}$, (d) $60^{\circ}\text{S}-40^{\circ}\text{S}$ and $40^{\circ}\text{N}-60^{\circ}\text{N}$.

3.5.11 ΔSSS sorted as geophysical conditions

In Figure 71, we classify the match-up differences ΔSSS (ISAS - *in situ*) as function of the geophysical conditions at match-up points. The mean and std of ΔSSS (ISAS - TSG (LEGOS-Survostral)) is thus evaluated as function of the

- *in situ* SSS values per bins of width 0.2,
- *in situ* SST values per bins of width 1°C ,
- ASCAT daily wind values per bins of width 1 m/s,
- CMORPH 3-hourly rain rates per bins of width 1 mm/h, and,

- distance to coasts per bins of width 50 km,
- *in situ* measurement depth (if relevant).

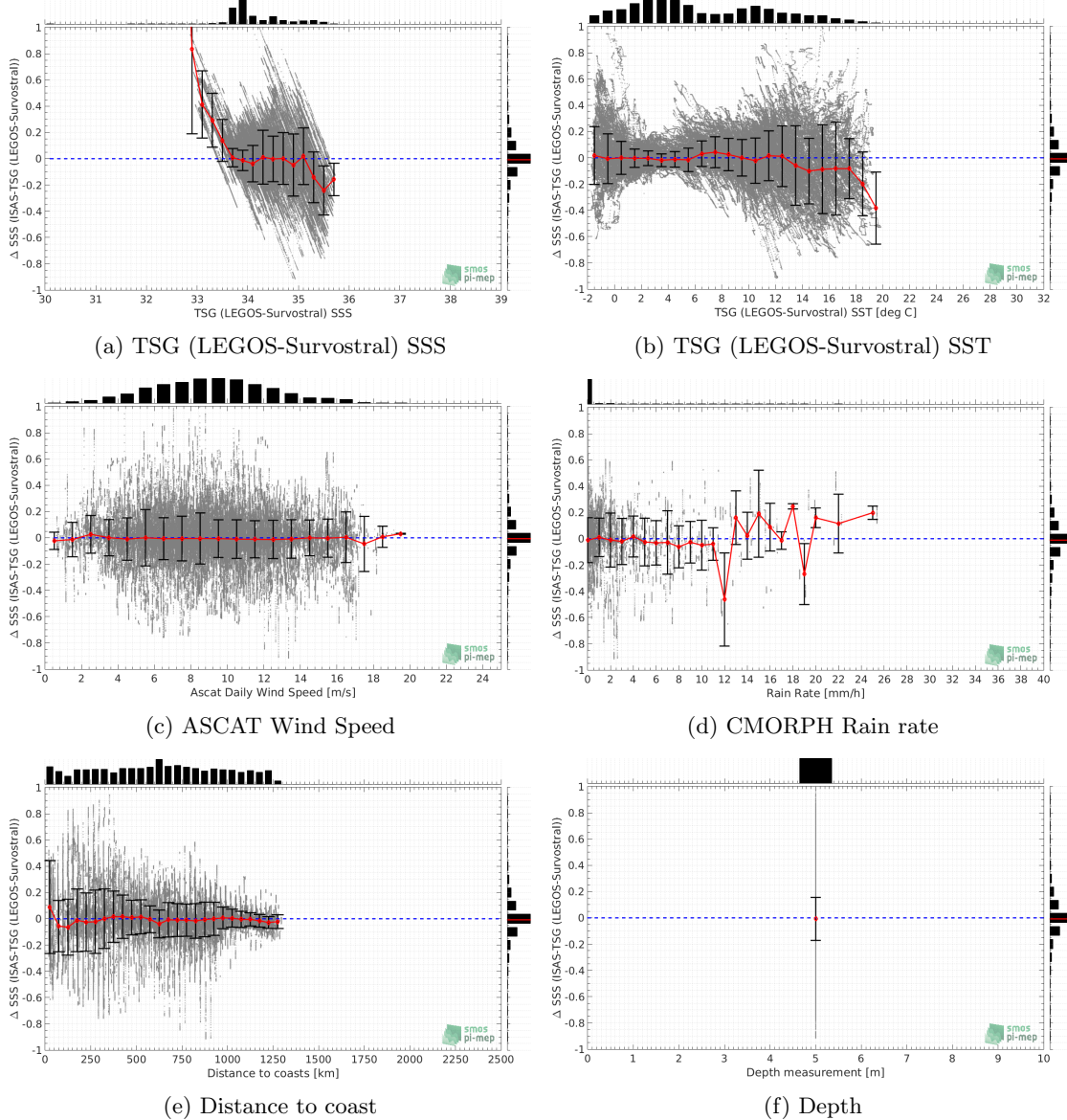


Figure 71: Δ SSS (ISAS - TSG (LEGOS-Survostral)) sorted as geophysical conditions: TSG (LEGOS-Survostral) SSS a), TSG (LEGOS-Survostral) SST b), ASCAT Wind speed c), CMORPH rain rate d), distance to coast (e) and depth measurements (f).

3.5.12 Δ SSS maps and statistics for different geophysical conditions

In Figures 72 and 73, we focus on sub-datasets of the match-up differences Δ SSS (ISAS - *in situ*) for the following specific geophysical conditions:

- **C1:**if the local value at *in situ* location of estimated rain rate is zero, mean daily wind is in the range [3, 12] m/s, the SST is $> 5^{\circ}\text{C}$ and distance to coast is > 800 km.
- **C2:**if the local value at *in situ* location of estimated rain rate is zero, mean daily wind is in the range [3, 12] m/s.
- **C3:**if the local value at *in situ* location of estimated rain rate is high (ie. > 1 mm/h) and mean daily wind is low (ie. < 4 m/s).
- **C5:**if the *in situ* data is located where the climatological SSS standard deviation is low (ie. above < 0.2).
- **C6:**if the *in situ* data is located where the climatological SSS standard deviation is high (ie. above > 0.2).

For each of these conditions, the temporal mean (gridded over spatial boxes of size $1^{\circ} \times 1^{\circ}$) and the histogram of the difference ΔSSS (ISAS - *in situ*) are presented.

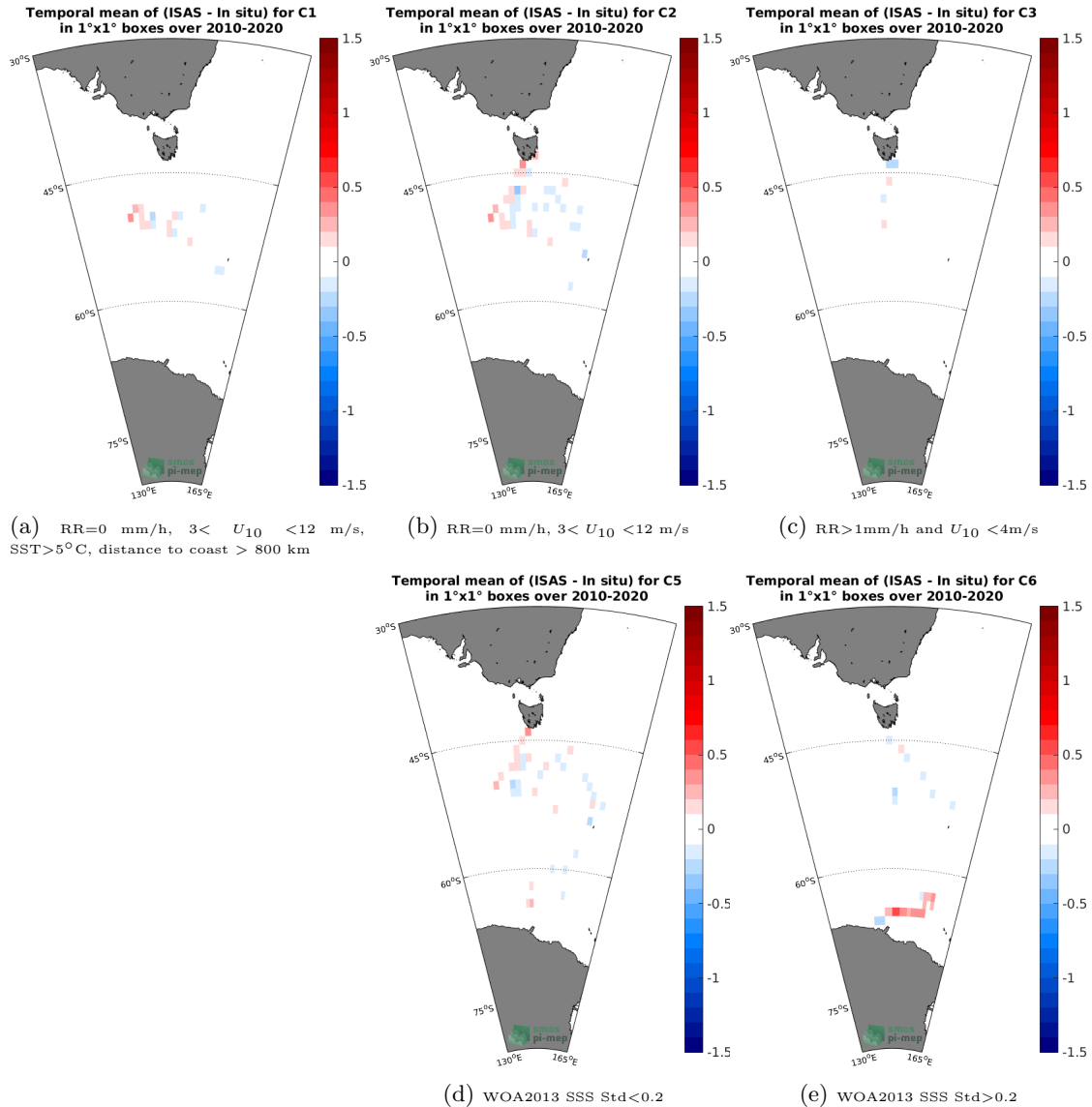


Figure 72: Temporal mean gridded over spatial boxes of size $1^\circ \times 1^\circ$ of ΔSSS (ISAS - TSG (LEGOS-Survostral)) for 5 different subdatasets corresponding to: RR=0 mm/h, $3 < U_{10} < 12 \text{ m/s}$, SST> 5°C , distance to coast > 800 km (a), RR=0 mm/h, $3 < U_{10} < 12 \text{ m/s}$ (b), RR>1mm/h and $U_{10} < 4 \text{ m/s}$ (c), WOA2013 SSS Std<0.2 (d), WOA2013 SSS Std>0.2 (e).

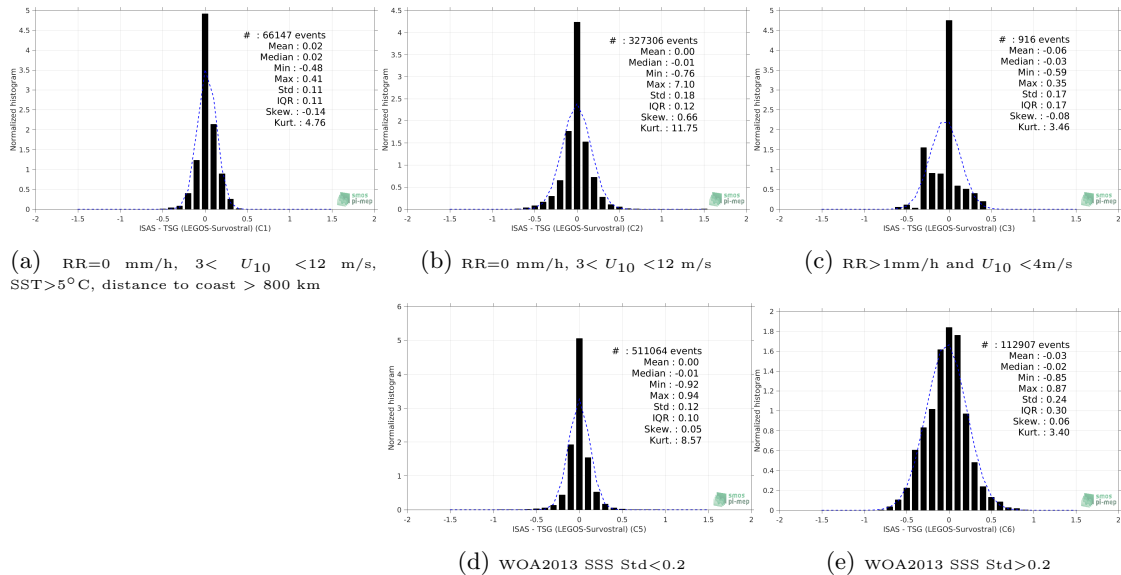


Figure 73: Normalized histogram of ΔSSSS (ISAS - TSG (LEGOS-Survostral)) for 5 different subdatasets corresponding to: RR=0 mm/h, $3 < U_{10} < 12$ m/s, SST> 5° C, distance to coast > 800 km (a), RR=0 mm/h, $3 < U_{10} < 12$ m/s (b), RR>1mm/h and $U_{10} < 4$ m/s (c), WOA2013 SSS Std<0.2 (d), WOA2013 SSS Std>0.2 (e).

3.5.13 Summary

Table 1 shows the mean, median, standard deviation (Std), root mean square (RMS), interquartile range (IQR), correlation coefficient (r^2) and robust standard deviation (Std*) of the match-up differences ΔSSSS (ISAS - TSG (LEGOS-Survostral)) for the following conditions:

- all: All the match-up pairs satellite/in situ SSS values are used to derive the statistics
- C1: only pairs where RR=0 mm/h, $3 < U_{10} < 12$ m/s, SST> 5° C, distance to coast > 800 km
- C2: only pairs where RR=0 mm/h, $3 < U_{10} < 12$ m/s
- C3: only pairs where RR>1mm/h and $U_{10} < 4$ m/s
- C5: only pairs where WOA2013 SSS Std<0.2
- C6: only pairs where WOA2013 SSS Std>0.2
- C7a: only pairs with a distance to coast < 150 km.
- C7b: only pairs with a distance to coast in the range [150, 800] km.
- C7c: only pairs with a distance to coast > 800 km.
- C8a: only pairs where SST is < 5° C.
- C8b: only pairs where SST is in the range [$5, 15$]°C.
- C8c: only pairs where SST is > 15° C.

- C9a: only pairs where SSS is < 33 .
- C9b: only pairs where SSS is in the range [33, 37].
- C9c: only pairs where SSS is > 37 .

Table 1: Statistics of Δ SSS (ISAS - TSG (LEGOS-Survostral))

Condition	#	Median	Mean	Std	RMS	IQR	r^2	Std*
all	652976	-0.01	0.00	0.16	0.16	0.12	0.90	0.09
C1	66147	0.02	0.02	0.11	0.11	0.11	0.74	0.08
C2	327306	-0.01	0.00	0.18	0.18	0.12	0.90	0.09
C3	916	-0.03	-0.06	0.17	0.18	0.17	0.92	0.08
C5	511064	-0.01	0.00	0.12	0.12	0.10	0.92	0.07
C6	112907	-0.02	-0.03	0.24	0.24	0.30	0.86	0.22
C7a	63782	0.00	0.02	0.29	0.29	0.30	0.85	0.22
C7b	368723	-0.01	-0.01	0.17	0.17	0.15	0.90	0.11
C7c	220471	-0.01	0.00	0.09	0.09	0.08	0.74	0.05
C8a	308616	-0.01	0.00	0.10	0.10	0.08	0.53	0.06
C8b	295347	0.00	0.00	0.18	0.18	0.19	0.85	0.14
C8c	42997	-0.10	-0.08	0.32	0.33	0.36	0.01	0.27
C9a	400	0.92	1.73	1.27	2.15	1.77	0.15	0.76
C9b	652576	-0.01	0.00	0.15	0.15	0.12	0.91	0.09
C9c	0	NaN	NaN	NaN	NaN	NaN	NaN	NaN

Table 1 numerical values can be downloaded as a csv file [here](#).

3.6 TSG (LEGOS-Survostral-Adelie)

3.6.1 Introduction

The TSG-LEGOS-Surv-Adel dataset correspond to delayed mode regional dataset along the Adelie coast provided by the [Survostral project](#) and available via [ftp](#). Adjusted values when available and only collected TSG data that exhibit quality flags=1 and 2 were used.

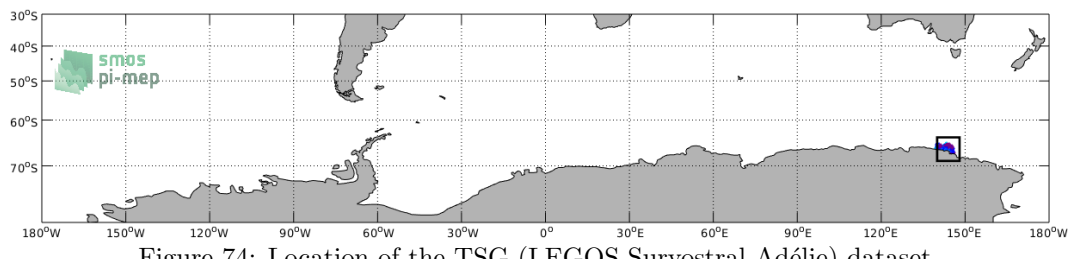


Figure 74: Location of the TSG (LEGOS-Survostral-Adélie) dataset.

3.6.2 Number of SSS data as a function of time and distance to coast

Figure 75 shows the time (a) and distance to coast (b) distributions of the TSG (LEGOS-Survostral-Adélie) *in situ* dataset.

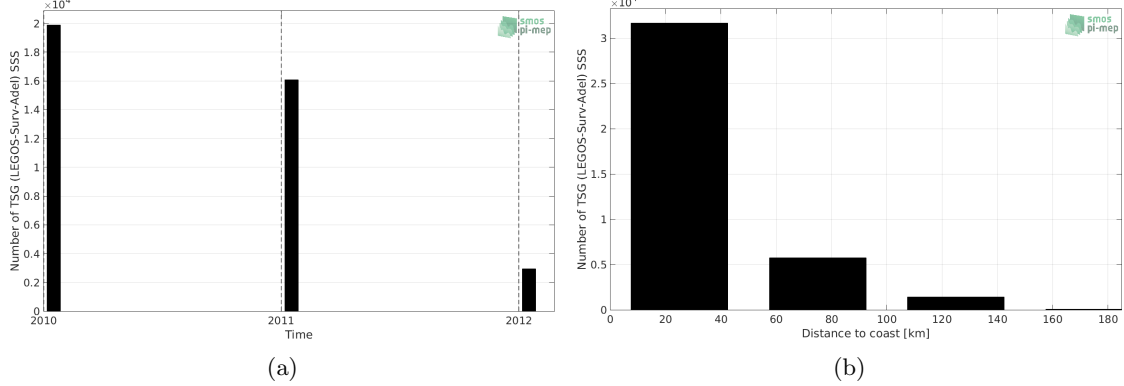


Figure 75: Number of SSS from TSG (LEGOS-Survostral-Adélie) as a function of time (a) and distance to coast (b).

3.6.3 Histograms of SSS

Figure 76 shows the SSS distribution of the TSG (LEGOS-Survostral-Adélie) (a) and colocalized ISAS (b) dataset.

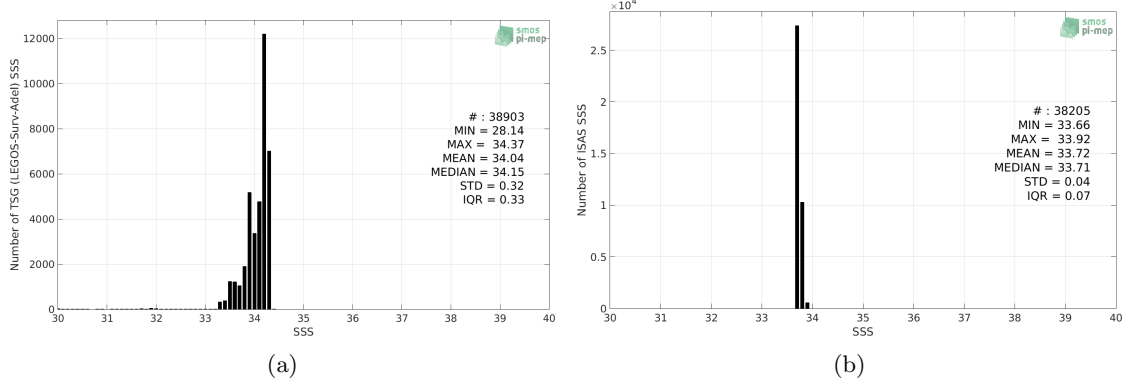


Figure 76: Histograms of SSS from TSG (LEGOS-Survostral-Adélie) (a) and ISAS (b) per bins of 0.1.

3.6.4 Distribution of *in situ* SSS depth measurements

In Figure 77, we show the depth distribution of the *in situ* salinity dataset (a) and the spatial distribution of the depth temporal mean in $1^\circ \times 1^\circ$ boxes and considering the full *in situ* dataset period (b).

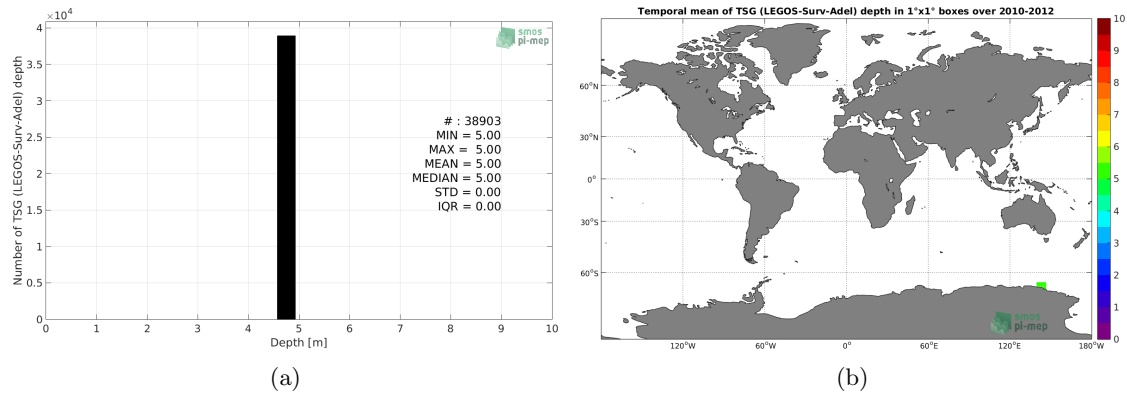


Figure 77: Depth distribution of the upper level SSS measurements from TSG (LEGOS-Survostral-Adélie) (a) and spatial distribution of the *in situ* SSS depth measurements showing the mean value in 1°x1° boxes and considering the full *in situ* dataset period (b).

3.6.5 Spatial distribution of SSS

In Figure 78, the number of TSG (LEGOS-Survostral-Adélie) SSS measurements in 1°x1° boxes is shown.

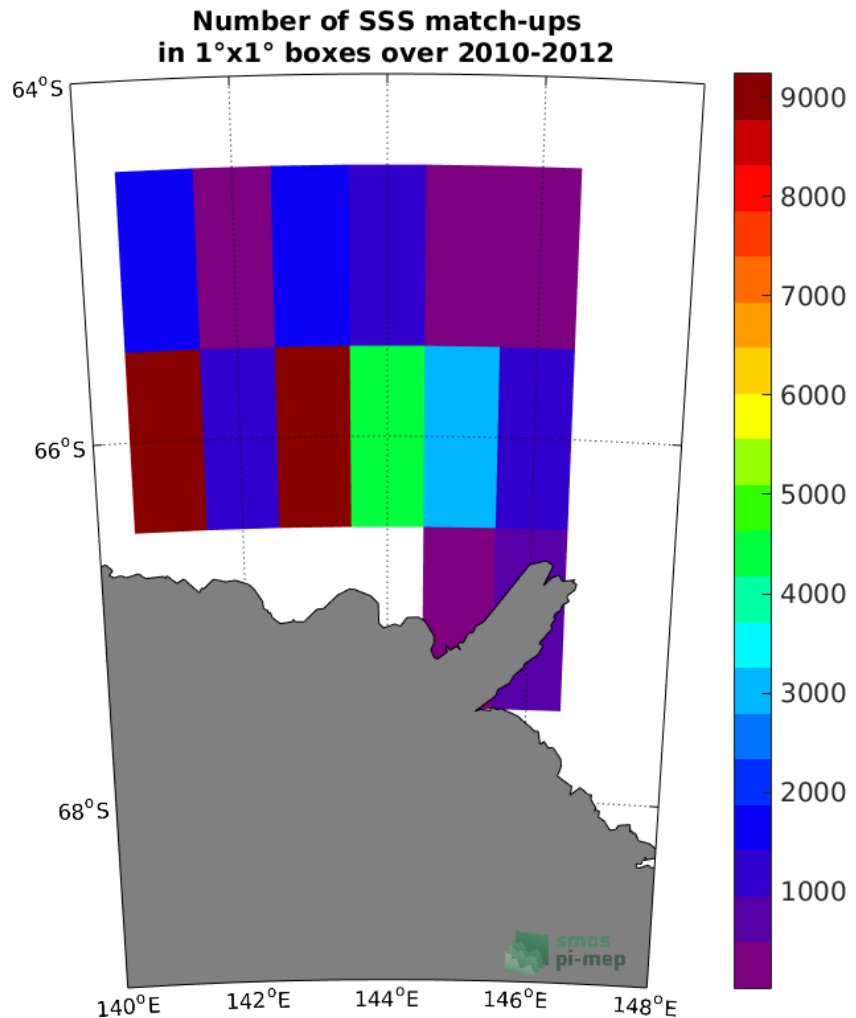


Figure 78: Number of SSS from TSG (LEGOS-Survostral-Adélie) in $1^\circ \times 1^\circ$ boxes.

3.6.6 Spatial Maps of the Temporal mean and Std of *in situ* and ISAS SSS and of the difference (Δ SSS)

In Figure 79, we show maps of temporal mean (left) and standard deviation (right) of ISAS (top), TSG (LEGOS-Survostral-Adélie) *in situ* dataset (middle) and the difference Δ SSS (ISAS - TSG (LEGOS-Survostral-Adélie)) (bottom). The temporal mean and std are calculated using all match-up pairs falling in spatial boxes of size $1^\circ \times 1^\circ$ over the full TSG (LEGOS-Survostral-Adélie) dataset period.

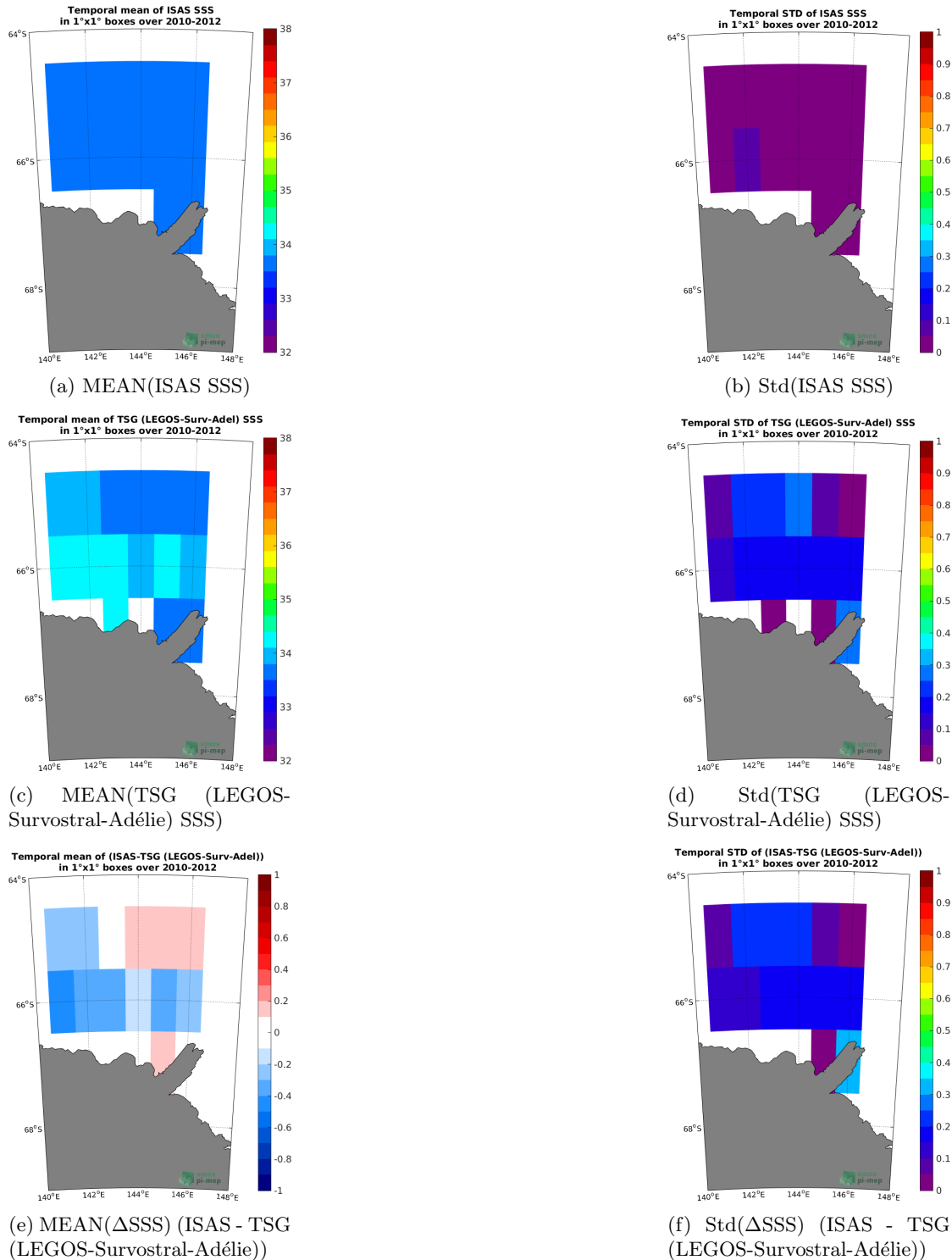


Figure 79: Temporal mean (left) and Std (right) of SSS from ISAS (top), TSG (LEGOS-Survostral-Adélie) (middle), and of Δ SSS (ISAS - TSG (LEGOS-Survostral-Adélie)). Only match-up pairs are used to generate these maps.

3.6.7 Time series of the monthly median and Std of *in situ* and ISAS SSS and of the difference (Δ SSS)

In the top panel of Figure 80, we show the time series of the monthly median SSS estimated for both ISAS SSS product (in black) and the TSG (LEGOS-Survostral-Adélie) *in situ* dataset (in blue) at the collected Pi-MEP match-up pairs.

In the middle panel of Figure 80, we show the time series of the monthly median of Δ SSS (ISAS - TSG (LEGOS-Survostral-Adélie)) for the collected Pi-MEP match-up pairs.

In the bottom panel of Figure 80, we show the time series of the monthly standard deviation of the Δ SSS (ISAS - TSG (LEGOS-Survostral-Adélie)) for the collected Pi-MEP match-up pairs.

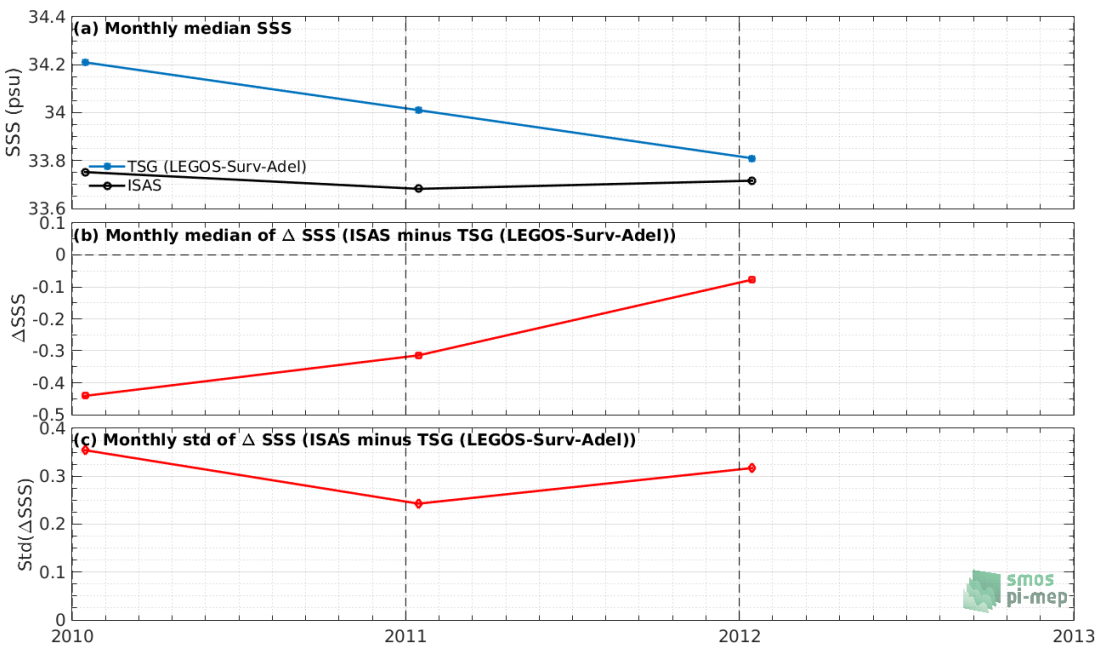


Figure 80: Time series of the monthly median SSS (top), median of Δ SSS (ISAS - TSG (LEGOS-Survostral-Adélie)) and Std of Δ SSS (ISAS - TSG (LEGOS-Survostral-Adélie)) considering all match-ups collected by the Pi-MEP.

3.6.8 Zonal mean and Std of *in situ* and ISAS SSS and of the difference Δ SSS

In Figure 81 left panel, we show the zonal mean SSS considering all Pi-MEP match-up pairs for both ISAS SSS product (in black) and the TSG (LEGOS-Survostral-Adélie) *in situ* dataset (in blue). The full *in situ* dataset period is used to derive the mean.

In the right panel of Figure 81, we show the zonal mean of Δ SSS (ISAS - TSG (LEGOS-Survostral-Adélie)) for all the collected Pi-MEP match-up pairs estimated over the full *in situ* dataset period.

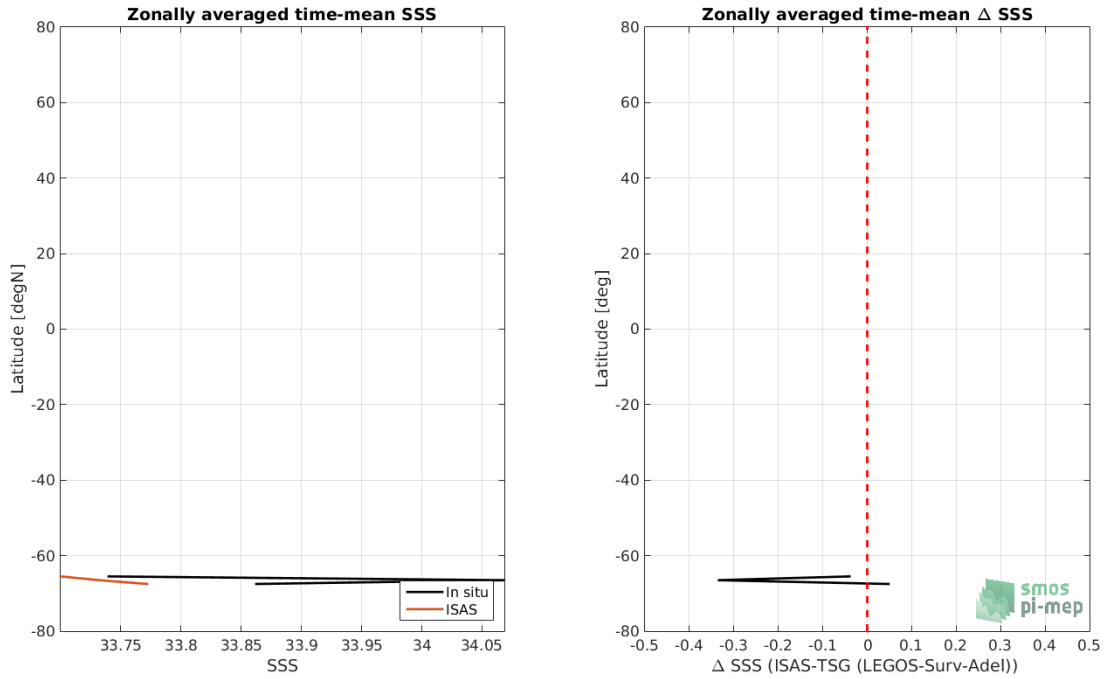


Figure 81: Left panel: Zonal mean SSS from ISAS product (black) and from TSG (LEGOS-Survostral-Adélie) (blue). Right panel: Zonal mean of Δ SSS (ISAS - TSG (LEGOS-Survostral-Adélie)) for all the collected Pi-MEP match-up pairs estimated over the full *in situ* dataset period.

3.6.9 Scatterplots of ISAS vs *in situ* SSS by latitudinal bands

In Figure 82, contour maps of the concentration of ISAS SSS (y-axis) versus TSG (LEGOS-Survostral-Adélie) SSS (x-axis) at match-up pairs for different latitude bands: (a) 80°S-80°N, (b) 20°S-20°N, (c) 40°S-20°S and 20°N-40°N and (d) 60°S-40°S and 40°N-60°N. For each plot, the red line shows $x=y$. The black thin and dashed lines indicate a linear fit through the data cloud and the $\pm 95\%$ confidence levels, respectively. The number match-up pairs n , the slope and R^2 coefficient of the linear fit, the root mean square (RMS) and the mean bias between ISAS and *in situ* data are indicated for each latitude band in each plots.

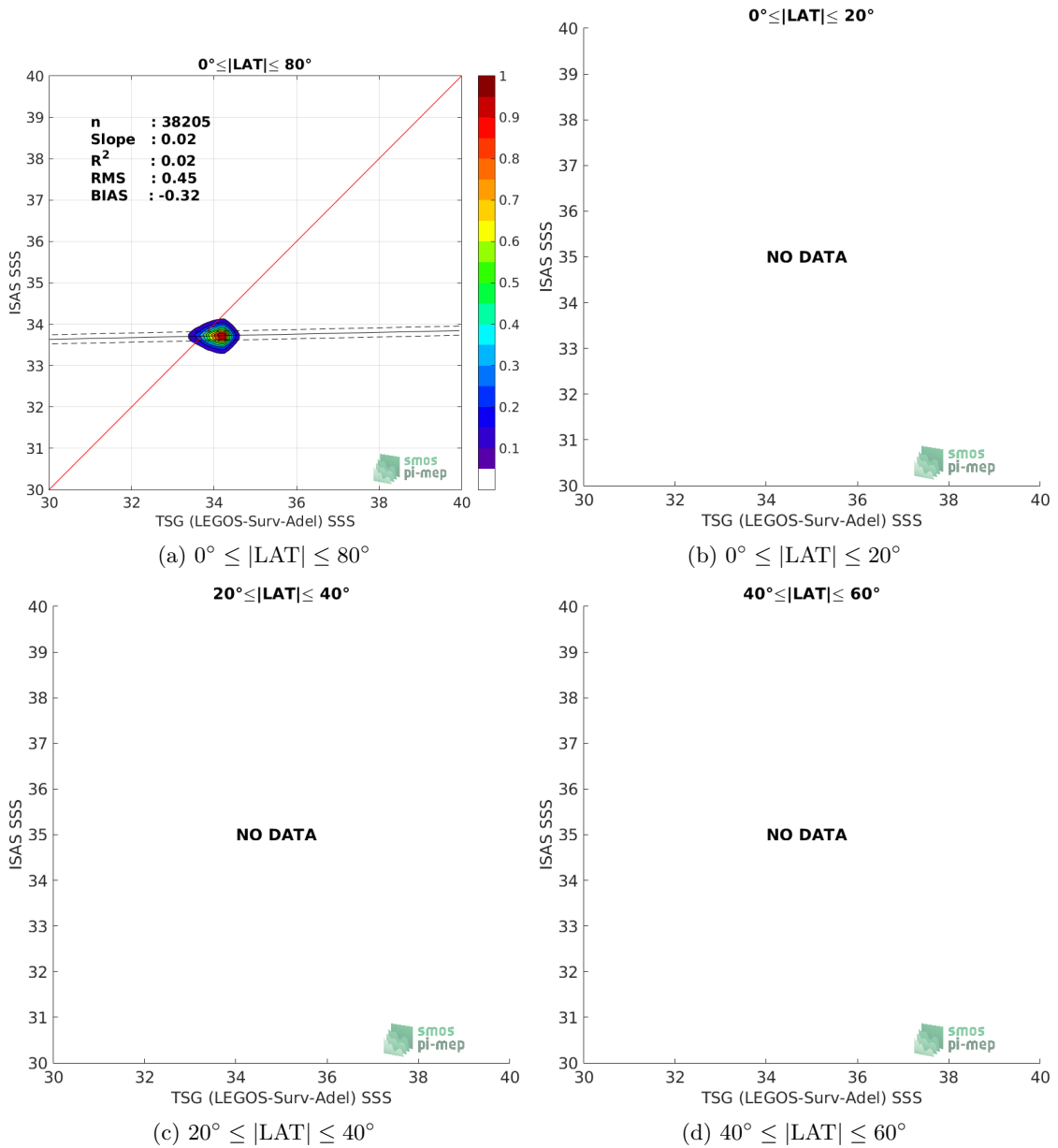


Figure 82: Contour maps of the concentration of ISAS SSS (y-axis) versus TSG (LEGOS-Survostral-Adélie) SSS (x-axis) at match-up pairs for different latitude bands. For each plot, the red line shows $x=y$. The black thin and dashed lines indicate a linear fit through the data cloud and the $\pm 95\%$ confidence levels, respectively. The number match-up pairs n , the slope and R^2 coefficient of the linear fit, the root mean square (RMS) and the mean bias between ISAS and *in situ* data are indicated for each latitude band in each plots.

3.6.10 Time series of the monthly median and Std of the difference ΔSSS sorted by latitudinal bands

In Figure 83, time series of the monthly median (red curves) of ΔSSS (ISAS - TSG (LEGOS-Survostral-Adélie)) and ± 1 Std (black vertical thick bars) as function of time for all the collected Pi-MEP match-up pairs estimated for the full *in situ* dataset period are shown for different latitude bands: (a) $80^{\circ}\text{S}-80^{\circ}\text{N}$, (b) $20^{\circ}\text{S}-20^{\circ}\text{N}$, (c) $40^{\circ}\text{S}-20^{\circ}\text{S}$ and $20^{\circ}\text{N}-40^{\circ}\text{N}$ and (d) $60^{\circ}\text{S}-40^{\circ}\text{S}$ and $40^{\circ}\text{N}-60^{\circ}\text{N}$.

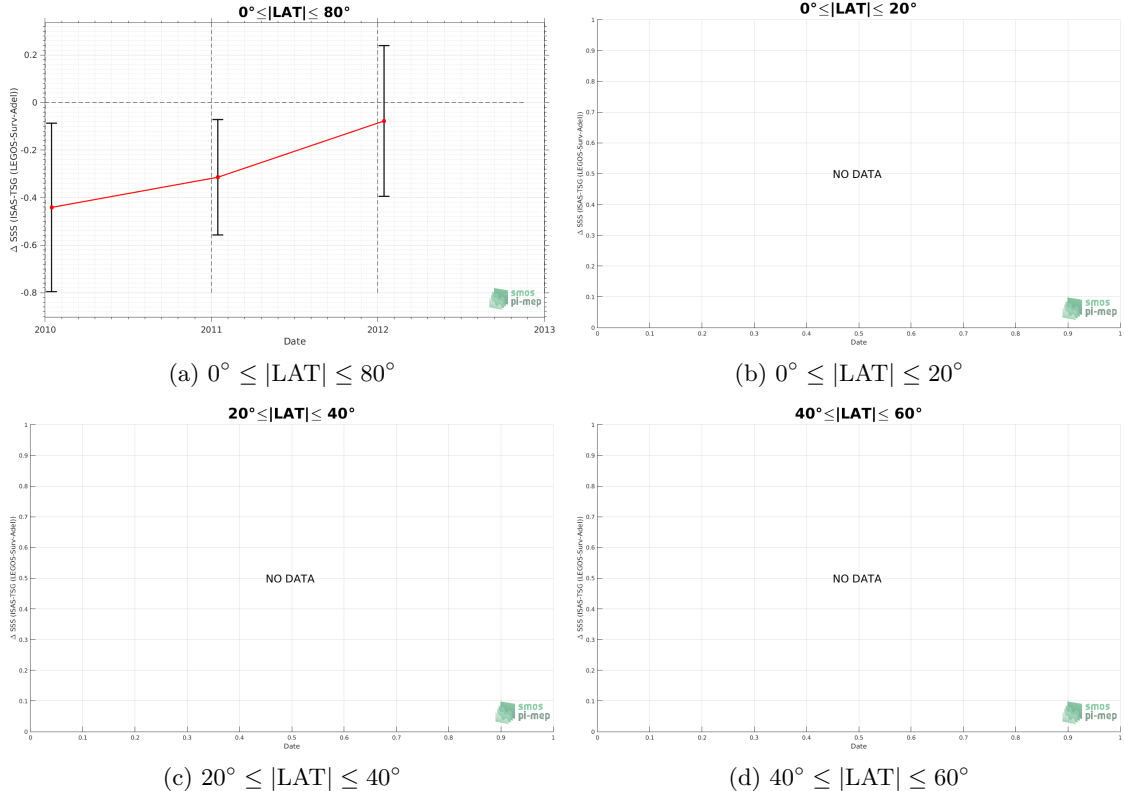


Figure 83: Monthly median (red curves) of ΔSSS (ISAS - TSG (LEGOS-Survostral-Adélie)) and ± 1 Std (black vertical thick bars) as function of time for all the collected Pi-MEP match-up pairs for the full *in situ* dataset period are shown for different latitude bands: (a) $80^{\circ}\text{S}-80^{\circ}\text{N}$, (b) $20^{\circ}\text{S}-20^{\circ}\text{N}$, (c) $40^{\circ}\text{S}-20^{\circ}\text{S}$ and $20^{\circ}\text{N}-40^{\circ}\text{N}$ and (d) $60^{\circ}\text{S}-40^{\circ}\text{S}$ and $40^{\circ}\text{N}-60^{\circ}\text{N}$.

3.6.11 ΔSSS sorted as geophysical conditions

In Figure 84, we classify the match-up differences ΔSSS (ISAS - *in situ*) as function of the geophysical conditions at match-up points. The mean and std of ΔSSS (ISAS - TSG (LEGOS-Survostral-Adélie)) is thus evaluated as function of the

- *in situ* SSS values per bins of width 0.2,
- *in situ* SST values per bins of width 1°C ,
- ASCAT daily wind values per bins of width 1 m/s,
- CMORPH 3-hourly rain rates per bins of width 1 mm/h, and,

- distance to coasts per bins of width 50 km,
- *in situ* measurement depth (if relevant).

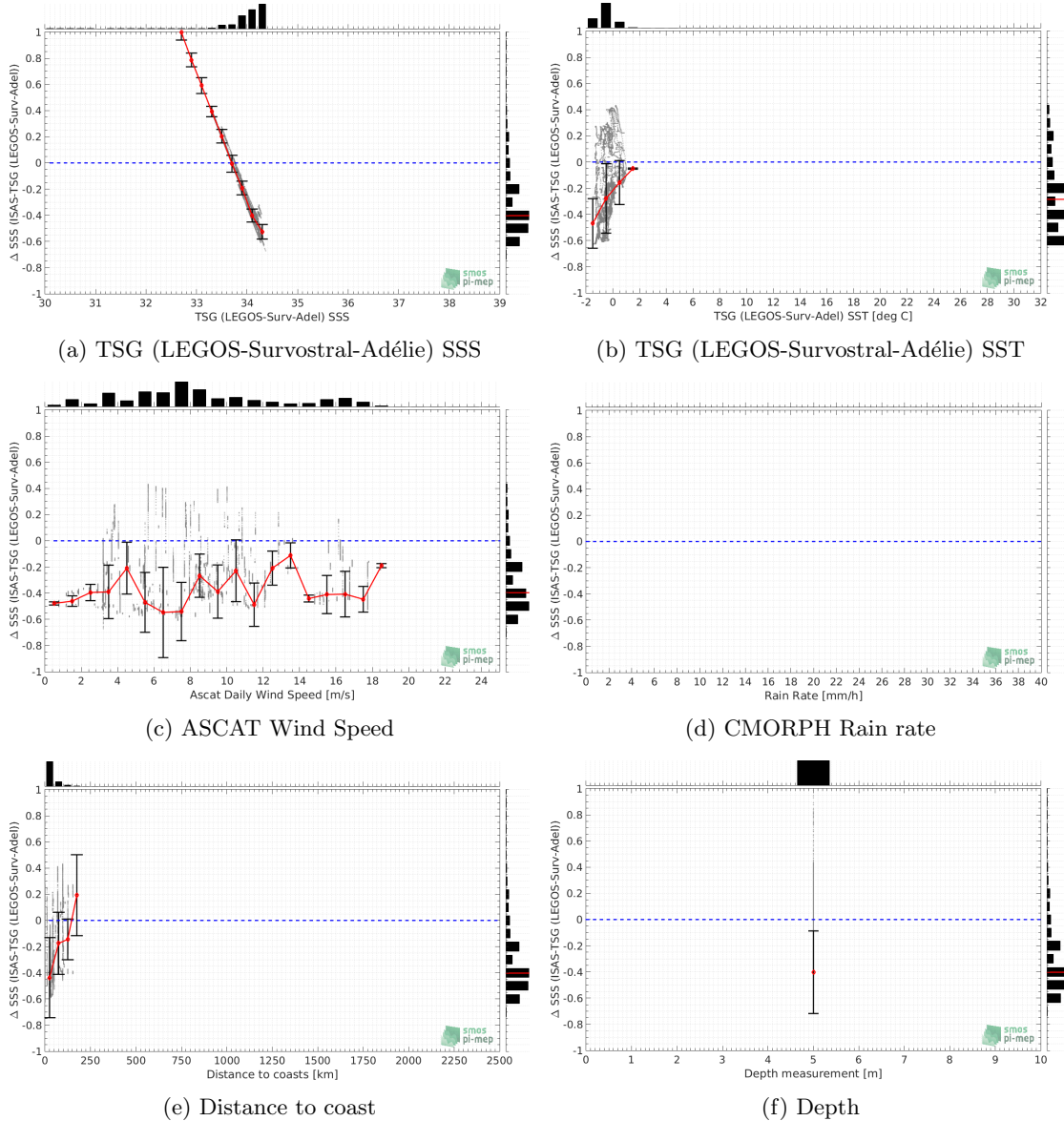


Figure 84: ΔSSS (ISAS - TSG (LEGOS-Survostral-Adélie)) sorted as geophysical conditions: TSG (LEGOS-Survostral-Adélie) SSS a), TSG (LEGOS-Survostral-Adélie) SST b), ASCAT Wind speed c), CMORPH rain rate d), distance to coast (e) and depth measurements (f).

3.6.12 ΔSSS maps and statistics for different geophysical conditions

In Figures 85 and 86, we focus on sub-datasets of the match-up differences ΔSSS (ISAS - *in situ*) for the following specific geophysical conditions:

- **C1:**if the local value at *in situ* location of estimated rain rate is zero, mean daily wind is in the range [3, 12] m/s, the SST is $> 5^{\circ}\text{C}$ and distance to coast is > 800 km.
- **C2:**if the local value at *in situ* location of estimated rain rate is zero, mean daily wind is in the range [3, 12] m/s.
- **C3:**if the local value at *in situ* location of estimated rain rate is high (ie. > 1 mm/h) and mean daily wind is low (ie. < 4 m/s).
- **C5:**if the *in situ* data is located where the climatological SSS standard deviation is low (ie. above < 0.2).
- **C6:**if the *in situ* data is located where the climatological SSS standard deviation is high (ie. above > 0.2).

For each of these conditions, the temporal mean (gridded over spatial boxes of size $1^{\circ} \times 1^{\circ}$) and the histogram of the difference ΔSSS (ISAS - *in situ*) are presented.

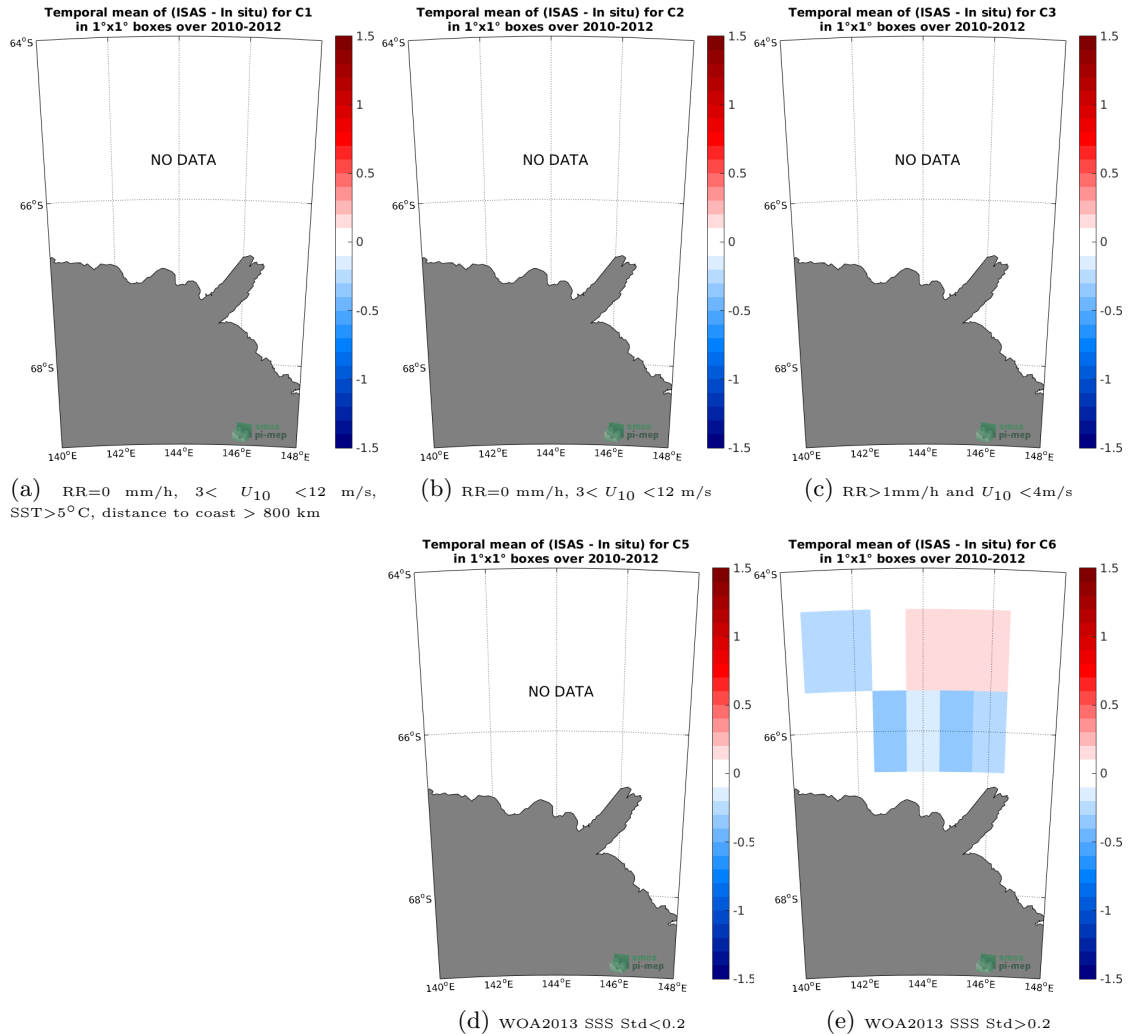


Figure 85: Temporal mean gridded over spatial boxes of size $1^\circ \times 1^\circ$ of ΔSSS (ISAS - TSG (LEGOS-Survostral-Adélie)) for 5 different subdatasets corresponding to: RR=0 mm/h, $3 < U_{10} < 12$ m/s, SST > 5°C, distance to coast > 800 km (a), RR=0 mm/h, $3 < U_{10} < 12$ m/s (b), RR > 1mm/h and $U_{10} < 4$ m/s (c), WOA2013 SSS Std < 0.2 (d), WOA2013 SSS Std > 0.2 (e).

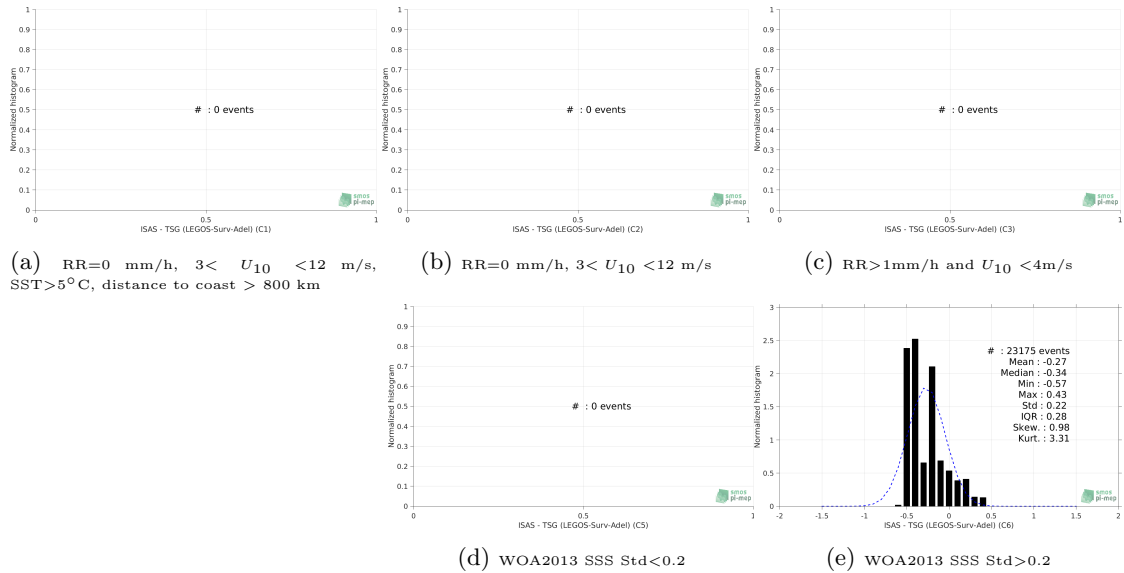


Figure 86: Normalized histogram of ΔSSS (ISAS - TSG (LEGOS-Survostral-Adélie)) for 5 different subdatasets corresponding to: $RR=0 \text{ mm/h}, 3 < U_{10} < 12 \text{ m/s}, SST > 5^\circ\text{C}, \text{distance to coast} > 800 \text{ km}$ (a), $RR=0 \text{ mm/h}, 3 < U_{10} < 12 \text{ m/s}$ (b), $RR > 1\text{mm/h} \text{ and } U_{10} < 4\text{m/s}$ (c), WOA2013 SSS Std < 0.2 (d), WOA2013 SSS Std > 0.2 (e).

3.6.13 Summary

Table 1 shows the mean, median, standard deviation (Std), root mean square (RMS), interquartile range (IQR), correlation coefficient (r^2) and robust standard deviation (Std^*) of the match-up differences ΔSSS (ISAS - TSG (LEGOS-Survostral-Adélie)) for the following conditions:

- all: All the match-up pairs satellite/in situ SSS values are used to derive the statistics
- C1: only pairs where $RR=0 \text{ mm/h}, 3 < U_{10} < 12 \text{ m/s}, SST > 5^\circ\text{C}, \text{distance to coast} > 800 \text{ km}$
- C2: only pairs where $RR=0 \text{ mm/h}, 3 < U_{10} < 12 \text{ m/s}$
- C3: only pairs where $RR > 1\text{mm/h} \text{ and } U_{10} < 4\text{m/s}$
- C5: only pairs where WOA2013 SSS Std < 0.2
- C6: only pairs where WOA2013 SSS Std > 0.2
- C7a: only pairs with a distance to coast < 150 km.
- C7b: only pairs with a distance to coast in the range [150, 800] km.
- C7c: only pairs with a distance to coast > 800 km.
- C8a: only pairs where SST is < 5°C .
- C8b: only pairs where SST is in the range $[5, 15]^\circ\text{C}$.
- C8c: only pairs where SST is > 15°C .

- C9a: only pairs where SSS is < 33.
- C9b: only pairs where SSS is in the range [33, 37].
- C9c: only pairs where SSS is > 37.

Table 1: Statistics of Δ SSS (ISAS - TSG (LEGOS-Survostral-Adélie))

Condition	#	Median	Mean	Std	RMS	IQR	r ²	Std*
all	38205	-0.40	-0.32	0.32	0.45	0.30	0.02	0.20
C1	0	NaN	NaN	NaN	NaN	NaN	NaN	NaN
C2	0	NaN	NaN	NaN	NaN	NaN	NaN	NaN
C3	0	NaN	NaN	NaN	NaN	NaN	NaN	NaN
C5	0	NaN	NaN	NaN	NaN	NaN	NaN	NaN
C6	23175	-0.34	-0.27	0.22	0.35	0.28	0.40	0.21
C7a	38109	-0.40	-0.32	0.32	0.45	0.30	0.02	0.20
C7b	96	0.19	0.00	0.31	0.31	0.65	0.99	0.12
C7c	0	NaN	NaN	NaN	NaN	NaN	NaN	NaN
C8a	18615	-0.29	-0.27	0.26	0.37	0.34	0.22	0.26
C8b	0	NaN	NaN	NaN	NaN	NaN	NaN	NaN
C8c	0	NaN	NaN	NaN	NaN	NaN	NaN	NaN
C9a	270	1.76	2.09	1.16	2.39	0.93	0.00	0.59
C9b	37935	-0.40	-0.34	0.22	0.40	0.30	0.03	0.20
C9c	0	NaN	NaN	NaN	NaN	NaN	NaN	NaN

Table 1 numerical values can be downloaded as a csv file [here](#).

3.7 TSG (Polarstern)

3.7.1 Introduction

The TSG-POLARSTERN dataset has been gathered through the <https://www.pangaea.de/> data warehouse utility using the following criteria: basis:”Polarstern”, device:”Underway cruise track measurements (CT)”, time coverage form 2010/01/01 to present. The result of the query is a collection of 77 different datasets with the following identification numbers: 736345, 742729, 753224, 753225, 753226, 753227, 758080, 760120, 760121, 761277, 770034, 770035, 770828, 776596, 776597, 780004, 802809, 802810, 802811, 802812, 803312, 803431, 808835, 808836, 808838, 809727, 810678, 816055, 819831, 823259, 831976, 832269, 839406, 839407, 839408, 845130, 848615, 858879, 858880, 858881, 858882, 858883, 858884, 858885, 863228, 863229, 863230, 863231, 863232, 863234, 873145, 873147, 873151, 873153, 873155, 873156, 873158, 887767, 889444, 889513, 889515, 889516, 889517, 889535, 889542, 889548, 895578, 895579, 895581, 898225, 898233, 898266, 905555, 905562, 905608, 905610, 905734.

3.7.2 Number of SSS data as a function of time and distance to coast

Figure 87 shows the time (a) and distance to coast (b) distributions of the TSG (Polarstern) *in situ* dataset.

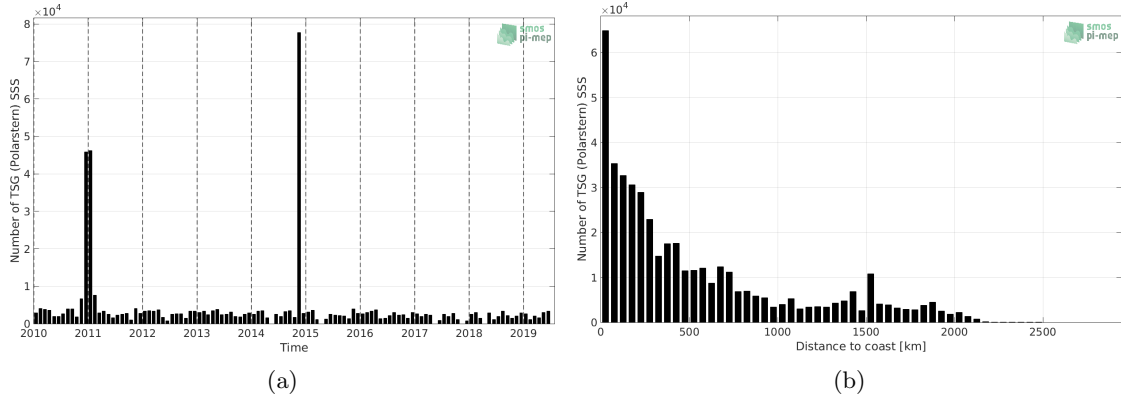


Figure 87: Number of SSS from TSG (Polarstern) as a function of time (a) and distance to coast (b).

3.7.3 Histograms of SSS

Figure 88 shows the SSS distribution of the TSG (Polarstern) (a) and colocalized ISAS (b) dataset.

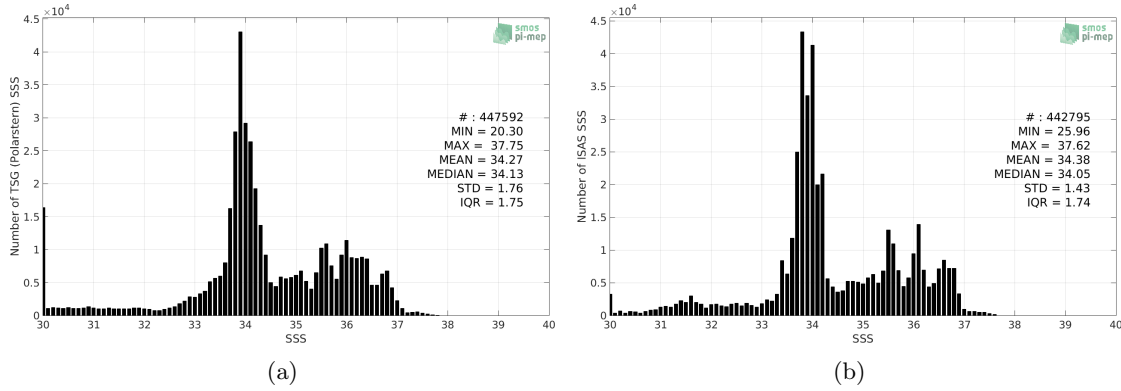


Figure 88: Histograms of SSS from TSG (Polarstern) (a) and ISAS (b) per bins of 0.1.

3.7.4 Distribution of *in situ* SSS depth measurements

In Figure 89, we show the depth distribution of the *in situ* salinity dataset (a) and the spatial distribution of the depth temporal mean in $1^\circ \times 1^\circ$ boxes and considering the full *in situ* dataset period (b).

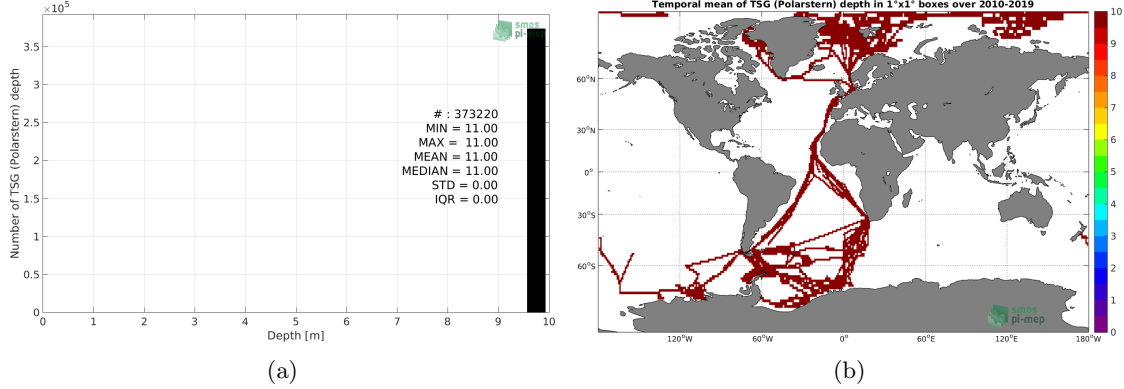


Figure 89: Depth distribution of the upper level SSS measurements from TSG (Polarstern) (a) and spatial distribution of the *in situ* SSS depth measurements showing the mean value in 1°x1° boxes and considering the full *in situ* dataset period (b).

3.7.5 Spatial distribution of SSS

In Figure 90, the number of TSG (Polarstern) SSS measurements in 1°x1° boxes is shown.

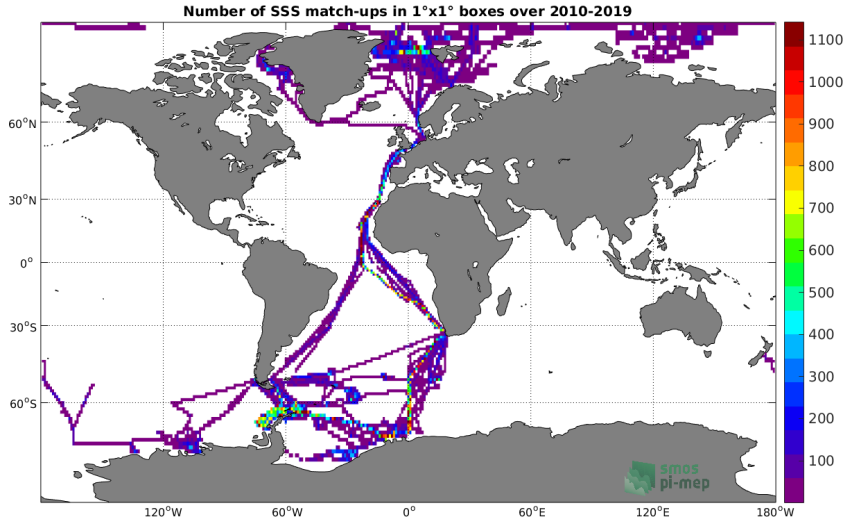


Figure 90: Number of SSS from TSG (Polarstern) in 1°x1° boxes.

3.7.6 Spatial Maps of the Temporal mean and Std of *in situ* and ISAS SSS and of the difference (Δ SSS)

In Figure 91, we show maps of temporal mean (left) and standard deviation (right) of ISAS (top), TSG (Polarstern) *in situ* dataset (middle) and the difference Δ SSS(ISAS -TSG (Polarstern)) (bottom). The temporal mean and std are calculated using all match-up pairs falling in spatial boxes of size 1°x1° over the full TSG (Polarstern) dataset period.

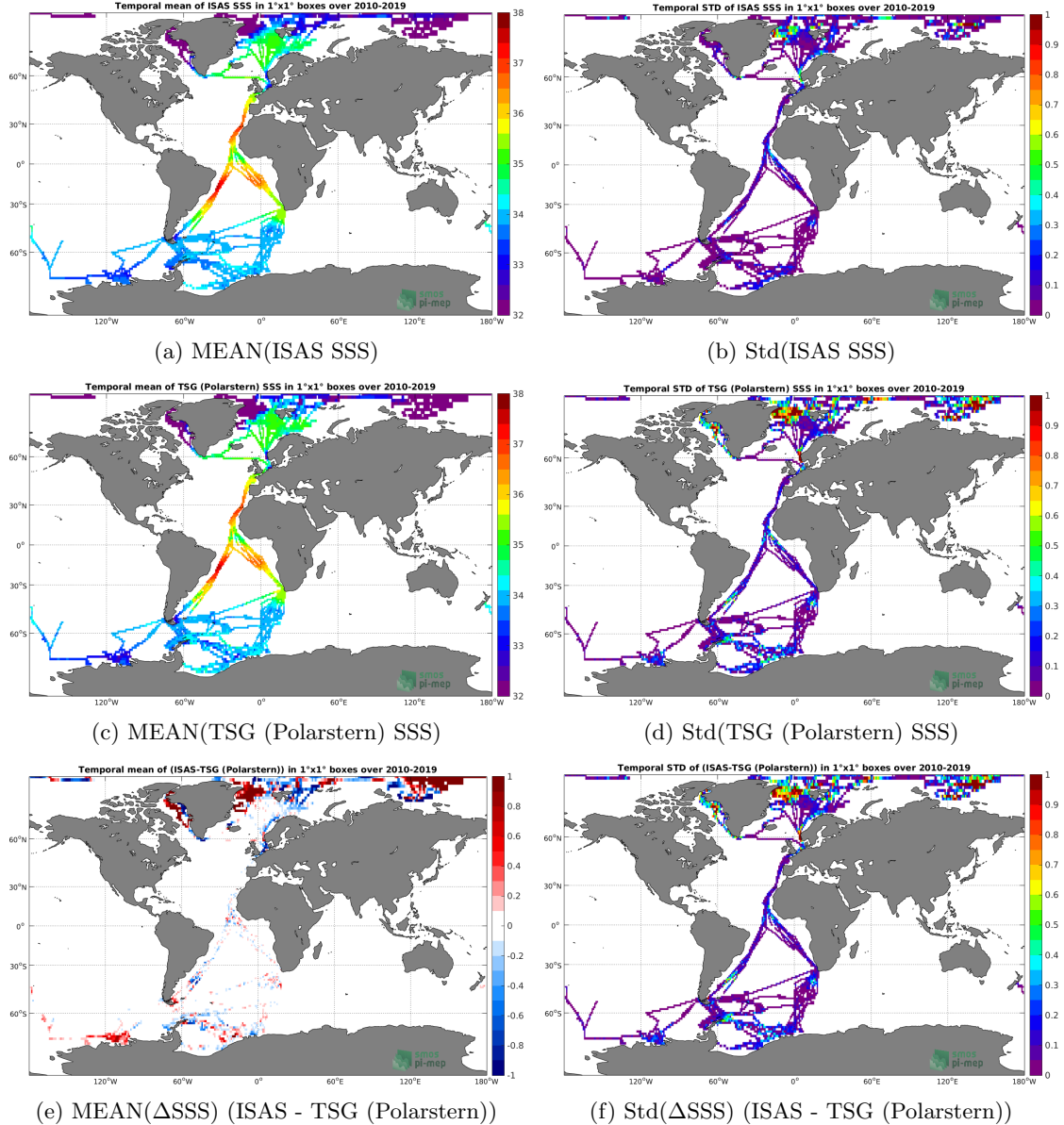


Figure 91: Temporal mean (left) and Std (right) of SSS from ISAS (top), TSG (Polarstern) (middle), and of Δ SSS (ISAS - TSG (Polarstern)). Only match-up pairs are used to generate these maps.

3.7.7 Time series of the monthly median and Std of *in situ* and ISAS SSS and of the difference (Δ SSS)

In the top panel of Figure 92, we show the time series of the monthly median SSS estimated for both ISAS SSS product (in black) and the TSG (Polarstern) *in situ* dataset (in blue) at the collected Pi-MEP match-up pairs.

In the middle panel of Figure 92, we show the time series of the monthly median of Δ SSS (ISAS - TSG (Polarstern)) for the collected Pi-MEP match-up pairs.

In the bottom panel of Figure 92, we show the time series of the monthly standard deviation of the ΔSSS (ISAS - TSG (Polarstern)) for the collected Pi-MEP match-up pairs.

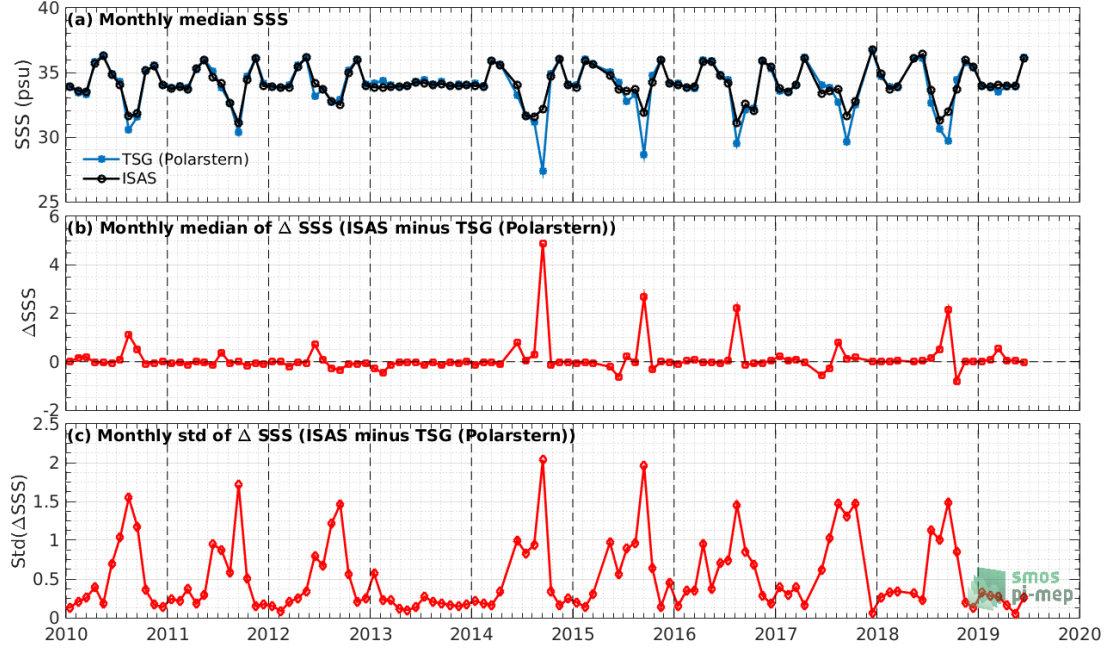


Figure 92: Time series of the monthly median SSS (top), median of ΔSSS (ISAS - TSG (Polarstern)) and Std of ΔSSS (ISAS - TSG (Polarstern)) considering all match-ups collected by the Pi-MEP.

3.7.8 Zonal mean and Std of *in situ* and ISAS SSS and of the difference ΔSSS

In Figure 93 left panel, we show the zonal mean SSS considering all Pi-MEP match-up pairs for both ISAS SSS product (in black) and the TSG (Polarstern) *in situ* dataset (in blue). The full *in situ* dataset period is used to derive the mean.

In the right panel of Figure 93, we show the zonal mean of ΔSSS (ISAS - TSG (Polarstern)) for all the collected Pi-MEP match-up pairs estimated over the full *in situ* dataset period.

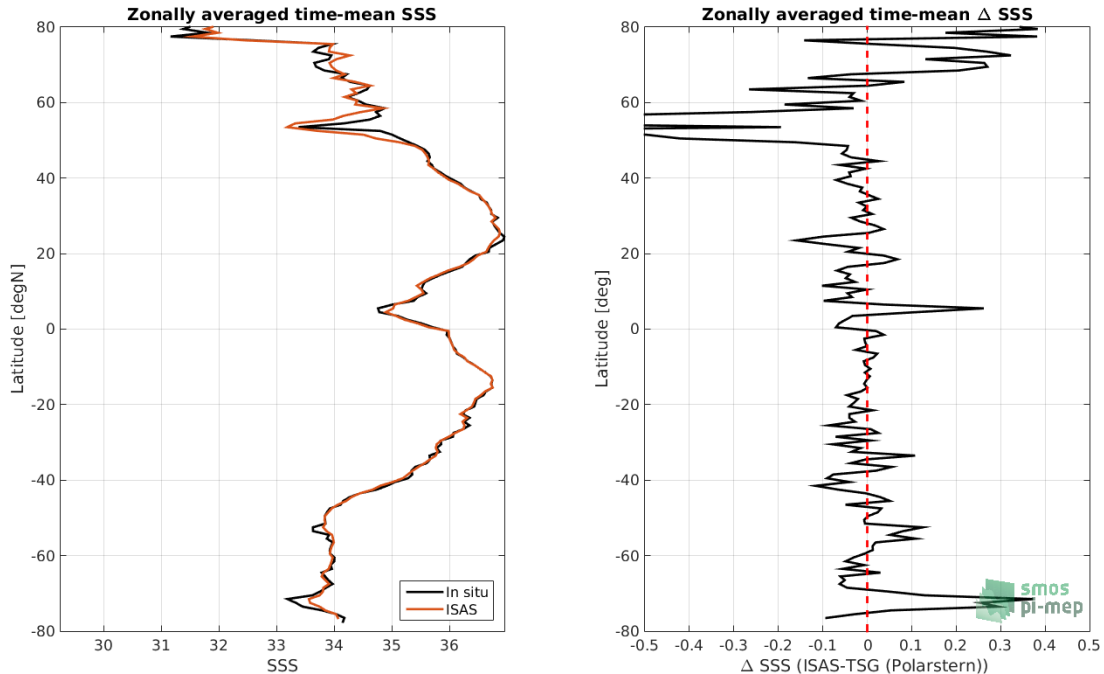


Figure 93: Left panel: Zonal mean SSS from ISAS product (black) and from TSG (Polarstern) (blue). Right panel: Zonal mean of Δ SSS (ISAS - TSG (Polarstern)) for all the collected Pi-MEP match-up pairs estimated over the full *in situ* dataset period.

3.7.9 Scatterplots of ISAS vs *in situ* SSS by latitudinal bands

In Figure 94, contour maps of the concentration of ISAS SSS (y-axis) versus TSG (Polarstern) SSS (x-axis) at match-up pairs for different latitude bands: (a) 80°S-80°N, (b) 20°S-20°N, (c) 40°S-20°S and 20°N-40°N and (d) 60°S-40°S and 40°N-60°N. For each plot, the red line shows $x=y$. The black thin and dashed lines indicate a linear fit through the data cloud and the $\pm 95\%$ confidence levels, respectively. The number match-up pairs n , the slope and R^2 coefficient of the linear fit, the root mean square (RMS) and the mean bias between ISAS and *in situ* data are indicated for each latitude band in each plots.

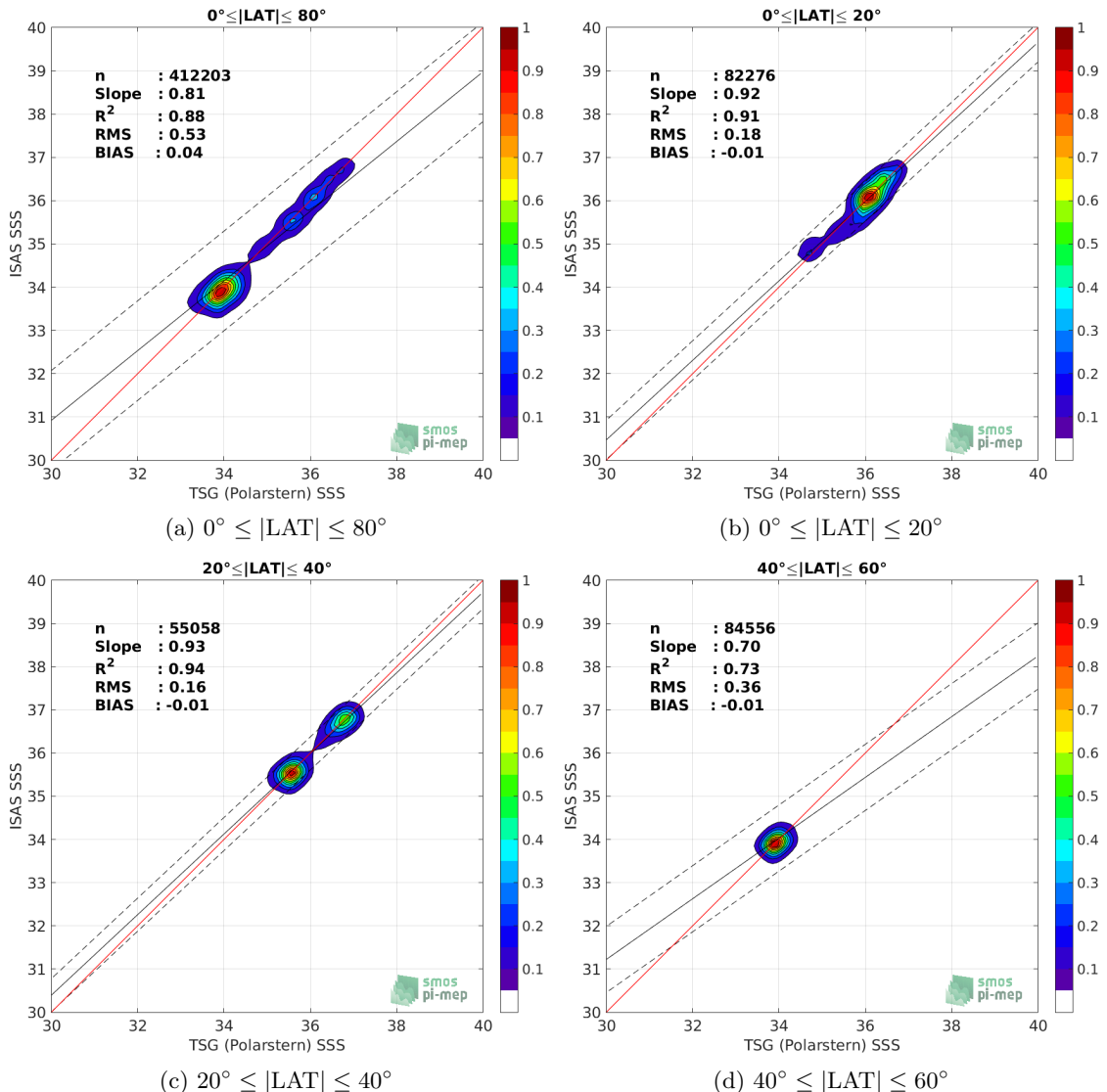


Figure 94: Contour maps of the concentration of ISAS SSS (y-axis) versus TSG (Polarstern) SSS (x-axis) at match-up pairs for different latitude bands. For each plot, the red line shows $x=y$. The black thin and dashed lines indicate a linear fit through the data cloud and the $\pm 95\%$ confidence levels, respectively. The number match-up pairs n , the slope and R^2 coefficient of the linear fit, the root mean square (RMS) and the mean bias between ISAS and *in situ* data are indicated for each latitude band in each plots.

3.7.10 Time series of the monthly median and Std of the difference ΔSSS sorted by latitudinal bands

In Figure 95, time series of the monthly median (red curves) of Δ SSS (ISAS - TSG (Polarstern)) and ± 1 Std (black vertical thick bars) as function of time for all the collected Pi-MEP match-up pairs estimated for the full *in situ* dataset period are shown for different latitude bands: (a) 80°S-80°N, (b) 20°S-20°N, (c) 40°S-20°S and 20°N-40°N and (d) 60°S-40°S and 40°N-60°N.

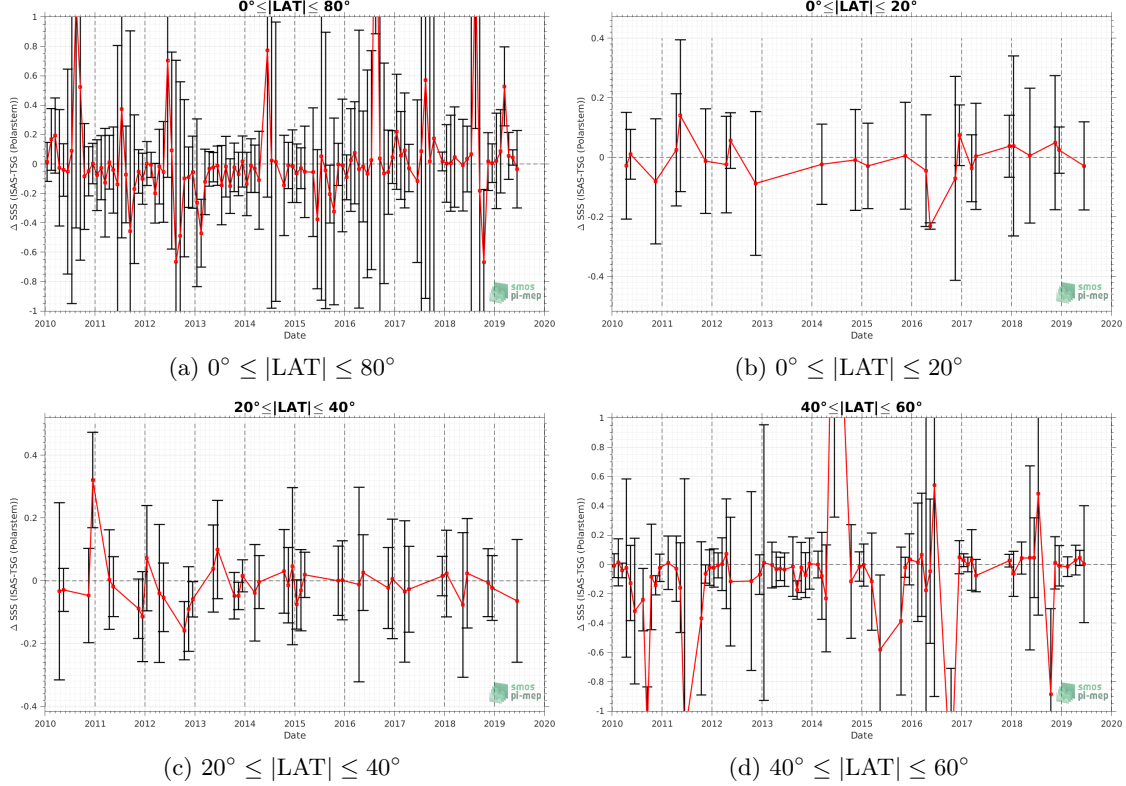


Figure 95: Monthly median (red curves) of ΔSSS (ISAS - TSG (Polarstern)) and ± 1 Std (black vertical thick bars) as function of time for all the collected Pi-MEP match-up pairs for the full *in situ* dataset period are shown for different latitude bands: (a) $80^\circ\text{S}-80^\circ\text{N}$, (b) $20^\circ\text{S}-20^\circ\text{N}$, (c) $40^\circ\text{S}-20^\circ\text{S}$ and $20^\circ\text{N}-40^\circ\text{N}$ and (d) $60^\circ\text{S}-40^\circ\text{S}$ and $40^\circ\text{N}-60^\circ\text{N}$.

3.7.11 ΔSSS sorted as geophysical conditions

In Figure 96, we classify the match-up differences ΔSSS (ISAS - *in situ*) as function of the geophysical conditions at match-up points. The mean and std of ΔSSS (ISAS - TSG (Polarstern)) is thus evaluated as function of the

- *in situ* SSS values per bins of width 0.2,
- *in situ* SST values per bins of width 1°C ,
- ASCAT daily wind values per bins of width 1 m/s,
- CMORPH 3-hourly rain rates per bins of width 1 mm/h, and,
- distance to coasts per bins of width 50 km,
- *in situ* measurement depth (if relevant).

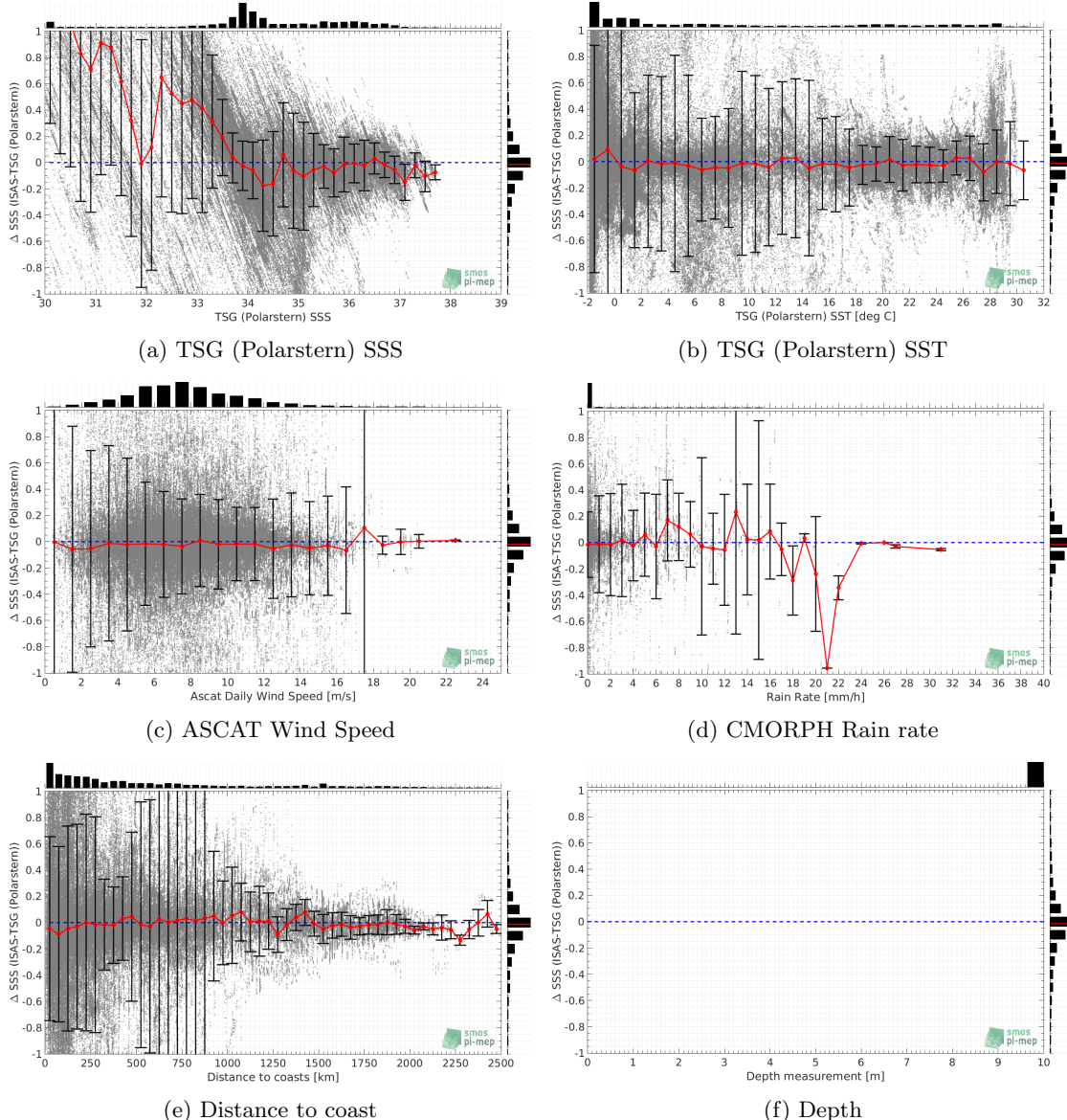


Figure 96: ΔSSS (ISAS - TSG (Polarstern)) sorted as geophysical conditions: TSG (Polarstern) SSS a), TSG (Polarstern) SST b), ASCAT Wind speed c), CMORPH rain rate d), distance to coast (e) and depth measurements (f).

3.7.12 ΔSSS maps and statistics for different geophysical conditions

In Figures 97 and 98, we focus on sub-datasets of the match-up differences ΔSSS (ISAS - *in situ*) for the following specific geophysical conditions:

- **C1:** if the local value at *in situ* location of estimated rain rate is zero, mean daily wind is in the range [3, 12] m/s, the SST is $> 5^\circ\text{C}$ and distance to coast is > 800 km.
- **C2:** if the local value at *in situ* location of estimated rain rate is zero, mean daily wind is

in the range [3, 12] m/s.

- **C3:** if the local value at *in situ* location of estimated rain rate is high (ie. $> 1 \text{ mm/h}$) and mean daily wind is low (ie. $< 4 \text{ m/s}$).
- **C5:** if the *in situ* data is located where the climatological SSS standard deviation is low (ie. above < 0.2).
- **C6:** if the *in situ* data is located where the climatological SSS standard deviation is high (ie. above > 0.2).

For each of these conditions, the temporal mean (gridded over spatial boxes of size $1^\circ \times 1^\circ$) and the histogram of the difference ΔSSS (ISAS - *in situ*) are presented.

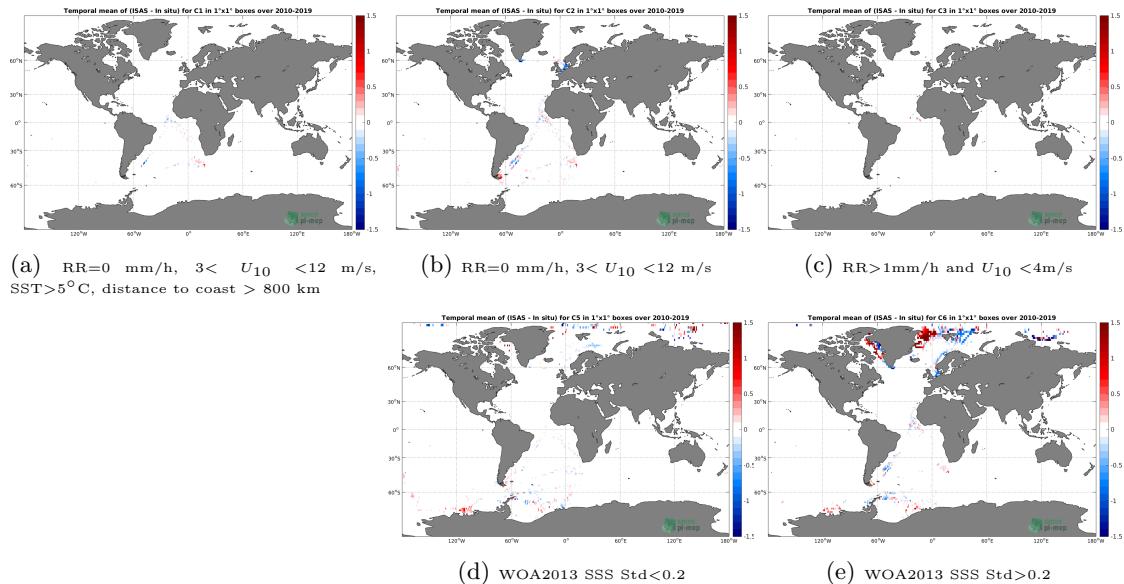


Figure 97: Temporal mean gridded over spatial boxes of size $1^\circ \times 1^\circ$ of ΔSSS (ISAS - TSG (Polarstern)) for 5 different subdatasets corresponding to: $\text{RR}=0 \text{ mm/h}$, $3 < U_{10} < 12 \text{ m/s}$, $\text{SST}>5^\circ\text{C}$, distance to coast $> 800 \text{ km}$ (a), $\text{RR}=0 \text{ mm/h}$, $3 < U_{10} < 12 \text{ m/s}$ (b), $\text{RR}>1\text{mm/h}$ and $U_{10} < 4\text{m/s}$ (c), WOA2013 SSS Std < 0.2 (d), WOA2013 SSS Std > 0.2 (e).

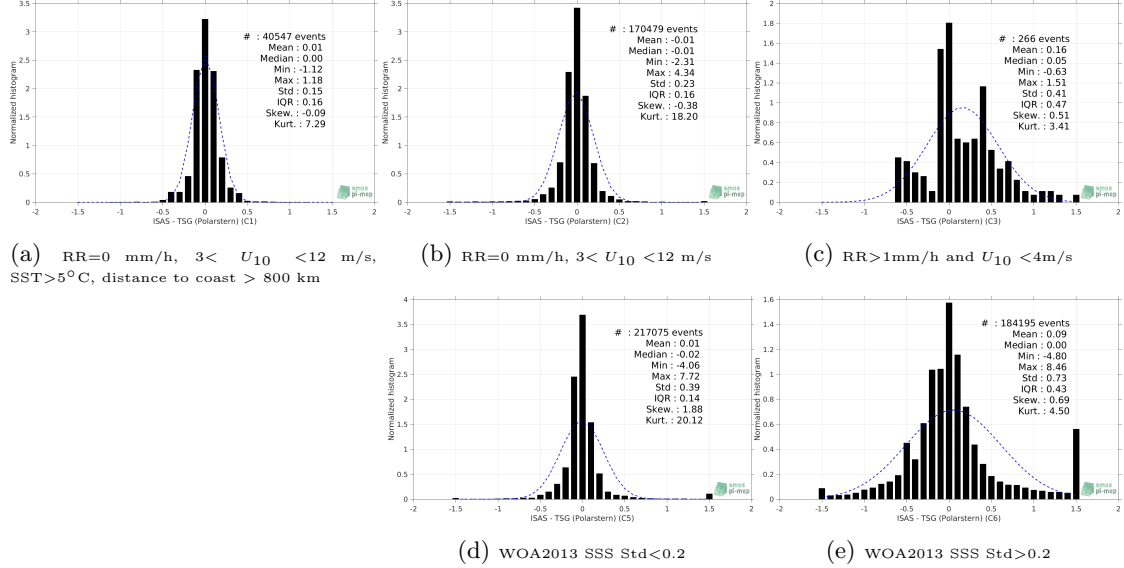


Figure 98: Normalized histogram of ΔSSS (ISAS - TSG (Polarstern)) for 5 different subdatasets corresponding to: RR=0 mm/h, $3 < U_{10} < 12$ m/s, SST $>5^{\circ}\text{C}$, distance to coast > 800 km (a), RR=0 mm/h, $3 < U_{10} < 12$ m/s (b), RR $>1\text{mm/h}$ and $U_{10} < 4\text{m/s}$ (c), WOA2013 SSS Std <0.2 (d), WOA2013 SSS Std >0.2 (e).

3.7.13 Summary

Table 1 shows the mean, median, standard deviation (Std), root mean square (RMS), interquartile range (IQR), correlation coefficient (r^2) and robust standard deviation (Std*) of the match-up differences ΔSSS (ISAS - TSG (Polarstern)) for the following conditions:

- all: All the match-up pairs satellite/in situ SSS values are used to derive the statistics
- C1: only pairs where RR=0 mm/h, $3 < U_{10} < 12$ m/s, SST $>5^{\circ}\text{C}$, distance to coast > 800 km
- C2: only pairs where RR=0 mm/h, $3 < U_{10} < 12$ m/s
- C3: only pairs where RR $>1\text{mm/h}$ and $U_{10} < 4\text{m/s}$
- C5: only pairs where WOA2013 SSS Std <0.2
- C6: only pairs where WOA2013 SSS Std >0.2
- C7a: only pairs with a distance to coast < 150 km.
- C7b: only pairs with a distance to coast in the range [150, 800] km.
- C7c: only pairs with a distance to coast > 800 km.
- C8a: only pairs where SST is $< 5^{\circ}\text{C}$.
- C8b: only pairs where SST is in the range [5, 15] $^{\circ}\text{C}$.
- C8c: only pairs where SST is $> 15^{\circ}\text{C}$.

- C9a: only pairs where SSS is < 33 .
- C9b: only pairs where SSS is in the range [33, 37].
- C9c: only pairs where SSS is > 37 .

Table 1: Statistics of Δ SSS (ISAS - TSG (Polarstern))

Condition	#	Median	Mean	Std	RMS	IQR	r^2	Std*
all	442795	-0.01	0.10	0.75	0.76	0.24	0.83	0.18
C1	40547	0.00	0.01	0.15	0.15	0.16	0.97	0.12
C2	170479	-0.01	-0.01	0.23	0.23	0.16	0.96	0.12
C3	266	0.05	0.16	0.41	0.44	0.47	0.88	0.37
C5	217075	-0.02	0.01	0.39	0.39	0.14	0.92	0.11
C6	184195	0.00	0.09	0.73	0.74	0.43	0.83	0.33
C7a	128460	-0.06	0.03	0.72	0.72	0.40	0.81	0.30
C7b	206389	0.00	0.17	0.87	0.89	0.26	0.81	0.18
C7c	107909	-0.01	0.04	0.50	0.50	0.15	0.88	0.11
C8a	234510	0.00	0.21	0.96	0.99	0.34	0.66	0.25
C8b	66643	-0.04	-0.04	0.57	0.57	0.26	0.69	0.19
C8c	105714	-0.02	-0.02	0.20	0.20	0.18	0.91	0.13
C9a	51684	0.98	1.26	1.64	2.07	1.92	0.25	1.40
C9b	386802	-0.03	-0.05	0.29	0.29	0.20	0.93	0.15
C9c	4309	-0.09	-0.11	0.13	0.17	0.20	0.74	0.15

Table 1 numerical values can be downloaded as a csv file [here](#).

3.8 TSG (NCEI-0170743)

3.8.1 Introduction

The TSG-NCEI-0170743 dataset ([Aulicino et al. \(2018\)](#)) contains sea surface temperature and salinity data collected from 2010 to 2017 in the South Atlantic Ocean and Southern Ocean from S.A. Agulhas and Agulhas-II research vessels, in the framework of South African National Antarctic Programme ([SANAP](#)), South African Department of Environmental Affairs ([DEA](#)) and Italian National Antarctic Research Programme ([PNRA](#)) scientific activities. Measurements have been obtained through termosalinograph (TSG) during several cruises to both Antarctica and sub-Antarctic islands. On-board TSG devices have been regularly calibrated and continuously monitored in-between cruises; no appreciable sensor drift emerged. Independent water samples taken along the cruises have been used to validate the data; salinity measurement error was a few hundredths of a unit on the practical salinity scale. A careful quality control allowed to discard bad data for each single campaign.

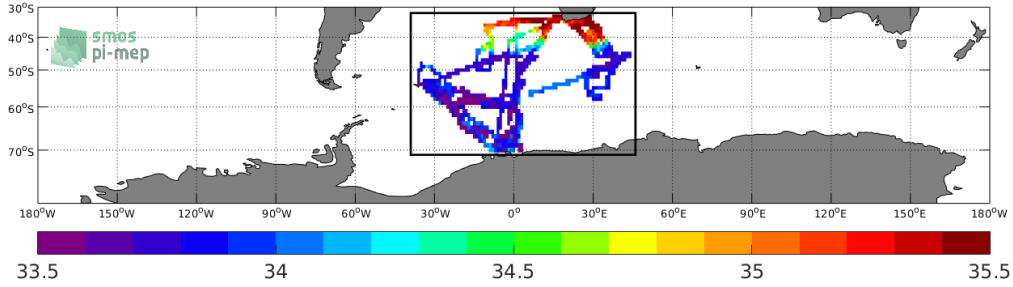


Figure 99: Location of the TSG (NCEI-0170743) dataset.

3.8.2 Number of SSS data as a function of time and distance to coast

Figure 100 shows the time (a) and distance to coast (b) distributions of the TSG (NCEI-0170743) *in situ* dataset.

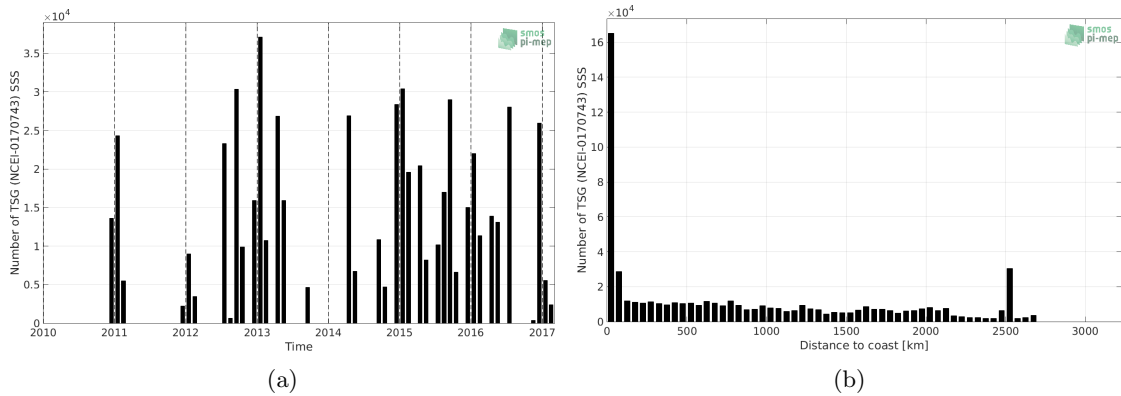


Figure 100: Number of SSS from TSG (NCEI-0170743) as a function of time (a) and distance to coast (b).

3.8.3 Histograms of SSS

Figure 101 shows the SSS distribution of the TSG (NCEI-0170743) (a) and colocalized ISAS (b) dataset.

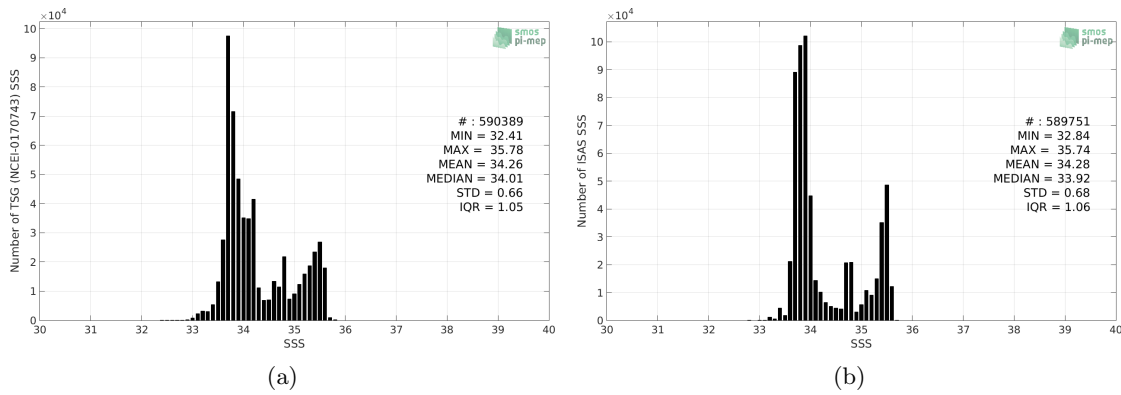


Figure 101: Histograms of SSS from TSG (NCEI-0170743) (a) and ISAS (b) per bins of 0.1.

3.8.4 Distribution of *in situ* SSS depth measurements

In Figure 102, we show the depth distribution of the *in situ* salinity dataset (a) and the spatial distribution of the depth temporal mean in $1^\circ \times 1^\circ$ boxes and considering the full *in situ* dataset period (b).

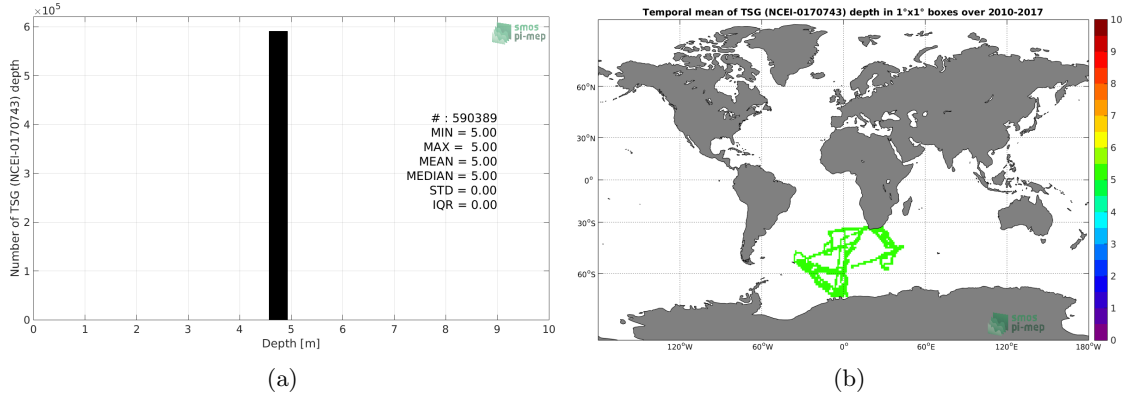


Figure 102: Depth distribution of the upper level SSS measurements from TSG (NCEI-0170743) (a) and spatial distribution of the *in situ* SSS depth measurements showing the mean value in $1^\circ \times 1^\circ$ boxes and considering the full *in situ* dataset period (b).

3.8.5 Spatial distribution of SSS

In Figure 103, the number of TSG (NCEI-0170743) SSS measurements in $1^\circ \times 1^\circ$ boxes is shown.

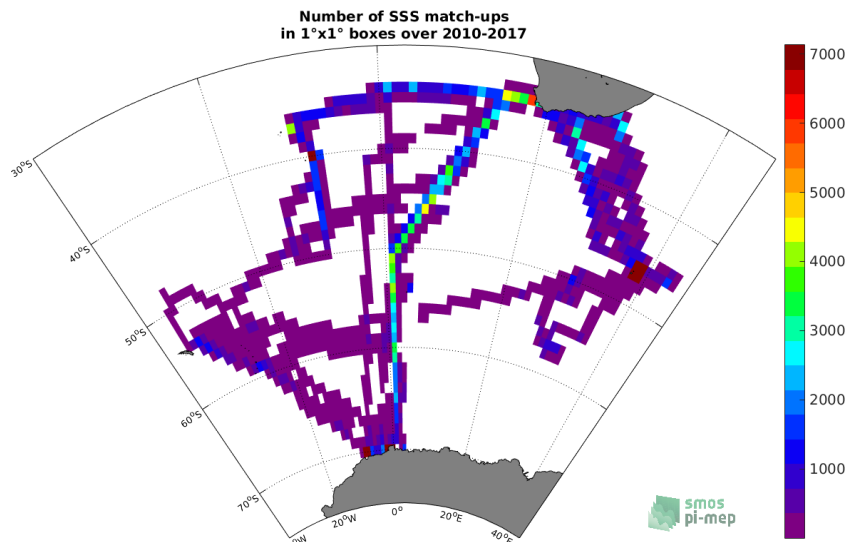


Figure 103: Number of SSS from TSG (NCEI-0170743) in $1^\circ \times 1^\circ$ boxes.

3.8.6 Spatial Maps of the Temporal mean and Std of *in situ* and ISAS SSS and of the difference (Δ SSS)

In Figure 104, we show maps of temporal mean (left) and standard deviation (right) of ISAS (top), TSG (NCEI-0170743) *in situ* dataset (middle) and the difference Δ SSS(ISAS -TSG (NCEI-0170743)) (bottom). The temporal mean and std are calculated using all match-up pairs falling in spatial boxes of size $1^\circ \times 1^\circ$ over the full TSG (NCEI-0170743) dataset period.

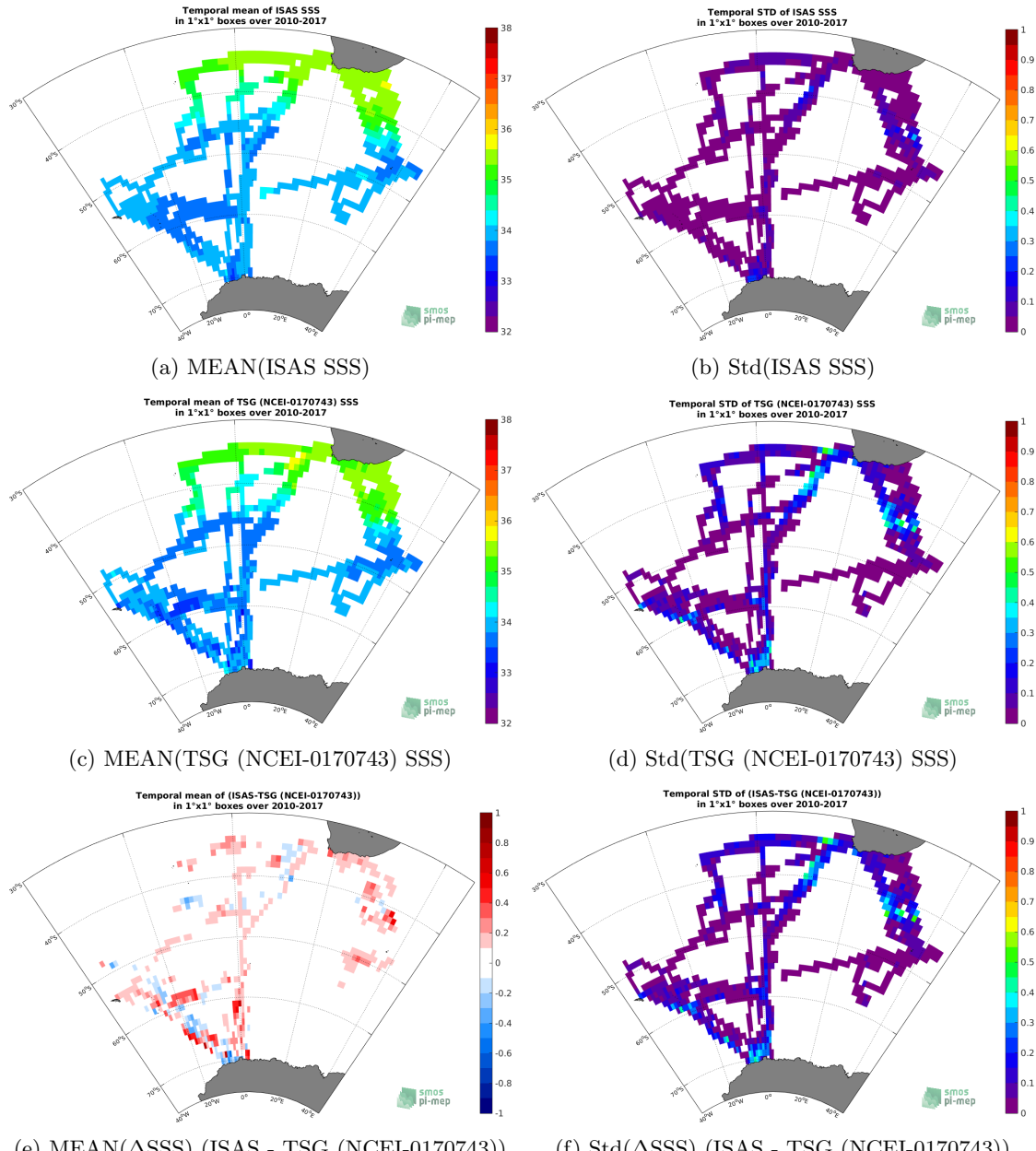


Figure 104: Temporal mean (left) and Std (right) of SSS from ISAS (top), TSG (NCEI-0170743) (middle), and of Δ SSS (ISAS - TSG (NCEI-0170743)). Only match-up pairs are used to generate these maps.

3.8.7 Time series of the monthly median and Std of *in situ* and ISAS SSS and of the difference (Δ SSS)

In the top panel of Figure 105, we show the time series of the monthly median SSS estimated for both ISAS SSS product (in black) and the TSG (NCEI-0170743) *in situ* dataset (in blue) at the collected Pi-MEP match-up pairs.

In the middle panel of Figure 105, we show the time series of the monthly median of ΔSSS (ISAS - TSG (NCEI-0170743)) for the collected Pi-MEP match-up pairs.

In the bottom panel of Figure 105, we show the time series of the monthly standard deviation of the ΔSSS (ISAS - TSG (NCEI-0170743)) for the collected Pi-MEP match-up pairs.

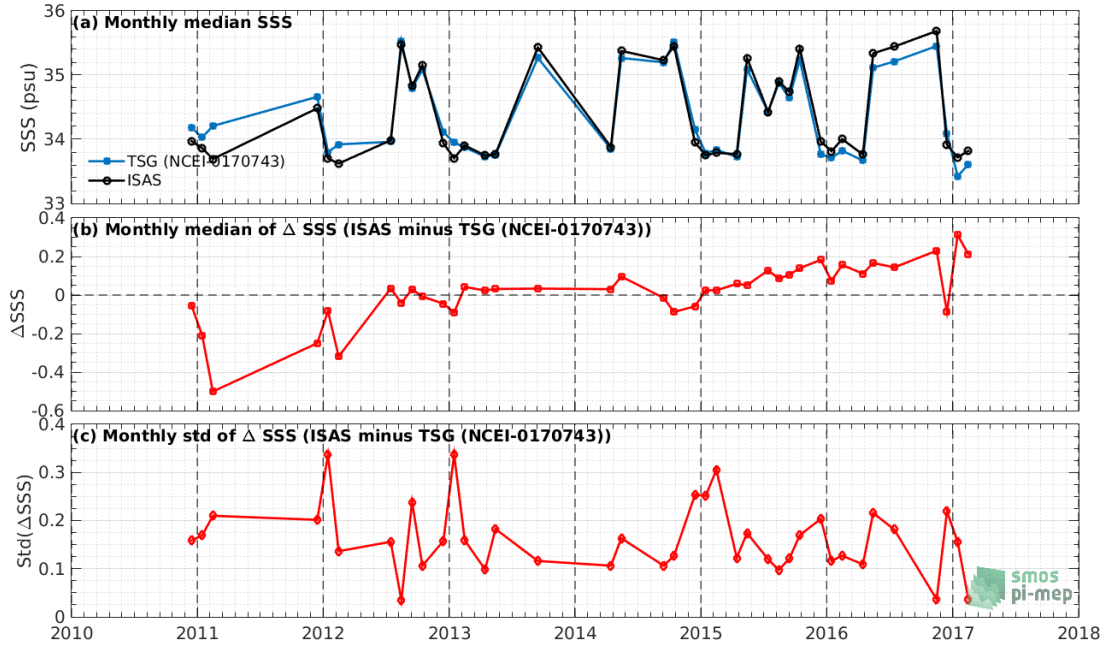


Figure 105: Time series of the monthly median SSS (top), median of ΔSSS (ISAS - TSG (NCEI-0170743)) and Std of ΔSSS (ISAS - TSG (NCEI-0170743)) considering all match-ups collected by the Pi-MEP.

3.8.8 Zonal mean and Std of *in situ* and ISAS SSS and of the difference ΔSSS

In Figure 106 left panel, we show the zonal mean SSS considering all Pi-MEP match-up pairs for both ISAS SSS product (in black) and the TSG (NCEI-0170743) *in situ* dataset (in blue). The full *in situ* dataset period is used to derive the mean.

In the right panel of Figure 106, we show the zonal mean of ΔSSS (ISAS - TSG (NCEI-0170743)) for all the collected Pi-MEP match-up pairs estimated over the full *in situ* dataset period.

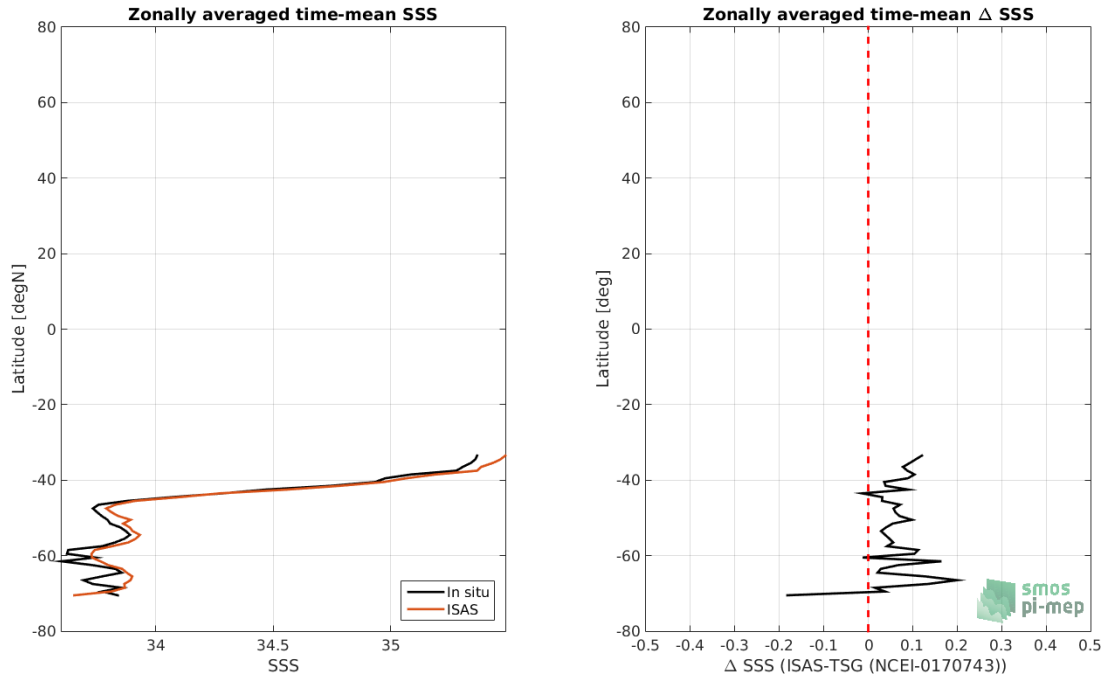


Figure 106: Left panel: Zonal mean SSS from ISAS product (black) and from TSG (NCEI-0170743) (blue). Right panel: Zonal mean of Δ SSS (ISAS - TSG (NCEI-0170743)) for all the collected Pi-MEP match-up pairs estimated over the full *in situ* dataset period.

3.8.9 Scatterplots of ISAS vs *in situ* SSS by latitudinal bands

In Figure 107, contour maps of the concentration of ISAS SSS (y-axis) versus TSG (NCEI-0170743) SSS (x-axis) at match-up pairs for different latitude bands: (a) 80°S-80°N, (b) 20°S-20°N, (c) 40°S-20°S and 20°N-40°N and (d) 60°S-40°S and 40°N-60°N. For each plot, the red line shows $x=y$. The black thin and dashed lines indicate a linear fit through the data cloud and the $\pm 95\%$ confidence levels, respectively. The number match-up pairs n , the slope and R^2 coefficient of the linear fit, the root mean square (RMS) and the mean bias between ISAS and *in situ* data are indicated for each latitude band in each plots.

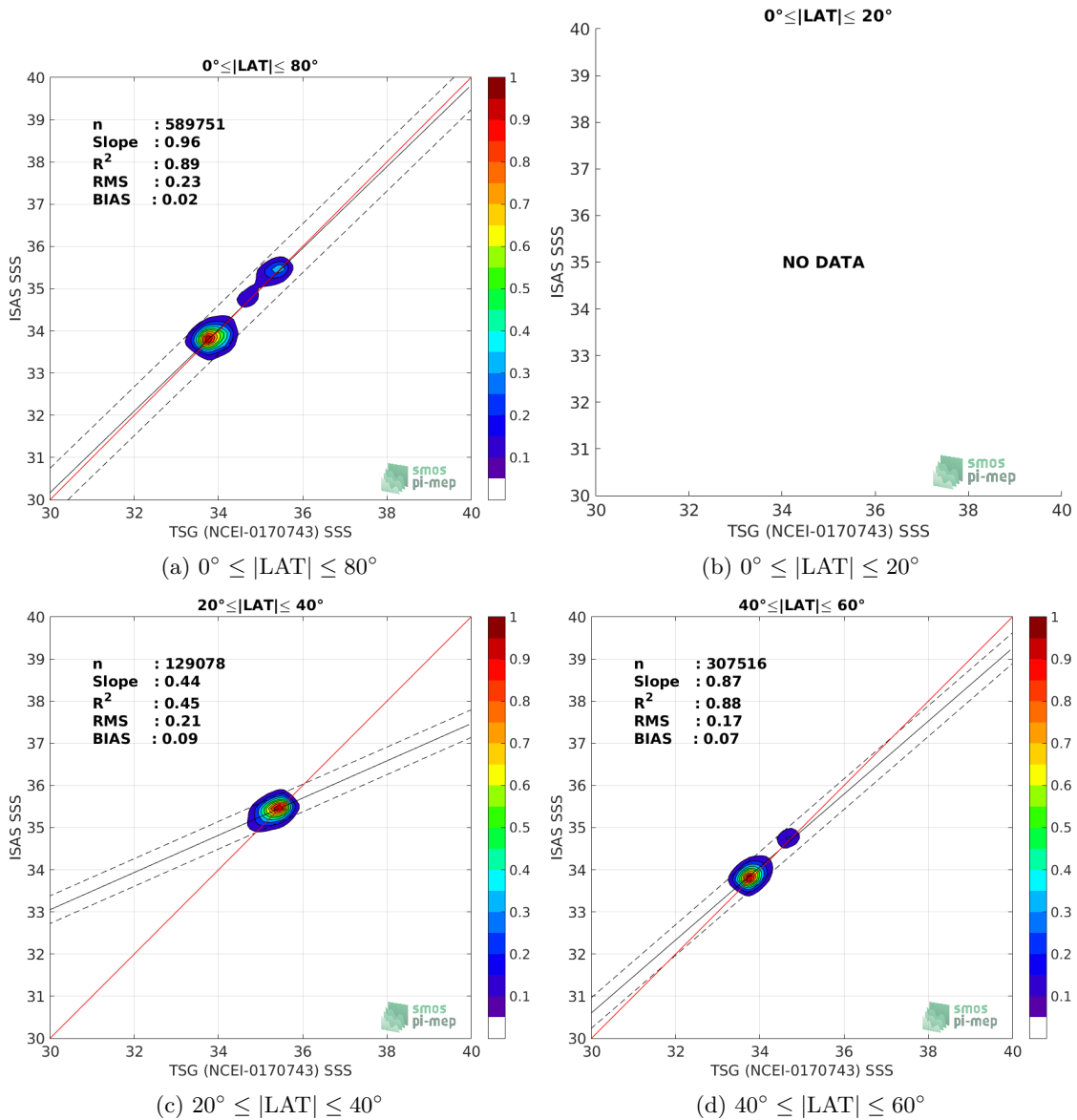


Figure 107: Contour maps of the concentration of ISAS SSS (y-axis) versus TSG (NCEI-0170743) SSS (x-axis) at match-up pairs for different latitude bands. For each plot, the red line shows $x=y$. The black thin and dashed lines indicate a linear fit through the data cloud and the $\pm 95\%$ confidence levels, respectively. The number match-up pairs n , the slope and R^2 coefficient of the linear fit, the root mean square (RMS) and the mean bias between ISAS and *in situ* data are indicated for each latitude band in each plots.

3.8.10 Time series of the monthly median and Std of the difference ΔSSS sorted by latitudinal bands

In Figure 108, time series of the monthly median (red curves) of ΔSSS (ISAS - TSG (NCEI-0170743)) and ± 1 Std (black vertical thick bars) as function of time for all the collected Pi-MEP

match-up pairs estimated for the full *in situ* dataset period are shown for different latitude bands: (a) 80°S-80°N, (b) 20°S-20°N, (c) 40°S-20°S and 20°N-40°N and (d) 60°S-40°S and 40°N-60°N.

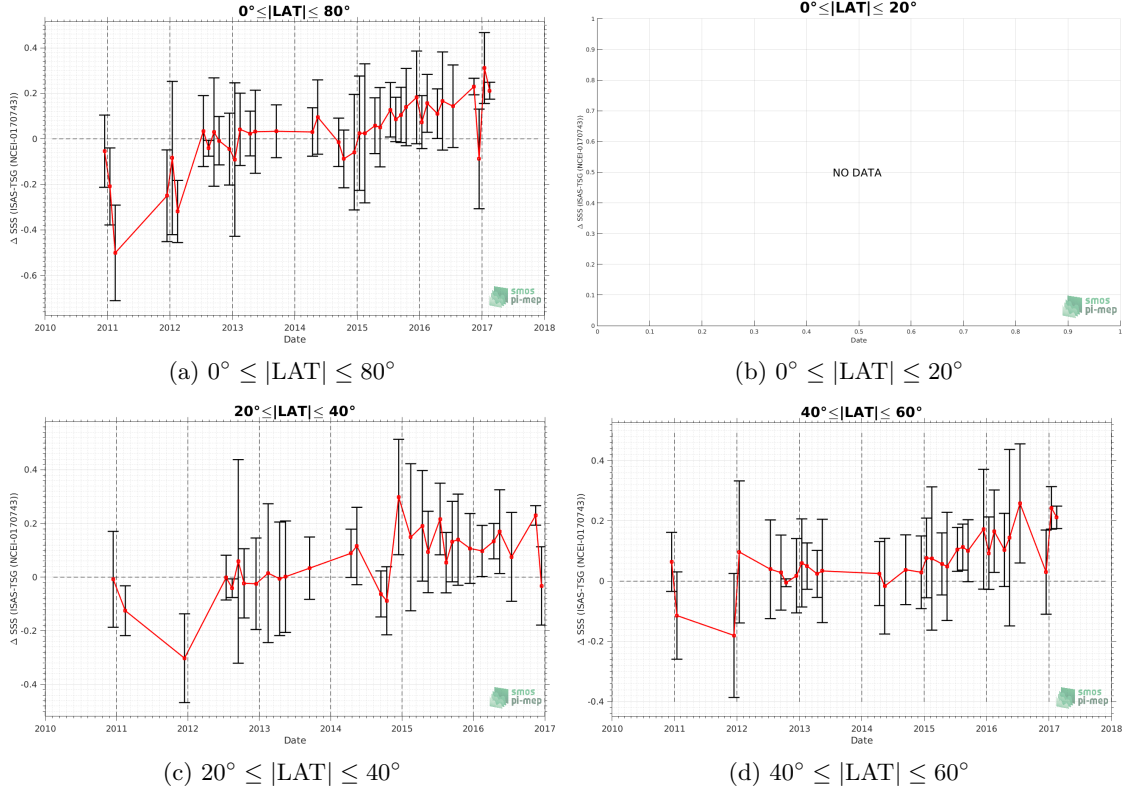


Figure 108: Monthly median (red curves) of ΔSSS (ISAS - TSG (NCEI-0170743)) and ± 1 Std (black vertical thick bars) as function of time for all the collected Pi-MEP match-up pairs for the full *in situ* dataset period are shown for different latitude bands: (a) 80°S-80°N, (b) 20°S-20°N, (c) 40°S-20°S and 20°N-40°N and (d) 60°S-40°S and 40°N-60°N.

3.8.11 ΔSSS sorted as geophysical conditions

In Figure 109, we classify the match-up differences ΔSSS (ISAS - *in situ*) as function of the geophysical conditions at match-up points. The mean and std of ΔSSS (ISAS - TSG (NCEI-0170743)) is thus evaluated as function of the

- *in situ* SSS values per bins of width 0.2,
- *in situ* SST values per bins of width 1°C,
- ASCAT daily wind values per bins of width 1 m/s,
- CMORPH 3-hourly rain rates per bins of width 1 mm/h, and,
- distance to coasts per bins of width 50 km,
- *in situ* measurement depth (if relevant).

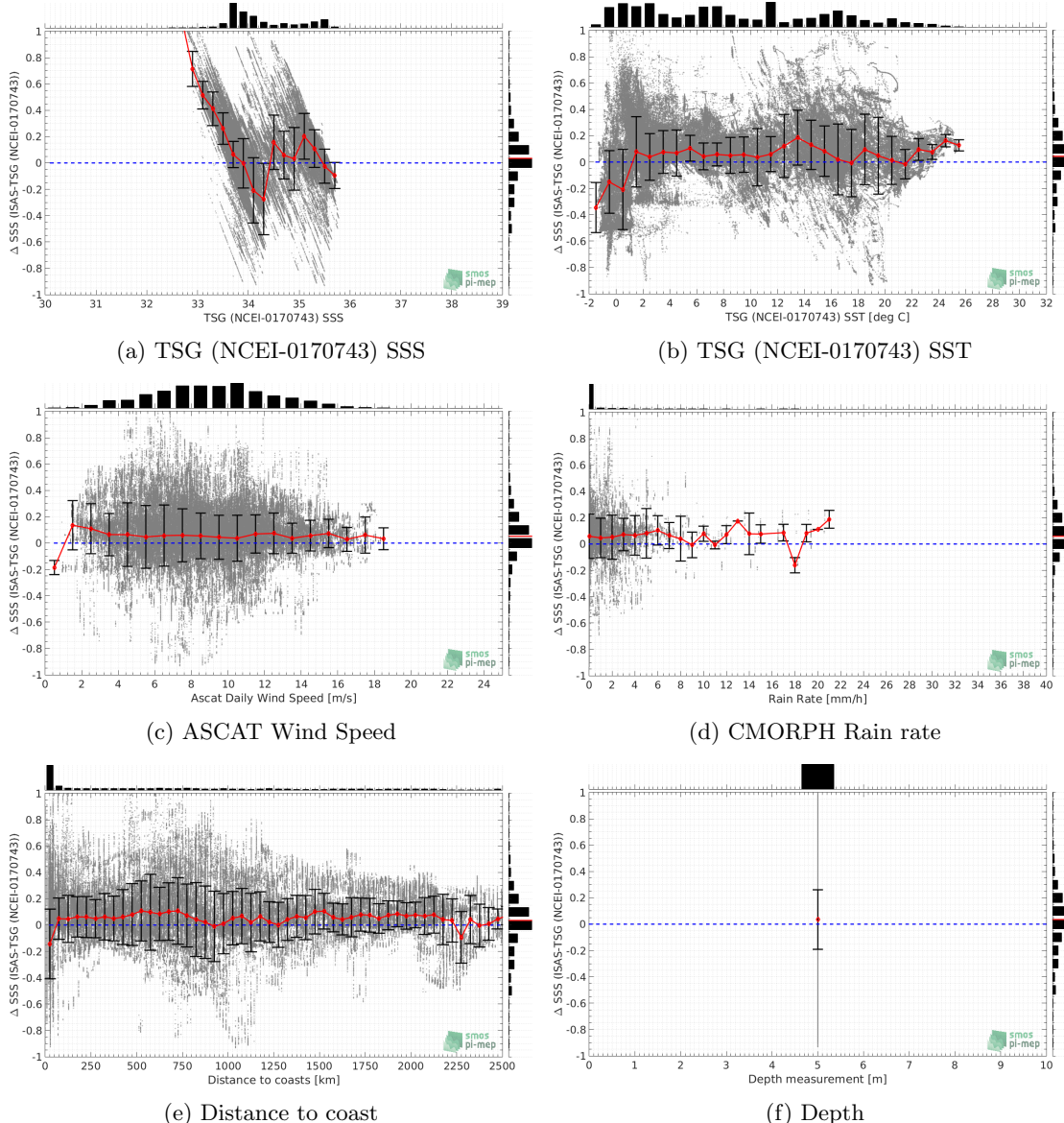


Figure 109: ΔSSS (ISAS - TSG (NCEI-0170743)) sorted as geophysical conditions: TSG (NCEI-0170743) SSS a), TSG (NCEI-0170743) SST b), ASCAT Wind speed c), CMORPH rain rate d), distance to coast (e) and depth measurements (f).

3.8.12 ΔSSS maps and statistics for different geophysical conditions

In Figures 110 and 111, we focus on sub-datasets of the match-up differences ΔSSS (ISAS - *in situ*) for the following specific geophysical conditions:

- **C1:** if the local value at *in situ* location of estimated rain rate is zero, mean daily wind is in the range [3, 12] m/s, the SST is $> 5^\circ\text{C}$ and distance to coast is > 800 km.
- **C2:** if the local value at *in situ* location of estimated rain rate is zero, mean daily wind is

in the range [3, 12] m/s.

- **C3:** if the local value at *in situ* location of estimated rain rate is high (ie. $> 1 \text{ mm/h}$) and mean daily wind is low (ie. $< 4 \text{ m/s}$).
- **C5:** if the *in situ* data is located where the climatological SSS standard deviation is low (ie. above < 0.2).
- **C6:** if the *in situ* data is located where the climatological SSS standard deviation is high (ie. above > 0.2).

For each of these conditions, the temporal mean (gridded over spatial boxes of size $1^\circ \times 1^\circ$) and the histogram of the difference ΔSSS (ISAS - *in situ*) are presented.

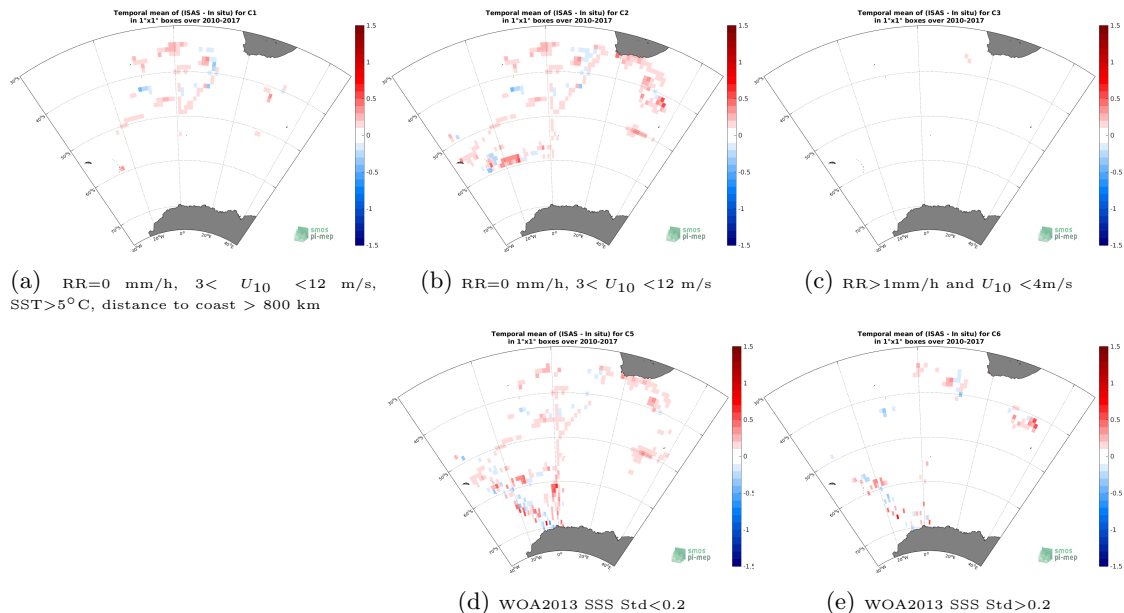


Figure 110: Temporal mean gridded over spatial boxes of size $1^\circ \times 1^\circ$ of ΔSSS (ISAS - TSG (NCEI-0170743)) for 5 different subdatasets corresponding to: $\text{RR}=0 \text{ mm/h}, 3 < U_{10} < 12 \text{ m/s}, \text{SST} > 5^\circ\text{C}, \text{distance to coast} > 800 \text{ km}$ (a), $\text{RR}=0 \text{ mm/h}, 3 < U_{10} < 12 \text{ m/s}$ (b), $\text{RR} > 1\text{mm/h and } U_{10} < 4\text{m/s}$ (c), WOA2013 SSS Std < 0.2 (d), WOA2013 SSS Std > 0.2 (e).

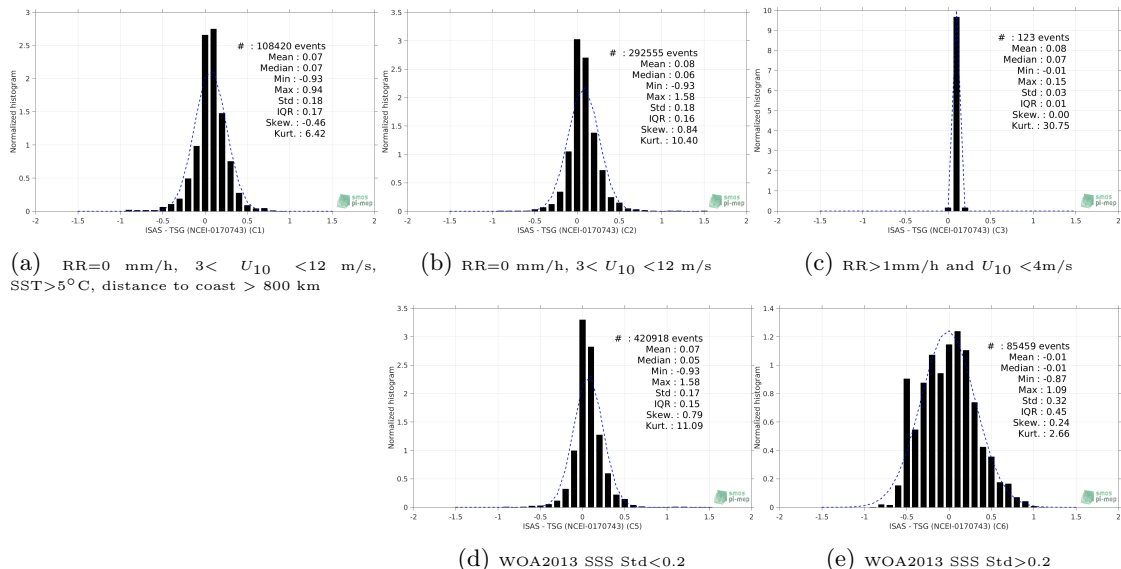


Figure 111: Normalized histogram of ΔSSS (ISAS - TSG (NCEI-0170743)) for 5 different sub-datasets corresponding to: RR=0 mm/h, $3 < U_{10} < 12$ m/s, SST>5°C, distance to coast > 800 km (a), RR=0 mm/h, $3 < U_{10} < 12$ m/s (b), RR>1mm/h and $U_{10} < 4$ m/s (c), WOA2013 SSS Std<0.2 (d), WOA2013 SSS Std>0.2 (e).

3.8.13 Summary

Table 1 shows the mean, median, standard deviation (Std), root mean square (RMS), interquartile range (IQR), correlation coefficient (r^2) and robust standard deviation (Std*) of the match-up differences ΔSSS (ISAS - TSG (NCEI-0170743)) for the following conditions:

- all: All the match-up pairs satellite/in situ SSS values are used to derive the statistics
- C1: only pairs where RR=0 mm/h, $3 < U_{10} < 12$ m/s, SST>5°C, distance to coast > 800 km
- C2: only pairs where RR=0 mm/h, $3 < U_{10} < 12$ m/s
- C3: only pairs where RR>1mm/h and $U_{10} < 4$ m/s
- C5: only pairs where WOA2013 SSS Std<0.2
- C6: only pairs where WOA2013 SSS Std>0.2
- C7a: only pairs with a distance to coast < 150 km.
- C7b: only pairs with a distance to coast in the range [150, 800] km.
- C7c: only pairs with a distance to coast > 800 km.
- C8a: only pairs where SST is < 5°C.
- C8b: only pairs where SST is in the range [5, 15]°C.
- C8c: only pairs where SST is > 15°C.

- C9a: only pairs where SSS is < 33 .
- C9b: only pairs where SSS is in the range [33, 37].
- C9c: only pairs where SSS is > 37 .

Table 1: Statistics of ΔSSS (ISAS - TSG (NCEI-0170743))

Condition	#	Median	Mean	Std	RMS	IQR	r^2	Std*
all	589751	0.03	0.02	0.23	0.23	0.21	0.89	0.16
C1	108420	0.07	0.07	0.18	0.19	0.17	0.91	0.13
C2	292555	0.06	0.08	0.18	0.19	0.16	0.94	0.12
C3	123	0.07	0.08	0.03	0.09	0.01	1.00	0.01
C5	420918	0.05	0.07	0.17	0.18	0.15	0.94	0.11
C6	85459	-0.01	-0.01	0.32	0.32	0.45	0.79	0.34
C7a	205194	-0.01	-0.08	0.26	0.27	0.35	0.79	0.25
C7b	138113	0.07	0.09	0.21	0.23	0.22	0.93	0.16
C7c	246444	0.06	0.07	0.17	0.18	0.16	0.92	0.12
C8a	194461	0.00	-0.03	0.26	0.26	0.35	0.04	0.24
C8b	219434	0.06	0.08	0.15	0.17	0.13	0.92	0.09
C8c	124692	0.04	0.06	0.23	0.23	0.22	0.78	0.16
C9a	940	0.87	0.86	0.20	0.88	0.31	0.20	0.27
C9b	588811	0.03	0.02	0.22	0.22	0.21	0.89	0.15
C9c	0	NaN	NaN	NaN	NaN	NaN	NaN	NaN

Table 1 numerical values can be downloaded as a csv file [here](#).

4 Surface drifters

4.1 Introduction

The skin depth of the L-band radiometer signal over the ocean is about 1 cm whereas classical surface salinity measured by ships or Argo floats are performed at a few meters depth. In order to improve the knowledge of the SSS variability in the first 50 cm depth, to better document the SSS variability in a satellite pixel and to provide ground-truth as close as possible to the sea surface for validating satellite SSS, the L-band remotely sensed community proposed to deploy numerous surface drifters over various parts of the ocean. Surface drifter data are provided by the LOCEAN (see <https://www.locean-ipsl.upmc.fr/smos/drifters/>). Only validated data are considered with uncertainty order of 0.01 and 0.1.

4.2 Number of SSS data as a function of time and distance to coast

Figure 112 shows the time (a) and distance to coast (b) distributions of the Surface drifters *in situ* dataset.

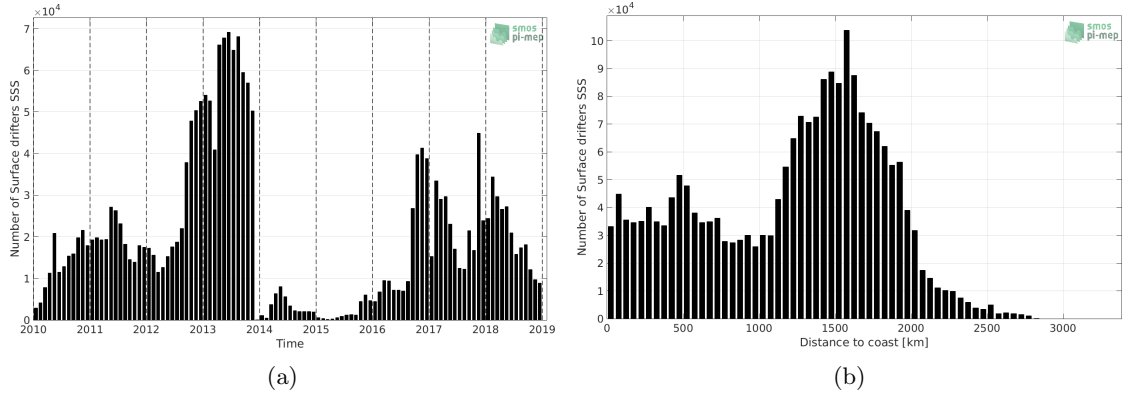


Figure 112: Number of SSS from Surface drifters as a function of time (a) and distance to coast (b).

4.3 Histograms of SSS

Figure 113 shows the SSS distribution of the Surface drifters (a) and colocalized ISAS (b) dataset.

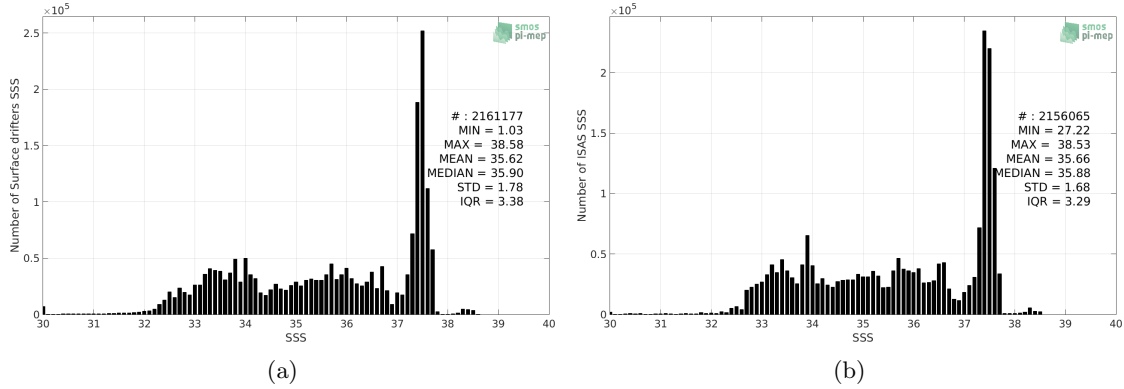


Figure 113: Histograms of SSS from Surface drifters (a) and ISAS (b) per bins of 0.1.

4.4 Distribution of *in situ* SSS depth measurements

In Figure 114, we show the depth distribution of the *in situ* salinity dataset (a) and the spatial distribution of the depth temporal mean in $1^\circ \times 1^\circ$ boxes and considering the full *in situ* dataset period (b).

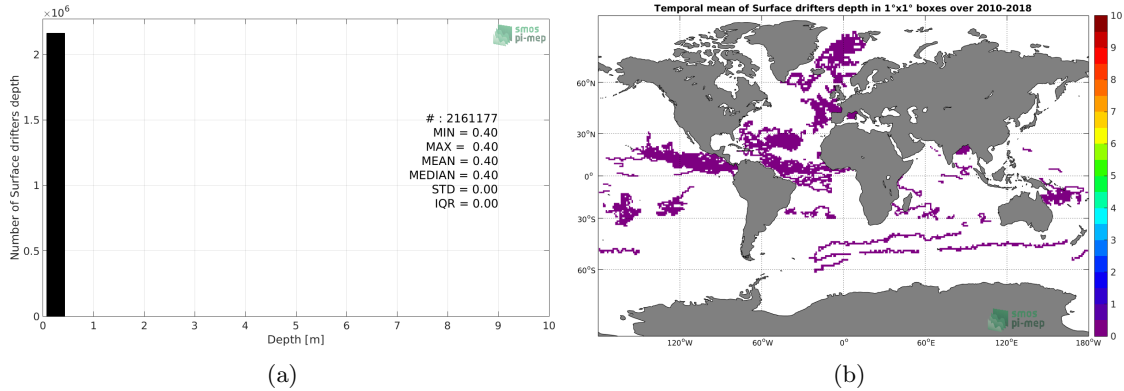


Figure 114: Depth distribution of the upper level SSS measurements from Surface drifters (a) and spatial distribution of the *in situ* SSS depth measurements showing the mean value in $1^\circ \times 1^\circ$ boxes and considering the full *in situ* dataset period (b).

4.5 Spatial distribution of SSS

In Figure 115, the number of Surface drifters SSS measurements in $1^\circ \times 1^\circ$ boxes is shown.

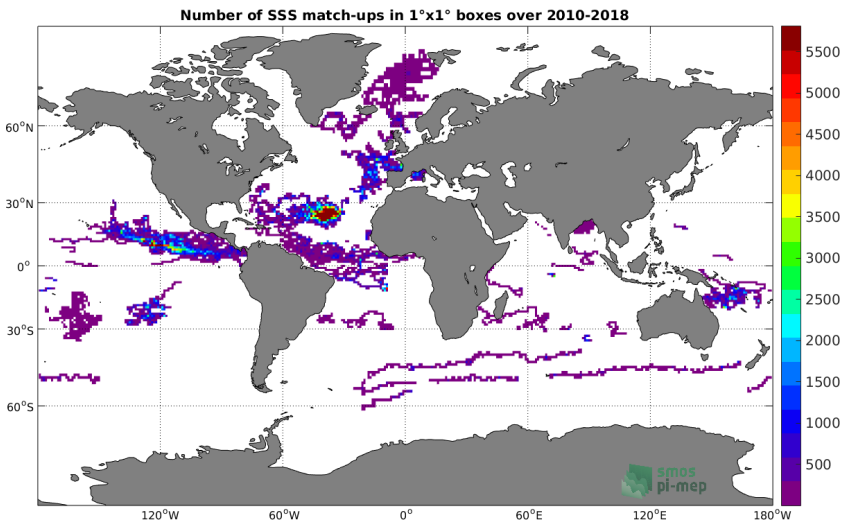


Figure 115: Number of SSS from Surface drifters in $1^\circ \times 1^\circ$ boxes.

4.6 Spatial Maps of the Temporal mean and Std of *in situ* and ISAS SSS and of the difference (Δ SSS)

In Figure 116, we show maps of temporal mean (left) and standard deviation (right) of ISAS (top), Surface drifters *in situ* dataset (middle) and the difference Δ SSS(ISAS -Surface drifters) (bottom). The temporal mean and std are calculated using all match-up pairs falling in spatial boxes of size $1^\circ \times 1^\circ$ over the full Surface drifters dataset period.

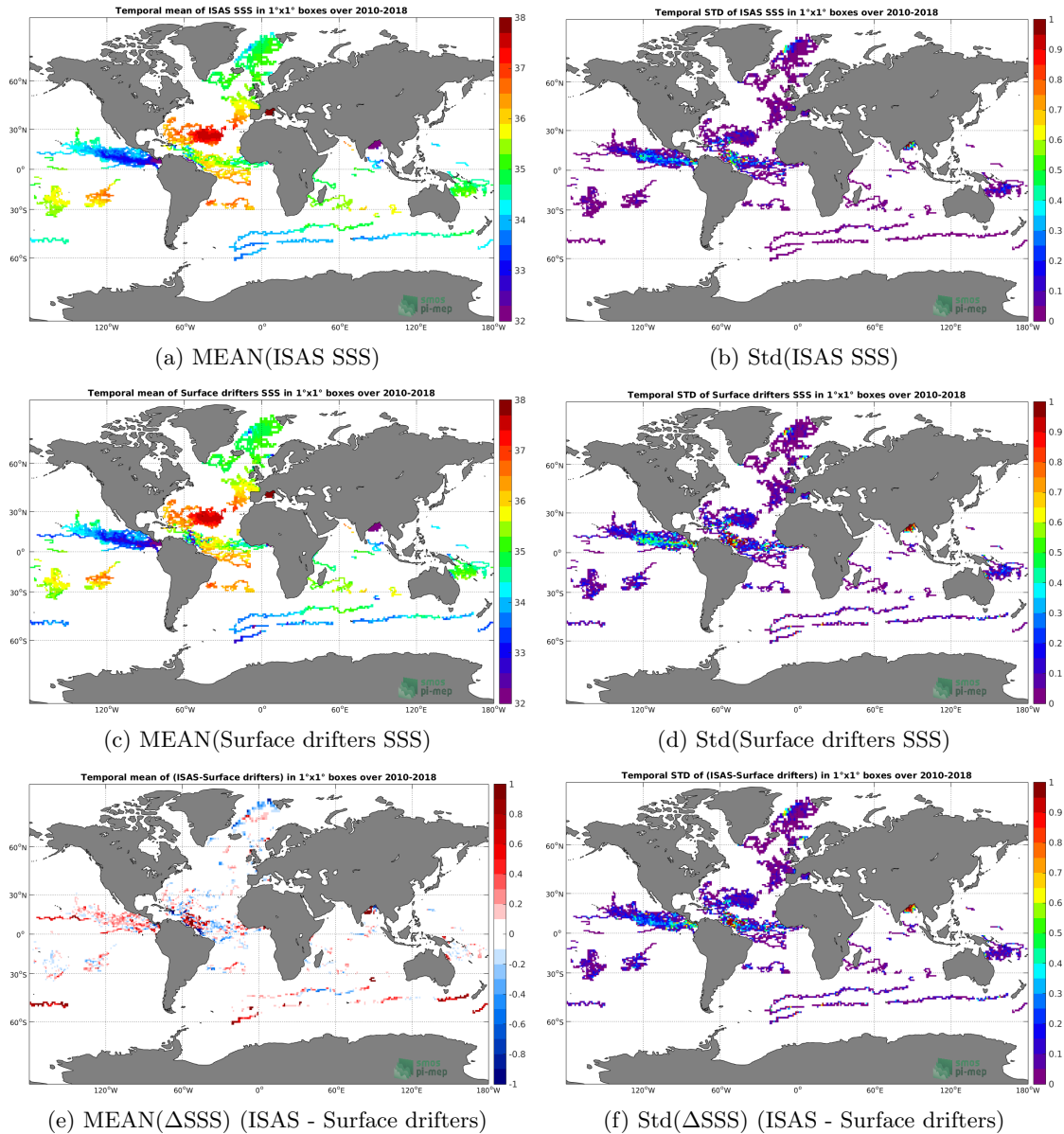


Figure 116: Temporal mean (left) and Std (right) of SSS from ISAS (top), Surface drifters (middle), and of Δ SSS (ISAS - Surface drifters). Only match-up pairs are used to generate these maps.

4.7 Time series of the monthly median and Std of *in situ* and ISAS SSS and of the difference (Δ SSS)

In the top panel of Figure 117, we show the time series of the monthly median SSS estimated for both ISAS SSS product (in black) and the Surface drifters *in situ* dataset (in blue) at the collected Pi-MEP match-up pairs.

In the middle panel of Figure 117, we show the time series of the monthly median of Δ SSS

(ISAS - Surface drifters) for the collected Pi-MEP match-up pairs.

In the bottom panel of Figure 117, we show the time series of the monthly standard deviation of the ΔSSS (ISAS - Surface drifters) for the collected Pi-MEP match-up pairs.

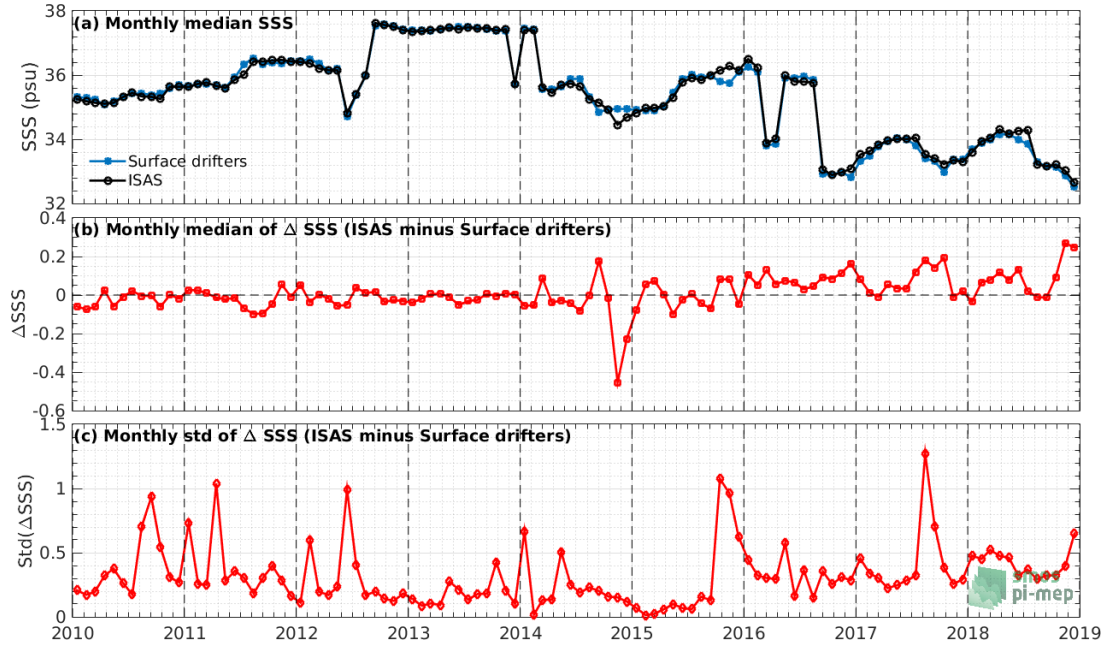


Figure 117: Time series of the monthly median SSS (top), median of ΔSSS (ISAS - Surface drifters) and Std of ΔSSS (ISAS - Surface drifters) considering all match-ups collected by the Pi-MEP.

4.8 Zonal mean and Std of *in situ* and ISAS SSS and of the difference ΔSSS

In Figure 118 left panel, we show the zonal mean SSS considering all Pi-MEP match-up pairs for both ISAS SSS product (in black) and the Surface drifters *in situ* dataset (in blue). The full *in situ* dataset period is used to derive the mean.

In the right panel of Figure 118, we show the zonal mean of ΔSSS (ISAS - Surface drifters) for all the collected Pi-MEP match-up pairs estimated over the full *in situ* dataset period.

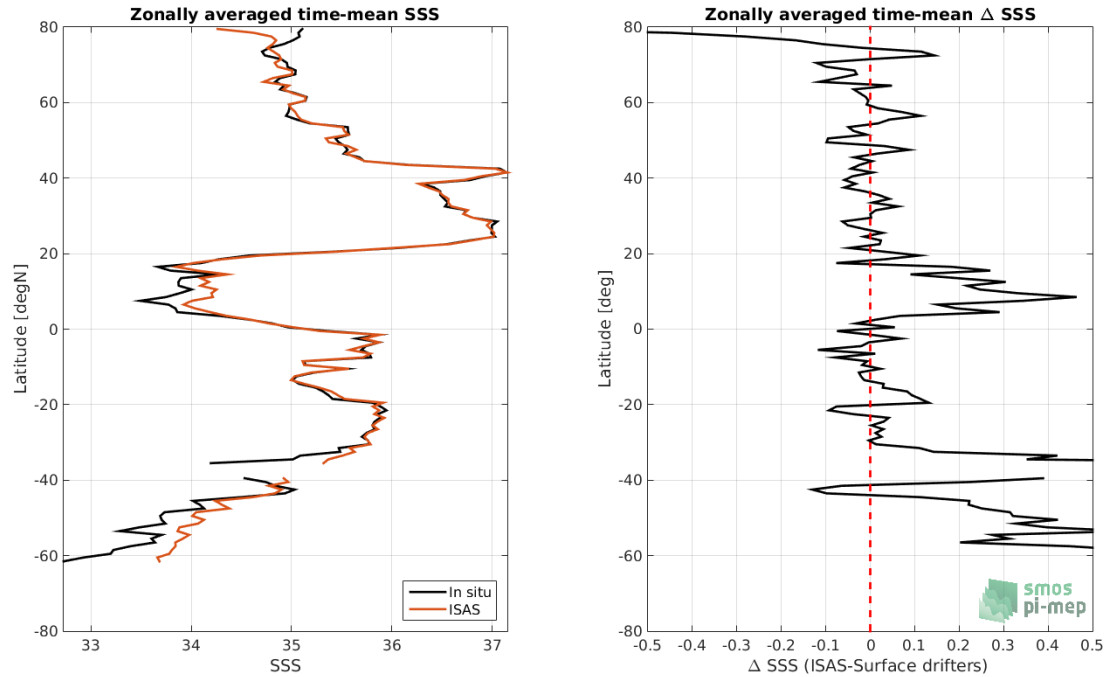


Figure 118: Left panel: Zonal mean SSS from ISAS product (black) and from Surface drifters (blue). Right panel: Zonal mean of Δ SSS (ISAS - Surface drifters) for all the collected Pi-MEP match-up pairs estimated over the full *in situ* dataset period.

4.9 Scatterplots of ISAS vs *in situ* SSS by latitudinal bands

In Figure 119, contour maps of the concentration of ISAS SSS (y-axis) versus Surface drifters SSS (x-axis) at match-up pairs for different latitude bands: (a) 80°S-80°N, (b) 20°S-20°N, (c) 40°S-20°S and 20°N-40°N and (d) 60°S-40°S and 40°N-60°N. For each plot, the red line shows $x=y$. The black thin and dashed lines indicate a linear fit through the data cloud and the $\pm 95\%$ confidence levels, respectively. The number match-up pairs n , the slope and R^2 coefficient of the linear fit, the root mean square (RMS) and the mean bias between ISAS and *in situ* data are indicated for each latitude band in each plots.

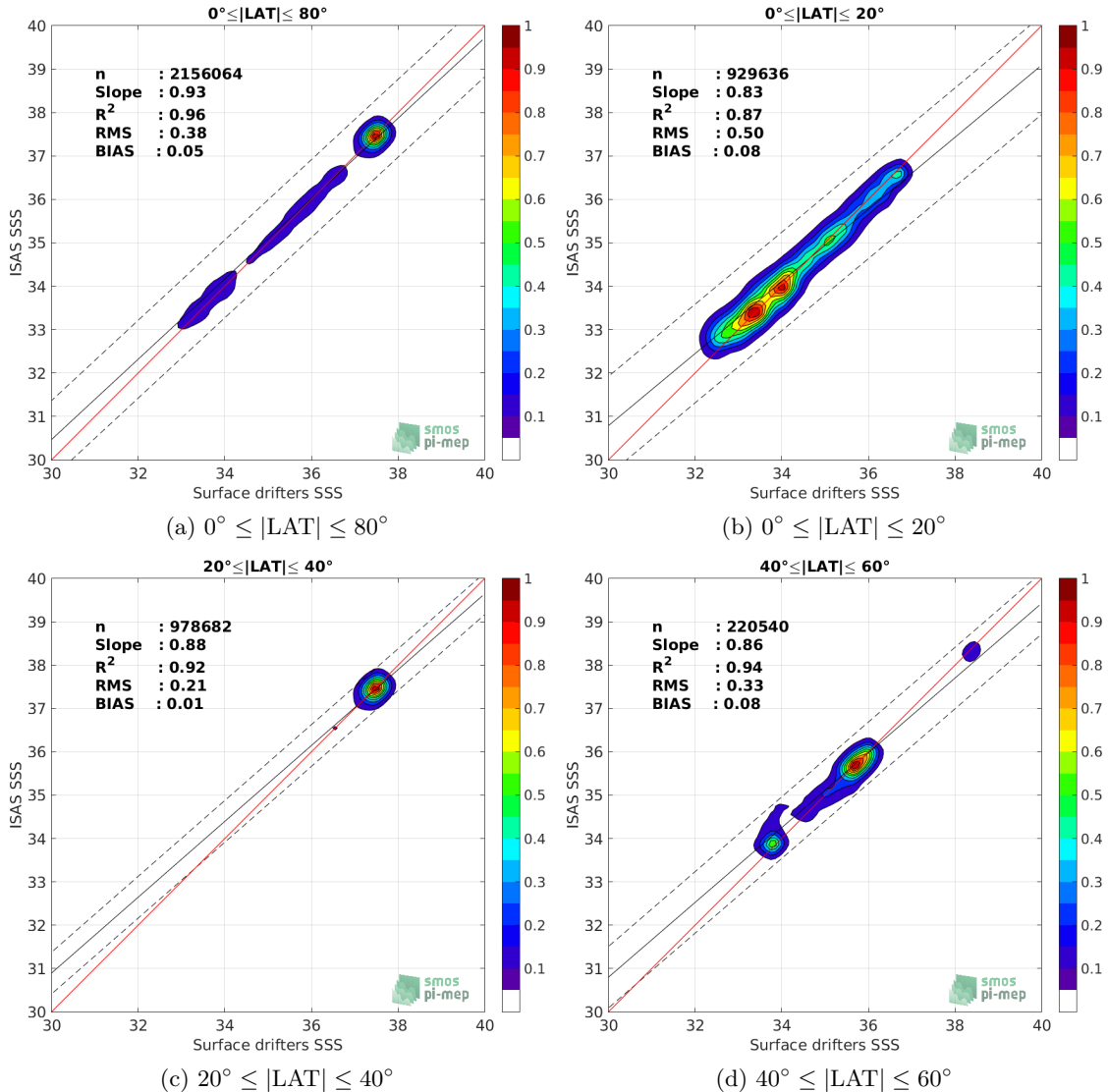


Figure 119: Contour maps of the concentration of ISAS SSS (y-axis) versus Surface drifters SSS (x-axis) at match-up pairs for different latitude bands. For each plot, the red line shows $x=y$. The black thin and dashed lines indicate a linear fit through the data cloud and the $\pm 95\%$ confidence levels, respectively. The number match-up pairs n , the slope and R^2 coefficient of the linear fit, the root mean square (RMS) and the mean bias between ISAS and *in situ* data are indicated for each latitude band in each plots.

4.10 Time series of the monthly median and Std of the difference ΔSSS sorted by latitudinal bands

In Figure 120, time series of the monthly median (red curves) of ΔSSS (ISAS - Surface drifters) and ± 1 Std (black vertical thick bars) as function of time for all the collected Pi-MEP match-up pairs estimated for the full *in situ* dataset period are shown for different latitude bands: (a) $80^\circ\text{S}-80^\circ\text{N}$, (b) $20^\circ\text{S}-20^\circ\text{N}$, (c) $40^\circ\text{S}-20^\circ\text{S}$ and $20^\circ\text{N}-40^\circ\text{N}$ and (d) $60^\circ\text{S}-40^\circ\text{S}$ and $40^\circ\text{N}-60^\circ\text{N}$.

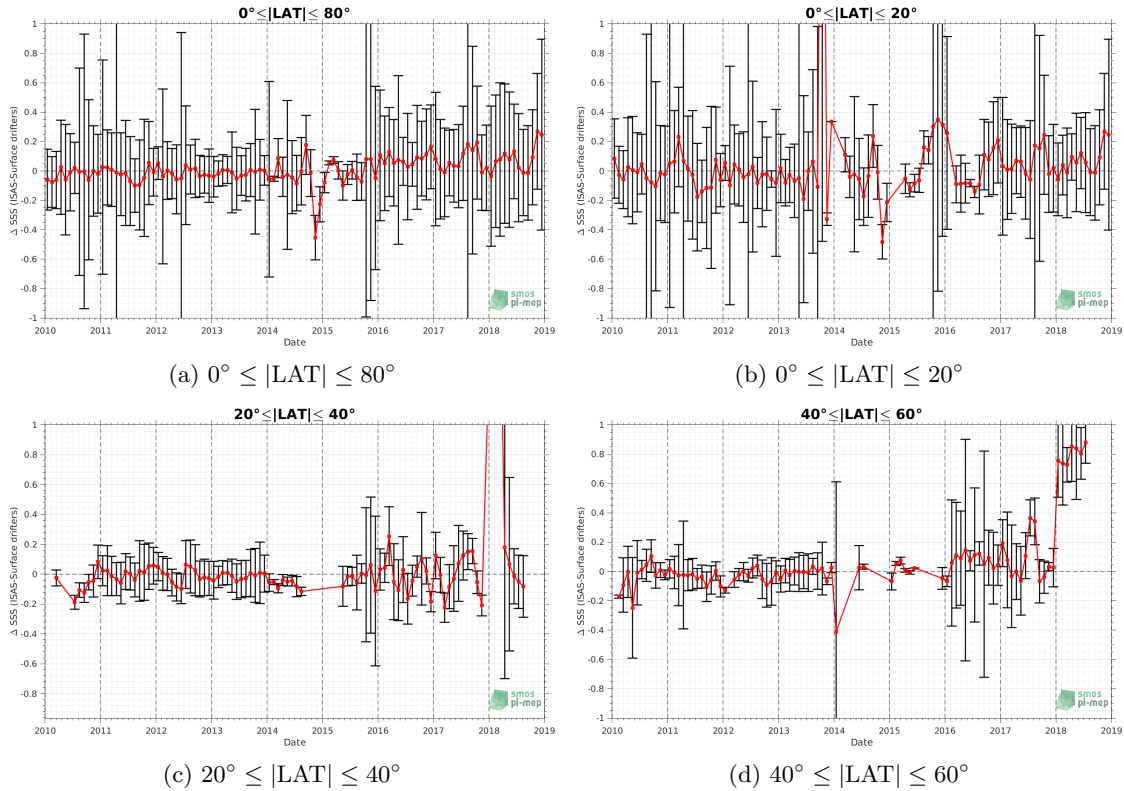


Figure 120: Monthly median (red curves) of ΔSSS (ISAS - Surface drifters) and ± 1 Std (black vertical thick bars) as function of time for all the collected Pi-MEP match-up pairs for the full *in situ* dataset period are shown for different latitude bands: (a) $80^\circ\text{S}-80^\circ\text{N}$, (b) $20^\circ\text{S}-20^\circ\text{N}$, (c) $40^\circ\text{S}-20^\circ\text{S}$ and $20^\circ\text{N}-40^\circ\text{N}$ and (d) $60^\circ\text{S}-40^\circ\text{N}$ and $40^\circ\text{N}-60^\circ\text{N}$.

4.11 ΔSSS sorted as geophysical conditions

In Figure 121, we classify the match-up differences ΔSSS (ISAS - *in situ*) as function of the geophysical conditions at match-up points. The mean and std of ΔSSS (ISAS - Surface drifters) is thus evaluated as function of the

- *in situ* SSS values per bins of width 0.2,
- *in situ* SST values per bins of width 1°C ,
- ASCAT daily wind values per bins of width 1 m/s,
- CMORPH 3-hourly rain rates per bins of width 1 mm/h, and,
- distance to coasts per bins of width 50 km,
- *in situ* measurement depth (if relevant).

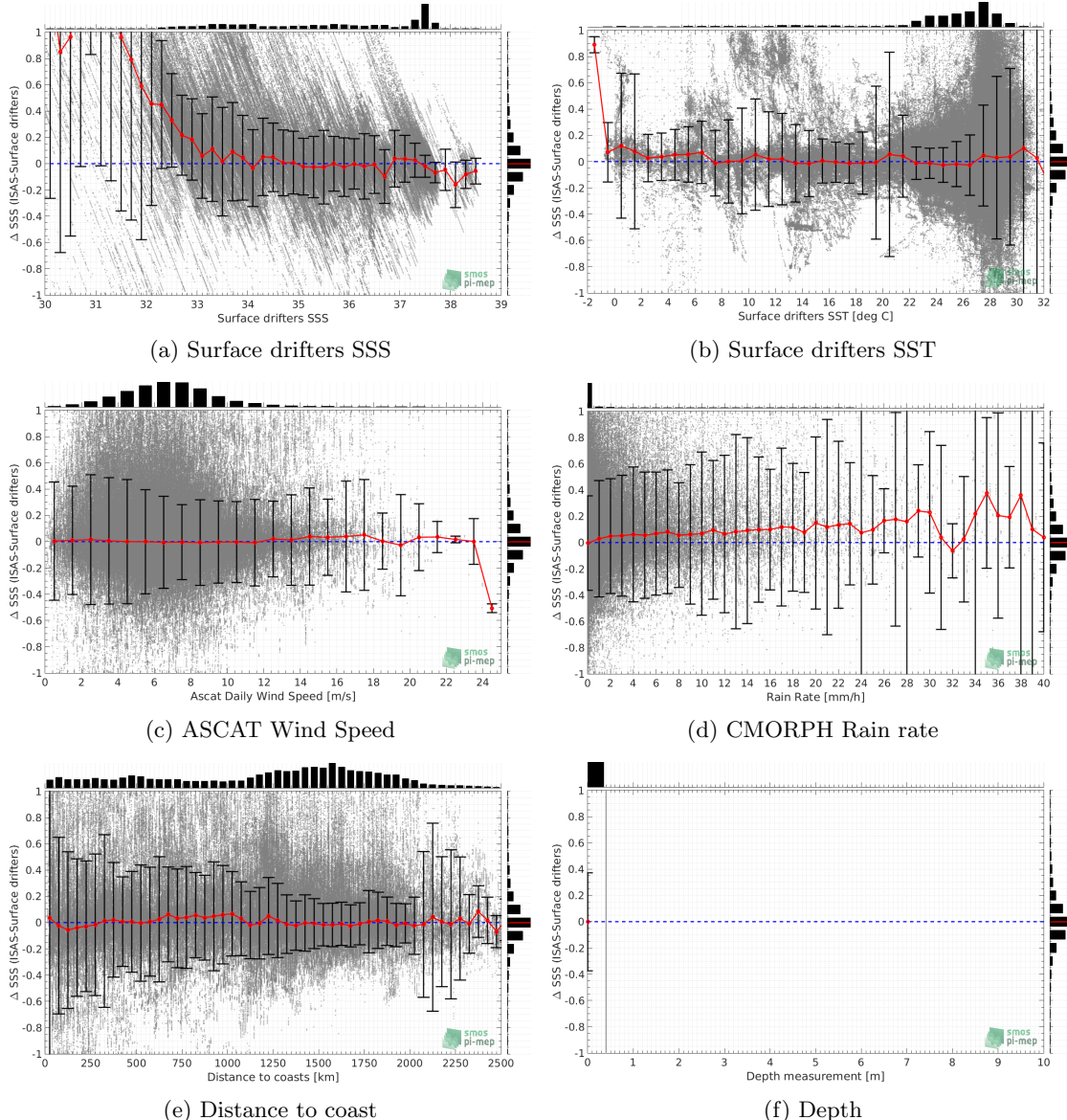


Figure 121: ΔSSS (ISAS - Surface drifters) sorted as geophysical conditions: Surface drifters SSS a), Surface drifters SST b), ASCAT Wind speed c), CMORPH rain rate d), distance to coast (e) and depth measurements (f).

4.12 ΔSSS maps and statistics for different geophysical conditions

In Figures 122 and 123, we focus on sub-datasets of the match-up differences ΔSSS (*ISAS - in situ*) for the following specific geophysical conditions:

- **C1:** if the local value at *in situ* location of estimated rain rate is zero, mean daily wind is in the range [3, 12] m/s, the SST is $> 5^{\circ}\text{C}$ and distance to coast is > 800 km.
- **C2:** if the local value at *in situ* location of estimated rain rate is zero, mean daily wind is

in the range [3, 12] m/s.

- **C3:** if the local value at *in situ* location of estimated rain rate is high (ie. $> 1 \text{ mm/h}$) and mean daily wind is low (ie. $< 4 \text{ m/s}$).
- **C5:** if the *in situ* data is located where the climatological SSS standard deviation is low (ie. above < 0.2).
- **C6:** if the *in situ* data is located where the climatological SSS standard deviation is high (ie. above > 0.2).

For each of these conditions, the temporal mean (gridded over spatial boxes of size $1^\circ \times 1^\circ$) and the histogram of the difference ΔSSS (ISAS - *in situ*) are presented.

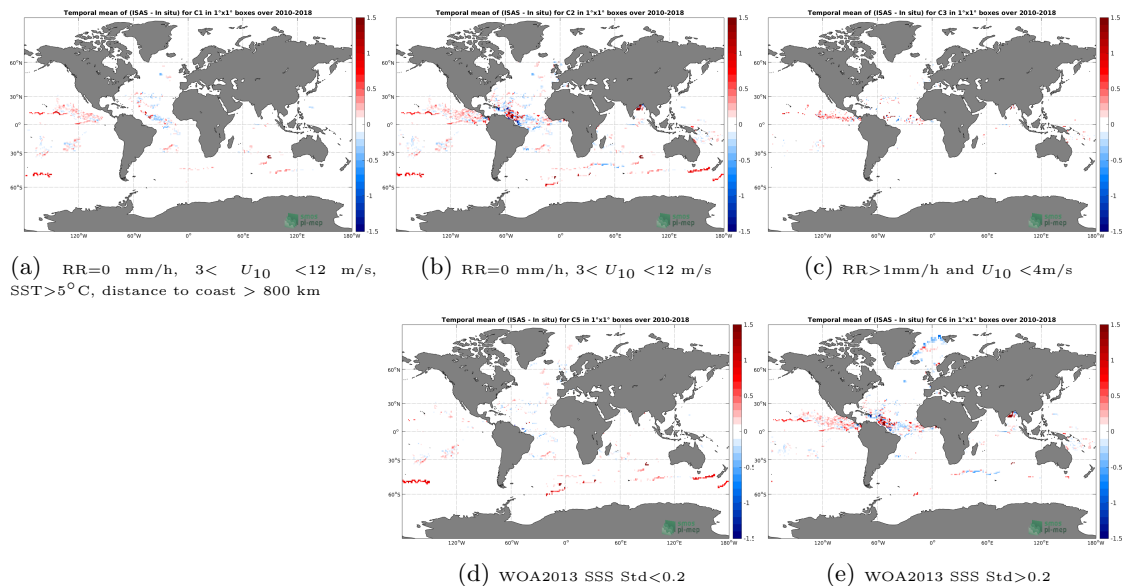


Figure 122: Temporal mean gridded over spatial boxes of size $1^\circ \times 1^\circ$ of ΔSSS (ISAS - Surface drifters) for 5 different subdatasets corresponding to: $\text{RR}=0 \text{ mm/h}, 3 < U_{10} < 12 \text{ m/s}, \text{SST} > 5^\circ\text{C}$, distance to coast $> 800 \text{ km}$ (a), $\text{RR}=0 \text{ mm/h}, 3 < U_{10} < 12 \text{ m/s}$ (b), $\text{RR} > 1 \text{ mm/h} \text{ and } U_{10} < 4 \text{ m/s}$ (c), WOA2013 SSS Std < 0.2 (d), WOA2013 SSS Std > 0.2 (e).

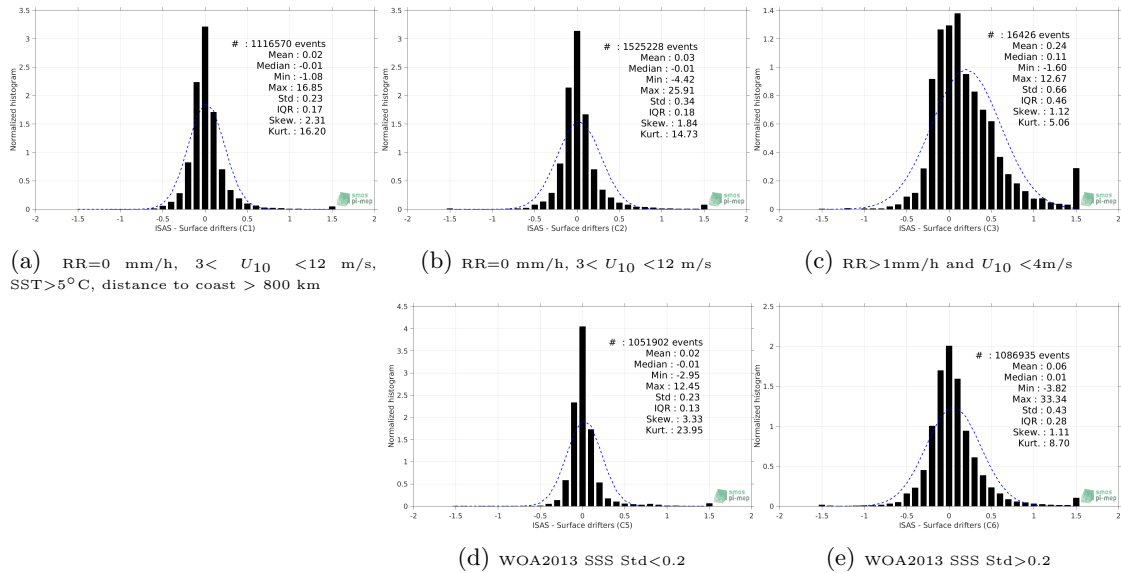


Figure 123: Normalized histogram of ΔSSS (ISAS - Surface drifters) for 5 different subdatasets corresponding to: RR=0 mm/h, $3 < U_{10} < 12$ m/s, SST > 5°C, distance to coast > 800 km (a), RR=0 mm/h, $3 < U_{10} < 12$ m/s (b), RR > 1 mm/h and $U_{10} < 4$ m/s (c), WOA2013 SSS Std < 0.2 (d), WOA2013 SSS Std > 0.2 (e).

4.13 Summary

Table 1 shows the mean, median, standard deviation (Std), root mean square (RMS), interquartile range (IQR), correlation coefficient (r^2) and robust standard deviation (Std*) of the match-up differences ΔSSS (ISAS - Surface drifters) for the following conditions:

- all: All the match-up pairs satellite/in situ SSS values are used to derive the statistics
- C1: only pairs where RR=0 mm/h, $3 < U_{10} < 12$ m/s, SST > 5°C, distance to coast > 800 km
- C2: only pairs where RR=0 mm/h, $3 < U_{10} < 12$ m/s
- C3: only pairs where RR > 1 mm/h and $U_{10} < 4$ m/s
- C5: only pairs where WOA2013 SSS Std < 0.2
- C6: only pairs where WOA2013 SSS Std > 0.2
- C7a: only pairs with a distance to coast < 150 km.
- C7b: only pairs with a distance to coast in the range [150, 800] km.
- C7c: only pairs with a distance to coast > 800 km.
- C8a: only pairs where SST is < 5°C.
- C8b: only pairs where SST is in the range [5, 15]°C.
- C8c: only pairs where SST is > 15°C.

- C9a: only pairs where SSS is < 33.
- C9b: only pairs where SSS is in the range [33, 37].
- C9c: only pairs where SSS is > 37.

Table 1: Statistics of Δ SSS (ISAS - Surface drifters)

Condition	#	Median	Mean	Std	RMS	IQR	r^2	Std*
all	2156065	0.00	0.05	0.37	0.38	0.19	0.96	0.14
C1	1116570	-0.01	0.02	0.23	0.23	0.17	0.98	0.13
C2	1525228	-0.01	0.03	0.34	0.34	0.18	0.96	0.13
C3	16426	0.11	0.24	0.66	0.70	0.46	0.84	0.32
C5	1051902	-0.01	0.02	0.23	0.23	0.13	0.97	0.10
C6	1086935	0.01	0.06	0.43	0.44	0.28	0.93	0.21
C7a	110201	-0.02	0.12	0.94	0.94	0.26	0.81	0.19
C7b	491121	0.01	0.07	0.46	0.46	0.21	0.88	0.15
C7c	1554687	0.00	0.03	0.26	0.26	0.19	0.98	0.14
C8a	31421	0.07	0.18	0.45	0.49	0.11	0.58	0.08
C8b	140829	0.01	0.08	0.33	0.34	0.16	0.93	0.11
C8c	1978206	0.00	0.04	0.37	0.38	0.19	0.96	0.14
C9a	164016	0.29	0.48	0.96	1.07	0.44	0.16	0.31
C9b	1231999	0.00	0.03	0.29	0.29	0.24	0.94	0.18
C9c	760050	-0.02	-0.02	0.11	0.11	0.11	0.71	0.08

Table 1 numerical values can be downloaded as a csv file [here](#).

5 Sea mammals

5.1 Introduction

Instrumentation of southern elephant seals with satellite-linked CTD tags proposes unique temporal and spatial coverage. This includes extensive data from the Antarctic continental slope and shelf regions during the winter months, which is outside the conventional areas of Argo autonomous floats and ship-based studies. The use of elephant seals has been particularly effective to sample the Southern Ocean and the North Pacific. Other seal species have been successfully used in the North Atlantic, such as hooded seals. The marine mammal dataset ([MEOP-CTD database](#)) is quality controlled and calibrated using delayed-mode techniques involving comparisons with other existing profiles as well as cross-comparisons similar to established protocols within the Argo community, with a resulting accuracy of ± 0.03 °C in temperature and ± 0.05 in salinity or better ([Treasure et al. \(2017\)](#)). The marine mammal data were collected and made freely available by the International MEOP Consortium and the national programs that contribute to it (<http://www.meop.net>). This dataset is updated once a year and can be downloaded [here](#) ([Roquet et al. \(2018\)](#)). A preprocessing stage is applied to the database before being used by the Pi-MEP which consist to keep only profile with salinity, temperature and pressure quality flags set to 1 or 2 and if at least one measurement



is in the top 10 m depth. Marine mammal SSS correspond to the top (shallowest) profile salinity data provided that profile depth is 10 m or less.

5.2 Number of SSS data as a function of time and distance to coast

Figure 124 shows the time (a) and distance to coast (b) distributions of the Sea mammals *in situ* dataset.

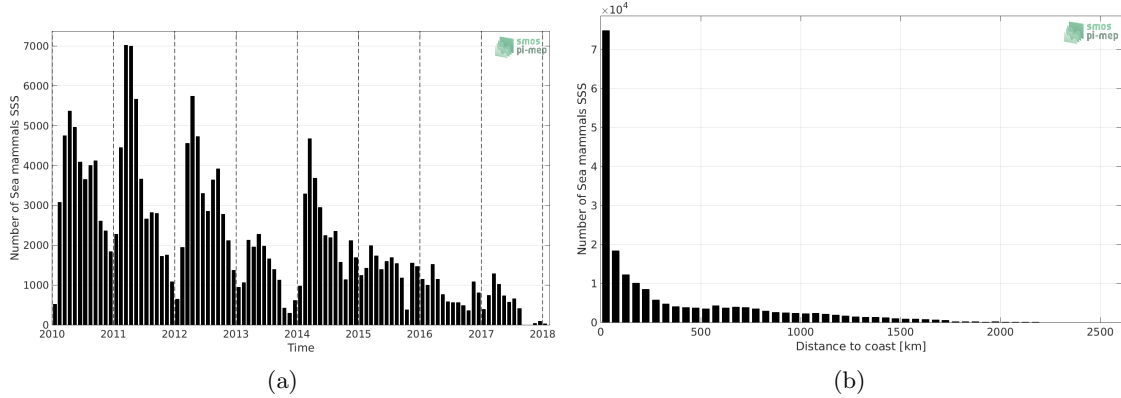


Figure 124: Number of SSS from Sea mammals as a function of time (a) and distance to coast (b).

5.3 Histograms of SSS

Figure 125 shows the SSS distribution of the Sea mammals (a) and colocalized ISAS (b) dataset.

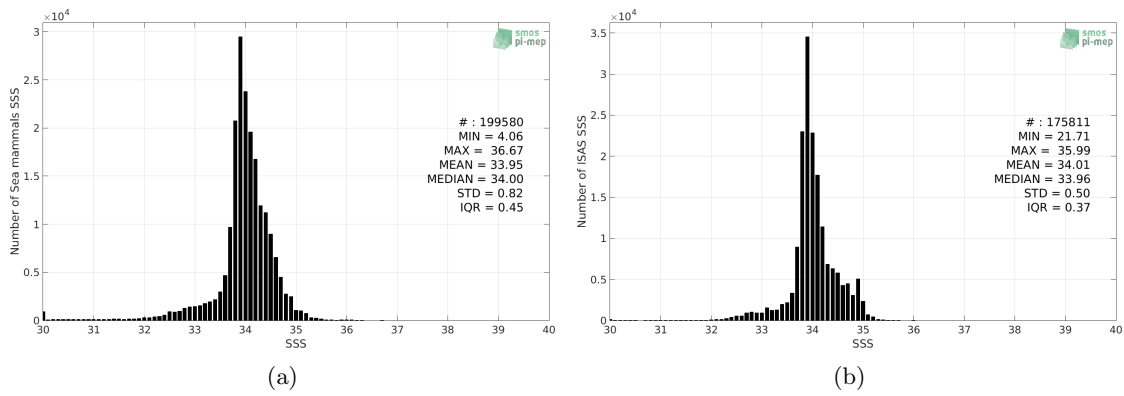


Figure 125: Histograms of SSS from Sea mammals (a) and ISAS (b) per bins of 0.1.

5.4 Distribution of *in situ* SSS depth measurements

In Figure 126, we show the depth distribution of the *in situ* salinity dataset (a) and the spatial distribution of the depth temporal mean in $1^\circ \times 1^\circ$ boxes and considering the full *in situ* dataset period (b).

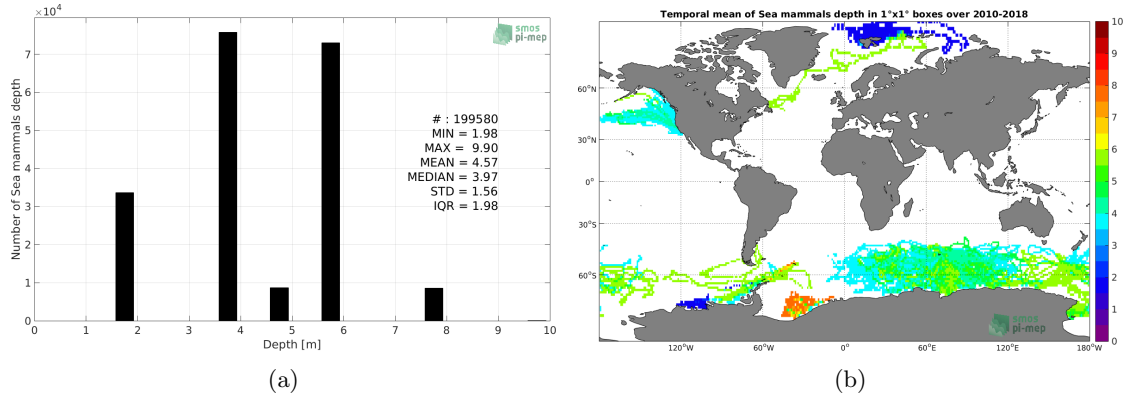


Figure 126: Depth distribution of the upper level SSS measurements from Sea mammals (a) and spatial distribution of the *in situ* SSS depth measurements showing the mean value in 1°x1° boxes and considering the full *in situ* dataset period (b).

5.5 Spatial distribution of SSS

In Figure 127, the number of Sea mammals SSS measurements in 1°x1° boxes is shown.

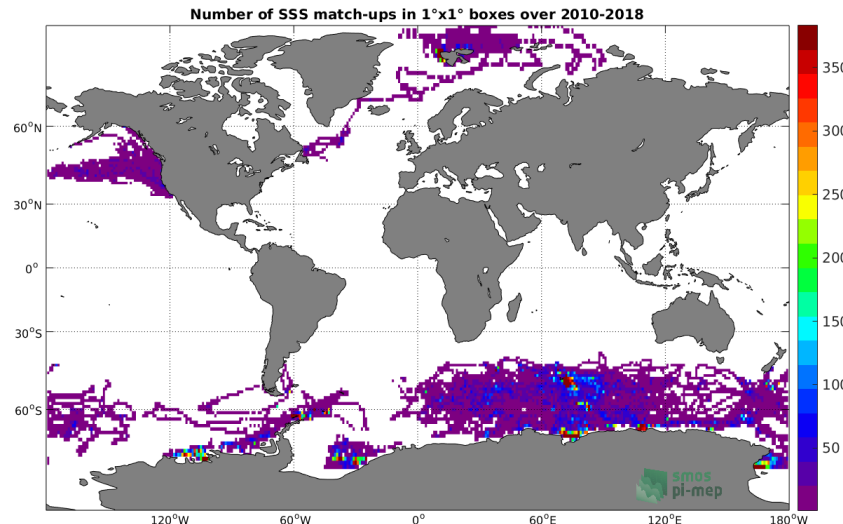


Figure 127: Number of SSS from Sea mammals in 1°x1° boxes.

5.6 Spatial Maps of the Temporal mean and Std of *in situ* and ISAS SSS and of the difference (Δ SSS)

In Figure 128, we show maps of temporal mean (left) and standard deviation (right) of ISAS (top), Sea mammals *in situ* dataset (middle) and the difference Δ SSS(ISAS -Sea mammals) (bottom). The temporal mean and std are calculated using all match-up pairs falling in spatial boxes of size 1°x1° over the full Sea mammals dataset period.

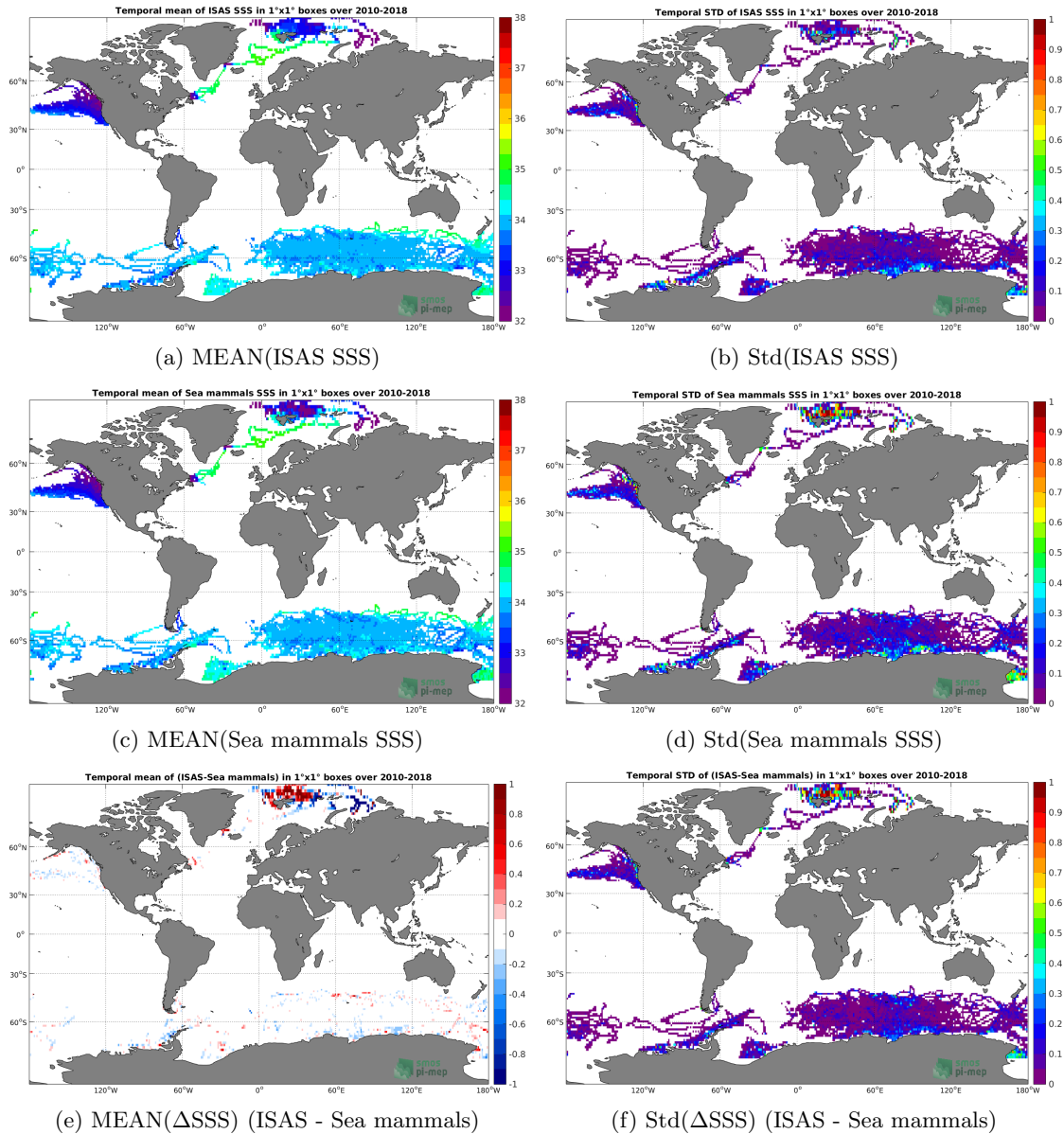


Figure 128: Temporal mean (left) and Std (right) of SSS from ISAS (top), Sea mammals (middle), and of Δ SSS (ISAS - Sea mammals). Only match-up pairs are used to generate these maps.

5.7 Time series of the monthly median and Std of *in situ* and ISAS SSS and of the difference (Δ SSS)

In the top panel of Figure 129, we show the time series of the monthly median SSS estimated for both ISAS SSS product (in black) and the Sea mammals *in situ* dataset (in blue) at the collected Pi-MEP match-up pairs.

In the middle panel of Figure 129, we show the time series of the monthly median of Δ SSS (ISAS - Sea mammals) for the collected Pi-MEP match-up pairs.

In the bottom panel of Figure 129, we show the time series of the monthly standard deviation of the Δ SSS (ISAS - Sea mammals) for the collected Pi-MEP match-up pairs.

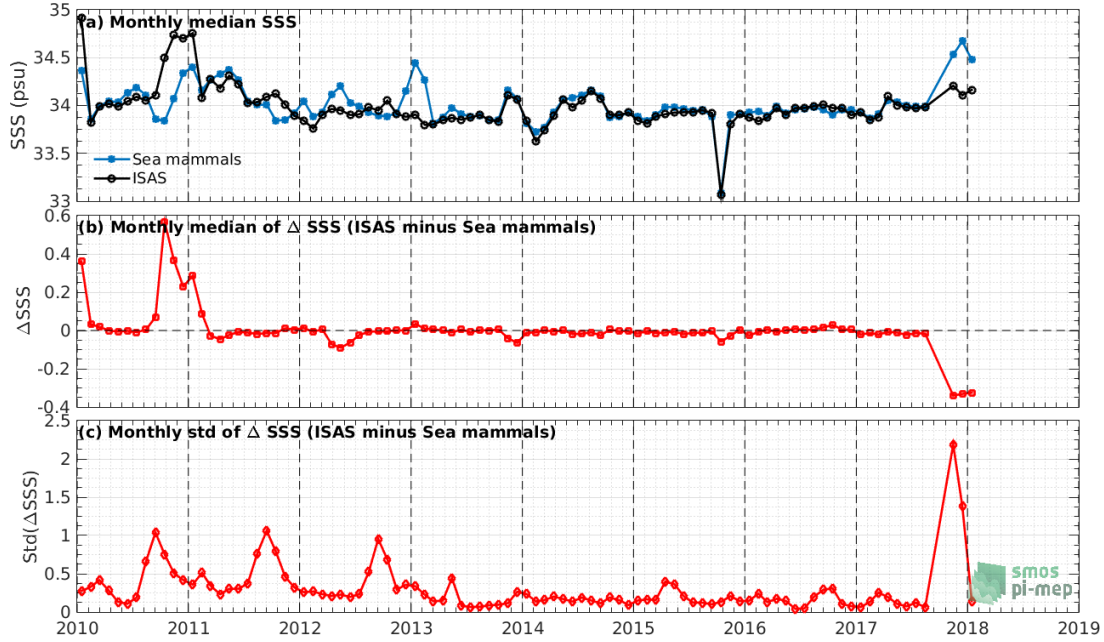


Figure 129: Time series of the monthly median SSS (top), median of Δ SSS (ISAS - Sea mammals) and Std of Δ SSS (ISAS - Sea mammals) considering all match-ups collected by the Pi-MEP.

5.8 Zonal mean and Std of *in situ* and ISAS SSS and of the difference Δ SSS

In Figure 130 left panel, we show the zonal mean SSS considering all Pi-MEP match-up pairs for both ISAS SSS product (in black) and the Sea mammals *in situ* dataset (in blue). The full *in situ* dataset period is used to derive the mean.

In the right panel of Figure 130, we show the zonal mean of Δ SSS (ISAS - Sea mammals) for all the collected Pi-MEP match-up pairs estimated over the full *in situ* dataset period.

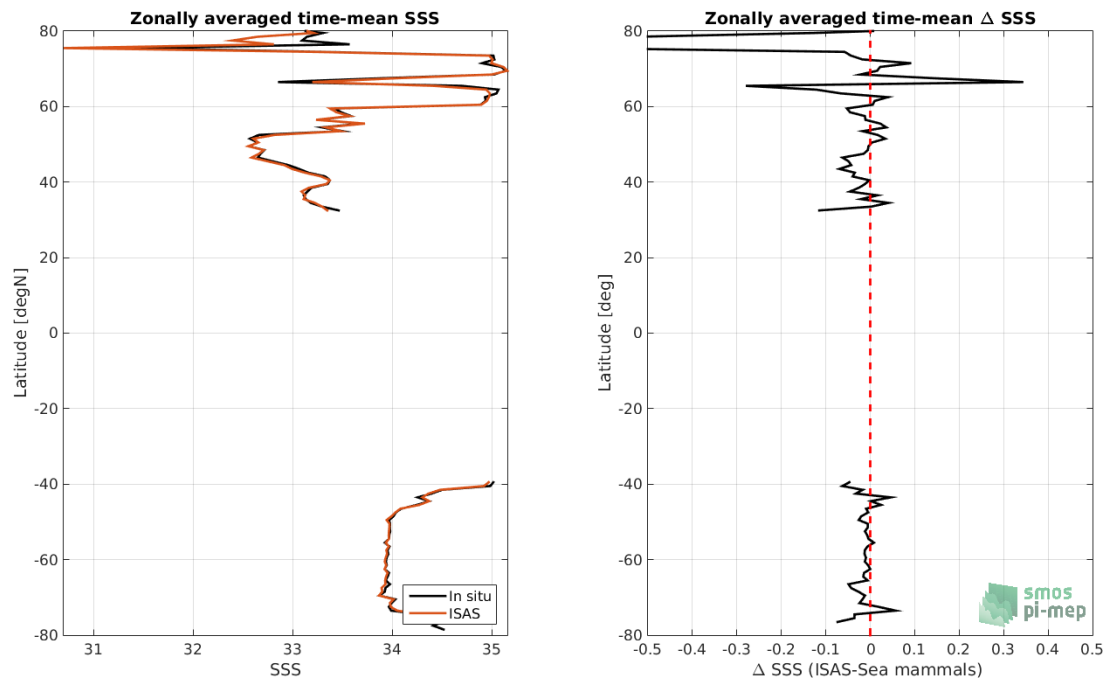


Figure 130: Left panel: Zonal mean SSS from ISAS product (black) and from Sea mammals (blue). Right panel: Zonal mean of Δ SSS (ISAS - Sea mammals) for all the collected Pi-MEP match-up pairs estimated over the full *in situ* dataset period.

5.9 Scatterplots of ISAS vs *in situ* SSS by latitudinal bands

In Figure 131, contour maps of the concentration of ISAS SSS (y-axis) versus Sea mammals SSS (x-axis) at match-up pairs for different latitude bands: (a) 80°S-80°N, (b) 20°S-20°N, (c) 40°S-20°S and 20°N-40°N and (d) 60°S-40°S and 40°N-60°N. For each plot, the red line shows $x=y$. The black thin and dashed lines indicate a linear fit through the data cloud and the $\pm 95\%$ confidence levels, respectively. The number match-up pairs n , the slope and R^2 coefficient of the linear fit, the root mean square (RMS) and the mean bias between ISAS and *in situ* data are indicated for each latitude band in each plots.

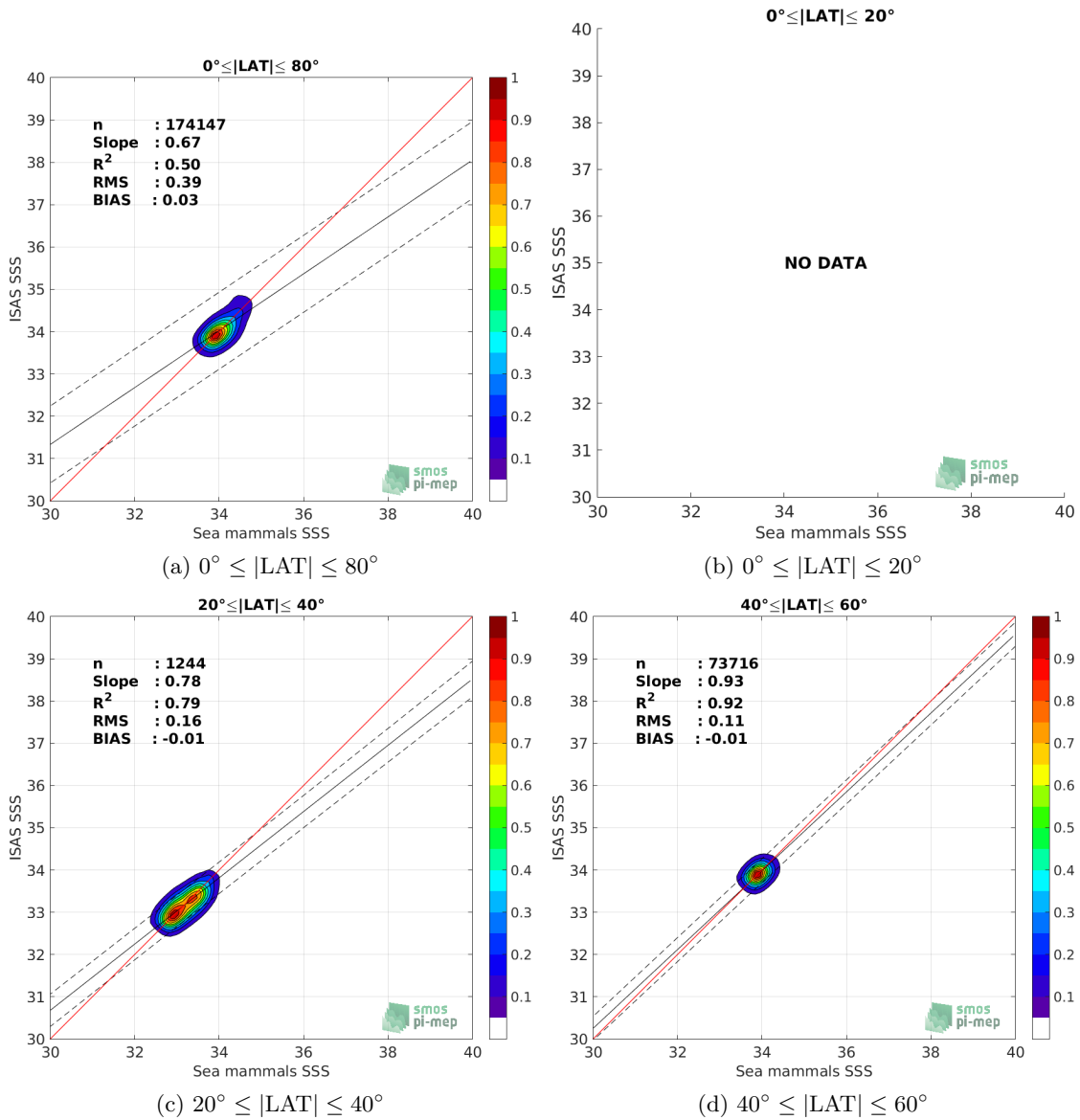


Figure 131: Contour maps of the concentration of ISAS SSS (y-axis) versus Sea mammals SSS (x-axis) at match-up pairs for different latitude bands. For each plot, the red line shows $x=y$. The black thin and dashed lines indicate a linear fit through the data cloud and the $\pm 95\%$ confidence levels, respectively. The number match-up pairs n , the slope and R^2 coefficient of the linear fit, the root mean square (RMS) and the mean bias between ISAS and *in situ* data are indicated for each latitude band in each plots.

5.10 Time series of the monthly median and Std of the difference ΔSSS sorted by latitudinal bands

In Figure 132, time series of the monthly median (red curves) of ΔSSS (ISAS - Sea mammals) and ± 1 Std (black vertical thick bars) as function of time for all the collected Pi-MEP match-up

pairs estimated for the full *in situ* dataset period are shown for different latitude bands: (a) $80^{\circ}\text{S}-80^{\circ}\text{N}$, (b) $20^{\circ}\text{S}-20^{\circ}\text{N}$, (c) $40^{\circ}\text{S}-20^{\circ}\text{S}$ and $20^{\circ}\text{N}-40^{\circ}\text{N}$ and (d) $60^{\circ}\text{S}-40^{\circ}\text{S}$ and $40^{\circ}\text{N}-60^{\circ}\text{N}$.

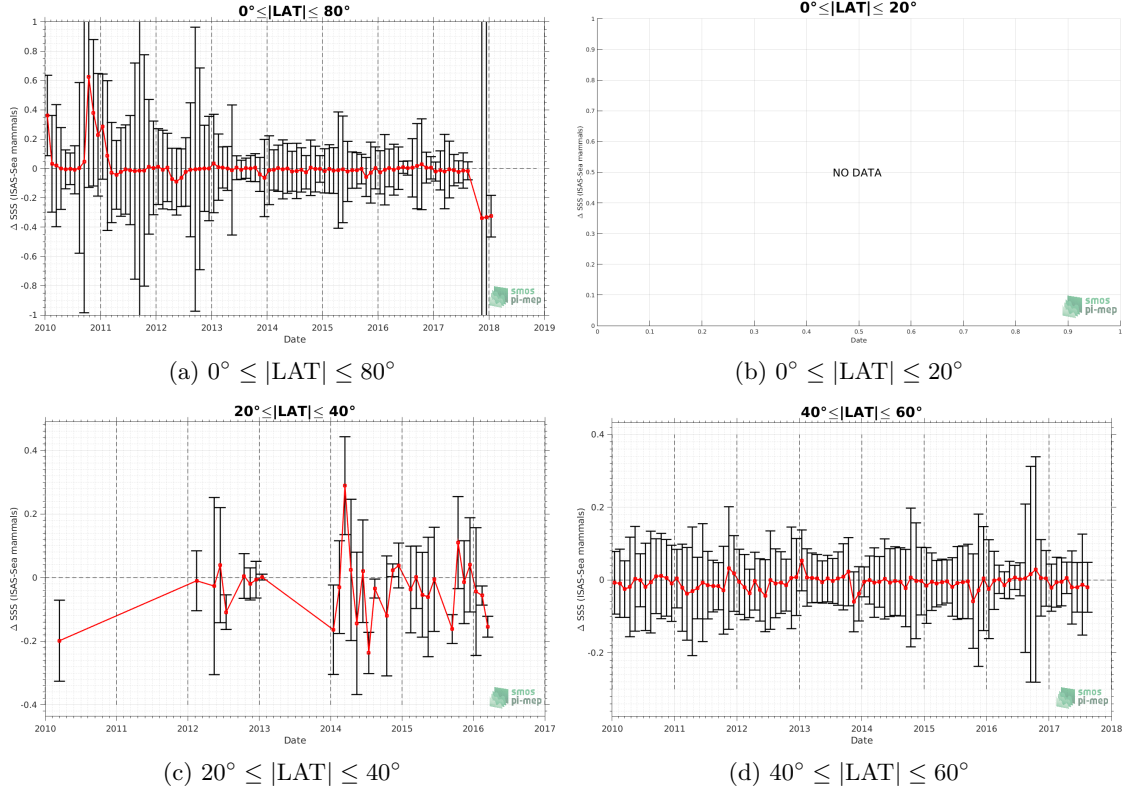


Figure 132: Monthly median (red curves) of ΔSSS (ISAS - Sea mammals) and ± 1 Std (black vertical thick bars) as function of time for all the collected Pi-MEP match-up pairs for the full *in situ* dataset period are shown for different latitude bands: (a) $80^{\circ}\text{S}-80^{\circ}\text{N}$, (b) $20^{\circ}\text{S}-20^{\circ}\text{N}$, (c) $40^{\circ}\text{S}-20^{\circ}\text{S}$ and $20^{\circ}\text{N}-40^{\circ}\text{N}$ and (d) $60^{\circ}\text{S}-40^{\circ}\text{S}$ and $40^{\circ}\text{N}-60^{\circ}\text{N}$.

5.11 ΔSSS sorted as geophysical conditions

In Figure 133, we classify the match-up differences ΔSSS (ISAS - *in situ*) as function of the geophysical conditions at match-up points. The mean and std of ΔSSS (ISAS - Sea mammals) is thus evaluated as function of the

- *in situ* SSS values per bins of width 0.2,
- *in situ* SST values per bins of width 1°C ,
- ASCAT daily wind values per bins of width 1 m/s,
- CMORPH 3-hourly rain rates per bins of width 1 mm/h, and,
- distance to coasts per bins of width 50 km,
- *in situ* measurement depth (if relevant).

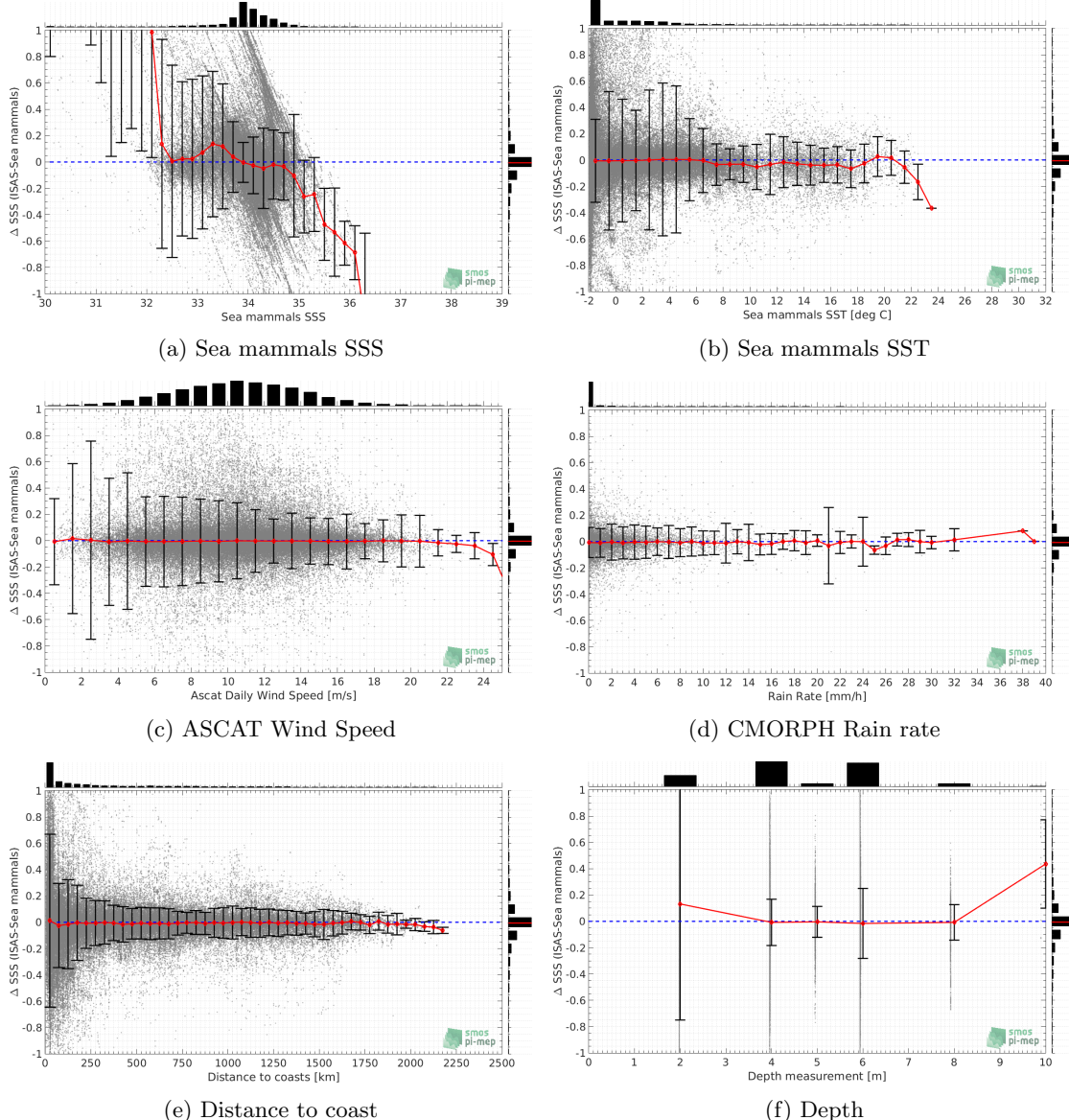


Figure 133: ΔSSS (ISAS - Sea mammals) sorted as geophysical conditions: Sea mammals SSS a), Sea mammals SST b), ASCAT Wind speed c), CMORPH rain rate d), distance to coast (e) and depth measurements (f).

5.12 ΔSSS maps and statistics for different geophysical conditions

In Figures 134 and 135, we focus on sub-datasets of the match-up differences ΔSSS (ISAS - *in situ*) for the following specific geophysical conditions:

- **C1:** if the local value at *in situ* location of estimated rain rate is zero, mean daily wind is in the range [3, 12] m/s, the SST is $> 5^\circ\text{C}$ and distance to coast is > 800 km.
- **C2:** if the local value at *in situ* location of estimated rain rate is zero, mean daily wind is

in the range [3, 12] m/s.

- **C3:**if the local value at *in situ* location of estimated rain rate is high (ie. $> 1 \text{ mm/h}$) and mean daily wind is low (ie. $< 4 \text{ m/s}$).
- **C4:**if the mixed layer is shallow with depth $< 20\text{m}$.
- **C5:**if the *in situ* data is located where the climatological SSS standard deviation is low (ie. above < 0.2).
- **C6:**if the *in situ* data is located where the climatological SSS standard deviation is high (ie. above > 0.2).

For each of these conditions, the temporal mean (gridded over spatial boxes of size $1^\circ \times 1^\circ$) and the histogram of the difference ΔSSS (ISAS - *in situ*) are presented.

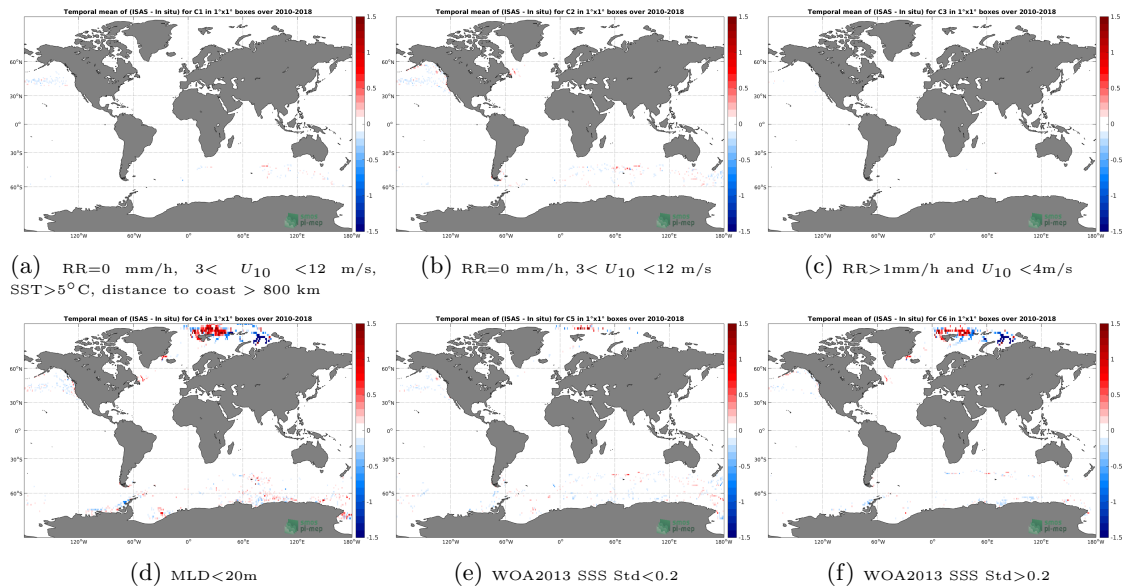


Figure 134: Temporal mean gridded over spatial boxes of size $1^\circ \times 1^\circ$ of ΔSSS (ISAS - Sea mammals) for 6 different subdatasets corresponding to: RR=0 mm/h, $3 < U_{10} < 12 \text{ m/s}$, SST $>5^\circ\text{C}$, distance to coast $> 800 \text{ km}$ (a), RR=0 mm/h, $3 < U_{10} < 12 \text{ m/s}$ (b), RR $>1\text{mm/h}$ and $U_{10} < 4\text{m/s}$ (c), MLD $<20\text{m}$ (d), WOA2013 SSS Std <0.2 (e), WOA2013 SSS Std >0.2 (f).

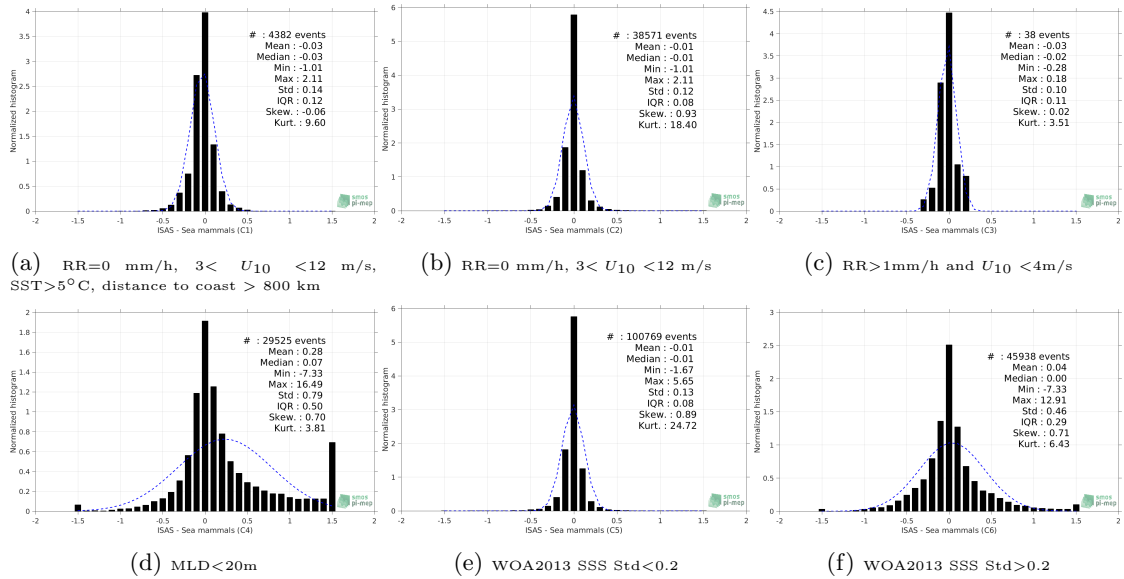


Figure 135: Normalized histogram of ΔSSS (ISAS - Sea mammals) for 6 different subdatasets corresponding to: RR=0 mm/h, $3 < U_{10} < 12$ m/s, SST > 5°C, distance to coast > 800 km (a), RR=0 mm/h, $3 < U_{10} < 12$ m/s (b), RR > 1mm/h and $U_{10} < 4$ m/s (c), WOA2013 SSS Std < 0.2 (d), WOA2013 SSS Std > 0.2 (e).

5.13 Summary

Table 1 shows the mean, median, standard deviation (Std), root mean square (RMS), interquartile range (IQR), correlation coefficient (r^2) and robust standard deviation (Std*) of the match-up differences ΔSSS (ISAS - Sea mammals) for the following conditions:

- all: All the match-up pairs satellite/in situ SSS are used to derive the statistics
- C1: only pairs where RR=0 mm/h, $3 < U_{10} < 12$ m/s, SST > 5°C, distance to coast > 800 km
- C2: only pairs where RR=0 mm/h, $3 < U_{10} < 12$ m/s
- C3: only pairs where RR > 1mm/h and $U_{10} < 4$ m/s
- C4: only pairs where MLD < 20m
- C5: only pairs where WOA2013 SSS Std < 0.2
- C6: only pairs where WOA2013 SSS Std > 0.2
- C7a: only pairs where distance to coast is < 150 km.
- C7b: only pairs where distance to coast is in the range [150, 800] km.
- C7c: only pairs where distance to coast is > 800 km.
- C8a: only pairs where in situ SST is < 5°C.
- C8b: only pairs where in situ SST is in the range [5, 15]°C.

- C8c: only pairs where in situ SST is $> 15^{\circ}\text{C}$.
- C9a: only pairs where in situ SSS is < 33 .
- C9b: only pairs where in situ SSS is in the range [33, 37].
- C9c: only pairs where in situ SSS is > 37 .

Table 1: Statistics of ΔSSS (ISAS - Sea mammals)

Condition	#	Median	Mean	Std	RMS	IQR	r^2	Std*
all	175811	-0.01	0.03	0.40	0.40	0.12	0.49	0.09
C1	4382	-0.03	-0.03	0.14	0.14	0.12	0.94	0.09
C2	38571	-0.01	-0.01	0.12	0.12	0.08	0.93	0.06
C3	38	-0.02	-0.03	0.10	0.10	0.11	0.97	0.09
C4	29525	0.07	0.28	0.79	0.84	0.50	0.36	0.29
C5	100769	-0.01	-0.01	0.13	0.13	0.08	0.87	0.06
C6	45938	0.00	0.04	0.46	0.46	0.29	0.63	0.21
C7a	81623	0.00	0.07	0.56	0.57	0.24	0.32	0.18
C7b	63015	-0.01	-0.01	0.17	0.17	0.09	0.86	0.06
C7c	31148	-0.01	-0.01	0.10	0.10	0.07	0.92	0.05
C8a	154749	0.00	0.03	0.42	0.42	0.12	0.38	0.09
C8b	18630	-0.02	-0.01	0.22	0.22	0.12	0.90	0.09
C8c	2432	-0.04	-0.04	0.14	0.15	0.16	0.91	0.12
C9a	7650	0.08	0.60	1.29	1.42	0.98	0.11	0.29
C9b	168161	-0.01	0.00	0.28	0.28	0.12	0.51	0.09
C9c	0	NaN	NaN	NaN	NaN	NaN	NaN	NaN

Table 1 numerical values can be downloaded as a csv file [here](#).

6 Moorings

6.1 Introduction

The Pi-MEP collects data from the Global Tropical Moored Buoy Array ([GTMBA](#)), a multi-national effort to provide data in real-time for climate research and forecasting. Major components include the TAO/TRITON array in the Pacific, PIRATA in the Atlantic, and RAMA in the Indian Ocean. Data collected within TAO/TRITON, PIRATA and RAMA comes primarily from ATLAS and TRITON moorings. These two mooring systems are functionally equivalent in terms of sensors, sample rates, and data quality. The data are directly downloaded from [ftp.pmel.noaa.gov](ftp://pmel.noaa.gov) every day and stored in the Pi-MEP. Only salinity data measured at 1 or 1.5 meter depth with standard (pre-deployment calibration applied) and highest quality (pre/post calibration agree) are considered. A careful filtering of suspicious bad mooring salinity data when compared with all satellite data has also been performed (cf. [presentation](#)). The Pi-MEP project acknowledges the GTMBA Project Office of NOAA/PMEL for providing the data. Data from the Ocean Station [PAPA](#) are also added to the Pi-MEP *in situ* database.

From the [Upper Ocean Processes Group](#) at Woods Hole Oceanographic Institution ([WHOI](#)), delayed mode surface mooring salinity records under the stratus cloud deck in the eastern tropical Pacific ([Stratus](#)), in the trade wind region of the northwest tropical Atlantic ([NTAS](#)), 100 km north of Oahu at the WHOI Hawaii Ocean Time-series Site ([WHOTS](#)), in the salinity maximum region of the subtropical North Atlantic ([SPURS-1](#)) and in the Pacific intertropical convergence zone ([SPURS-2](#)) are also included in the Pi-MEP.

6.2 Number of SSS data as a function of time and distance to coast

Figure 136 shows the time (a) and distance to coast (b) distributions of the Moorings *in situ* dataset.

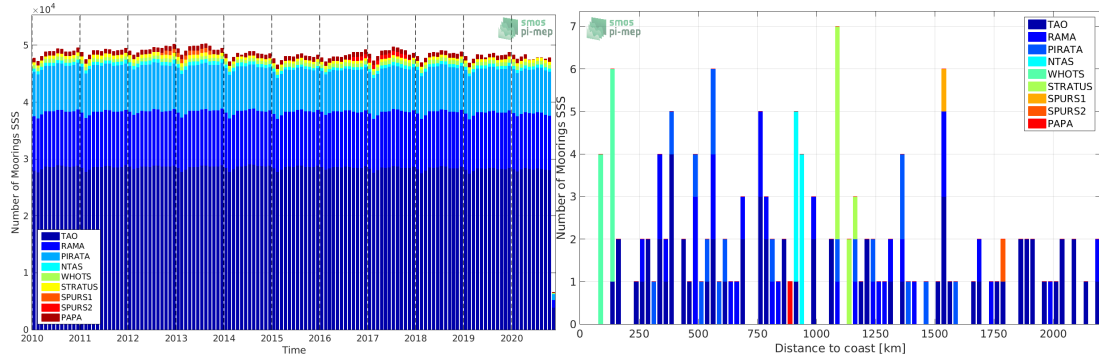


Figure 136: Number of SSS from Moorings as a function of time (left) and distance to coast (right).

6.3 Histogram of SSS

Figure 137 shows the SSS distribution of the Moorings.

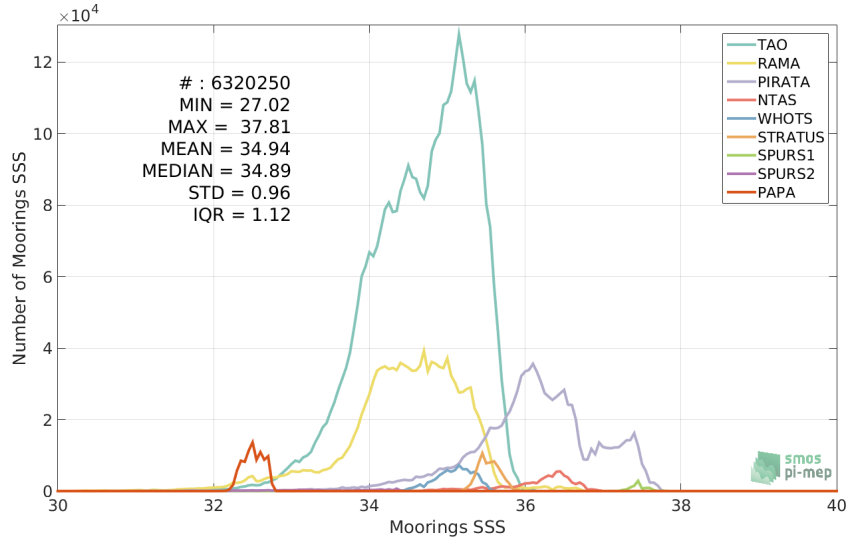


Figure 137: Distribution of SSS from Moorings per bins of 0.1.

6.4 Temporal mean of shallowest salinity

Figure 138 show a map of the mooring locations and the color of each circle indicates the temporal mean calculated using the full time series from 2010 to now of each mooring.

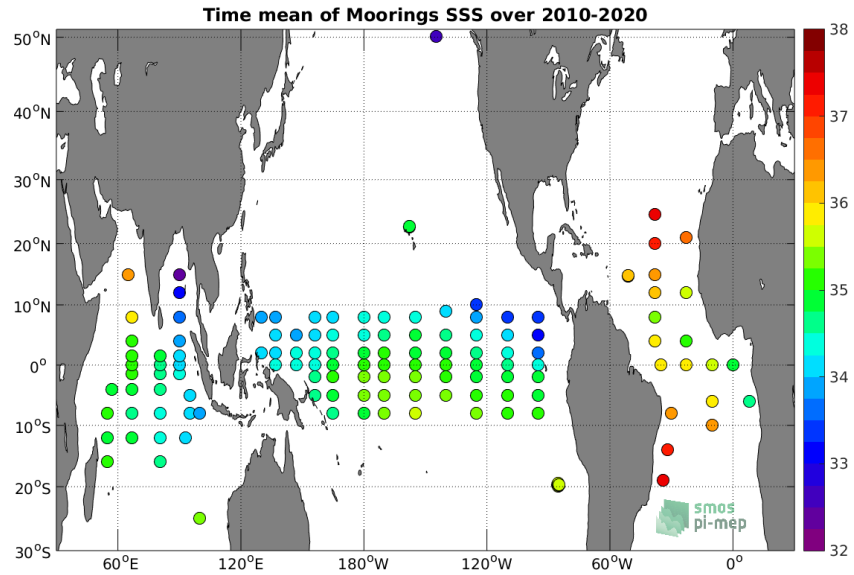


Figure 138: Temporal mean SSS from Moorings.

6.5 Temporal Std of shallowest salinity

Figure 139 show maps of the mooring locations and the color of each circle indicates the temporal standard deviation calculated using the full time series from 2010 to now of each mooring.

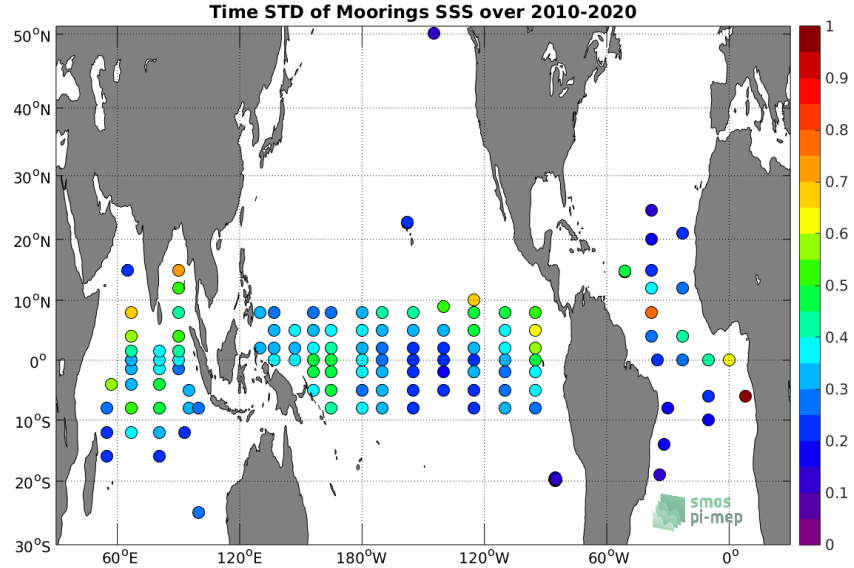


Figure 139: Temporal Std of SSS from Moorings.

6.6 Number of shallowest salinity

Figure 140 show maps of the mooring locations and the color of each circle indicates the number of SSS data measured by each mooring from 2010 to now.

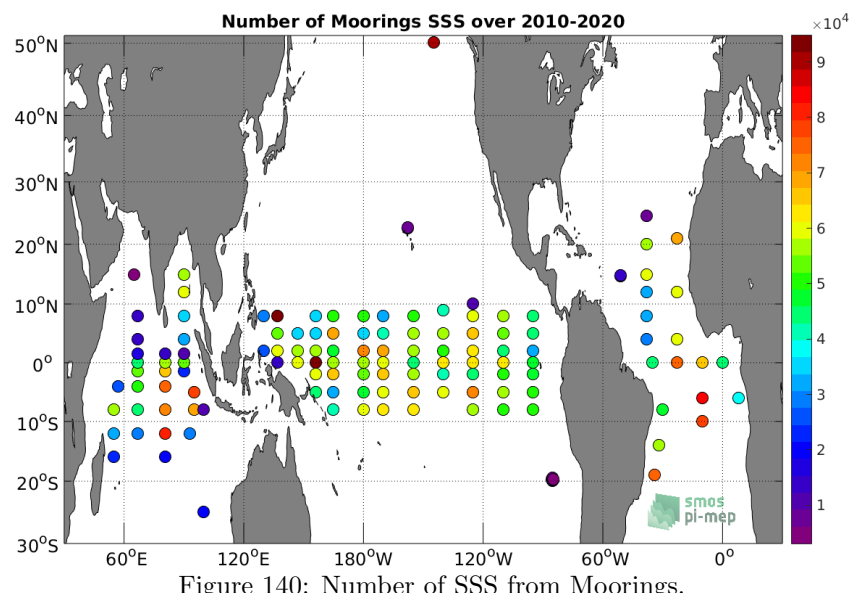


Figure 140: Number of SSS from Moorings.

6.7 Time series of shallowest salinity

The following figures (141) show time series of shallowest salinity for each mooring. To switch from a mooring to another, you can play with the arrows between the plot and the caption.

Figure 141: Time series of mooring shallowest salinity

7 Summary

In the following summary section, some of the plots presented in the previous sections corresponding to the time distribution [7.1], SSS distribution [7.2], temporal mean [7.3] and std [7.4], and spatial density [7.5], are combined to emphasize similarities/differences between each *in situ* datasets. Some characteristics of each *in situ* datasets for each Pi-MEP region are also presented in 7.6.

7.1 Number of SSS data as a function of time

Figures 142 show the time distribution of the different *in situ* datasets.

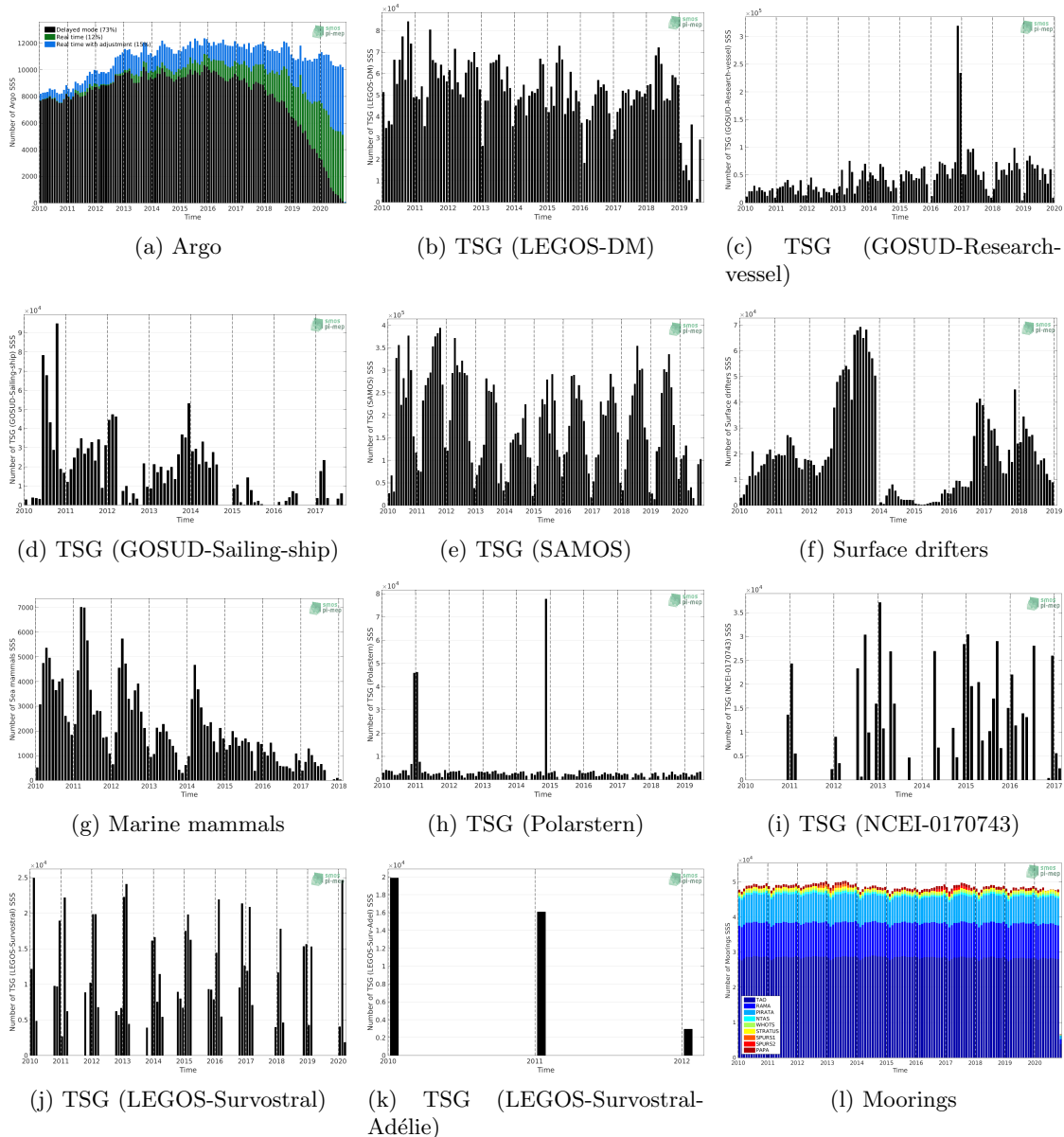


Figure 142: Number of SSS data as a function of time of the different *in situ* datasets

7.2 Histogram of SSS

Figures 143 show the SSS distribution of the different *in situ* datasets.

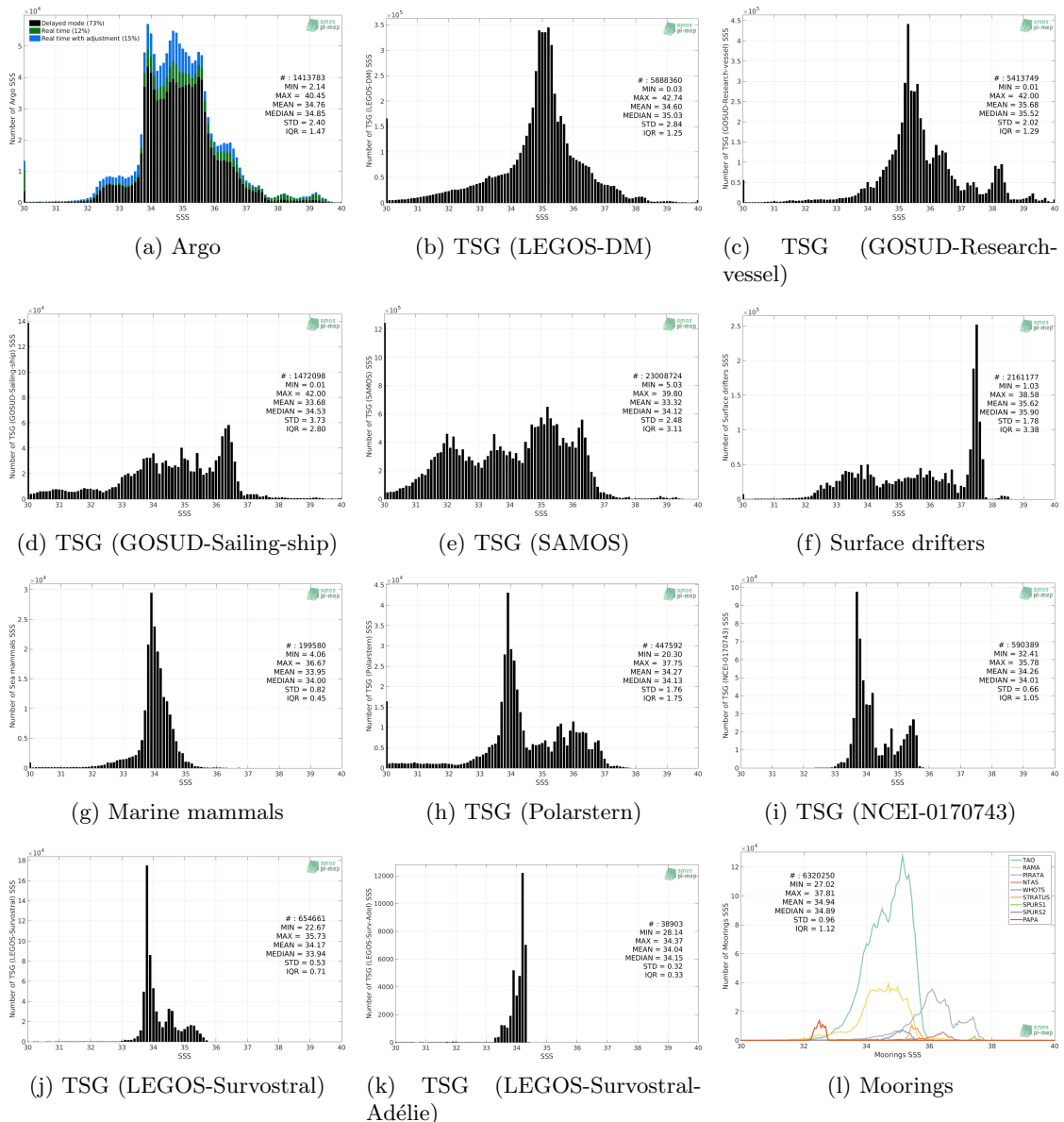


Figure 143: Distribution of SSS per bins of 0.1 of the different *in situ* datasets.

7.3 Temporal mean of SSS

Figures 144 show the temporal mean gridded over spatial boxes of size $1^\circ \times 1^\circ$ using the full period of each *in situ* datasets.

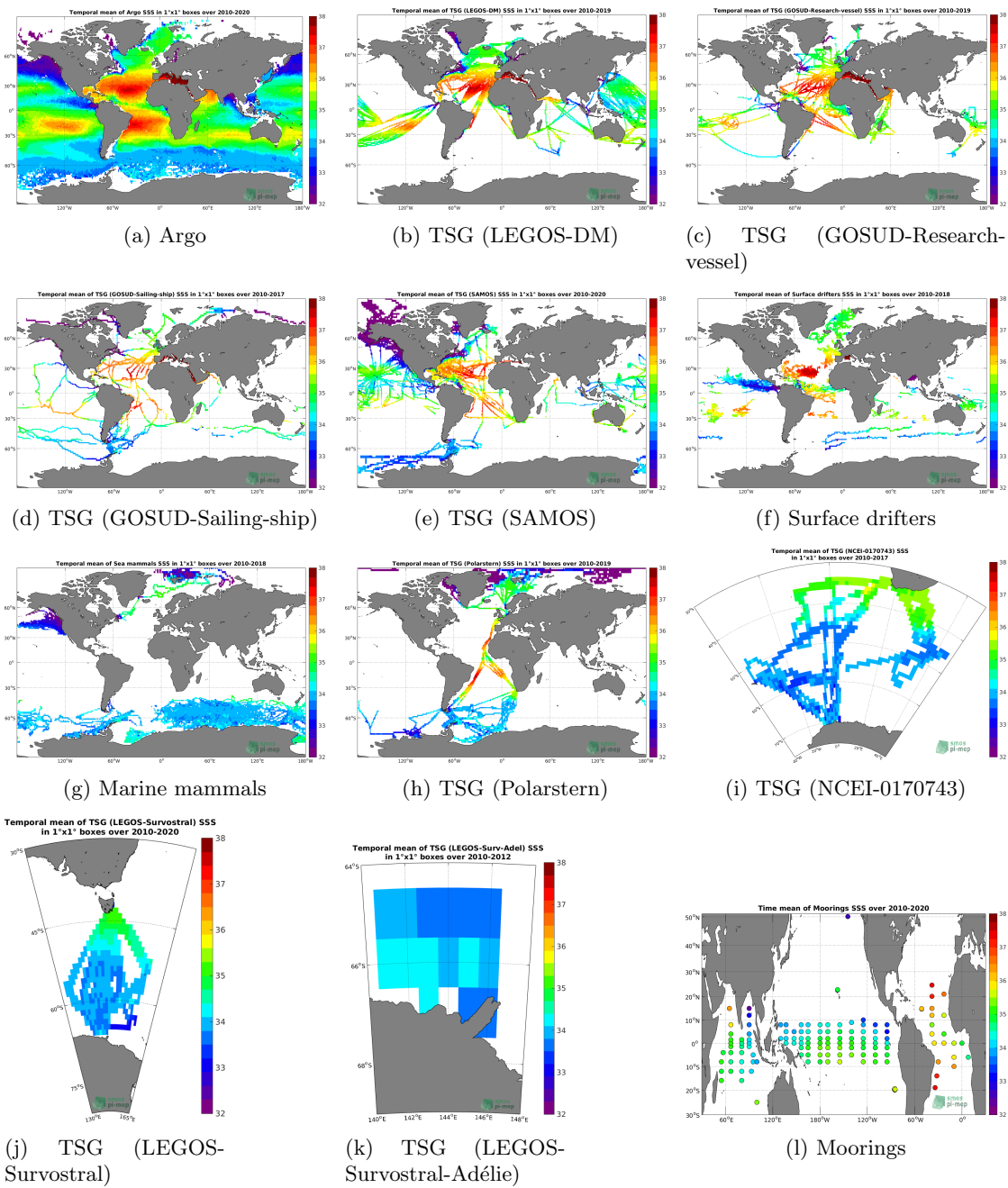


Figure 144: Temporal mean of SSS in $1^\circ \times 1^\circ$ boxes.

7.4 Temporal Std of SSS

Figures 145 show the temporal standard deviation (std) gridded over spatial boxes of size $1^\circ \times 1^\circ$ using the full period of each *in situ* datasets.

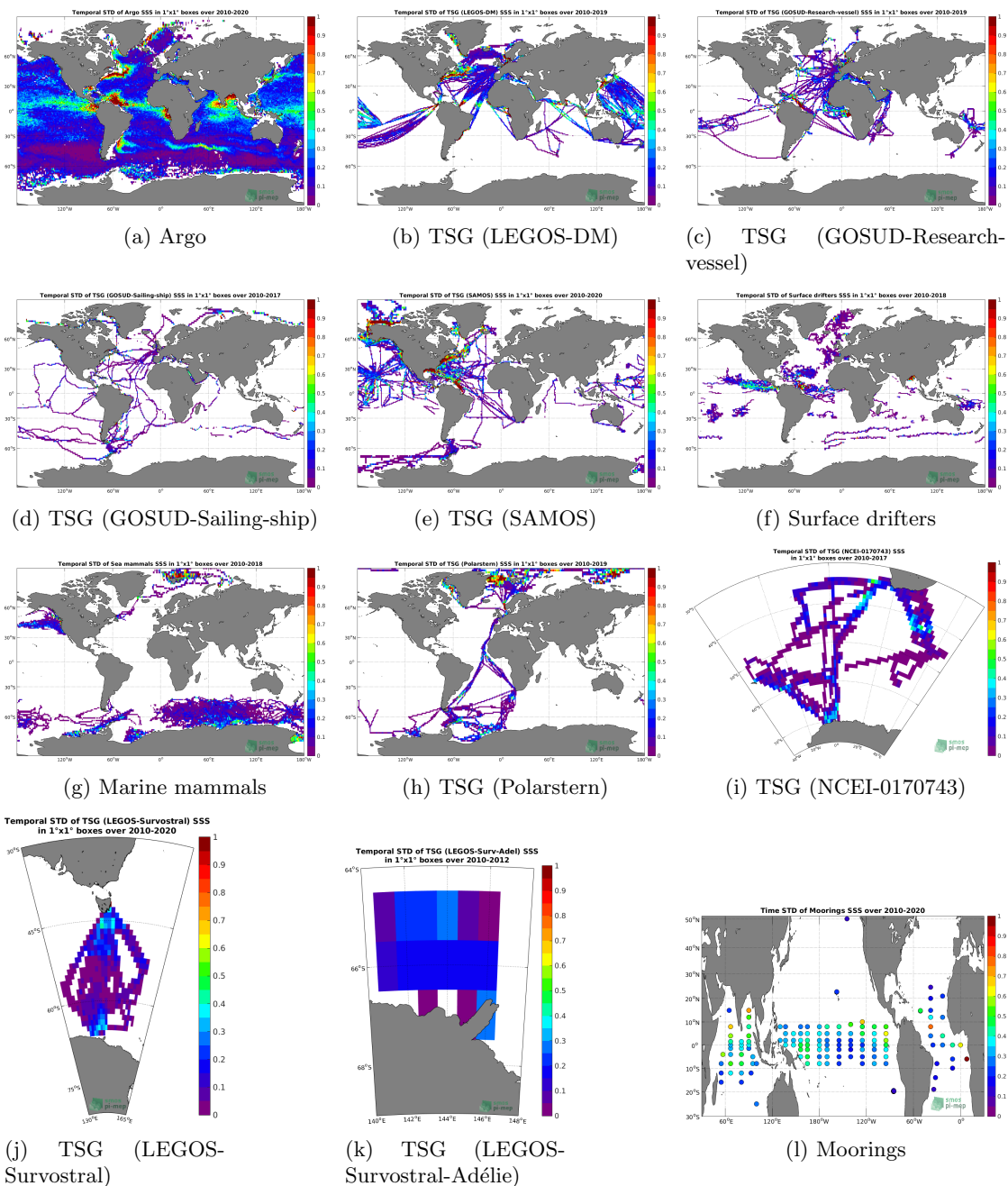


Figure 145: Temporal Std of SSS in $1^\circ \times 1^\circ$ boxes.

7.5 Spatial density of SSS

Figures 146 show the spatial distribution of SSS gridded over spatial boxes of size $1^\circ \times 1^\circ$ using the full period of each *in situ* datasets.

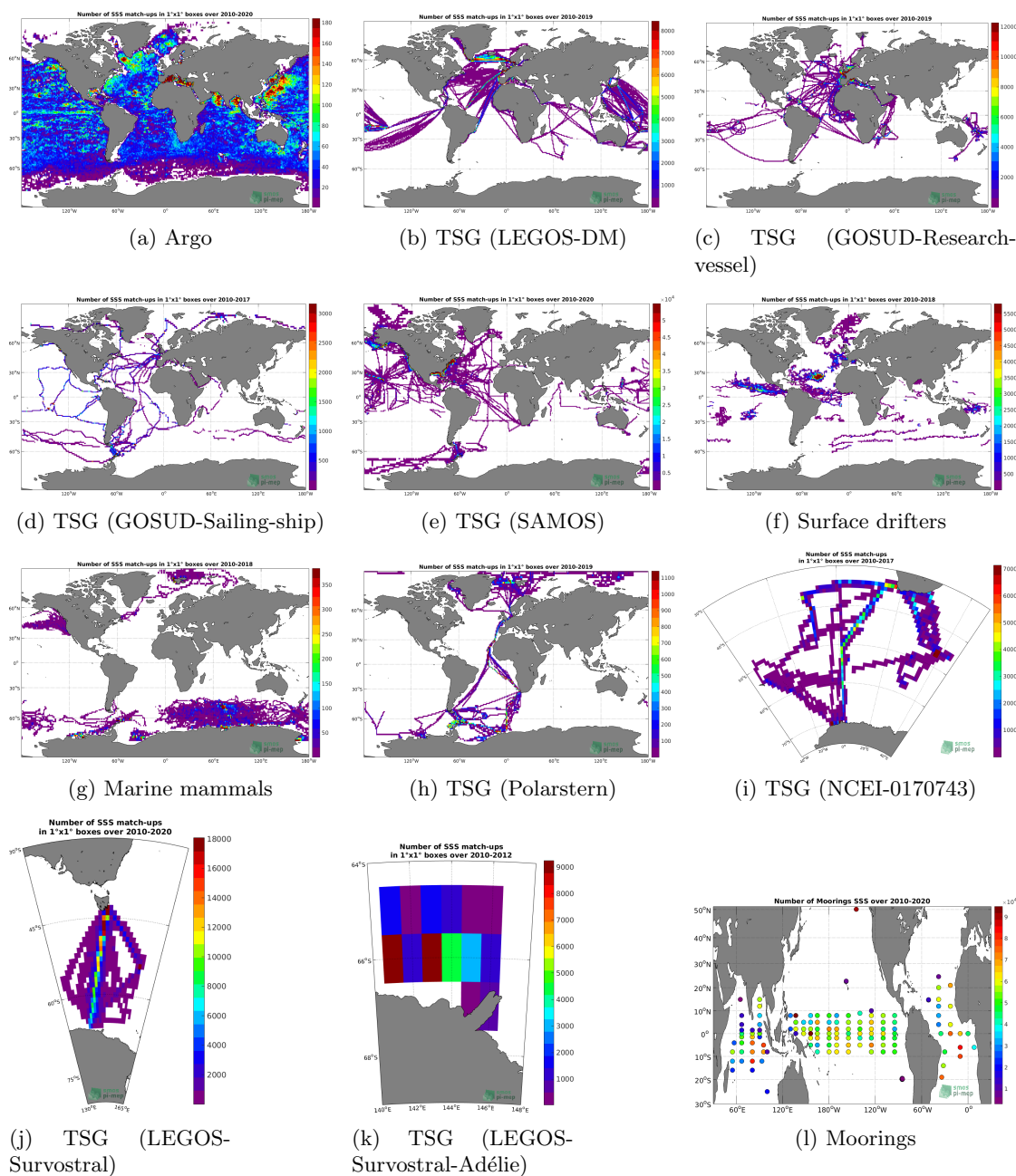


Figure 146: Number of SSS in $1^\circ \times 1^\circ$ boxes.

7.6 Characteristics for each Pi-MEP region

The following tables show some characteristics of each *in situ* dataset after applying the different Pi-MEP region masks described [here](#). To switch from a region to another, you can play with the arrows between the plot and the caption.

References

- Gaël Alory, T. Delcroix, P. Téchiné, D. Diverrès, D. Varillon, S. Cravatte, Y. Gouriou, J. Grelet, S. Jacquin, E. Kestenare, and et al. The French contribution to the voluntary observing ships network of sea surface salinity. *Deep-Sea Res. Pt. I*, 105:1–18, November 2015. ISSN 0967-0637. doi: [10.1016/j.dsr.2015.08.005](https://doi.org/10.1016/j.dsr.2015.08.005).
- Argo. Argo float data and metadata from Global Data Assembly Centre (Argo GDAC), 2000. doi: [10.17882/42182](https://doi.org/10.17882/42182).
- Giuseppe Aulicino, Yuri Cotroneo, Isabelle Ansorge, and Marcel Van Den Berg. Sea surface temperature and salinity collected aboard the S.A. AGULHAS II and S.A. AGULHAS in the South Atlantic Ocean and Southern Ocean from 2010-12-08 to 2017-02-02 (NCEI Accession 0170743), 2018. doi: [10.7289/v56m3545](https://doi.org/10.7289/v56m3545).
- Abderrahim Bentamy and Denis Croize Fillon. Gridded surface wind fields from Metop/ASCAT measurements. *Int. J. Remote Sens.*, 33(6):1729–1754, March 2012. ISSN 1366-5901. doi: [10.1080/01431161.2011.600348](https://doi.org/10.1080/01431161.2011.600348).
- Abderrahim Bentamy, Semyon A. Grodsky, James A. Carton, Denis Croizé-Fillon, and Bertrand Chapron. Matching ASCAT and QuikSCAT winds. *J. Geophys. Res.*, 117(C2), February 2012. ISSN 0148-0227. doi: [10.1029/2011JC007479](https://doi.org/10.1029/2011JC007479).
- Jaqueline Boutin, Y. Chao, W. E. Asher, T. Delcroix, R. Drucker, K. Drushka, N. Kolodziejczyk, T. Lee, N. Reul, G. Reverdin, J. Schanze, A. Soloviev, L. Yu, J. Anderson, L. Brucker, E. Dinnat, A. S. Garcia, W. L. Jones, C. Maes, T. Meissner, W. Tang, N. Vinogradova, and B. Ward. Satellite and In Situ Salinity: Understanding Near-Surface Stratification and Sub-footprint Variability. *Bull. Am. Meterol. Soc.*, 97(8):1391–1407, 2016. ISSN 1520-0477. doi: [10.1175/bams-d-15-00032.1](https://doi.org/10.1175/bams-d-15-00032.1).
- Ralph R. Ferraro. SSM/I derived global rainfall estimates for climatological applications. *J. Geophys. Res.*, 102(D14):16715–16736, 07 1997. doi: [10.1029/97JD01210](https://doi.org/10.1029/97JD01210).

Ralph R. Ferraro, Fuzhong Weng, Norman C. Grody, and Limin Zhao. Precipitation characteristics over land from the NOAA-15 AMSU sensor. *Geophys. Res. Lett.*, 27(17):2669–2672, 2000. doi: [10.1029/2000GL011665](https://doi.org/10.1029/2000GL011665).

Fabienne Gaillard, E. Autret, V. Thierry, P. Galaup, C. Coatanoan, and T. Loubrieu. Quality Control of Large Argo Datasets. *J. Atmos. Oceanic Technol.*, 26(2):337–351, 2009. doi: [10.1175/2008JTECHO552.1](https://doi.org/10.1175/2008JTECHO552.1).

Fabienne Gaillard, Thierry Reynaud, Virginie Thierry, Nicolas Kolodziejczyk, and Karina von Schuckmann. In Situ-Based Reanalysis of the Global Ocean Temperature and Salinity with ISAS: Variability of the Heat Content and Steric Height. *J. Clim.*, 29(4):1305–1323, February 2016. ISSN 1520-0442. doi: [10.1175/jcli-d-15-0028.1](https://doi.org/10.1175/jcli-d-15-0028.1).

Robert J. Joyce, John E. Janowiak, Phillip A. Arkin, and Pingping Xie. CMORPH: A Method that Produces Global Precipitation Estimates from Passive Microwave and Infrared Data at High Spatial and Temporal Resolution. *J. Hydrometeorol.*, 5(3):487–503, June 2004. doi: [10.1175/1525-7541\(2004\)005<0487:camtpg>2.0.co;2](https://doi.org/10.1175/1525-7541(2004)005<0487:camtpg>2.0.co;2).

Nicolas Kolodziejczyk, Denis Diverres, Stéphane Jacquin, Yves Gouriou, Jacques Grelet, Marc Le Menn, Joelle Tassel, Gilles Reverdin, Christophe Maes, and Fabienne Gaillard. Sea Surface Salinity from French RESearch Vessels : Delayed mode dataset, annual release, 2015a. doi: [10.17882/39475](https://doi.org/10.17882/39475).

Nicolas Kolodziejczyk, Gilles Reverdin, and Alban Lazar. Interannual Variability of the Mixed Layer Winter Convection and Spice Injection in the Eastern Subtropical North Atlantic. *J. Phys. Oceanogr.*, 45(2):504–525, Feb 2015b. ISSN 1520-0485. doi: [10.1175/jpo-d-14-0042.1](https://doi.org/10.1175/jpo-d-14-0042.1).

Christian Kummerow, Y. Hong, W. S. Olson, S. Yang, R. F. Adler, J. McCollum, R. Ferraro, G. Petty, D-B. Shin, and T. T. Wilheit. The Evolution of the Goddard Profiling Algorithm (GPROF) for Rainfall Estimation from Passive Microwave Sensors. *J. Appl. Meteorol.*, 40(11):1801–1820, 2001. doi: [10.1175/1520-0450\(2001\)040<1801:TEOTGP>2.0.CO;2](https://doi.org/10.1175/1520-0450(2001)040<1801:TEOTGP>2.0.CO;2).

Rosemary Morrow and Elodie Kestenare. Nineteen-year changes in surface salinity in the southern ocean south of australia. *J. Mar. Sys.*, 129:472–483, January 2014. doi: [10.1016/j.jmarsys.2013.09.011](https://doi.org/10.1016/j.jmarsys.2013.09.011).

Thierry Reynaud, Floriane Desprez De Gesincourt, Fabienne Gaillard, Hervé Le Goff, and Gilles Reverdin. Sea Surface Salinity from Sailing ships : Delayed mode dataset, annual release, 2015. doi: [10.17882/39476](https://doi.org/10.17882/39476).

Fabien Roquet, Christophe Guinet, Jean-Benoit Charrassin, Daniel P. Costa, Kit M Kovacs, Christian Lydersen, Horst Bornemann, Marthan N. Bester, Monica C. Muelbert, Mark A. Hindell, Clive R. McMahon, Rob Harcourt, Lars Boehme, and Mike A. Fedak. MEOP-CTD in-situ data collection: a Southern ocean Marine-mammals calibrated sea water temperatures and salinities observations, 2018. doi: [10.17882/45461](https://doi.org/10.17882/45461).

Shawn R. Smith, Jeremy J. Rolph, Kristen Briggs, and Mark A. Bourassa. Quality-Controlled Underway Oceanographic and Meteorological Data from the Center for Ocean-Atmospheric Predictions Center (COAPS) - Shipboard Automated Meteorological and Oceanographic System (SAMOS), 2009. doi: [10.7289/v5qj7f8r](https://doi.org/10.7289/v5qj7f8r).

Anne Treasure, Fabien Roquet, Isabelle Ansorge, Marthán Bester, Lars Boehme, Horst Bornemann, Jean-Benoît Charrassin, Damien Chevallier, Daniel Costa, Mike Fedak, Christophe

Guinet, Mike Hammill, Robert Harcourt, Mark Hindell, Kit Kovacs, Mary-Anne Lea, Phil Lovell, Andrew Lowther, Christian Lydersen, Trevor McIntyre, Clive McMahon, Mônica Muelbert, Keith Nicholls, Baptiste Picard, Gilles Reverdin, Andrew Trites, Guy Williams, and P.J. Nico de Bruyn. Marine Mammals Exploring the Oceans Pole to Pole: A Review of the MEOP Consortium. *Oceanography*, 30(2):132–138, jun 2017. doi: [10.5670/oceanog.2017.234](https://doi.org/10.5670/oceanog.2017.234).